

CONTROLS OF MINERALIZATION IN
THE BETTS COVE OPHIOLITE

CENTRE FOR NEWFOUNDLAND STUDIES

TOTAL OF 10 PAGES ONLY
MAY BE XEROXED

(Without Author's Permission)

CYNTHIA MARGARET SAUNDERS

**CONTROLS OF MINERALIZATION
IN THE BETTS COVE OPHIOLITE**

BY

© Cynthia Margaret Saunders, B. Sc.

A thesis submitted to the School of Graduate

Studies in partial fulfillment of the

requirements for the degree of

Master of Science

Department of Earth Sciences

Memorial University of Newfoundland

February 1985

St. John's, Newfoundland

Abstract

The focus of this study is the Betts Cove massive sulphide deposit which is located within the Betts Cove Complex, an Ordovician ophiolite sequence that consists of, in ascending stratigraphic order, an ultramafic, a gabbroic, a sheeted dyke and a pillow lava member. The ophiolite is conformably overlain by the Ordovician Snooks Arm Group, a series of sedimentary rocks and basic to andesitic pyroclastic rocks which are intruded by diabasic sills. The ophiolite and the Snooks Arm Group are intruded by or are in fault or unconformable contact with the surrounding rock units. The pillow lava member of the ophiolite is characterized by variolitic textures which are the result of supercooling. The basaltic members of the ophiolite are characterized by unusually low TiO_2 and high Cr, Ni and MgO concentrations; they show similarities to boninites from the Western Pacific and may have formed in a supra-subduction environment. The Betts Cove sulphide deposit is located at the contact between the sheeted dyke and the pillow lava members. It consists of a massive pyrite-chalcopyrite-sphalerite body underlain by a stockwork of pyrite-chalcopyrite. The deposit has a distinctive footwall alteration zone which consists of a core of quartz-chlorite and a halo of chlorite-albite-quartz. These zones are superimposed on a background greenschist assemblage of actinolite-epidote-chlorite-albite-quartz with relict clinopyroxene commonly preserved. The footwall alteration zones can be related to the amount of water which has passed through the rock. The core zone was the area of highest fluid flux (high water/rock ratio); CaO, Na_2O , Sr, and to some extent, light rare earth elements were leached from this zone. The background assemblage was produced by a low water/rock ratio and that of the halo zone by an intermediate water/rock ratio. Fluid inclusion studies show that the fluids had a composition similar to that of seawater. The Betts Cove deposit

shows many similarities to the classic Troodos massive sulphide deposits and is thought to have formed in the same way - by re-deposition of metals which were leached from the ocean crust by circulating seawater. Comparable deposits are currently being formed at the East Pacific Rise and the Galapagos Ridge. The site of upwelling of metal-bearing hydrothermal fluids, probably along faults and fracture zones, is the area of greatest fluid flux; thus the core alteration zone underlying the Betts Cove deposit is interpreted to represent the conduit for the mineralizing fluids which deposited the massive sulphide mineralization. The fluids may have been focussed along faults and permeable zones.

Acknowledgments

I would like to thank my supervisor, Dr. D. F. Strong, for his enormous help and patience. Dr. R. K. Stevens served as second supervisor and provided many helpful hints along the way. Paul Dean and Baxter Kean of the Newfoundland Department of Mines and Energy provided field supervision and shared their ideas on the ophiolites and massive sulphides of central Newfoundland. Anne Hogan is thanked for cheerful field assistance even when carrying staggering loads of rocks from the mine to the camp. Drs. D. Wilton, T. Rivers, B. Fryer and C. Hughes assisted with various aspects of the thesis. I would also like to thank Desiree King for help with draughting, Dave Press for help with computer programs, Gert Andrews for major element analyses, Patricia Finn for help with rare earth element analyses, Wilf Marsh for help with photography, Dr. H. Longerich for assistance with the electron microprobe and Foster Thornhill, Lloyd Warford, Gerry Ford and Rick Soper for making thin and polished sections. Finally, I would like to thank my husband, Phil, for his patience and support. Financial support was provided through a university fellowship and an ASARCO scholarship. Financial assistance was also provided by NSERC operating grant no. A7975 to Dr. D. F. Strong. The Geological Survey of Canada supplied my salary during the summer of 1982 and the Newfoundland Department of Mines and Energy provided field support.

Table of Contents

1. GENERAL GEOLOGY AND LITERATURE REVIEW	1
1.1. Introduction	1
1.2. Location and Access	2
1.3. Previous Work	2
1.4. Regional Geology	6
1.5. General Description of the Ophiolite and Snooks Arm Group	10
1.5.1. The Betts Cove Complex	11
1.5.1.1. The Ultramafic Member	11
1.5.1.2. The Gabbroic Member	12
1.5.1.3. The Sheeted Dyke Member	13
1.5.1.4. The Pillow Lava Member	13
1.5.2. The Snooks Arm Group	13
1.5.2.1. The Bobby Cove and Balsam Bud Cove Formations	14
1.5.2.2. The Venams Bight and Round Harbour Formations	14
1.6. Mineralization in the Betts Cove Ophiolite	16
1.7. Cyprus Type Deposits	17
1.8. Experimental Work	21
1.9. Modern Sub-sea Hydrothermal Systems	21
1.10. Summary	24
2. FIELD OBSERVATIONS AND PETROGRAPHY	25
2.1. Introduction	25
2.2. Gabbroic Rocks	25
2.3. Sheeted Dyke Member	28
2.3.1. Dyke Breccia	31
2.4. Pillow Lava Member	31
2.4.1. Significance of Variolitic Textures	33
2.4.2. Pillow Breccia	45
2.5. Summary	47
3. GEOCHEMISTRY	48
3.1. Introduction	48
3.2. Elemental Mobility	50
3.3. Results	51
3.3.1. Discussion	59
3.4. Tectonic Environment	62
3.5. Summary	65

4. MINERALIZATION AND RELATED ALTERATION	66
4.1. Introduction	66
4.2. Outcrop Description	66
4.3. Metal Contents of Sulphide Samples	72
4.4. Sulphide Textures	74
4.4.1. Comparison with Troodos and East Pacific Rise Deposits	79
4.5. Alteration	84
4.5.1. Variation Diagrams	88
4.5.2. Comparison With Other Deposits	96
4.5.2.1. Eurasian Ophiolite Deposits	96
4.5.2.2. Newfoundland Ophiolite Deposits	97
4.5.2.3. Canadian Archean Deposits	98
4.5.2.4. Summary	99
4.5.3. Discussion	99
4.5.3.1. Experimental Studies	99
4.5.3.2. Application of Experimental Results to the Present Study	101
4.5.3.3. Natural Systems	106
4.5.3.4. Implications for Betts Cove	110
4.6. Fluid Inclusions	111
4.6.1. Introduction	111
4.6.2. Description of Inclusions	111
4.6.3. Freezing Results	122
4.6.3.1. Fluid Composition	122
4.6.3.2. Salinity	124
4.6.4. Homogenization Temperatures	124
4.7. Structural and Stratigraphic Control	127
4.8. Summary	129
5. CONCLUSIONS	133
REFERENCES	136
Appendix A. Petrographic Table Illustrating Mineralogy of Samples	159
Appendix B. Analytical Methods	168
Appendix C. Major and Trace Element Analyses	170
Appendix D. Sulphide Analyses	190
Appendix E. Electron Microprobe Data - Chlorites	193
Appendix F. Fluid Inclusion Methodology	199

List of Tables

Table 1-1:	Published works and theses concerning the Betts Cove ophiolite in general	3
Table 1-2:	Published works and theses concerning mineralization in the Betts Cove ophiolite	4
Table 1-3:	Private reports on mineralization in the Betts Cove ophiolite	5
Table 2-1:	Explanation of crystal morphology terminology	41
Table 3-1:	Variation of major and trace element abundances from varioles to matrix and core to rim of individual pillows	53
Table 4-1:	Geochemical characteristics of alteration zones	87
Table 4-2:	Cu and Zn concentrations in dykes	95
Table 4-3:	Concentrations (ppm) of components in modern vent solutions at EPR and Galapagos	107
Table 4-4:	Characteristics of fluid inclusion solid phases	113
Table 4-5:	Characteristics of fluid inclusions	114
Table 4-6:	Eutectic temperatures of aqueous chloride systems	123

List of Figures

Figure 1-1:	General geology of the Burlington Peninsula	7
Figure 1-2:	Geology of the Betts Cove - Tilt Cove area	9
Figure 1-3:	Stratigraphic section for Betts Cove - Tilt Cove area	15
Figure 1-4:	Diagrammatic section through a typical Cyprus sulphide deposit	19
Figure 2-1:	Geology and sample locations - Betts Cove area	26
Figure 2-2:	Enlargement of mine area from Fig. 2-1	27
Figure 2-3:	Photographs of gabbro and plagiogranite thin-sections and sheeted dyke outcrops	29
Figure 2-4:	Photographs of variolitic dyke outcrop and dyke breccia and photomicrographs of dyke breccia	32
Figure 2-5:	Photographs of typical outcrops of variolitic pillows	34
Figure 2-6:	Photographs illustrating mode of variole distribution within pillows	35
Figure 2-7:	Photomicrographs of phenocryst pseudomorphs	36
Figure 2-8:	Photomicrographs of representative variolitic textures	37
Figure 2-9:	Photomicrographs of pyroxene crystal textures	38
Figure 2-10:	Photomicrographs of variole-matrix contact	39
Figure 2-11:	Progression of crystal textures produced by increasing degrees of supercooling	40
Figure 2-12:	The basic spherulite morphologies	42
Figure 2-13:	Experimentally produced plagioclase spherulites	42
Figure 2-14:	Photomicrographs of significant crystallization textures	43
Figure 2-15:	Photographs of pillow breccia (thin-sections, outcrop and cut slab)	46
Figure 3-1:	Variation diagrams	54
Figure 3-2:	Variation diagrams	55
Figure 3-3:	Variation diagrams	57
Figure 3-4:	Variation diagrams	58
Figure 3-5:	Variation diagrams	60
Figure 3-6:	Diagram illustrating environment of ophiolite formation and mode of ophiolite obduction	64
Figure 4-1:	Photograph of old mine site	67
Figure 4-2:	Photographs of outcrops of stockwork mineralization	69
Figure 4-3:	Photomicrographs of sulphide textures	75

Figure 4-4:	Photographs of tectonic fabric in sulphides	76
Figure 4-5:	Photographs of sulphide textures	78
Figure 4-6:	Photomicrographs of cobaltite and primary pyrite	80
Figure 4-7:	Photomicrographs of gangue minerals	81
Figure 4-8:	Photomicrographs of mineralization-related alteration	85
Figure 4-9:	Photographs of albite veins (in outcrop and thin-section)	89
Figure 4-10:	Variation diagrams	91
Figure 4-11:	Variation diagrams	92
Figure 4-12:	Cr (in whole rock) vs. Fe/Mg (in chlorites).	93
Figure 4-13:	Triangular plot of FeO vs. Al ₂ O ₃ vs. MgO in chlorites;	94
Figure 4-14:	Alteration assemblages produced by varying water/rock ratios	103
Figure 4-15:	Sub-seafloor convection cell model	104
Figure 4-16:	Flow geometry of sub-seafloor hydrothermal convection system	105
Figure 4-17:	Photomicrographs of growth zones in quartz	116
Figure 4-18:	Photomicrographs of two-phase inclusions	117
Figure 4-19:	Photomicrographs of multiphase inclusions	118
Figure 4-20:	Photomicrographs of multiphase inclusions	119
Figure 4-21:	Photomicrographs of multiphase inclusions	120
Figure 4-22:	Photomicrographs of multiphase inclusions	121
Figure 4-23:	Fluid inclusion salinity and homogenization temperature histograms	125
Figure 4-24:	Fault control of mineralization	130
Figure F-1:	Calibration curve for fluid inclusion heating runs	200

Chapter 1

GENERAL GEOLOGY AND LITERATURE REVIEW

1.1. Introduction

The aim of this thesis is to describe the mineralogical and chemical characteristics of the Betts Cove copper deposit as a means to providing some insight into its mode of formation.

The deposit is contained in the Betts Cove Complex, a Lower Ordovician ophiolite which is located on the east coast of the Burlington or Baie Verte Peninsula in north-central Newfoundland. The Betts Cove deposit is an "ophiolite type" massive sulphide deposit (Upadhyay, 1973; Upadhyay and Strong, 1973). Accordingly a brief description of the type deposits is presented as a framework in which to describe the Betts Cove deposit.

Ideas concerning the formation of ophiolitic massive sulphides have been verified and refined by recent experimental work on seawater-basalt interaction, and by new information provided by recent discoveries of natural hydrothermal fluids which are actively depositing sulphides on the seafloor. The findings of both lines of research are briefly summarized in this chapter.

1.2. Location and Access

The Betts Cove Ophiolite is located on the east side of the Burlington Peninsula (Fig. 1-1). Access is most convenient by boat from Nippers Harbour, 6 km to the southwest.

1.3. Previous Work

The Burlington Peninsula has long been a center of geological activity in Newfoundland. It has been explored extensively by both academic researchers and mining company geologists, and geological interpretations of the area have kept pace with changing geological concepts. During the early seventies the area was the focus of much attention by researchers concerned with unravelling the then new theory of plate tectonics. Since then ideas have undergone much revision and refinement but the area still affords ample material for further study.

Some of the most important and influential contributions were provided by Snelgrove (1931), Watson (1943, 1947), Baird (1947, 1951), Neale (1957, 1958a,b, 1959, 1967), Neale et al. (1960), Neale and Nash (1963), Neale and Kennedy (1967), Neale et al. (1975), Church (1965, 1966, 1969), Church and Stevens (1971), Kennedy (1971, 1975a,b), Kennedy and Phillips (1971), Kennedy et al. (1972), Dewey (1969), Dewey and Bird (1971), Bird and Dewey (1970), Upadhyay et al. (1971), Upadhyay (1973), Kidd (1974, 1977), Kidd et al. (1978), de Wit (1972, 1974, 1980), Bursnall (1975), Bursnall and de Wit (1975), Bursnall and Hibbard (1980), DeGrace et al. (1976), Williams (1977, 1978), Williams and Hibbard (1977), Williams et al. (1977), Williams and St. Julien (1978, 1982), Hibbard (1982, 1983), Hibbard and Gagnon (1980), Hibbard et al. (1980a,b). Hibbard (1983) has presented a comprehensive account of the development of geological ideas on the peninsula in which he lists the individual accomplishments of the above authors. The works which directly concern the Betts Cove Ophiolite are summarized here in Tables 1-1, 1-2 and 1-2.

**Table 1-1: Published works and theses concerning
the Betts Cove ophiolite in general**

Year	Author(s)	Subject
1957	Neale	Nature of contact between the ultramafic belt and surrounding units.
1971	Upadhyay <u>et al.</u>	Description and interpretation of mode of formation of the ophiolite.
1971	Schroeter	M.Sc. thesis on Nippers Harbour ophiolite.
1972	Riccio	M.Sc. thesis on ophiolite in Betts Cove area.
1973	Upadhyay	Ph.D. thesis on the entire ophiolite.
1974	Brock	Proposed sheeted dykes need not mean spreading.
1974	Church and Riccio	Discussion of Brock (1974).
1975	Strong and Malpas	Discussion of Brock (1974).
1975	Neale <u>et al.</u>	Described unconformity between the ophiolite and overlying Cape St. John Group.
1977	Coish	Ph.D thesis on geochemistry of the mafic units of the ophiolite near Betts Cove.
1977	Coish	Paper on subsea metamorphism in the ophiolite.
1978	Upadhyay	Proposed that some lavas within the ophiolite are komatiitic.
1979	Coish and Church	Described geochemistry of the mafic units of the ophiolite near Betts Cove.
1982	Upadhyay	Paper on komatiitic lavas from the ophiolite.
1982	Coish <u>et al.</u>	Paper on REE geochemistry of mafic rocks from the ophiolite.

Table 1-2: Published works and theses concerning mineralization in the Betts Cove ophiolite

Year	Author(s)	Subject
1881	Murray and Howley	Description of Murray's 1864 regional survey and his visits to the Betts Cove and Tilt Cove deposits in 1865, 1867 and 1875.
1918	Murray and Howley	Howley reported on progress at the Betts Cove and Tilt Cove mines.
1923	Sampson	Paper on ferruginous chert formations of Notre Dame Bay.
1931	Snelgrove	Ph.D thesis on geology and ore deposits at Betts Cove and Tilt Cove.
1940	Douglas <u>et al.</u>	Description of Newfoundland copper deposits.
1947	Baird	Ph.D thesis on Betts Cove and Tilt Cove deposits.
1948	Baird	Paper on copper deposits in the Betts Cove - Stocking Harbour district.
1959	Donoghue <u>et al.</u>	Description of mining operations at Tilt Cove.
1964	Papezik	Paper on nickel minerals at Tilt Cove.
1967	Craig	B.Sc. thesis on East Mine, Tilt Cove.
1973	Upadhyay and Strong	Proposed genetic model for Betts Cove deposit.
1978	Dean	M.Sc. thesis on stratigraphy and metallogeny of Notre Dame Bay.
1981	Squires	B.Sc. thesis on Tilt Cove deposit.
1983	Saunders	Paper describing results of mapping in area of Betts Cove deposit.

**Table 1-3: Private reports on mineralization in the
Betts Cove ophiolite**

Year	Author(s)	Subject
1899	Bainbridge, Seymour and Co.	Report to Reid Newfoundland Co. on the Betts Cove copper mine.
1929	Snelgrove	Report to Norseman Co. on Betts Cove deposit.
1953	Hudson	Falconbridge Nickel Mines Ltd. diamond drill logs, Betts Big Pond area (no locations in report).
1954	Baragar	Report to Falconbridge Nickel Mines Ltd. on the Betts Big Pond showing.
1955	Carrigan	Advocate Mines diamond drill logs, Betts Cove Mine.
1956	O'Toole	Advocate Mines diamond drill logs, Mt. Misery showing.
1958	Bichan	Report to Maritime Mining on Tilt Cove.
1963	James <u>et al.</u>	Report on Maritime Mining property at Tilt Cove.
1975	Riccio	Report to Phillips Management on mineral potential in area.
1974	Upadhyay	Report to Consolidated Morrison on mineral potential in the ophiolite.
1980	Strong	Report to Newmont Mining Canada Ltd. on Tilt Cove area.
1982	Kusmirski and Norman	Report to Newmont Mining Canada Ltd. on Tilt Cove area.

As well there are numerous Tilt Cove Mine drill logs on file at the
Mines Branch of the Newfoundland Department of Mines and Energy.

1.4. Regional Geology

Williams (1976) divided the island of Newfoundland into four tectonic subdivisions; from west to east they are the Humber, Dunnage, Gander and Avalon Zones. The central Dunnage Zone is a largely volcanic terrane containing many ophiolitic remnants of an ancient ocean which are overlain by island arc sequences. It is sandwiched between the Humber and Gander Zones which are two continental margins of dominantly carbonate and clastic character respectively. The fourth zone, the Avalon, is a Precambrian-Cambrian platform of disputed origin which is separated from the Gander Zone by a major structural break. The Burlington Peninsula straddles the Baie Verte-Brompton Line which represents the junction between the Humber and Dunnage Zones (Williams and St. Julien, 1978).

Hibbard (1983) has produced a memoir on the geology of the entire peninsula and DeGrace et al. (1976) have described the geology of the Nippers Harbour map sheet (2E/13). Their works are heavily relied on here.

Hibbard (1983) has informally termed that part of the peninsula to the east of the Baie Verte-Brompton Line as the Baie Verte Belt. It contains three ophiolitic units which can be separated on the basis of geographical distribution and structural history, namely the Advocate, Point Rouse and Betts Cove Complexes. A fourth unit, the Pacquet Harbour Group, has characteristics of both ophiolitic and island arc volcanics. The Lushs Bight Group on the nearby Springdale Peninsula is a sequence of ophiolitic pillow lavas and sheeted dykes. The ophiolites are overlain conformably and unconformably by later volcanic cover sequences and are cut by later intrusions. Distribution of these units is shown in Fig. 1-1.

The Betts Cove Ophiolite occupies an arcuate belt stretching from Tilt Cove in the north to Betts Cove in the south (Figs. 1-1 and 1-2). The Nippers Harbour Group to the south was recognized as an ophiolite suite by Schroeter (1971) and is

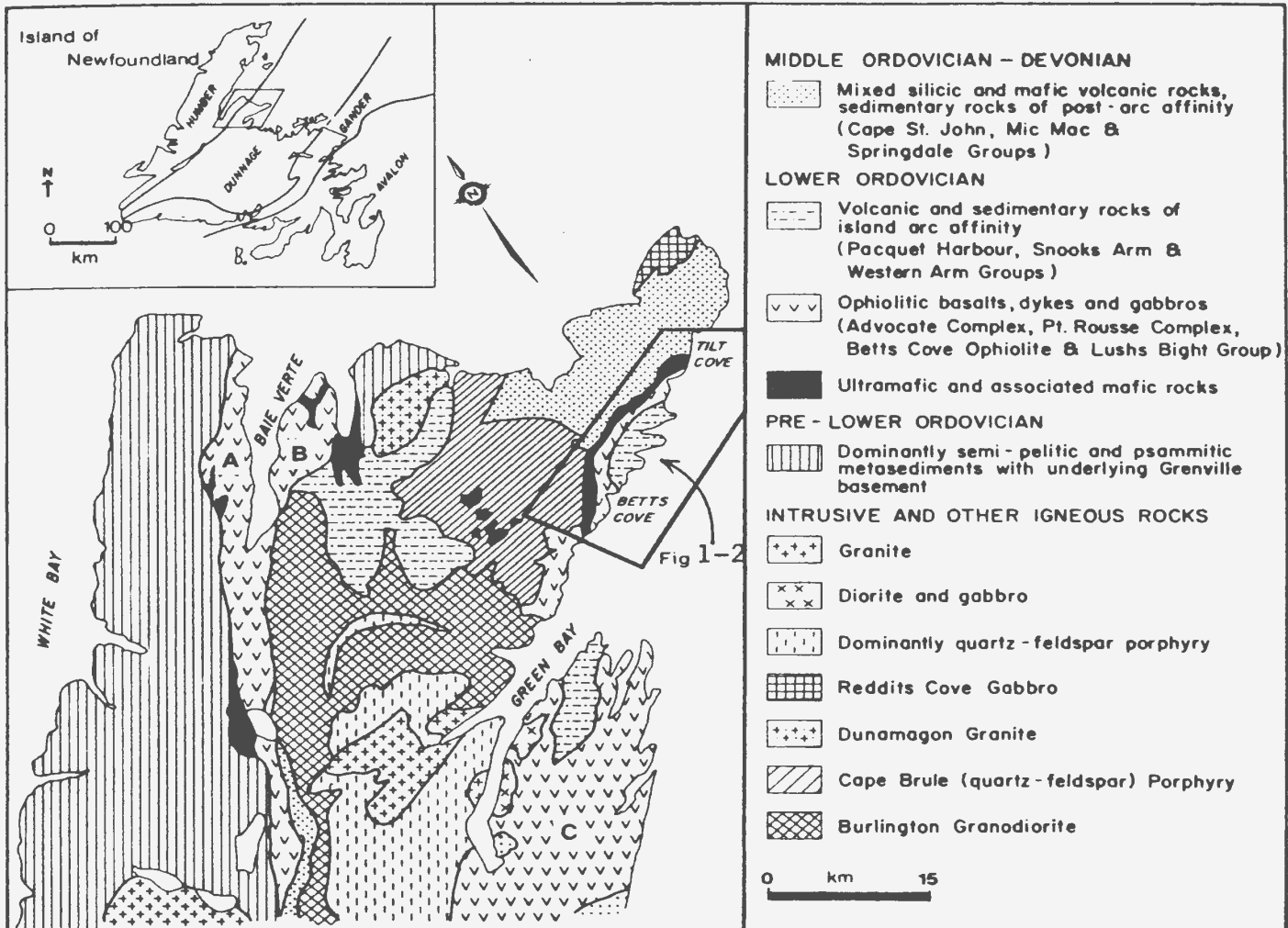


Figure 1-1: General geology of the Burlington Peninsula

From Strong (1984) - simplified from DeGrace *et al.* (1976) and Hibbard (1983); A - Advocate Complex, B - Point Rouse Complex, C - Lushs Bight Group

an extension of the Betts Cove Ophiolite (DeGrace et al., 1976). The Betts Cove Ophiolite is composed of, from top to bottom, an ultramafic, a gabbroic, a sheeted dyke and a pillow lava unit (Figs. 1-2 and 1-3). It is conformably overlain by a sequence of mafic volcanic, volcanoclastic, and sedimentary rocks. The ophiolite and these overlying units were named the Snooks Arm Group by Snelgrove (1931). Snelgrove (1931) found Arenigian graptolites in the Snooks Arm Group sediments which overlie the ophiolitic rocks. Dunning (1984) obtained a U/Pb-zircon date of $488.6 \pm 3.1/-1.8$ Ma for the gabbro member of the ophiolite in the Tilt Cove area.

Further description of the internal stratigraphy of the ophiolite and the conformably overlying units is given in section 1.5.

For much of its length the ophiolite is faulted against or unconformably overlain (Neale, 1957; Neale et al., 1975; DeGrace et al., 1976) by the Silurian Cape St. John Group. This group is a subaerial sequence of conglomerates, sandstones, basic pyroclastics and flows, and assorted andesitic to rhyolitic tuffs, breccias, agglomerates and ignimbrites (DeGrace et al., 1976). The conglomerates, sandstones and pyroclastics contain detrital chromite and fragments of ultramafic rock (DeGrace et al., 1976) which were derived from the ophiolite.

The Ordovician Burlington Granodiorite, which intrudes the Nippers Harbour Ophiolite, is a medium to coarse-grained multi-phase pluton. The different phases are hornblende and biotite granite, granodiorite and quartz diorite (DeGrace et al., 1976). Various geochronological methods have yielded ages which cluster about three different dates- 460, 410 and 345 Ma (Hibbard, 1983). The oldest of these is interpreted as the age of emplacement of the granodiorite; the other two are interpreted to be the result of slow cooling of the body and of an Acadian thermal event respectively (Hibbard, 1983). Mattinson (1975) produced a U/Pb-zircon date of 463 ± 6 Ma on a dyke which cuts the Nippers Harbour Ophiolite. This dyke is believed to be related to the Burlington Granodiorite (D. F. Strong, pers. comm. to G. Dunning 1980; Epstein, 1983).

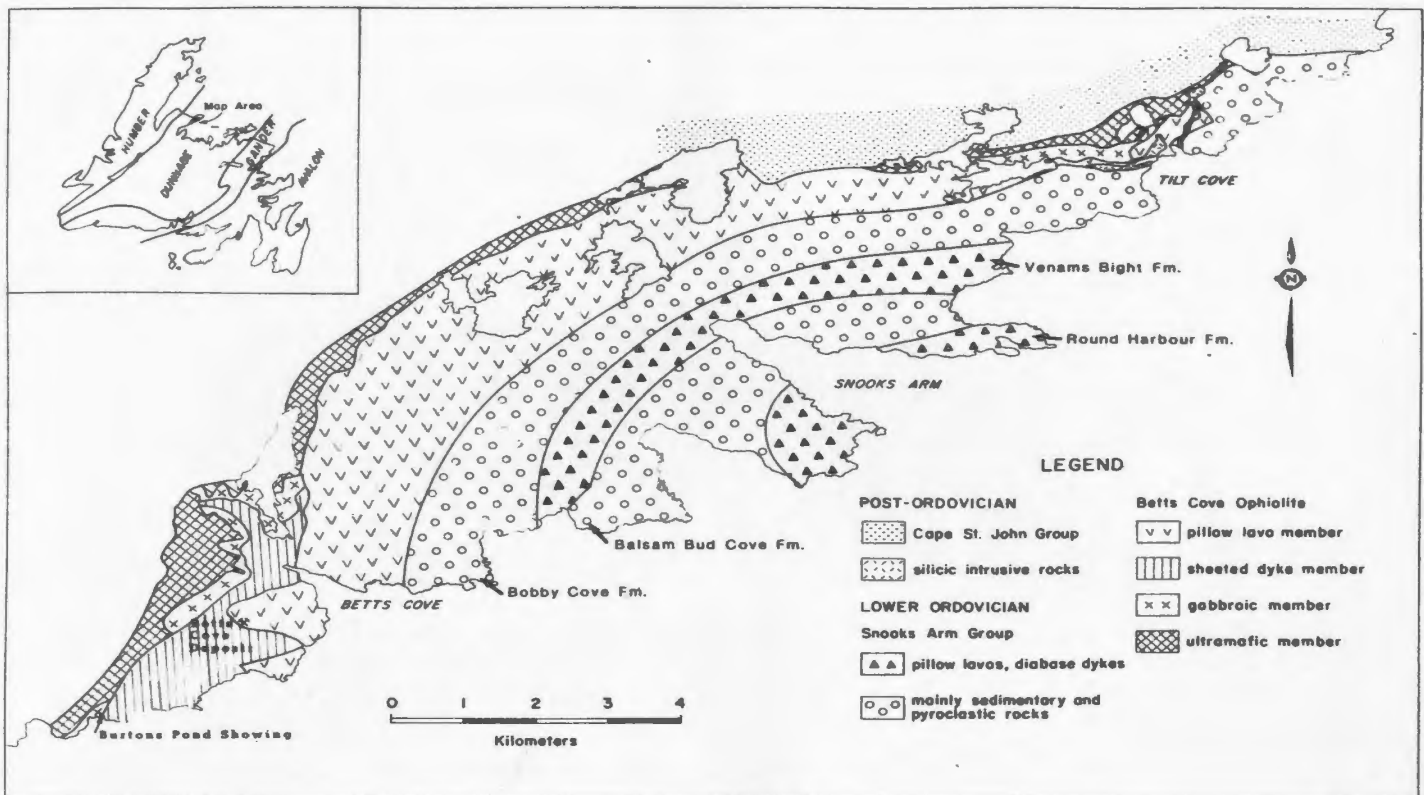


Figure 1-2: Geology of the Betts Cove - Tilt Cove area

From Strong (1984) - after Upadhyay (1973)

The Cape Brule Porphyry is a Late Silurian to Early Devonian (Hibbard, 1983) extremely heterogenous high-level pluton (DeGrace *et al.*, 1976). It consists of two main units: a finer-grained porphyry with a felsic matrix, and a coarse-grained unit with a matrix rich in mafic minerals. Riccio (1972) and Upadhyay (1973) referred to that part of the pluton near Burtons Pond as the Burtons Pond Porphyry, and they demonstrated that it intrudes the Betts Cove and Nippers Harbour Ophiolites. It contains many inclusions of the ophiolitic rocks and the Cape St. John Group which range from about 1 cm to roof pendants hundreds of metres across (DeGrace *et al.*, 1976). Of three age dates determined for the porphyry, Hibbard (1983) considered the Rb/Sr whole rock age of 404 +/- 25 Ma (Bell and Blenkinsop, 1977) to be the most consistent with stratigraphic relationships.

1.5. General Description of the Ophiolite and Snooks Arm Group

The Snooks Arm Group was originally defined (Snelgrove, 1931) to include the units now known as the Bobby Cove, Venams Bight, Balsam Bud Cove, and Round Harbour Formations plus the gabbroic, sheeted dyke, and pillow lava members of the Betts Cove Ophiolite. The ultramafic member was considered to be an intrusion and hence was not included. Church and Stevens (1971) and Upadhyay *et al.* (1971) recognized the ultramafic, gabbroic, and sheeted dyke units and the lowermost pillow lava unit as members of an ophiolite suite which formed the base of the Snooks Arm Group. Hibbard (1983) has recently proposed that the term Snooks Arm Group be restricted to the four units which overlie the ophiolite and that the Betts Cove and Nippers Harbour Ophiolites be together known as the Betts Cove Complex. In this thesis, for convenience, the terms Betts Cove Ophiolite and Nippers Harbour Ophiolite are used to distinguish between the ophiolites of the two areas.

1.5.1. The Betts Cove Complex

The Betts Cove Ophiolite has most recently been mapped in its entirety by Upadhyay (1973). Riccio (1972) mapped that part extending from Burtons Pond to Betts Big Pond; Coish (1977b) sampled the same area and essentially relied on the mapping of Upadhyay and Riccio. The Nippers Harbour Ophiolite was mapped by Schroeter (1971) and DeGrace *et al.* (1976).

The Betts Cove Ophiolite contains the four characteristic members of an ophiolite: an ultramafic, a gabbroic, a sheeted dyke and a pillow lava unit. The entire sequence is best exposed and least disturbed at Betts Cove.

Upadhyay (1973) pointed out some broad differences in the character of the ophiolite at Betts Cove and Tilt Cove: (1) at Betts Cove the ophiolite is about 3000 m thick and dips about 45 degrees SE but at Tilt Cove it narrows to about 750 m and dips sub-vertically; (2) in the Tilt Cove area the ophiolite is more highly faulted; (2) at Tilt Cove the sheeted dyke member is largely represented by dyke breccia.

The Nippers Harbour Ophiolite consists mainly of gabbro and sheeted dykes. Ultramafic rocks occur as scattered outcrops, and pillow lavas are rare.

The following descriptions are concerned mainly with the Betts Cove Ophiolite.

1.5.1.1. The Ultramafic Member

The ultramafic member is exposed throughout the length of the belt. At Betts Cove it is overlain by the gabbroic member but for much of the belt it is in fault contact with the pillow lava member. Upadhyay (1973) considered the gabbroic and sheeted dyke members to have been faulted out. Although Strong (1980) prefers this interpretation, he has suggested the possibility that they may never have been present, i.e. that the lavas could have been deposited onto ultramafic rocks that were exposed on the seafloor by faulting.

The ultramafic member is best exposed in the Kitty pond area where it reaches a maximum thickness of 750 m (Upadhyay, 1973). Here, compositional layering is well developed and primary textures are best preserved. The dip of the layering varies between 20 and 75 degrees; it changes abruptly in some areas (Upadhyay, 1973). The full range of ultramafic rock types is represented by the alternating layers, including dunite, harzburgite, orthopyroxenite, websterite, wehrlite, clinopyroxenite and lherzolite (Ricchio, 1972; Upadhyay, 1973). Upadhyay (1973) describes pegmatitic clinopyroxenite dykes which cut the ultramafic member.

The portion of the ultramafic member stretching from Betts Big Pond to Tilt Cove is largely altered to serpentinite and talc-carbonate rock. The only relatively fresh ultramafic rock exposed near Tilt Cove is a coarse-grained clinopyroxenite which occurs near the top of the member (Upadhyay, 1973).

1.5.1.2. The Gabbroic Member

The gabbroic member is best developed at Betts Cove where it is in fault contact with the ultramafic and sheeted dyke members. It does in places have a gradational contact with the sheeted dyke member (see chapter 2). At its base the gabbroic member consists of interlayered clinopyroxenite and gabbro. Upadhyay (1973) interpreted this as a gradational contact between the ultramafic and gabbroic members. Ricchio (1972) described this interlayered sequence as the "lower member of the Mafic Zone". Both geologists observed ultramafic xenoliths within this unit. Ricchio (1972) cited the xenoliths and the pegmatitic clinopyroxenite dykes (see paragraph 1.5.1.1) as evidence for intrusion of the gabbroic member into the ultramafic member. The proportion of clinopyroxenite bands decreases upwards from 50 % near the base (Ricchio, 1972) to nil near the top of the member (Upadhyay, 1973).

The gabbroic member is absent from most of the inland portion of the belt but reappears in the Long Pond area. Its maximum thickness is about 330 m in the Betts Cove area (Upadhyay, 1973).

1.5.1.3. The Sheeted Dyke Member

The sheeted dyke member is best developed in the Betts Cove area where the dykes trend generally east-west and dip vertically to sub-vertically. It varies in thickness from about 400 to 1600 m (Upadhyay, 1973). The contacts between the sheeted dyke member and the gabbro and pillow lava members are commonly sharp or faulted, but in places gradational relationships do exist (see chapter 2). The trend of the dykes is generally perpendicular to the strike of the pillow lavas, but Upadhyay (1973) reported that in places the dykes become irregularly oriented as they approach the contact with the pillow lava member and finally assume the attitude of sills.

The sheeted dyke member is represented at Tilt Cove mainly by dyke breccia (Upadhyay, 1973) which at Betts Cove forms a minor part of the member.

1.5.1.4. The Pillow Lava Member

The pillow lava member is the most extensive unit of the ophiolite; it outcrops from Betts Cove to Tilt Cove and varies in thickness from 1500 to 40 m (Upadhyay, 1973). A 60 m wide argillite unit occurs throughout much of the inland portion of the pillow lava unit (Upadhyay, 1973). The contacts between the pillow lava member and the other members have been discussed above and in chapter 2. Upadhyay (1973, 1978, 1982) has described ultramafic and komatiitic pillows from the Betts Cove area. Strong (1980) has mapped ultramafic pillow lavas at Tilt Cove. The pillow lavas are described more extensively in chapter 2; their chemistry is discussed in chapter 3.

1.5.2. The Snooks Arm Group

The Snooks Arm Group as redefined by Hibbard (1983) is made up of four members. From bottom to top they are: the Bobby Cove Formation, the Venams Bight Formation, the Balsam Bud Cove Formation and the Round Harbour Formation (Figs. 1-3 and 1-2). The Bobby Cove and Balsam Bud Cove Formations are similar and are dominantly sedimentary. The Venams Bight and

Round Harbour Formations are dominantly basaltic. The ophiolitic pillow lava unit passes conformably upward into the Bobby Cove Formation. The following descriptions are summarized from Upadhyay (1973); maximum stratigraphic thicknesses are given in Fig. 1-3.

1.5.2.1. The Bobby Cove and Balsam Bud Cove Formations

The Bobby Cove and Balsam Bud Cove Formations are composed mainly of sediments and volcanoclastic rocks, including argillites, greywackes, cherts, agglomerates and tuffs. Agglomerate and tuff are more volumetrically important in the Bobby Cove Formation. The agglomerate clasts, which range from a few centimetres to half a metre across are predominantly andesite; other lithologies include gabbro, foliated amphibolite, pyroxenite and hornblendite. The agglomerate grades into poorly sorted, bedded tuff which in turn grades into andesitic flysch. Greywacke units are a few centimetres to several metres thick and are generally associated with argillite. Chert and argillite occur as thinly bedded units which alternate to form green, red, grey and buff ribboned sediments. Pillow lavas and diabase sills are important constituents of both formations. Pillow lava units, which vary in thickness from a few metres to a few tens of metres, occur at several levels. Individual sills may reach a thickness of 200 m and locally make up over 50 % of the stratigraphic column. Conglomerate forms a minor portion of the Snooks Arm Group.

1.5.2.2. The Venams Bight and Round Harbour Formations

These two formations are composed mainly of pillow lavas and sills with minor pillow breccia. Metamorphic grade is lower in the Round Harbour Formation (zeolite facies); this is reflected in the darker colour of its basalts. Pillow lava interstices are filled with chert. The dip of the Round Harbour Formation is relatively shallow (as low as 25 to 30 degrees). Sills form about 25 to 40 % of the Venams Bight and Round Harbour Formations. In places, they are "sheeted"; locally, pillow screens occur. Earlier sills may be split by later ones. Pillow breccia consists of complete and partial pillows commonly set in a chert or jasper matrix.

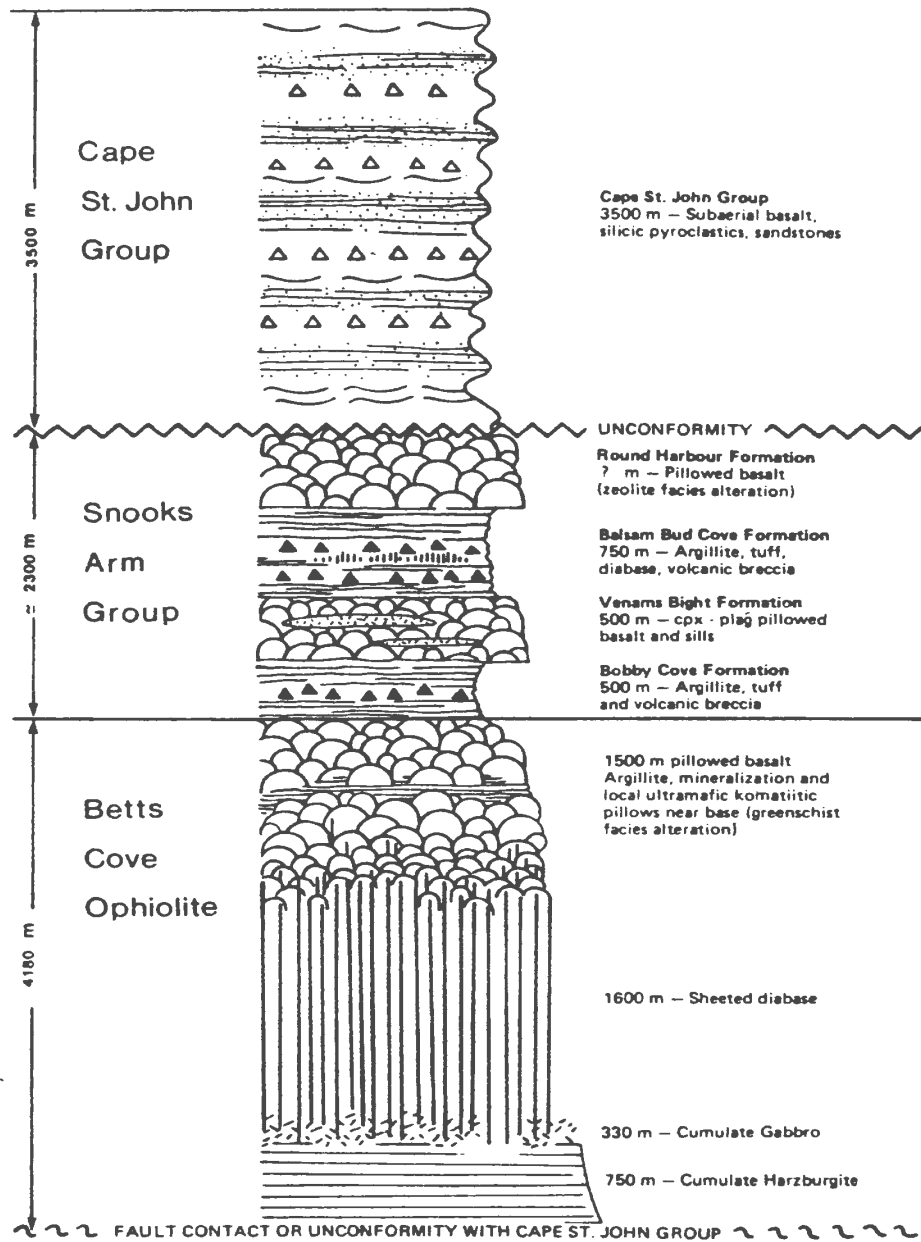


Figure 1-3: Stratigraphic section for Betts Cove - Tilt Cove area
From Strong (1984); data from Upadhyay (1973). Given thicknesses are maxima.

1.6. Mineralization in the Betts Cove Ophiolite

The Betts Cove mine was in operation from 1875 to 1885 and produced about 130,000 tons of hand-picked ore believed to average about 10 % Cu (Snelgrove and Baird, 1953). The mine was closed due to a cave-in and the grade or quantity of any remaining mineralization is not known. In the early 1900's, several unsuccessful attempts were made to reopen the mine. Little is now known about the shape or attitude of the mineralization. Martin (1983) has provided a fascinating account of the colourful history of the mine and the people who operated it. For the life of the mine Betts Cove was a thriving community of more than 3000 people with its own church, school, hospital and even its own currency.

The mineralization at Betts Cove (both the main and peripheral showings) is concentrated near the sheeted dyke-pillow lava contact. It occurs as massive lenses, stringers and disseminations characterized by chloritic shear zones (Upadhyay and Strong, 1973). Mineralization in the pillow lavas is concentrated in the pillow interstices but is also disseminated throughout the pillows. Locally, deformation has resulted in a sulphide-rich matrix surrounding pillow structures (Upadhyay and Strong, 1973). Most of the outcropping mineralization consists of disseminated and stringer pyrite and chalcopyrite. The only significant outcrop of massive sulphide is composed of relatively pure pyrite, but many massive sulphide samples from the dumps contain abundant chalcopyrite and/or sphalerite. Much of the massive sulphide is strongly banded. The significance of the banding and of the shear zones is discussed in chapter 4.

Tilt Cove in particular has had a long and profitable though sporadic mining history. The Tilt Cove mine was operated from 1864 to 1917 and was reopened in 1957 for ten years. About 9 million tons of ore was removed over the life of the mine. During the early years of production the grade of the ore was about 4 to 12 % Cu; in the 1960's it was only about 2 %. About 42,000 ounces of gold was produced during the later episode of mining (DeGrace et al. 1976). Gold

production statistics for the early mining period are not known but Howley in 1909 reported that the average grade was 1.5 dwts (2.3 ppm) and that production was "known to have reached in some years from 3000 to 5000 ounces" (Murray and Howley, 1918).

At Tilt Cove the mineralization is located in the pillow lava horizon. The sheeted dykes and gabbros are almost completely absent from the area around the mine due to the presence of numerous faults. The sheeted dyke unit is represented in places by dyke breccia. The host rocks are chloritized, sheared and brecciated pillow lavas and agglomerates (Upadhyay, 1973). Mineralization occurs as massive, fine-grained, steeply dipping pyrite-chalcopyrite bodies and in stringers and disseminations of pyrite and chalcopyrite. Subordinate minerals include magnetite, sphalerite, pyrrhotite, native silver and gold. Specular hematite and limonite are found along faults (Upadhyay 1973). Squires (1981) attributed the formation of hematite to a later oxidizing event.

From 1869 to 1876 a total of 411 tons of high-grade nickel ore was produced from Tilt Cove (Snelgrove, 1931; Papezik, 1964). The nickel mineralization occurs in two forms. The first-mined nickel ore consisted of nickel sulphides and arsenides in a talc-carbonate zone located at the contact between chloritized "andesite" and serpentized peridotite. During the second period of mining nickel arsenides in carbonate gangue were found in several narrow fractures (Papezik, 1964- pers. comm. from A. Wilson, 1963). The nickel was remobilized from the peridotite, transported a short distance and deposited in fractures (Papezik, 1964).

1.7. Cyprus Type Deposits

Pyrite-chalcopyrite deposits in ophiolites have become known as Cyprus Type Deposits because the Troodos ophiolite and associated deposits are the best known and perhaps least altered of any in the world. Since the advent of plate tectonics the theory that these deposits formed at ocean floor spreading centers has become

widely accepted. Most early ideas held that the Troodos massif and its ore deposits formed at a mid-ocean ridge but in the past several years various authors led by Miyashiro (1973) have suggested that the setting was most probably that of an island arc or a marginal ocean basin. These ideas are reviewed more completely in chapter 3 and by Gass (1980).

The Troodos ore deposits have been described by Hutchinson and Searle (1971), Searle (1972), Constantinou (1972, 1976, 1980), Constantinou and Govett (1972, 1973) and Clarke (1971). Spooner and Fyfe (1973), Spooner (1977) and Parmentier and Spooner (1978) have made important contributions to understanding the genesis of the deposits.

The Troodos Massif contains a large number of these deposits; they occur in groups of four or more in each of five mining districts (Constantinou, 1980). They range in size from about 50,000 to 20,000 tonnes with grades of less than 0.5 % to more than 4.5 % Cu (Constantinou, 1980). Sphalerite is an important constituent of some deposits.

Fig. 1-4 (Hutchinson and Searle, 1971) is a schematic section through a typical Troodos sulphide deposit. The deposits typically consist of a lensoid massive sulphide body and an underlying stockwork or stringer zone. Some deposits are capped by ochre, an iron oxide-rich chert believed to be the result of submarine weathering of the sulphides (Constantinou, 1976).

The ochre contains thin layers of massive porous sandy pyrite, boulders of compact banded pyrite and disseminated pyrite grains with fine graded bedding. The pyrite boulders increase in size and number towards the massive sulphide zone (Searle, 1972).

The massive ore consists of two main types. The most common ore type is a conglomeratic ore made up of angular, spheroidal or pillow-shaped blocks of sulphide in a matrix of sandy, friable and porous sulphides. The ore contains

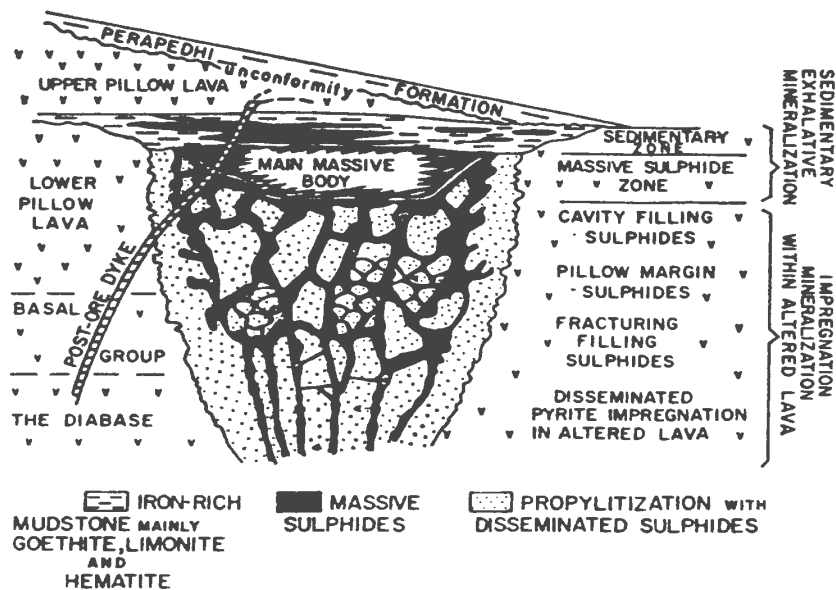


Figure 1-4: Diagrammatic section through a typical Cyprus sulphide deposit

from Hutchinson and Searle (1971)

interstitial Cu sulphides, sphalerite and quartz, and is characterized by colloform banding. The blocks of sulphide increase in size downwards and may pass into a compact ore consisting of large blocks of sulphide separated by fractures containing sandy friable ore or chalcopyrite with covellite coatings (Constantinou and Govett, 1973; Constantinou, 1980). The major mineral is pyrite and it is associated with chalcopyrite and sphalerite. Marcasite is common to rare. Other minerals include rare pyrrhotite and variable amounts of covellite, digenite, bornite and chalcocite (Constantinou, 1980).

The massive ore may be underlain by a relatively thin siliceous ore zone. Pyrite in this zone is commonly corroded and replaced by silica. Chalcopyrite and sphalerite occur in variable amounts. The sulphides are mixed with quartz and jasper (Constantinou and Govett, 1973; Constantinou 1976; 1980).

The lowermost zone is the stockwork zone. Constantinou (1980) described the

mineralogical and textural characteristics of this zone. The sulphides occur, with or without silica (quartz or chalcedony), as a breccia cement or as fillings of fractures in the basalt. The number of sulphide veins increases towards the top of the zone. Pyrite is the most common sulphide and where it occurs with quartz or chalcedony, it is intensely corroded and partially replaced by these minerals. Disseminated pyrite is found throughout the stockwork zone lavas, but chalcopyrite and sphalerite are confined to fractures, veins and vesicles. Original igneous textures are preserved, but quartz replaces and pseudomorphs plagioclase and pyroxene. The glassy matrix is altered to chalcedony, chlorite and commonly illite. Constantinou (1980) reported that analyses of hydrothermally altered lavas by X-ray diffraction revealed that: (a) quartz predominates in all samples, followed by pyrite and chlorite; (b) pyrite and chlorite abundances are negatively correlated; (c) minor illite was found in all samples and other clays were found at individual orebodies. The contacts between the ore veins and the host lavas is sharp with no evidence of replacement of lavas by sulphides. The stockwork zone is the root of the deposit and represents the feeder zone for the mineralization. The chemical signature of this zone as outlined by Constantinou (1980) is described in chapter 4.

Genetic models for the formation of these deposits have been presented by Sillitoe (1972), Spooner and Fyfe (1973), Upadhyay and Strong (1973), Andrews and Fyfe (1976), Fryer and Hutchinson (1976), Spooner (1977) and Parmentier and Spooner (1978). The orebodies are interpreted as the products of seawater circulation through the ocean crust, when heat generated at an ocean spreading center sets up convection cells. Cold seawater is drawn down into the crust and becomes heated by sub-ridge magma chambers. It is then forced up along fractures and permeable zones from which it debouches onto the seafloor. As it circulates through the crust it exchanges chemical components with the rock and the composition of both rock and water are significantly altered. One result of this exchange is that the seawater picks up significant quantities of metals which are deposited as sulphides onto the seafloor (the massive sulphide zone) and in the

immediately underlying conduit (the stockwork zone). The metals are believed to be derived from the rock column, but some authors don't discount the possibility that there may be some magmatic input.

1.8. Experimental Work

The experimental work of Bischoff and Dickson (1975) and Hajash (1975) showed that upon reaction with basaltic rock or glass seawater changes from an oxygenated slightly alkaline Na-Mg-SO₄-Cl solution to a reducing, acidic, metal-bearing Na-Ca-Cl solution. Magnesium is removed from seawater and incorporated into secondary alteration minerals. This exchange is accompanied by consumption of OH⁻; consequently H⁺ is left behind and pH is lowered. This enhances metal solubility and the metals are leached from the rock into the seawater. In a natural sub-seafloor circulation system this results in the metals being brought to the seafloor by convectively rising hydrothermal fluids. The findings of the experiments are discussed in depth in chapter 4 and the application of the results to natural systems (especially the Betts Cove deposit) are elaborated upon there.

1.9. Modern Sub-sea Hydrothermal Systems

For several years before their discovery the existence of active convecting hydrothermal systems at ocean spreading ridges had been predicted from thermal constraints (e.g. Elder, 1965; 1977; Lister, 1974) and from the study of ore deposits (e.g. Spooner and Fyfe, 1973; Andrews and Fyfe, 1976; Fryer and Hutchinson, 1976; Spooner, 1977; Parmentier and Spooner, 1978).

Even stronger evidence lay in the discoveries of metalliferous deposits on the seafloor. Bostrom and Peterson (1966) had discovered metalliferous sediments on the East Pacific Rise which they attributed to hydrothermal activity. Scott et al. (1974) described rapidly accumulating manganese deposits from the Mid-Atlantic Ridge; Moore and Vogt (1976) reported discovery of hydrothermal manganese crusts from the Galapagos area.

In the Red Sea, which represents very early seafloor spreading, iron-zinc mineralization is being precipitated from very saline brine pools (Degens and Ross, 1969; Bischoff, 1969). In the Salton Sea saline brines were discovered permeating deltaic sediments of the Colorado River (White et al., 1963).

In the mid-seventies several research groups were involved in exploration for active hydrothermal vents at mature spreading ridges in the deep ocean basin. Early searches were conducted using inadequate remote sensing devices. The first break came when a thermal anomaly which seemed to indicate hydrothermal activity was recorded over the Galapagos ridge (Williams et al., 1974). This was followed in 1977 by the first successful sampling of hydrothermal waters (Weiss et al. 1977). The sampled fluids had been extremely diluted by seawater and the resulting temperature anomaly was only $+0.1^{\circ}\text{C}$, but it was enough to record anomalous concentrations of Mn, Ba, Mg, Ca ^{222}Rn and ^3He . The latter isotope is a particularly strong indicator of hydrothermal activity because it is derived from the mantle (Craig et al. 1975).

In 1977, J. B. Corliss and J. M. Edmond, using the submersible Alvin, made the first visual observations of hydrothermal activity at the Galapagos spreading ridge (Corliss et al., 1979; Edmond and Von Damm, 1983). Four separate fields were discovered. Each is about 50 metres across and contains many individual vents. The vent solutions had produced a thin coating of Mn oxide on the surrounding pillow lavas. The hottest temperature recorded was 17°C which is 15°C above the background temperature. Edmond et al. (1979a) attributed the slightness of the thermal anomaly to sub-surface mixing of a hot end-member solution with cold seawater. They were able to determine the temperature of the end-member by assuming that it is devoid of Mg^{2+} and SO_4^{2-} as predicted by the experimental work of Bischoff and Dickson (1975). The temperature of the hydrothermal fluids could then be estimated by extrapolation of the seawater-vent water mixing lines to a zero concentration. Extrapolation of the mixing lines for these two species gave temperatures of 344°C and 380°C respectively.

In 1978 the CYAMEX research team discovered massive Fe-Zn sulphide mounds at 21°N on the East Pacific Rise (Francheteau *et al.*, 1979). Follow-up exploration, aided by the highly visible biological population, led to the discovery and sampling, in 1979, of hot end-member solutions (Speiss *et al.*, 1980). These solutions are currently venting onto the seafloor where mixing with cold alkaline seawater brings about immediate precipitation of fine particulate sulphide which resembles black smoke. They have therefore become known as "black smokers". As predicted the temperature of the solutions is 350°C and they are devoid of Mg^{2+} and SO_4^{2-} .

Edmond *et al.* (1979b) have proposed that differing degrees of sub-surface mixing of hot end-member solutions with cold seawater-like groundwater is responsible for the spectrum of metalliferous deposits found on the seafloor. If the hydrothermal fluids are diluted by cold groundwater in the sub-surface much of the sulphide-forming metals will precipitate in the conduit and the exhaling solution will produce MnO_2 deposits. If the conduit walls have become lined with impermeable minerals during initial precipitation the end-member may arrive at the seafloor with little dilution and will form sulphide-rich deposits. There exists a gradation between the two types. The East Pacific Rise solutions are of the latter type, and the Galapagos solutions border between pure Mn and Mn-Fe bearing (Edmond *et al.*, 1979b; Edmond, 1980).

Since these initial discoveries other active and inactive hydrothermal sites have been discovered. Rona (1984) has summarized knowledge to date and has compiled data on over 60 subsea metalliferous occurrences.

The chemistry of the solutions and the mineralogy of the sulphide mounds is discussed in more detail in chapter 4.

1.10. Summary

The Betts Cove Complex is a Lower Ordovician ophiolite suite, in which the four main constituents of an ophiolite, the ultramafic, gabbroic, sheeted dyke and pillow lava members, are represented. Individual members may be locally absent, but the complete sequence is exposed in the Betts Cove-Kitty Pond area. The ophiolite is conformably overlain by the Snooks Arm Group, a package of interbedded pillow basalts, sills and sediments. It is unconformably overlain by and in fault contact with the Silurian Cape St. John Group, and is intruded by the Burlington Granodiorite and the Cape Brule Porphyry.

Massive pyrite - chalcopyrite - sphalerite deposits are located near the pillow lava-sheeted dyke interface in the Betts Cove and Tilt Cove areas. These deposits are very similar to those found in other ophiolites and can be compared to the well-studied Troodos deposits. Insight into their origin can be derived from results of experimental studies and from comparison with modern sub-sea hydrothermal systems. Ideas about the genesis of the Betts Cove deposit which were gained from the literature on ore deposits, experiments and modern hydrothermal systems are discussed in chapter 4.

Chapter 2

FIELD OBSERVATIONS AND PETROGRAPHY

2.1. Introduction

The general geology of the ophiolite and its contact-relationships with surrounding units is described in chapter 1. This chapter includes the field observations and petrography for this study supplemented, where necessary, with those of previous workers especially Riccio (1972), Upadhyay (1973) and Coish (1977a,b). Only the upper three members of the ophiolite are represented in the map-area. Field descriptions and petrography of the mineralization and related alteration are presented in Chapter 4.

2.2. Gabbroic Rocks

This section contains descriptions of all the gabbroic rocks in the map-area, including pods of gabbro that outcrop high in the sheeted dyke unit.

The largest mass of gabbro in the area outcrops to the northwest of Joey's Pond where it is faulted in part against sheeted dykes. At its northeast end it does have a gradational contact with the sheeted dyke unit (Fig. 2-1), where screens of banded gabbro are found between the dykes. This gabbro, which was not sampled or mapped in detail, consists of approximately equal amounts of plagioclase and mafic minerals and minor quartz. Grain size averages 1 to 2 mm.

Numerous screens and several large pods of gabbro occur within the sheeted dykes to the west and south of the mine area. The largest pods outcrop west of

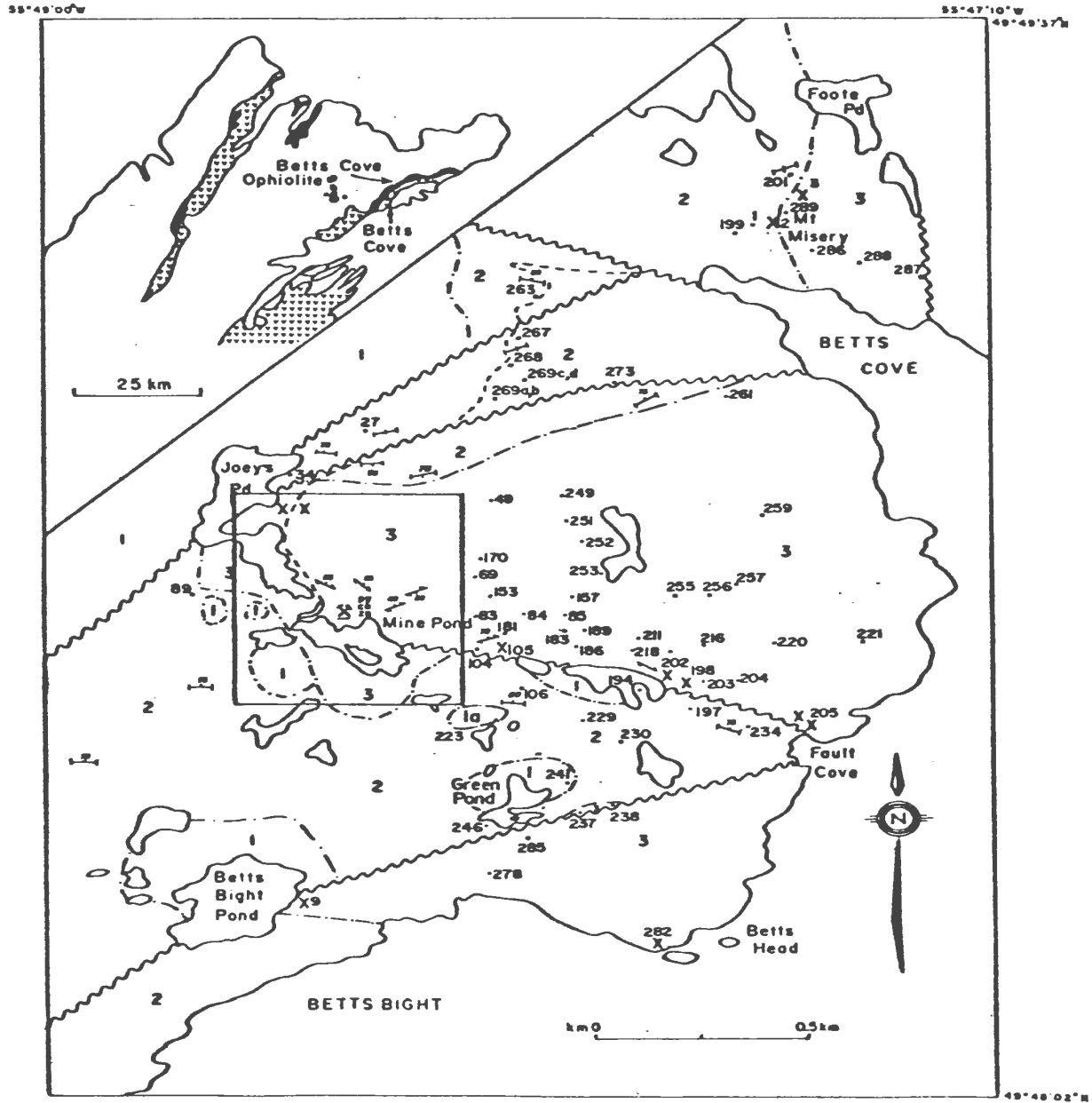
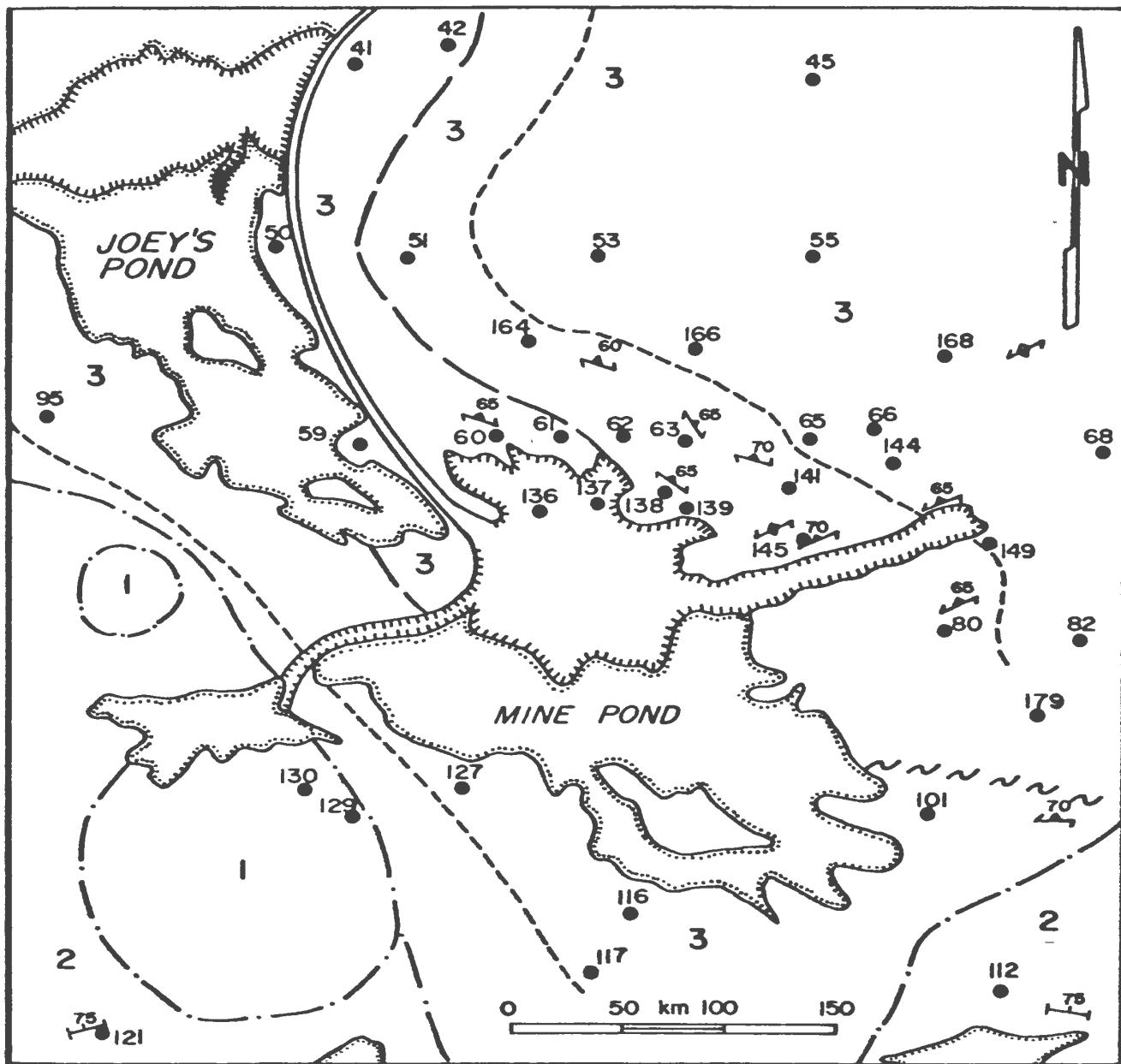


Figure 2-1: Geology and sample locations - Betts Cove area
 (1) gabbro; (1a) plagiogranite; (2) sheeted dyke unit; (3) pillow lava unit;
 X - sulphide showing; \longrightarrow trend of dykes; \longleftrightarrow chloritic shear zone;
 - · - · geological contact; ---- trail; · sample location; area in box is shown in more detail in Fig. 2-2



- Geological contact
- Chlorite-quartz core alteration zone
- - - - - Chlorite-albite-quartz halo alteration zone
- ~~~~~ Dump covered area
- ==== Trail

Figure 2-2: Enlargement of mine area from Fig. 2-1
 Symbols and geological units as in Fig. 2-1

Mine Pond and along the north side of Green Pond. They are cut by dykes which become more numerous towards the edges of the gabbro pods until they become sheeted and gabbro-free. The gabbro mass north of Betts Bight Pond, (Fig. 2-1) mapped by previous workers was not mapped for this study.

Most of the gabbro samples consist of equal parts plagioclase and clinopyroxene (partly or completely altered to actinolite or chlorite), locally with minor quartz. The plagioclase is generally albitized and heavily sericitized or locally altered to a very fine grained brown material. Coish (1977) described a similar alteration of plagioclase which he identified as a paragarnet-like substance. Fig. 2-3a is a photomicrograph of a typical gabbro.

One sample (223a) of a plagiogranite screen within the sheeted dykes consists of plagioclase (now albite), epidote, actinolite and chlorite surrounded by intergrowths of albite and quartz, in places dendritic and radially arranged (Fig. 2-3b).

Evidence suggests that the gabbro pods intruded the sheeted dyke and pillow lava units and were subsequently cut by dykes; e.g. locally, screens of gabbro and pillow lava are in close proximity within the sheeted dyke unit. The only definite intrusive contact was found on the shoreline at Betts Cove. There, a plagiogranite intrudes and is chilled against the sheeted dyke unit. A quartz-poor, calcareous gabbro, mineralogically similar to the pods of gabbro, later intruded the plagiogranite and the sheeted dyke unit and contains xenoliths of both.

2.3. Sheeted Dyke Member

The Sheeted Dyke Member outcrops to the north, west and south of the mine and its host block of pillow lavas (Fig. 2-1). The dykes strike generally east-west and dip steeply north, but their attitude varies locally, especially where there is a high percentage of gabbro screens. The dykes to the northeast of Joey's Pond are mostly sheeted although there are numerous gabbro screens near the gradational

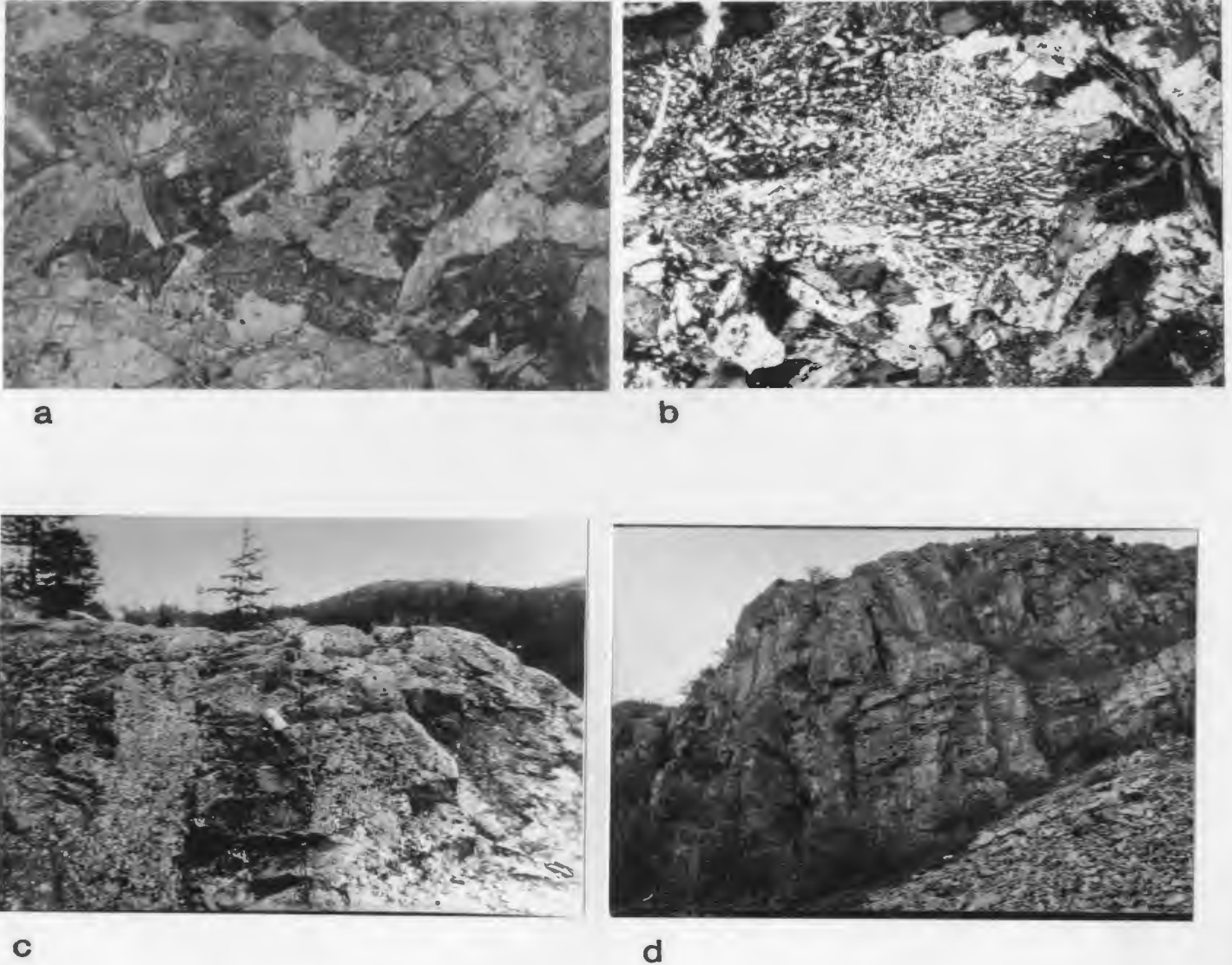


Figure 2-3: Photographs of gabbro and plagiogranite thin-sections and sheeted dyke outcrops

(a) Sample 234, PL, gabbro with subophitic plagioclase-clinopyroxene texture; (b) Sample 223a, XN, plagiogranite with graphic plagioclase-quartz intergrowths, (c,d) Sheeted dykes along Betts Cove Mine trail. Photo widths: (a) 2.7 mm, (b) 2.0 mm. In these and subsequent photomicrographs, PL - plane light; XN - crossed nichols; RL - reflected light.

contact with the gabbro unit. Dykes west of Joey's Pond and south of the Fault Cove Fault contain numerous screens and pods of gabbro. The dykes average 20 to 30 cm in width and weather red, red-brown, grey and green. Fig. 2-3c,d illustrate typical sheeted dykes. The red-weathering dykes are fine grained and may be black on fresh surface but more commonly are olive green. The grey and green weathering dykes are generally fine grained and dark green to black on fresh surface; plagioclase can be distinguished in most. Less common thin, aphanitic, green weathering dykes are also seen. These are commonly chilled against the other dykes which they generally cut at low angles.

A few east-west trending, very fine grained, siliceous dykes cut the pillow lavas north of Fault Cove. These dykes weather white and are pale green on fresh surface. They consist of actinolite laths in a matrix of untwinned plagioclase and quartz.

Several orange-red weathering, variolitic dykes (Fig. 2-4a) outcrop on Mount Misery (Fig. 2-1). The varioles average 3 to 5 mm, weather white, and are prominent on weathered surfaces. They are translucent brownish green, and have diffuse margins on fresh surfaces. The matrix to the varioles is fine grained and black.

A late siliceous dyke cuts at right angles to the sheeted dykes along the Betts Cove mine trail. This dyke is 40 cm wide, aphanitic, brownish yellow and consists of plagioclase, (commonly altered to calcite), and quartz phenocrysts set in a matrix of plagioclase and quartz.

Most dykes have at least one chilled margin, although the contacts are commonly obscured by fractures and shearing. The red weathering dykes are in places chilled against the green-grey weathering dykes but the reverse is also common. Rock analyses and observation of thin-sections has shown that there is little correspondence between the weathering colour of the dykes and their composition or mineralogy although actinolite is more commonly the dominant

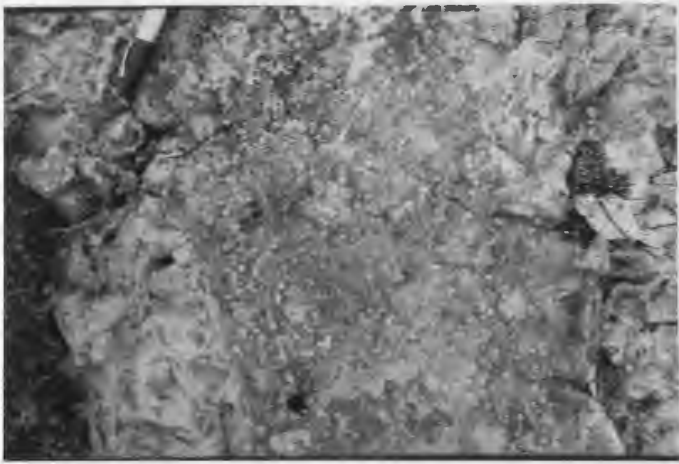
mafic mineral of the green weathering dykes and augite more common in the red weathering dykes. The augite is commonly affected by a reddish brown alteration (Fig. 2-7) and this may account for the reddish colour of the dykes. The dykes exhibit three main textures which grade into one another: (1) plagioclase laths set in a mafic matrix, (2) intergranular plagioclase and clinopyroxene/actinolite with interstitial chlorite, and (3) clinopyroxene/actinolite laths set in a plagioclase/quartz matrix. These textures are also exhibited by the pillow lavas and their significance will be discussed later.

2.3.1. Dyke Breccia

Dyke breccia outcrops sporadically throughout the sheeted dyke unit. It commonly follows the trend of the dykes and consists of subrounded to subangular fragments which average a few mm to a few cm, but locally are up to 30 cm across (Fig. 2-4b). The degree of brecciation varies; where it is light the fragments are all of the same type and may be difficult to see on the fresh surface (Fig. 2-4c). Where brecciation has been more intense there is a higher proportion of matrix, and fragments of several dykes or gabbro have been incorporated into the breccia (Fig. 2-4d). Some of the diabase fragments have chilled margins. The matrix is composed of smaller fragments, chlorite and locally a yellow epidotitic cement.

2.4. Pillow Lava Member

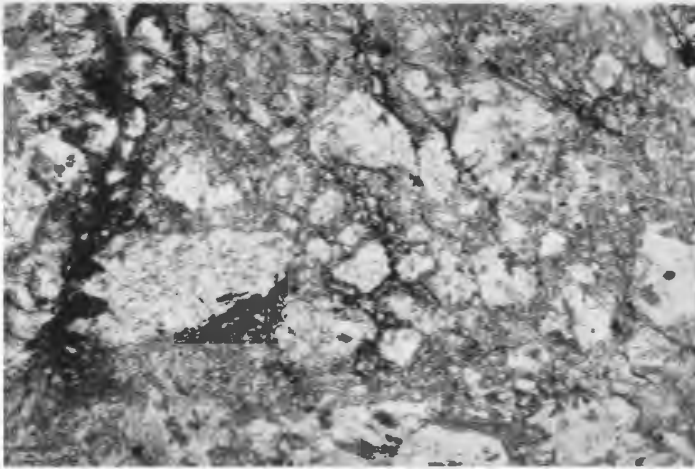
Pillow lavas are found in three parts of the map area; Mount Misery, to the immediate north of Betts Cove; south of Betts Cove, in the vicinity of and to the east of the mine; and on the coast near Betts Head (Fig. 2-1). They average 10 to 30 cm across, but may be 50 to 100 cm in places. Typical pillows are shown in Fig. 2-5a,b. Most are spherical or ellipsoidal; tubular pillows are also found especially about 1 km east of the mine. Near the mine the pillows are tightly packed and there is little interpillow material. Away from the mine area there is interstitial green to pale brown and, less commonly, red chert. Red chert is more



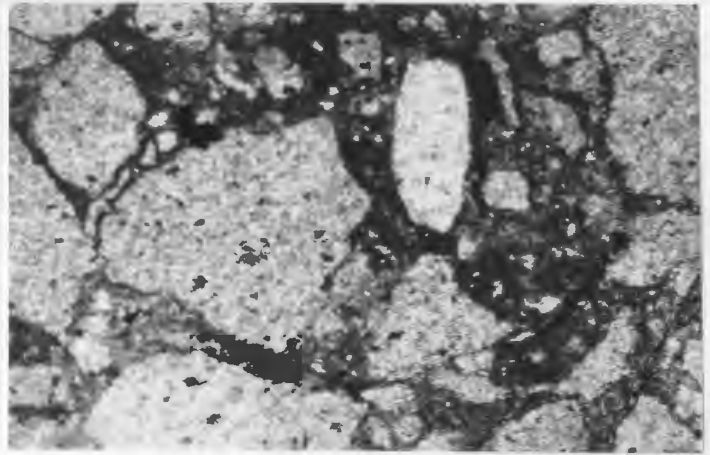
a



b



c



d

Figure 2-4: Photographs of variolitic dyke outcrop and dyke breccia and photomicrographs of dyke breccia

(a) Variolitic dyke, Mt. Misery (CS-201); (b) Dyke breccia, Green Pond (CS-246); (c) Sample 273, PL, less well developed dyke breccia; (d) Sample 230a, PL, well developed dyke breccia. Photo widths: (c,d) - 2.7 mm.

common on Mount Misery. Brecciated and broken pillows and hyaloclastic material are found in interstices where pillows are less tightly packed. Pillows are generally variolitic throughout the area, although in the vicinity of the mine at the gradational contact with the dykes they may contain only a few varioles.

2.4.1. Significance of Variolitic Textures

The term variole was originally given to spherical bodies visible on the weathered surfaces of diabases. The AGI Glossary (Gary *et al.* 1972) defines variole as "a pea-size spherule usually composed of radiating crystals of plagioclase or pyroxene." (They define spherule as "a little sphere or spherical body"). Both of these definitions attach no genetic meaning to the term variole, which is appropriate as their origin is disputed by some authors. There appears to be some confusion in the literature as to the use of the term variolite (it has been used interchangeably with variole). Terminology is used in this thesis following the recommendation of Gelinas *et al.* (1976), that is to use the term variole to denote the spherical body and the term variolite for a rock containing varioles, i.e. with variolitic texture.

At Betts Cove varioles average 2 to 4 mm in diameter, but range from 1 mm to, in one exceptional case, 4 cm. Commonly, variolitic texture begins 2 to 4 cm from the pillow rim and varioles increase in size and abundance towards the pillow center until they coalesce. Less commonly, they are randomly scattered and uniformly sized (relatively small) or are only present near the pillow margin (also small). Fig. 2-5 shows varioles as they appear on the weathered surfaces of outcrops, and Fig. 2-6 contains photos of cut slabs of rock illustrating variations in variole size and distribution. The varioles are most commonly pale green, although they are also cream, grey or brown. The matrix to the varioles is usually fine grained and grey to black. In places pillows are uniform pale green to grey and non-variolitic. The pillows are locally amygdaloidal, and vesicles are filled with chlorite (in places after glass), quartz, calcite and, less commonly, epidote.

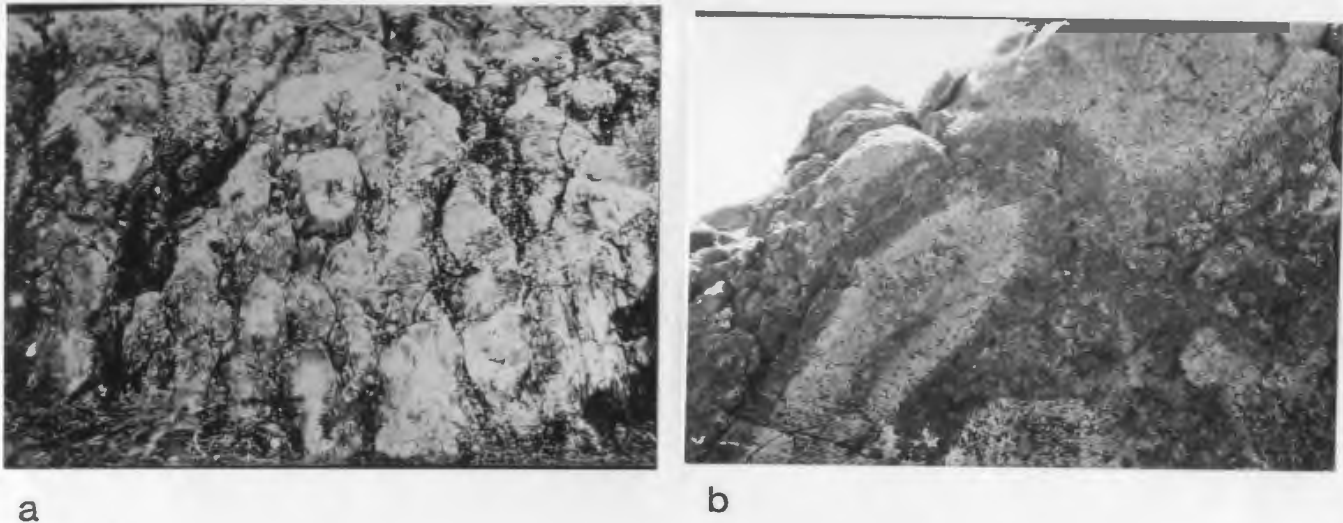


Figure 2-5: Photographs of typical outcrops of variolitic pillows

(a) Rounded pillows near CS-221; average pillow 30 cm across; (b) elongate pillow (about 45 cm across) at CS-257. Note concentration of varioles (white) at center of pillows.

Thin-sections show that many of the pillows were olivine-bearing. Olivine crystal outlines have been preserved but olivine has most commonly been altered to chlorite (plus or minus epidote) or quartz. Most olivine pseudomorphs contain clusters of euhedral chromite grains (Fig. 2-7a). Many pillows also contain pseudomorphs of clinopyroxene replaced by chlorite or actinolite. Some of these retain lamellae of relict clinopyroxene (Fig. 2-7b). Less altered phenocrysts of augite and altered plagioclase phenocrysts are found in many of the olivine-free pillows.

Varioles most commonly consist of augite microlites set in an aphanitic to fibrous groundmass. Representative varioles are shown in Fig. 2-8. The augite occurs in several habits; these include dendritic skeletal crystals, intrafasciculate (Drever *et al.* 1972) intergrowths with plagioclase, long slender prisms and chained crystals composed of well defined links (Fig. 2-9). Cross-sections of augites of the latter two habits are typically six-sided and are cored by a hydrous chlorite-like mixture (Fig. 2-10). Rarely, "normal" prismatic augite crystals are present as

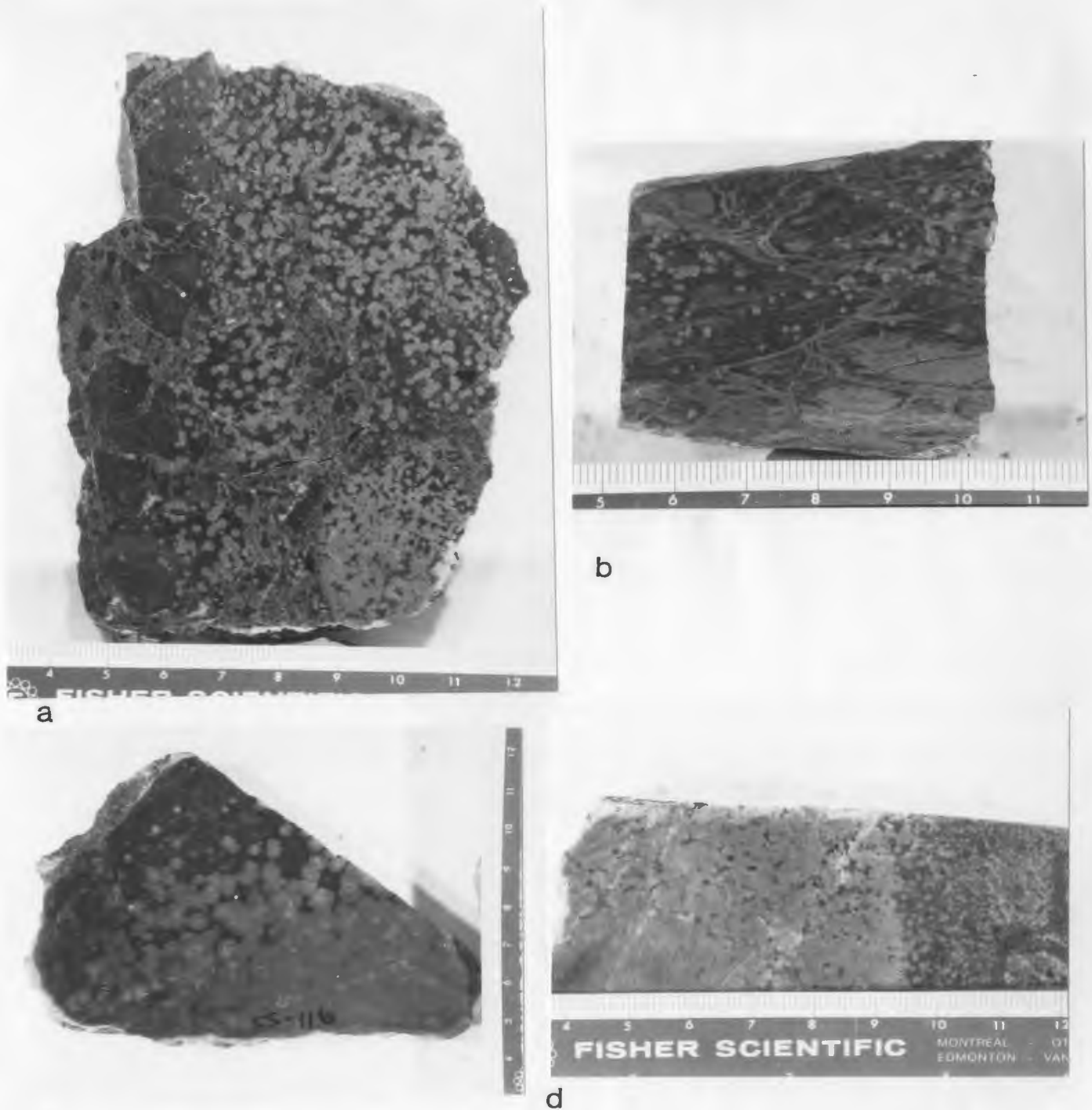


Figure 2-6: Photographs illustrating mode of variole distribution within pillows

(a,b) Samples 203a and 198c, scattered varioles in hyaloclastite; (c,d) Samples 116 and 257a, varioles increase in size towards center of pillows until they coalesce. Note scale with cm divisions.

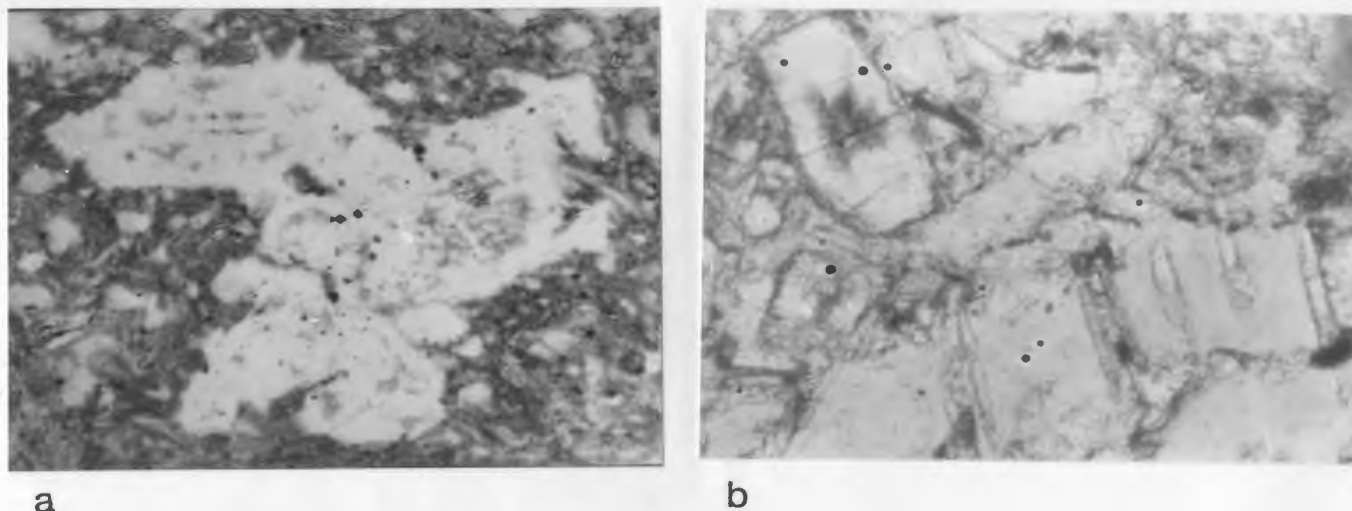


Figure 2-7: Photomicrographs of phenocryst pseudomorphs

(a) Sample 145, PL, quartz (white) pseudomorphing olivine. Note euhedral chromite grains in center; (b) Sample 82a, PL, chlorite (low relief, lower half of photo) replacing clinopyroxene. Note relict clinopyroxene lamellae. Clinopyroxene in upper left corner has reddish brown alteration in center. Photo widths: (a) 1.5 mm, (b) 0.75 mm.

phenocrysts in the varioles. The augite is relatively fresh, but is commonly altered to actinolite on the rims. The material of the groundmass in most of the varioles is a mixture of plagioclase (now albite) and quartz. In many samples a very fine grained fibrous intergrowth of plagioclase and clinopyroxene (commonly altered to actinolite) forms the groundmass. Commonly the groundmass material exhibits a radiating texture which is best seen under crossed nichols (Fig. 2-8d). This appears to be better developed or at least more easily seen where clinopyroxene is a constituent of the groundmass (Fig. 2-14a).

The matrix to the varioles most commonly consists of crystals of actinolite with interstitial chlorite (Fig. 2-10). The chlorite replaces glass and the actinolite replaces augite that was of the same habit as that found in the varioles of that particular sample. Rarely relict augite is found in the matrix (as in sample 55, Fig. 2-10a). Anhedral secondary quartz occurs in the matrix as isolated grains. The quartz forms because conversion of basaltic glass to chlorite releases excess silica (Mottl, 1983b).

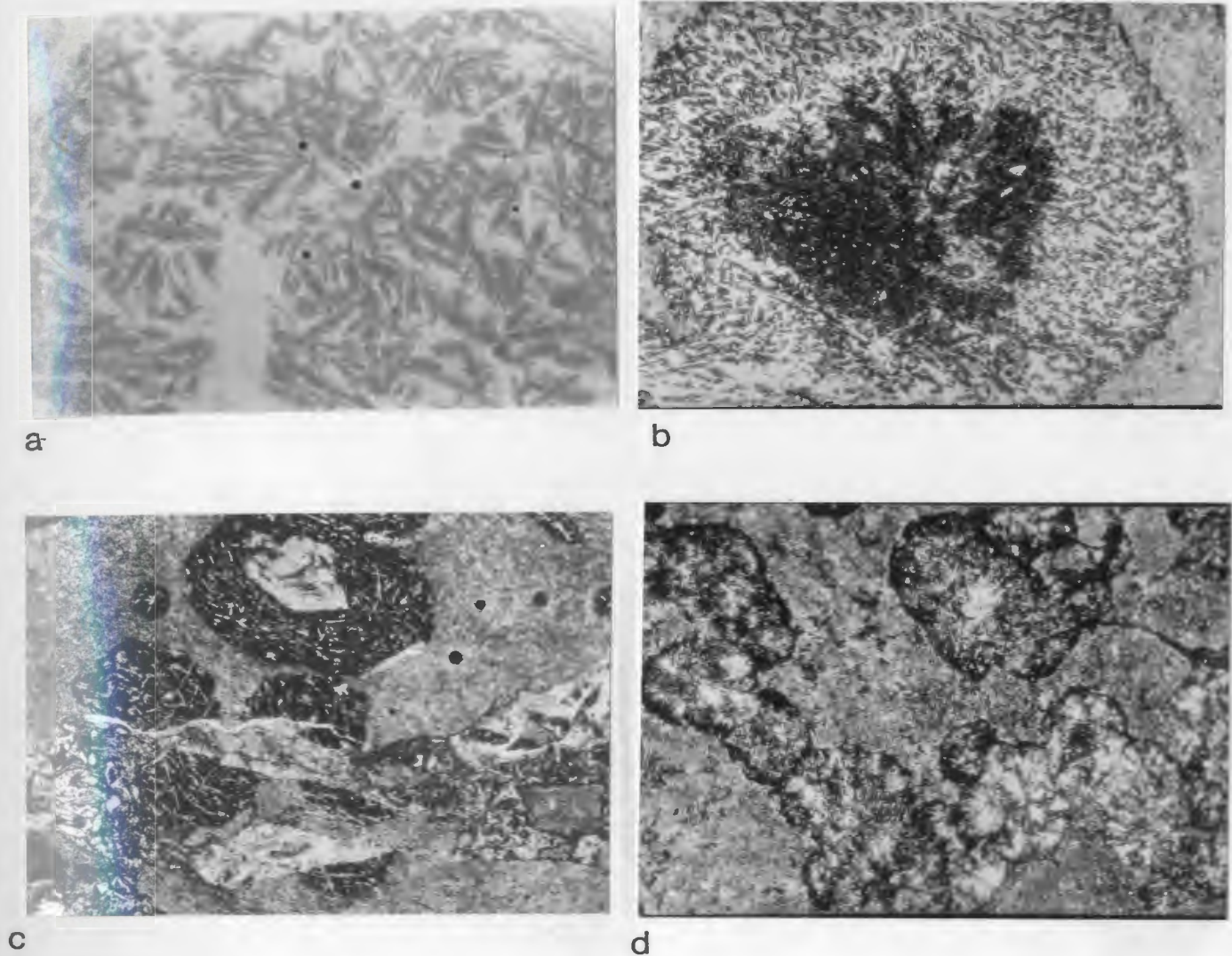
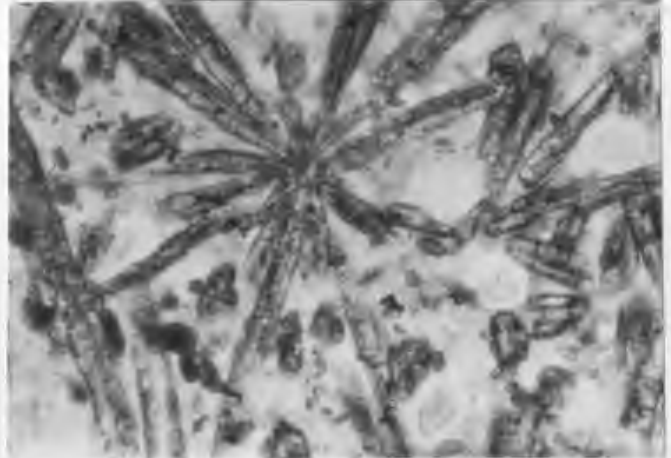


Figure 2-8: Photomicrographs of representative variolitic textures

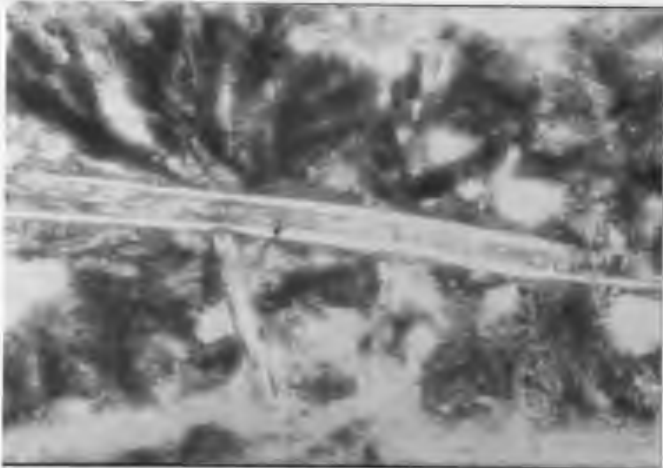
Varioles are set in a matrix of actinolite (after clinopyroxene) and chlorite. (a) Sample 85, PL, variole composed of plumose clinopyroxene (grey) set in felsic/silicic material; (b) Sample 116, PL, as above but clinopyroxene are hollow and have hexagonal cross-sections; dark mass in center is alteration; (c) Sample 203, PL, broken variolites (dark) in hyaloclastite - variolites are made up of intergrown quenched clinopyroxene and felsic/silicic material; note olivine pseudomorph in upper variole; (d) Sample 198a, XN, variolites composed of radiating intergrowths of feldspar, actinolite and chlorite - matrix is highly carbonatized. Photo widths: (a) 1.5 mm, (b,c,d) 6.5 mm.



a



b



c



d

Figure 2-9: Photomicrographs of pyroxene crystal textures

(a) Sample 249, PL, plumose clinopyroxene in variole; (b) Sample 45 PL, radial clinopyroxene arrangement in variole; (c) Sample 157, PL, "intrafasciculate" intergrowth of feldspar and clinopyroxene surrounded by feathery quench clinopyroxene in non-variolitic pillow; (d) Sample 53, PL, elongate hollow clinopyroxene in variole. Photo widths: (a) 0.67 mm, (b,c) 0.75 mm, (d) 4.3 mm.

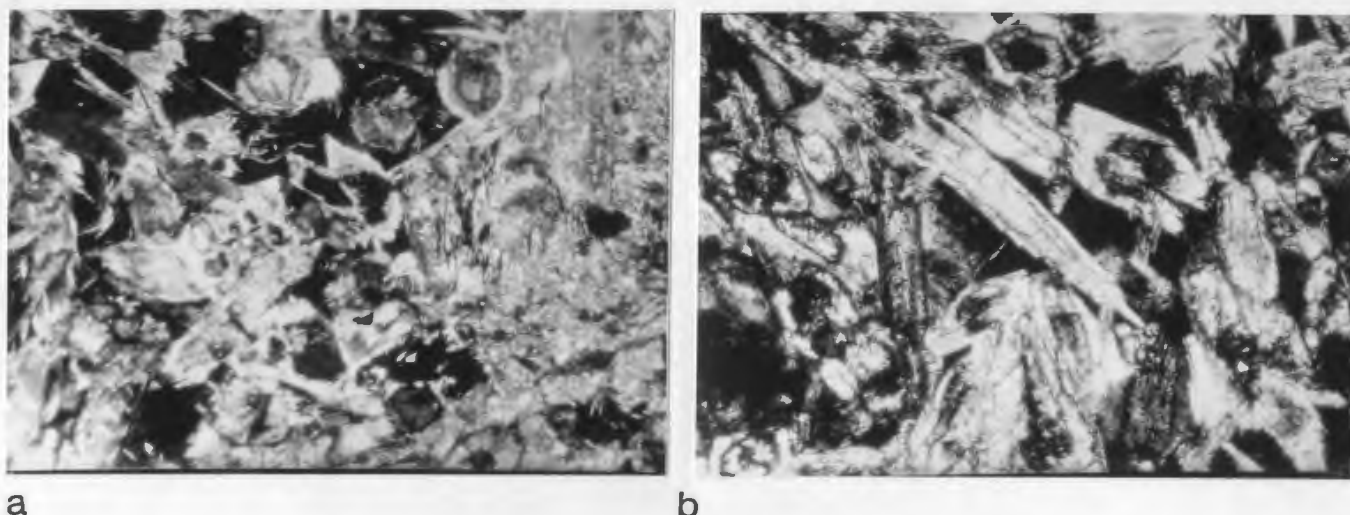


Figure 2-10: Photomicrographs of variole-matrix contact

(a) Sample 55, XN, right side of photo is variole - clinopyroxene set in an intergrowth of feldspar, quartz and actinolite; left side is matrix - actinolitized clinopyroxene set in chloritized glass; note hexagonal cross-sections of clinopyroxene; (b) Sample 181, XN, left side is variole - clinopyroxene set in intergrowth of feldspar and quartz; right side is matrix - actinolite (after clinopyroxene) set in chlorite; note hollow core and actinolite rim of clinopyroxene at top center of photo. Photo widths: (a) 1.8 mm, (b) 0.5 mm.

A mottled appearance (defined by varying shades of green) is exhibited by many of the pillows at Betts Cove. This is caused by a segregation of material into variole-like patches which have mineralogy similar to that of varioles but which have irregular shapes.

The varioles are obviously primary features rather than the result of devitrification or alteration. The skeletal nature of the pyroxenes and the radial disposition of the variole groundmass preclude any other interpretation. The three possible explanations are: (1) magma mixing, (2) liquid immiscibility, (3) the varioles are quench phenomena.

That quench crystallization features are present in the lavas is without doubt.

Table 2-1: Explanation of crystal morphology terminology

from Lofgren (1974)-ref.: (1) Gary et al. (1972), (2) Lofgren (1974), (3) Drever et al. (1972), (4) Drever et al. (1973), (5) Keith and Padden (1963), (6) Johannsen (1939)

Acicular	Needle-shaped: slender, like a needle or bristle, as some leaves or crystals.	(1)
Dendritic	A tree-like single crystal. The complexity of the crystallographic branching varies considerably, and the tree-like shape is not a necessary constraint. The important restriction is that all branches of the dendrite be part of a single crystal.	(2)
Equant	Crystals that have the same or nearly the same diameter in every direction.	(1)
Intrafasciculate	Plagioclase, generally tabular or acicular enclosing pyroxene, generally equant to acicular as a growth texture and not the simple inclusion of a pre-existing crystal during growth.	(3)
Radiate	A general term to describe rock textures comprised, at least in part, of spherulites of one or more morphologies and/or minerals.	(4)
Skeletal	Generally acicular crystals that are incomplete. They often appear hollow in thin section or have irregular outlines that form during crystal growth.	(2)
Spherulitic	"... a radiating array of crystalline fibers all having the same fiber axis and possessing, therefore, the unusual property of branching in such a way that the crystallographic orientation of a branch departs slightly but appreciably from that of its parent fiber... forming polycrystalline aggregates which are more or less radially symmetric." Spherulites with fibers greater than 3 to 5 m in diameter are coarse; those with fibers less than 3 to 5 m are fine. If there is visible melt or foreign material between fibers, the spherulite is open. If the fibers are tightly interwoven, the spherulite is closed.	(5)
Formal Modifying Adjectives of Spherulite		
Axiolitic	Spherulitic fibers radiating from a line and not a point. To be distinguished from spherical, bow-tie, or fan spherulites that may have nucleated and grown in a linear pattern.	(2)
Bow-tie	Spherulite fibers radiating in two fan-shaped arrays resembling in three dimensions two cones joined at their apices. The fan outlines need not be equal in size or symmetry.	(2)
Fan	Spherulite fibers radiating from a point in a fan-shaped array resembling half a bow-tie spherulite. In three dimensions the shape resembles a single cone.	(2)
Plumose	Spherulites that are coarse and open with extensive side branching on the principle fibers. They are usually fan spherulites.	(2)
Tabular	A crystal flattened parallel to one crystal axis relative to the others.	(1)
Variolitic	From the definition of variole. Spherical bodies appearing on the weathered surfaces or marginal portions of certain diabases. They are composed of various secondary minerals and are intimately intergrown with the rock. Often they are spherulites.	(6)

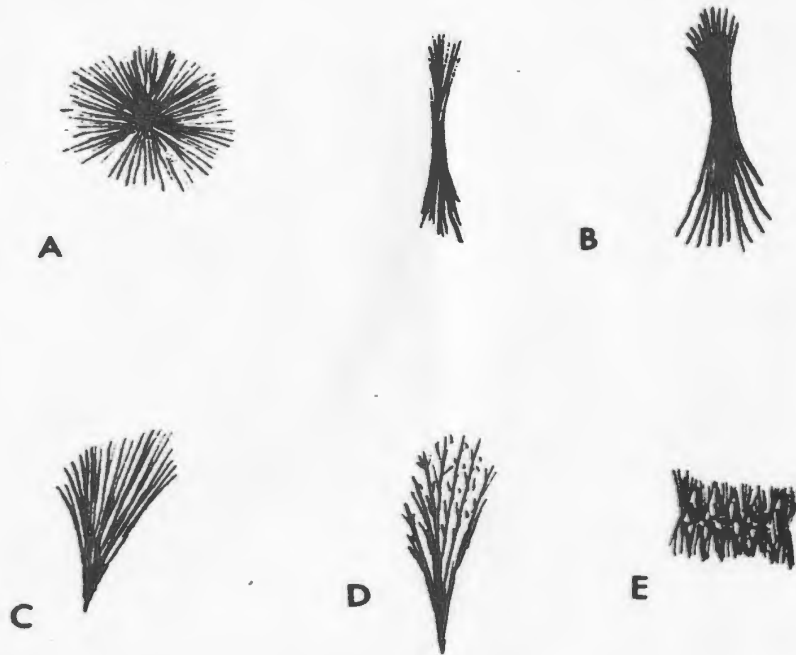
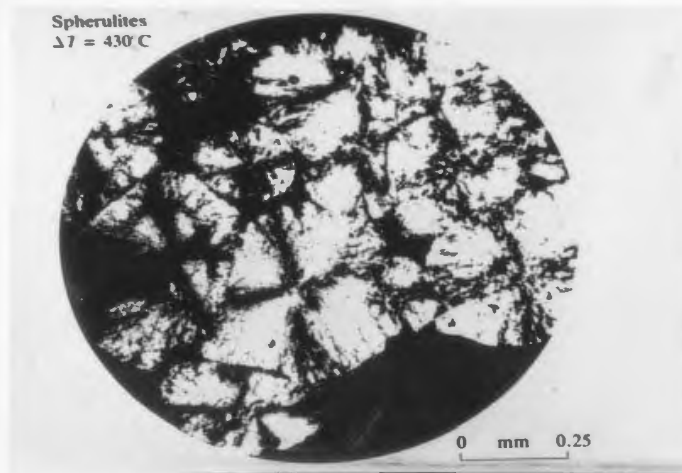


Figure 2-12: The basic spherulite morphologies (A) spherical, (B) bow-tie (C) fan, (D) plumose, (E) axialitic (Lofgren, 1974). Lofgren gives no scale.



from Lofgren, 1974

Figure 2-13: Experimentally produced plagioclase spherulites

growth as outlined by Lofgren (1974) and as concluded in this study; the other

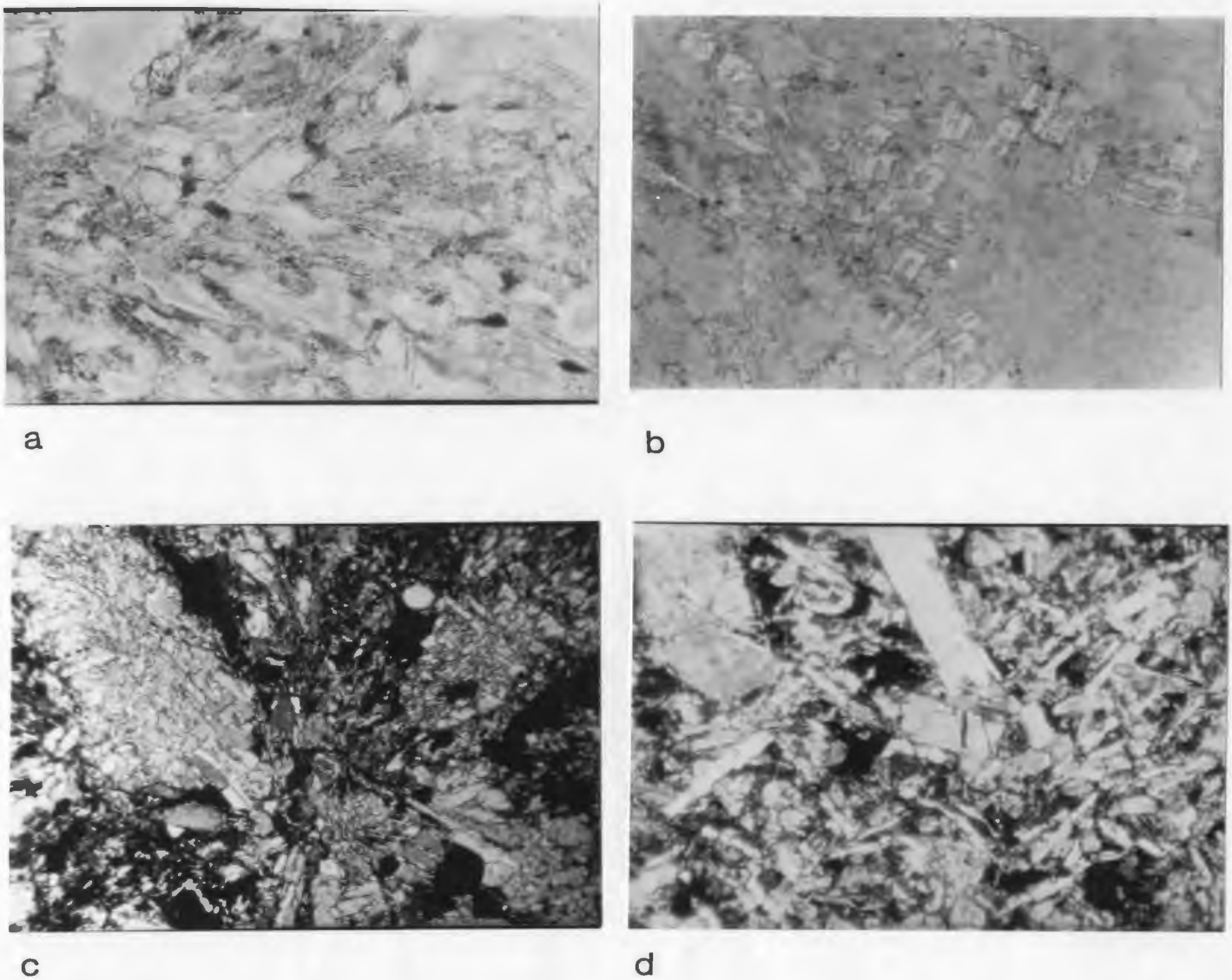


Figure 2-14: Photomicrographs of significant crystallization textures

(a) Sample 286a, PL, intergrowth of fibrous actinolite (after clinopyroxene) and feldspar within variole; (b) Sample 106a, PL, "Belt-buckle" texture - hollow feldspar set in actinolite matrix; (c) Sample 84, XN, intergrowth of clinopyroxene (grey) and feldspar (white) in non-variolitic pillow; (d) Sample 68, XN, plagioclase and clinopyroxene phenocryst-bearing dyke with intergranular texture. Photo widths: (a) 0.75 mm, (b,d) 1.5 mm, (c) 2.7 mm.

type they ascribed to quenched immiscible liquids. If varioles form by splitting of immiscible liquids it would seem likely that slow cooling would result in formation of varioles and matrix with equilibrium textures, however all variolitic lavas at Betts Cove have well developed quench textures. A liquid immiscibility origin also fails to explain the paucity of varioles in the Sheeted Dyke Unit where quenching of the lavas has generally not occurred.

The distribution of varioles within an individual pillow is also consistent with an origin related to quenching mechanisms. "In general we should expect comparatively few crystal nuclei with relatively high growth rates in slowly cooled basic magma, in contrast to many nuclei with small growth rates in quickly cooled basic magma" (Carmichael et al. 1974, page 23). This explains the distribution in some pillows of varioles which increase in size towards the center until they coalesce. The centers of the pillows cooled more slowly than the rims, therefore the high growth rate of varioles coupled with increased room for growth of individuals allows for larger sizes. The pillows that contain small scattered varioles were probably cooled at a quicker, more uniform rate. They therefore contained many variole nuclei and were characterized by relatively slow growth rates. Many of these pillows were small or were hyaloclastically brecciated (Fig. 2-6a,b). The small size of the varioles is owing in part to rapid solidification of the rock, perhaps in part to slower growth rates and, where varioles are tightly packed, to lack of room.

Like the dykes, the pillow lavas show a progression of textures from plagioclase crystals set in a matrix of mafic minerals (rare), to intergranular texture (Fig. 2-14c) and plagioclase-pyroxene intergrowths (Fig. 2-14d), to mafic minerals set in a matrix of plagioclase and quartz. These textures depend on whether plagioclase or pyroxene nucleated first. Variolitic pillows always have the latter texture although rocks with this texture are not always variolitic.

The composition of the pillows seems to have an effect on their textures. Chromium was used as an index of "maficity" because it is relatively immobile

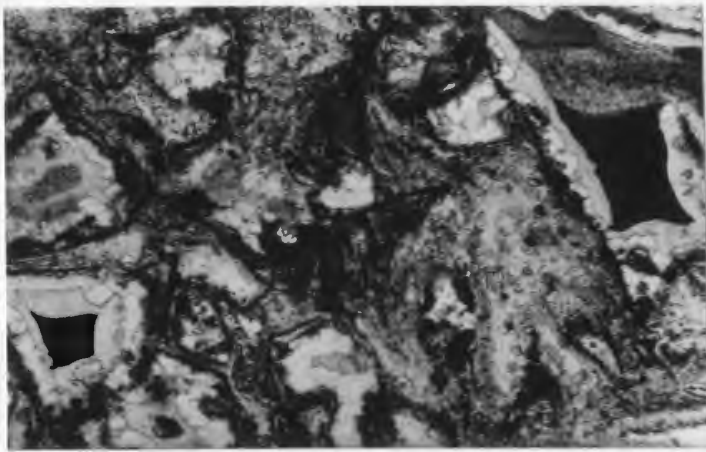
and is not affected by variole distribution as magnesium is (see chapter 3). Most of the least mafic pillows ($\text{Cr} < 300$ ppm) exhibit "plagioclase first" textures while most of the more mafic pillows exhibit "pyroxene first" textures. This relationship is less apparent for the dykes. Varioles are best developed in pillows that have a Cr content of 400 to 500 ppm. Pillows that have a Cr content of over 900 are characterized by mottled texture. The lower plagioclase content of such mafic lavas is surely the controlling factor. Variole development therefore seems to be affected by composition as well as degree of supercooling.

2.4.2. Pillow Breccia

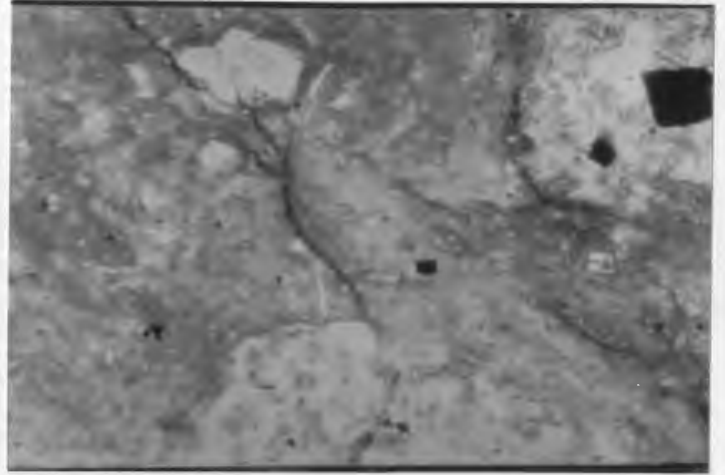
Different types of pillow breccia outcrop locally in the area. Hyaloclastic brecciation is caused by shattering of hot pillows as they become exposed to cold seawater. It is commonly confined to pillow interstices but may be developed on a larger scale. Fragments are very angular and may reach several cm in size. They are commonly set in a chloritic, siliceous, and/or epidotitic matrix (Fig. 2-15a).

The pillows have also been brecciated by hot gases or fluids in places, especially along the Fault Cove Fault at the contact between the pillow lava unit and the sheeted dyke unit. Numerous outcrops of breccia are found in the pillow lava unit in the vicinity of this fault. Several occurrences of dyke breccia outcrop just across the fault in the sheeted dyke unit. The fault may have been an original ocean floor feature which served as a pathway for hot fluids. Pillow breccias here contain angular glass fragments and rounded rock fragments of varying mineralogy set in an epidotitic, silicic and/or very fine grained fragmental matrix (Fig. 2-15b). The rounded shape of the rock fragments is proof that these breccias are not hyaloclastic in origin.

Pillows on Mount Misery are extensively brecciated (Fig. 2-15b,c). The matrix material (yellow in hand-specimen) is dominantly calcite. Drill hole logs from the area record extensive footage of carbonate-rich breccia which is probably the same rock type.



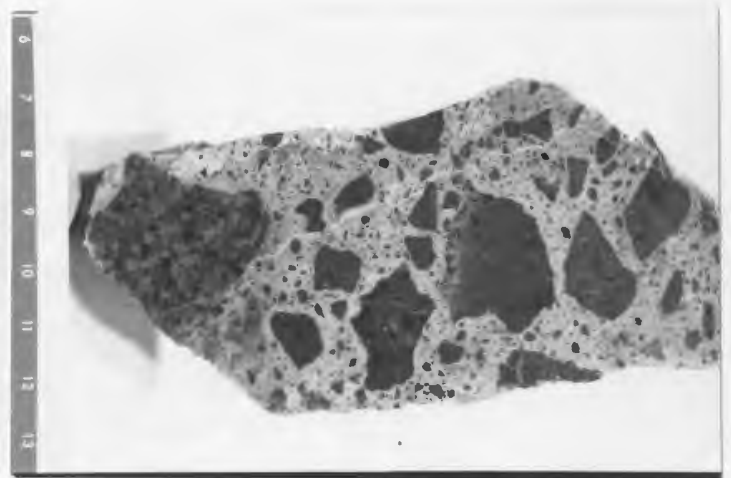
a



b



c



d

**Figure 2-15: Photographs of pillow breccia
(thin-sections, outcrop and cut slab)**

(a) Sample 183, PL hyaloclastite - altered angular glass fragments; (b) Sample 282a, PL, brecciation of pillow lava by hot fluids; (c) outcrop of pillow breccia with calcareous matrix at CS-288; (d) slab of same pillow breccia - note angular fragments. Photo widths: (a) 2.7 mm, (b) 1.5 mm.

2.5. Summary

The map area contains representatives of three of the members of the ophiolite. The ultramafic member is absent from the area studied. Contacts between the units are generally faulted, but locally gradational contacts occur. Where these gradational contacts exist, they occur over a short distance, commonly several metres.

The gabbro pods are in part intrusive into the sheeted dyke unit and to a lesser extent the pillow lava unit. The gabbro pods are cut by later dykes which become sheeted near the edges of the pods.

The variolitic nature of the pillow lavas is the result of quenching of the lavas as they erupted onto the seafloor. Where quench textures are not apparent, i.e. in some pillows and in 99 % of the dykes, variolitic textures are absent. Variolitic textures are controlled by degree of supercooling and pillow composition.

Chapter 3

GEOCHEMISTRY

3.1. Introduction

In order to determine the chemical changes which have affected the rocks at Betts Cove as a result of sulphide mineralization it is necessary to first determine the primary chemistry of the rocks, as well as the effects of more widespread sub-seafloor greenschist facies metamorphism. Separation of these three domains may be hampered by inhomogeneities in the primary chemistry and in the degree of greenschist metamorphism. As well as large scale compositional differences there are chemical differences between cores and rims of individual pillows, attributed at Betts Cove to variable distribution (Upadhyay 1978, 1982) and to seawater-rock interaction (Coish, 1977a,b).

Past geochemical analyses of the Betts Cove Sheeted Dyke and Pillow Lava Complexes have been carried out mainly by H.D. Upadhyay and R.A. Coish as part of their Ph.D theses and during follow-up work (Upadhyay, 1973; Upadhyay and Neale, 1979; Coish, 1977a,b; Coish *et al.*, 1982). Coish (1977a) divided the pillow lava unit into two geochemically distinct sequences which he named the upper and lower pillow lavas. This was later (Coish and Church, 1979) revised to include a third group, the intermediate lavas. Upadhyay (1978, 1982) outlined a two-fold subdivision corresponding to that of Coish (1977a). The lower lavas are those with $\text{TiO}_2 < 0.25\%$; intermediate lavas have TiO_2 contents between 0.25 and 0.50% ; upper lavas have $\text{TiO}_2 > 0.70\%$ (Coish and Church, 1979).

Many of the Betts Cove volcanics have geochemical and petrological

characteristics of basaltic komatiites and/or boninites ("high Mg-andesites") (Sun and Nesbitt, 1978; Upadhyay, 1978, 1982; Cameron et al. 1979; Cameron and Nisbet, 1982). Gale (1973) had earlier applied the term komatiitic basalt to low-Ti, high-Mg lavas of the Pacquet Harbour Group which outcrop south of the Rambler Mines 22 km NW of Betts Cove. Sun and Nesbitt (1978) objected to the use of this terminology to describe these and similar lavas from Cyprus (Simonian and Gass, 1978). They pointed out that at a given MgO content these ophiolitic basalts have much lower incompatible element contents than Archean komatiitic basalts, implying wet melting of a severely depleted source. They envisioned subducted crust as a source of water (water being necessary to promote melting of such a refractory source). They concluded that the low-Ti ophiolites of Newfoundland and Cyprus were most likely formed at a spreading center (as required by the presence of sheeted dykes) near a subduction zone, i.e. an interarc basin (back-arc ridge) or an incipient island arc. They suggested that use of the term komatiite implies a large amount of dry melting of an undepleted or relatively undepleted mantle. Smewing et al. (1975) and Coish and Church (1978) had earlier proposed that the low-Ti lavas of Troodos and Betts Cove respectively are the products of melting of a severely depleted source. The former suggested a marginal basin environment for the formation of the Troodos Massif. Coish and Church (1979) rejected the idea of spreading near a subduction zone, favouring instead melting of variously depleted sources within the same tectonic environment (mid-ocean ridge) as a means of producing a range of TiO_2 contents such as those found in the Betts Cove and the Blow-Me-Down ophiolites.

Sun and Nesbitt (1978) pointed out that the Betts Cove and Rambler low-Ti basalts resemble the low-Ti, "high-Mg andesites" (boninites) of Papua, the Bonin islands and the Mariana Trench which are rich in SiO_2 and MgO (>55% and 9% respectively (Hickey and Frey, 1982)) and poor in Al_2O_3 , CaO, Ti, P, Zr, Y and REE. Another group of basalts from Tonga which are similar but have lower SiO_2 and MgO and higher Al_2O_3 and CaO also have similarities to the Newfoundland examples. The type Boninites, from the Bonin Islands south of

Japan, contain abundant low-Ca pyroxene (high-Mg orthopyroxene and clinoenstatite); some authors require the presence of one or both of these for the definition of boninites. No relict low-Ca pyroxene was seen in the Betts Cove lavas, however, the underlying ultramafics contain abundant cumulus orthopyroxene. Cameron *et al.* (1979) define boninite as a "highly magnesian but relatively siliceous, glassy rock containing one or more varieties of pyroxene, some or all of which have a morphology characteristic of rapid growth, accessory magnesiochromite and, commonly, minor amounts of olivine. Laths of amphibole or plagioclase microlites are rare." They proposed that the uppermost Upper Pillow Lavas of the Troodos massif and Arakapas Fault Belt, Cyprus and the Agrilia Fm. of the Othris Mountains, Greece are boninites. The latter contain no low-Ca pyroxene.

Upadhyay (1982) classified several rocks from Betts Cove as komatiites and basaltic komatiites (he used an MgO content of 18% as a division between the terms komatiite and basaltic komatiite (after Arndt and Brooks, 1980)). The criteria he cited included skeletal quench crystallization textures, high MgO, Ni and Cr and low TiO₂ and K₂O values. He did, however, recognize that many of the rocks from Betts Cove are also similar in many respects to boninites, and suggested that they form a continuum from komatiite through boninite to magnesian andesite-andesite in an island arc-subduction zone environment. Upadhyay and Neale (1979) presented evidence for the island arc affinity of Betts Cove lavas (although some of their arguments involved highly mobile major elements, e.g. Na₂O and K₂O) and suggested that they formed in a marginal basin bounded on one side by an island arc and on the other by a continental margin.

3.2. Elemental Mobility

The usual approach to the problem of primary versus secondary composition is determination of major or trace element mobility. Analyses of ocean floor basalts show that most commonly the major element oxides SiO₂, total iron, MnO, MgO, CaO, Na₂O and K₂O have been mobilized (e.g. Hart, 1970; Andrews, 1977;

Humphris and Thompson, 1978a). Al_2O_3 in most cases appears to be immobile. TiO_2 and P_2O_5 along with the trace elements Zr, Nb, Y, V and Cr have been considered to be immobile (e.g. Cann, 1970; Pearce and Cann, 1973; Winchester and Floyd, 1976; Pearce, 1980). Recently, however, evidence has been accumulating for the mobility of some of these elements and the light REE (e.g. Humphris *et al.*, 1978; Ludden and Thompson, 1979; Hynes, 1980; Williams and Floyd, 1981; Finlow-Bates and Stumpfl, 1981; Baker and de Groot, 1983; Campbell *et al.* 1984). Caution must therefore be used in attempting to evaluate the primary chemistry of ocean floor basalts as the behaviour of even the most immobile elements may be suspect. Coish (1977a,b) determined that at Betts Cove the amount of Fe_2O_3 , MgO, Na_2O and H_2O increased in the rocks after alteration while CaO and Cu concentrations were lowered. SiO_2 , total Fe, K_2O , Ba and Rb concentrations were locally enhanced or depleted. TiO_2 , P_2O_5 , Zr, Y, Cr, Ni and possibly Al_2O_3 appeared to be immobile.

3.3. Results

Ninety-nine samples were analyzed for major and trace elements. Analytical methods are given in Appendix B and the results are presented in Appendix C. Varioles were separated from the enclosing rock for two samples, 116 and 257a. Separation was not complete in the case of sample 116 owing to the nature of variole distribution. The results are presented in Table 3-1 along with some core and rim analyses from Coish (1977a,b). He did not indicate whether the samples were variolitic, but the differences between the core and rim analyses are the same as those produced by the variole and matrix analyses. Major element abundances vary considerably from core to rim or variole to matrix but trace element abundances do not.

Coish (1977a) attributed these variations to major element mobility and to preferential nucleation of hydrous phases such as chlorite and actinolite in glassy rims. The varioles in samples 116 and 257a were concentrated in the centers of pillows. The actinolite in the matrix is after pyroxene microlites, but the chlorite

is after glass. Growth of the plagioclase spherulites would have left the residual material depleted in CaO and Al_2O_3 and enriched in MgO. Trace elements contained in phases which nucleated before variole growth (e.g. Ti, V, Cr in pyroxene and spinel) should be unaffected. If variolitic lavas are the result of liquid immiscibility, large differences in trace element abundances should be apparent. Alteration has also been responsible for some of the major element signatures of the varioles and matrix, for example metasomatism of the plagioclase in the varioles is responsible for their high Na_2O contents (and resulting loss of CaO). Strontium and Ba may have also been lost from the varioles during Na metasomatism; this would explain why their concentrations are not higher in the plagioclase-rich varioles than they are in the plagioclase-free matrix. There has possibly been movement of SiO_2 from the rims into the cores where it entered vesicles and replaced phenocrysts. The compositions of the variolitic pillows are the result of metasomatism of an already inhomogeneous body.

The results from this study indicate that TiO_2 , Zr, Y, Cr, Ni and FeOt/MgO are relatively immobile, as found by Coish (1977a,b). They will therefore be used most extensively to determine the characteristics of the Betts Cove basalts.

The most striking feature of the rocks is their extremely low TiO_2 contents (< 0.74%) and their high MgO and Cr contents. Fig. 3-1a is a plot of Ti vs. Zr, showing that pillow lavas with TiO_2 contents > 0.30% define a trend of increasing Ti with increasing Zr. There also appears to be a more gentle trend defined by less Ti-rich samples but there are fewer points at the high end. These trends may represent the intermediate and lower lavas respectively of Coish and Church (1979). None of the samples define any trend on the TiO_2 vs. FeOt/MgO diagram (not shown). Ti covaries systematically with Y (Fig. 3-1b) although there is some scatter, especially where concentrations are lower, but this can be accounted for by analytical error at such low abundances. Other low incompatible element abundances are highlighted in Figs. 3-1c and 3-2.

It was decided to use Cr rather than MgO as an index of "maficity" because of

Table 3-1: Variation of major and trace element abundances from varioles to matrix and core to rim of individual pillows

	Sample		Sample		Sample		Sample	
	257a		116		74-101		74-58	
	v	m	v	m	core	rim	core	rim
SiO ₂	61.40	46.50	54.40	51.40	61.74	45.70	55.14	49.14
TiO ₂	0.13	0.16	0.23	0.20	0.12	0.15	0.53	0.55
Al ₂ O ₃	13.40	12.30	14.50	13.60	11.94	11.76	16.80	16.35
Fe ₂ O ₃ t	4.73	10.40	7.96	11.19	6.20	13.10	7.29	9.82
MnO	0.09	0.16	0.12	0.17	0.15	0.20	0.16	0.17
MgO	5.90	14.16	9.60	10.86	7.77	16.58	8.17	11.07
CaO	5.79	13.39	5.08	5.07	6.86	12.42	8.38	12.56
Na ₂ O	5.95	0.29	5.50	3.90	5.14	0.55	4.05	1.96
K ₂ O	0.16	0.18	0.05	0.04	0.01	0.01	0.16	0.05
P ₂ O ₅	0.02	0.02	0.02	0.02	0.01	0.04	0.03	0.04
Rb	0	3	0	3	-	1	2	2
Sr	138	139	69	62	60	74	202	146
Y	6	4	7	10	8	11	13	14
Zr	11	14	12	12	16	20	20	20
Nb	0	2	1	4				
Zn	29	62	48	68				
Cu	81	93	31	46	113	133	79	54
Ni	97	116	141	156	268	231	224	244
Ba	35	52	45	41	28	12	28	8
V	220	273	240	323				
Cr	387	382	478	578	756	730	436	432
Ga	10	10	9	10				

v - variolitic core; m - non-variolitic rim ("matrix")
 Samples 74-101 and 74-58 are from Coish (1977a,b)

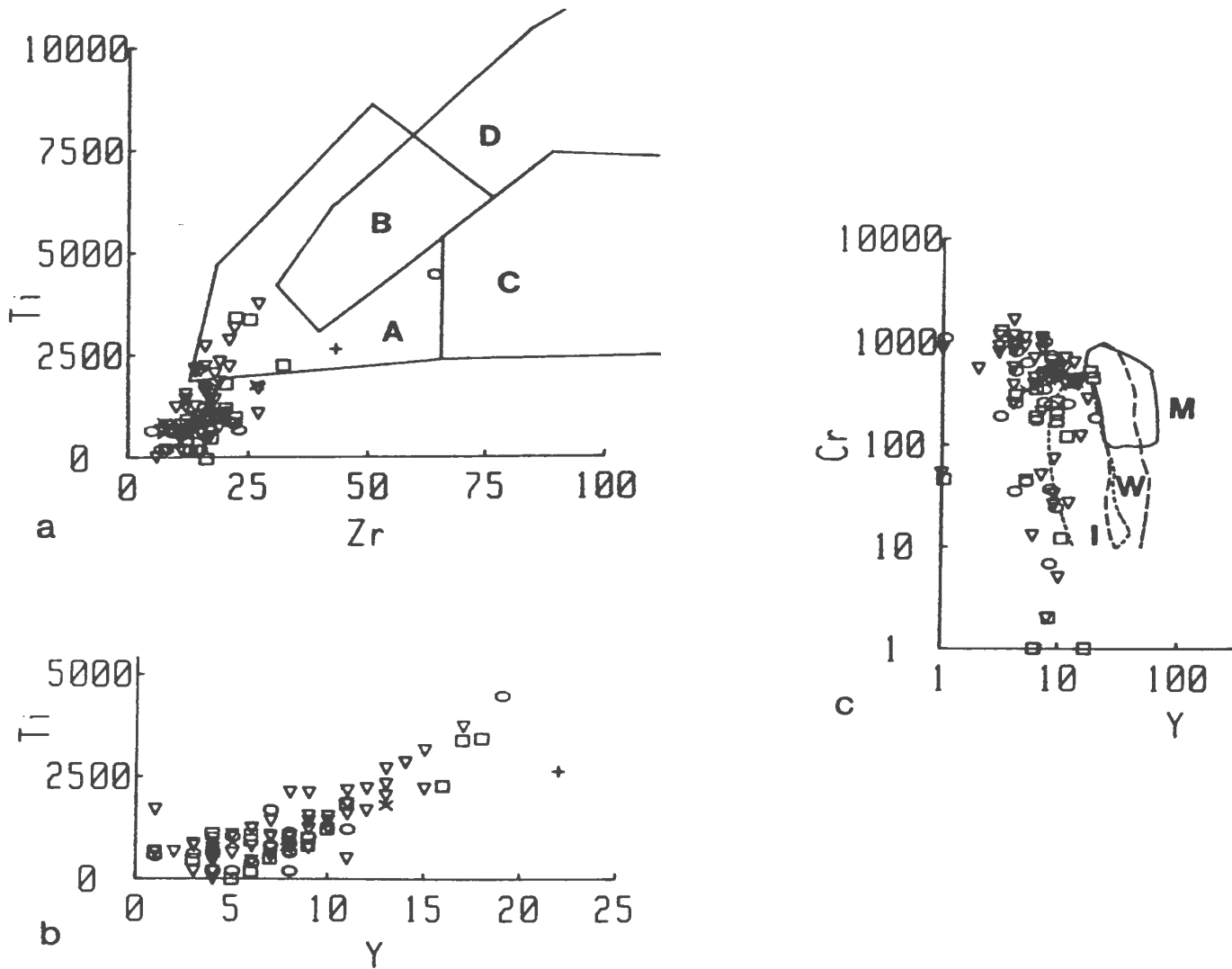


Figure 3-1: Variation diagrams

Majors elements in wt. %, trace elements in ppm; titanium as TiO_2 in %, as Ti in ppm. Symbols in this and following figures - triangles - pillow lavas, ovals - dykes, x - gabbro, + - plagiogranite, squares - mineralized lavas, * - leached lavas (latter two groupings discussed in chapter 4); (a) Ti vs. Zr - fields from Pearce and Cann (1973): low K tholeiites plot in fields A and B; ocean floor basalts plot in fields D and B; Calc-alkaline basalts plot in fields C and B; (b) Ti vs. Y; (c) $\log(\text{Cr})$ vs. $\log(\text{Y})$ - fields from Pearce (1980), I - island arc tholeiite, W - within-plate basalt, M - mid-ocean ridge basalt.

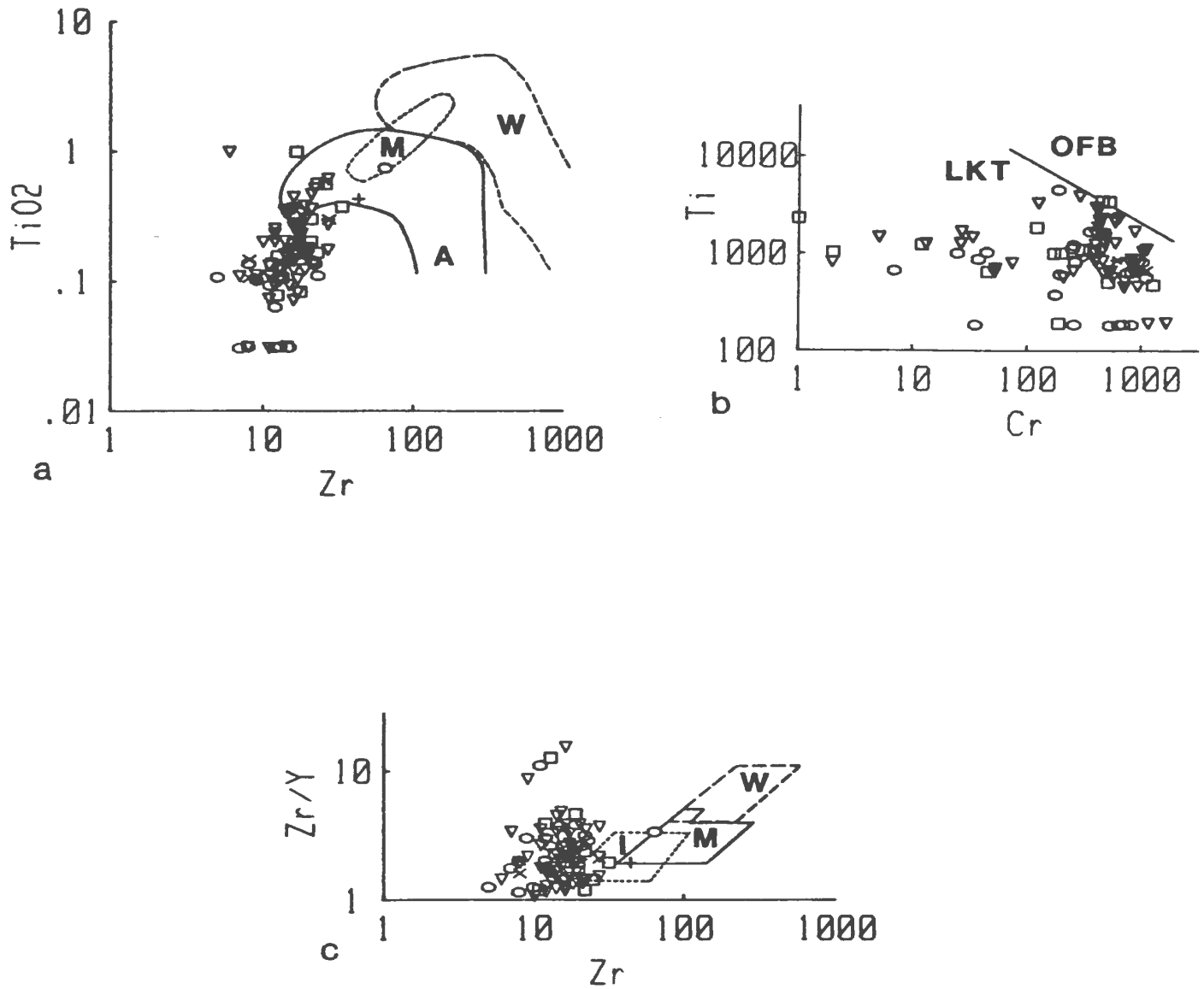


Figure 3-2: Variation diagrams

(a) $\log(\text{TiO}_2)$ vs. $\log(\text{Zr})$ - fields from Pearce (1980), A - arc lavas, W - within-plate lavas, M - mid-ocean ridge basalts; (b) $\log(\text{Ti})$ vs. $\log(\text{Cr})$ - fields from Pearce (1975) LKT - low potassium tholeiite, OFB - ocean-floor basalt; (c) $\log(\text{Zr}/\text{Y})$ vs. $\log(\text{Zr})$ - fields from Pearce (1980) as in Fig 3-1a.

its immobility. Cr abundances for the samples analyzed lie between 0 and 1250 ppm (except one at 1637). The majority of the dykes have Cr contents of < 300 , however, both high and low Cr contents are found in the gabbro, dyke and pillow lava units. MgO contents are higher than those for komatiitic basalts of equivalent Cr and Ni (Fig. 3-3a,b) contents owing to MgO addition during sub-seafloor alteration or to greater fractionation of Cr-spinel and olivine (or a combination of both). Some samples, e.g. 83a which has had extensive replacement of olivine phenocrysts by quartz, have also lost MgO. Cr and Ni contents covary systematically Fig. 3-3c and inversely with FeO/MgO (Fig. 3-4), indicating the latter have not changed greatly for most of the samples. Samples denoted with an open square or an asterisk are those affected by the mineralizing event and they will be discussed in chapter 4. The trend exhibited by the Ni vs. FeO/MgO plot (Fig. 3-4b) represents fractionation of Ni-bearing olivine from a basaltic magma; the flattening of the trend is brought about by the cessation of olivine crystallization. The similar trend shown by Cr (Fig. 3-4a) indicates that Cr-bearing phases were being fractionated along with olivine. The effects of fractionation of Cr-spinel (which is present as inclusions in pseudomorphs of olivine and as a free phase in basalts with a Cr content greater than about 300 ppm) should dominate and mask any effects of fractionation of Cr-bearing clinopyroxene.

Plots of immobile incompatible elements against Cr do not show any clearly defined trends, indicating that their abundances are controlled by factors other than simple differentiation, however they are useful as indicators of tectonic environment. Fields for determining tectonic environment are shown in Fig. 3-1 and 3-2 (Pearce and Cann, 1973; Pearce, 1975, 1980). In each case the Betts Cove samples plot partly in or near the island arc tholeiite or low potassium tholeiite fields. On the incompatible element diagrams they plot further towards the origin owing to their more depleted nature. Their chemistry is clearly quite different from that of average mid-ocean ridge basalt which is not depleted in incompatible elements.

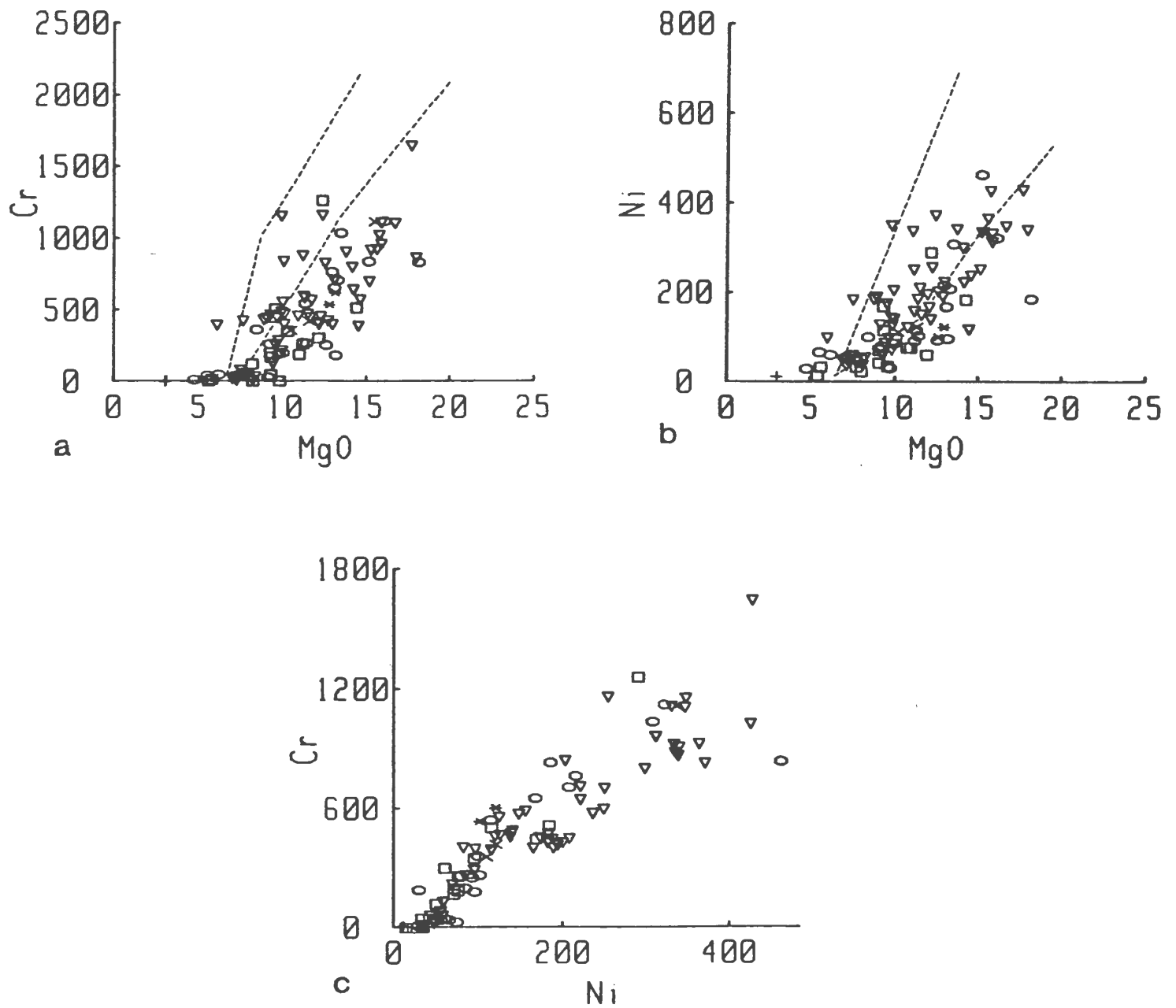


Figure 3-3: Variation diagrams

(a) Cr vs. MgO - Komatiitic basalts from Munro townships (Arndt and Nesbitt, 1982) fall into area between dashed lines; (b) Ni vs. MgO - field as above; (c) Cr vs. Ni

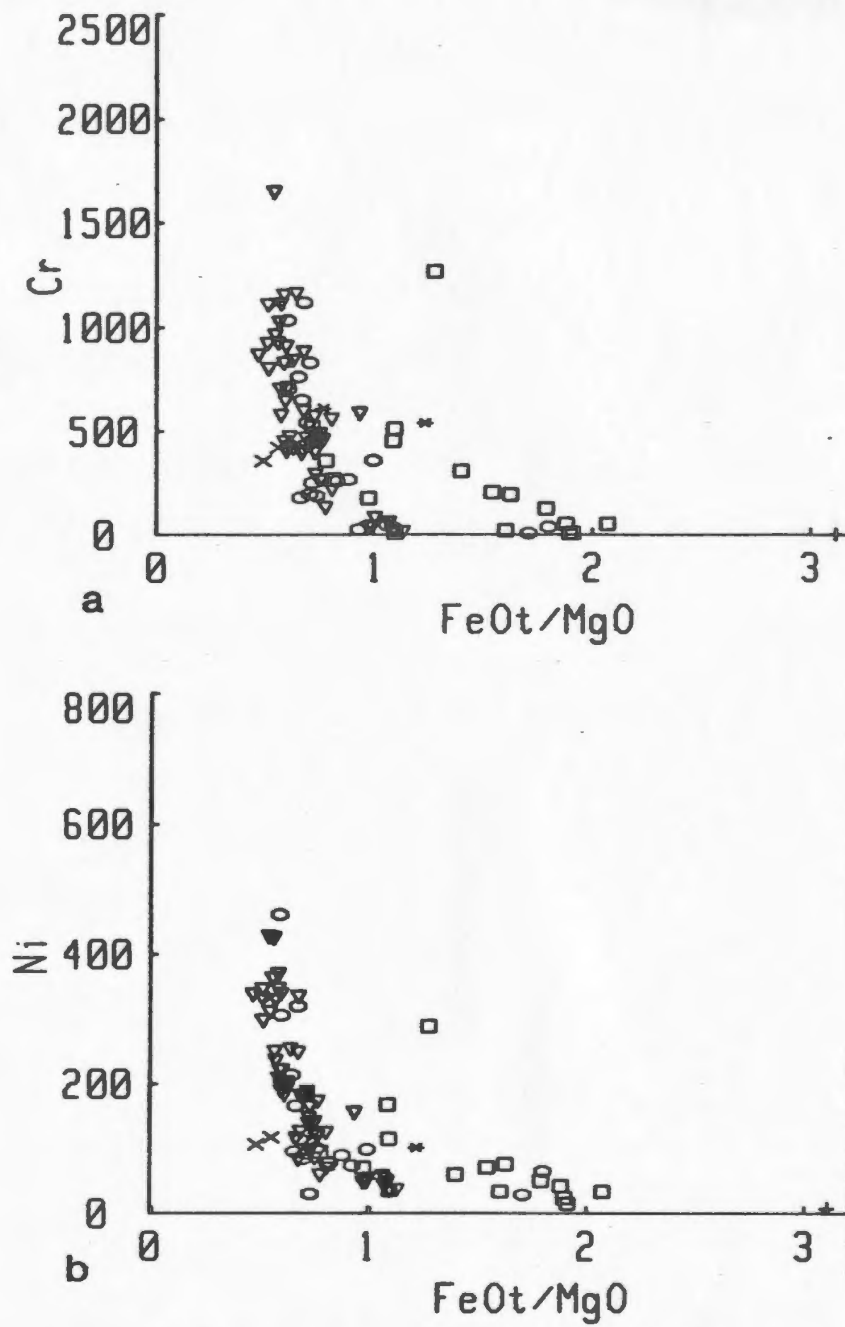


Figure 3-4: Variation diagrams
(a) Cr vs. FeOt/MgO; (b) Ni vs. FeOt/MgO.

The TiO_2 vs. $\text{Al}_2\text{O}_3/\text{TiO}_2$ and CaO/TiO_2 diagrams of Sun and Nesbitt (1978) are particularly useful as discriminators between MORB, komatiites and boninites. The $\text{Al}_2\text{O}_3/\text{TiO}_2$ and CaO/TiO_2 ratios of most Archean komatiites and their more evolved equivalents are close to chondritic, i.e. 20 and 17 respectively, or even lower, indicating that their source was undepleted. In contrast the $\text{Al}_2\text{O}_3/\text{TiO}_2$ and CaO/TiO_2 ratios of low-Ti ophiolitic basalts, including Betts Cove, are much higher (values displayed by Sun and Nesbitt (1978) approach 60). The $\text{Al}_2\text{O}_3/\text{TiO}_2$ ratios of basalts collected for this study are much higher still; most are shown in Fig. 3-5a but several are off scale, the highest being 492. The clearly defined trend highlights the immobility of these elements. In order to get these high ratios the source would have to be extremely depleted in TiO_2 . Fields for high-Mg ($> 9\%$) boninites from the South Pacific (Hickey and Frey, 1982), which are shown on Fig. 3-5a, parallel the trend shown by the Betts Cove samples although several of the latter are more depleted. The CaO/TiO_2 vs. TiO_2 diagram (not shown) has a less well defined trend owing to mobility of CaO, but nevertheless demonstrates the boninitic affinity of the Betts Cove basalts.

3.3.1. Discussion

The results quoted above lead to the conclusion that the Betts Cove basalts have an island arc-boninitic affinity as noted by Sun and Nesbitt (1978), Upadhyay and Neale (1979), Cameron *et al.* (1979, 1980) Upadhyay (1982) and Hibbard (1983). One of the characteristics of boninites is their relatively high ($> 55\%$) SiO_2 contents. The SiO_2 values of samples collected for this study range between 47 and 64% and most are between 52 and 58%. Undoubtedly some of the high values are owing to SiO_2 addition (e.g. sample 83a which has 64.21% SiO_2 and 1145 ppm Cr had abundant olivine phenocrysts which are now entirely replaced by quartz). Nevertheless, even if 10% of the SiO_2 is attributed to metasomatic addition, the rock would still have a relatively high SiO_2 content. Other samples which have a SiO_2 content higher than normal (e.g. 34b, 13Ob and 82a) are not cut by quartz veinlets nor do they contain quartz in vesicles or replacing phenocrysts.

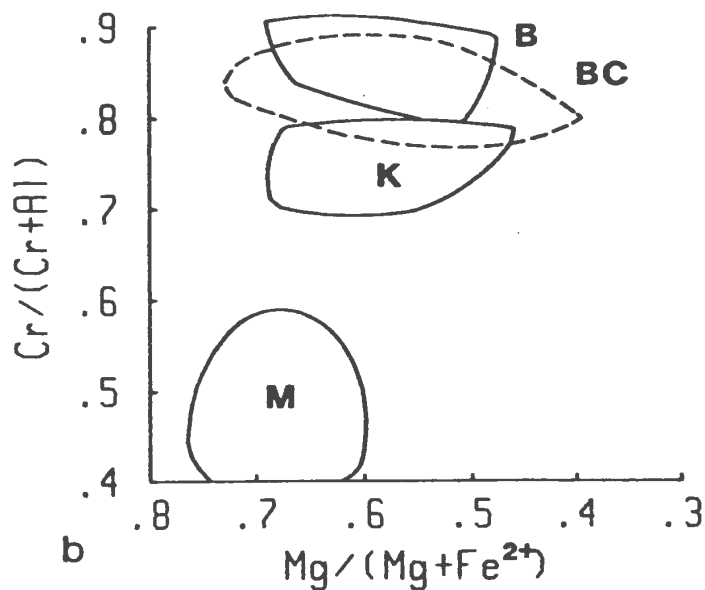
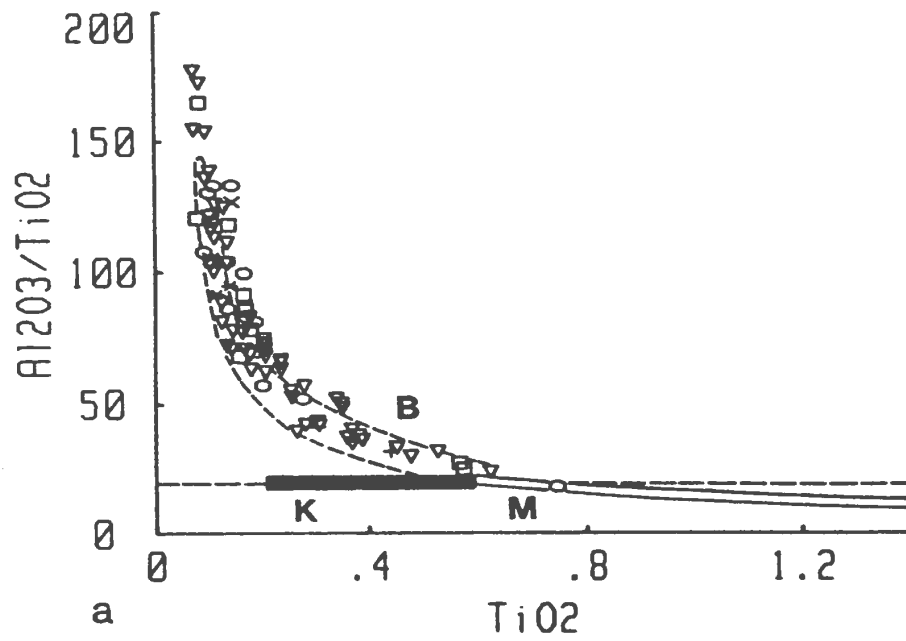


Figure 3-5: Variation diagrams

(a) $\text{Al}_2\text{O}_3/\text{TiO}_2$ vs. TiO_2 - from Sun and Nesbitt (1978) - K - archean komatiites; M - as previous; dotted line - chondritic values. B - field for boninites (Hickey and Frey, 1982); (b) $\text{Cr}/(\text{Cr}+\text{Al})$ vs. $\text{Mg}/(\text{Mg}+(\text{Fe}^{2+}))$ in chromites - fields for mid-Atlantic ridge (M), komatiites (K), and boninites from Cameron *et al.* (1979); field for Betts Cove (BC) from data of Coish and Church (1979).

Coish (1977a) determined that SiO_2 abundances at Betts Cove could be either enhanced or depleted during low grade alteration. According to Hart (1970) and Humphris and Thompson (1978a) basalts tend to lose SiO_2 during seawater-basalt interaction. The results of many experimental studies of seawater-rock interaction also indicate loss of SiO_2 from basalts (e.g. Hajash, 1975; Bischoff and Dickson, 1975; Hajash and Chandler, 1980; Seyfried and Bischoff, 1981). In areas of upwelling of hydrothermal fluids SiO_2 would be expected to precipitate but the general background SiO_2 content of the basalts would tend to be lowered.

The presence of low-Ca pyroxene is characteristic of boninites. The Betts Cove basalts do not contain any relict orthopyroxene, but according to Coish and Church (1979) the lower pillow lavas contain bastite (a serpentine) pseudomorphs of orthopyroxene. The cumulate section of the ophiolite contains abundant orthopyroxene; order of crystallization in this and the Papuan and Thetford ophiolites (which are also low in TiO_2) was olivine + chromite - orthopyroxene - clinopyroxene - plagioclase (Church and Riccio, 1977). The generalized order of crystallization in boninites was olivine + chromite - clinoenstatite - orthopyroxene - clinopyroxene - plagioclase (Cameron et al., 1980). In contrast, the Bay of Islands ophiolite, which has a higher TiO_2 content and a MORB type chemical signature, has little cumulus orthopyroxene and had a crystallization order of olivine + chromite - plagioclase - clinopyroxene - orthopyroxene (Church and Riccio, 1977). Cumulus orthopyroxene is rarely found in komatiites (Cameron et al., 1979).

The composition of chromites from Betts Cove is also similar to those from boninites (Fig. 3-5b). $\text{Cr}/\text{Cr}+\text{Al}$ ratios of chromite grains from picritic dykes at Betts Cove range between 0.80 and 0.90 (Coish and Church, 1979) as do most $\text{Cr}/\text{Cr}+\text{Al}$ ratios of chromites from boninites analysed by Cameron et al. (1979). $\text{Cr}/\text{Cr}+\text{Al}$ ratios of chromites from basaltic and peridotitic komatiites analysed by Cameron et al. (1979) range between 0.70 and 0.80. Chromites from ocean floor basalts are typified by $\text{Cr}/\text{Cr}+\text{Al}$ ratios < 0.60 .

The lower and intermediate Betts Cove lavas (Coish, 1977a,b) contain low REE concentrations - generally lower than 10 times chondrites (Coish et al. 1982). Some basalts from Betts Cove are characterized by convex upwards REE profiles (Coish et al. 1982) similar to those which are typical of boninites from the Mariana Trench and the Bonin Islands (Hickey and Frey, 1982).

3.4. Tectonic Environment

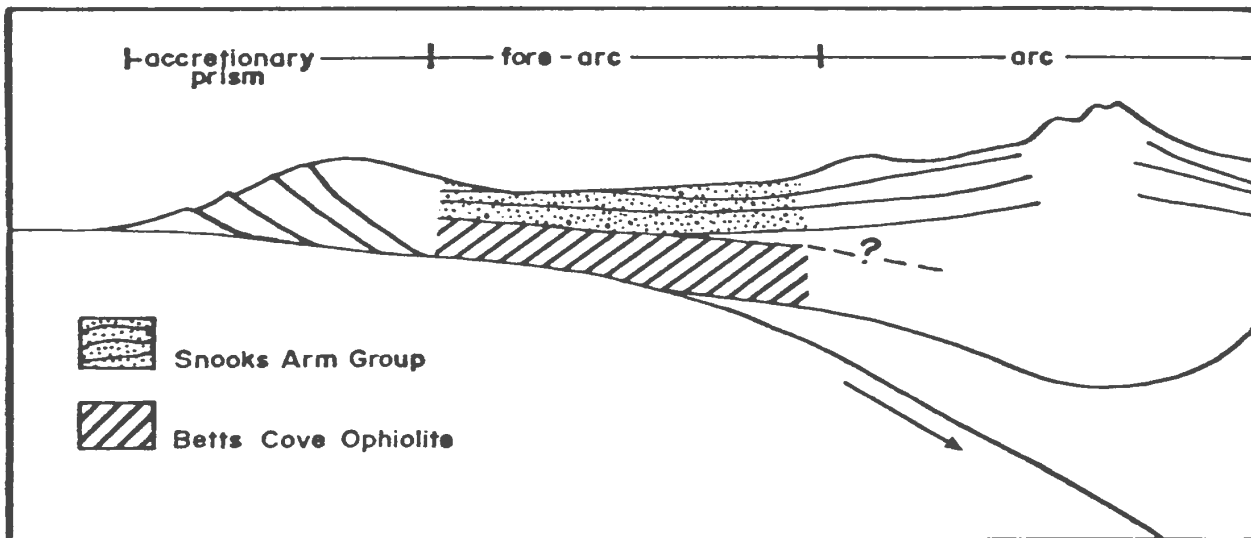
Upadhyay (1973) proposed that the Betts Cove Ophiolite formed in a marginal ocean basin. Coish (1977a,b) suggested that it formed at a mid-ocean ridge. Miyashiro (1973) and Pearce (1975) proposed an island arc and marginal basin environment respectively for the formation of the Troodos ophiolite. More recently various supra-subduction zone environments have been proposed as sites of formation of the Betts Cove ophiolite, e.g. incipient island arc or interarc basin (Sun and Nesbitt, 1978); interarc basin or back-arc basin (Coish et al., 1982).

However, boninites are most commonly found in fore-arc regions in the western Pacific (Cameron et al., 1980; Hickey and Frey, 1982). Gealey (1980) proposed that most of the major ophiolites of the world including Troodos and the Bay of Islands were produced in fore-arc regions making obduction during collision a relatively simple process. Crawford et al. (1981) suggested that the Betts Cove ophiolite may have formed in a fore-arc setting. Fig. 3-6 illustrates application of this model to Betts Cove. Fig. 3-6a represents the situation before collision and Fig. 3-6b is the generalized model of Gealey (1980) after collision. Strong (1974) and Malpas and Strong (1975) envisioned a similar environment of formation and mode of obduction for the ophiolites of the Burlington Peninsula. Hibbard (1983) proposed that the boninitic lavas of the Burlington Peninsula formed either at an oceanic ridge at or near the subduction zone, or within a fore-arc area extensional zone during ophiolite obduction. Although this general idea may be acceptable, there is no need to propose that magma generation in the fore-arc area be obduction-related. Cameron et al. (1980) suggested that boninite formation in fore-arc regions probably took place in catastrophic tensional regimes caused by

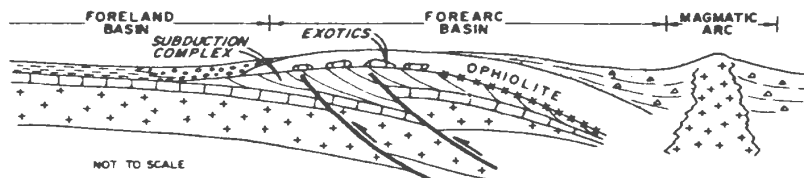
processes such as change in direction of plate movement or initiation of subduction when oceanic crust is rifted.

The overlying intercalated volcanics, sediments and pyroclastics of the Snooks Arm Group are visualized as products of arc volcanism, according to Upadhyay (1973), Upadhyay and Neale (1976), DeGrace et al. (1976) and Strong (1977). Jenner (1977) and Jenner and Fryer (1980), used geochemical arguments to disagree with this interpretation, preferring instead an ocean island or back-arc basin environment. Strong (1977) maintained that the geological relationships, which suggest an island-arc origin, outweigh the geochemistry, which negates this interpretation.

Alternatively, Coish et al. (1982) presented a model for formation of the Betts Cove ophiolite and overlying Snooks Arm Group based on the boninite formation model of Crawford et al. (1981). Crawford et al. (1981) proposed that boninites are generated beneath island arcs as a result of heat generated by a rising mantle diapir which initiates arc splitting. Heat from the rising diapir would cause melting of depleted mantle (depleted by previous formation of the island arc) to form boninites. The boninites are preferentially extruded into a fore-arc setting and would overlie arc lavas. Subsequent melting of the mantle diapir would lead to extrusion of MORB type lavas which would overlie the boninitic lavas as at Betts Cove and in Southeastern Australia (Crawford et al. 1981). Coish et al. (1982) suggested that the Betts Cove boninitic magmas were generated in much the same way, but they formed new oceanic crust in an interarc basin as arc splitting progressed. The overlying Snooks Arm Group would be formed by melting of the diapir itself.



a



b

Figure 3-6: Diagram illustrating environment of ophiolite formation and mode of ophiolite obduction

(a) Schematic diagram (not to scale) illustrating formation of Betts Cove ophiolite in a fore-arc basin. Snooks Arm Group rocks are the onlapping products of arc volcanism; (b) Model of Gealey (1980) for obduction of ophiolites. Accretionary prism (in a) = subduction complex (in b).

3.5. Summary

1) Determinations of elemental mobility are in agreement with the results of Coish (1977a,b) i.e. MgO and Na₂O abundances increased in most samples whereas CaO levels were lowered. SiO₂ has been locally redistributed. Al₂O₃, TiO₂, Zr, Y, Cr and Ni have remained immobile.

2) The Betts Cove basalts have an island arc-boninite affinity. Evidence in favour of this interpretation is: high MgO, Ni and Cr; extremely low TiO₂ and incompatible element contents and corresponding high Al₂O₃/TiO₂ and CaO/TiO₂ ratios; concave-upward REE profiles; crystallization order of olivine + chromite - orthopyroxene - clinopyroxene - plagioclase. Factors against this interpretation are: uncertainty regarding the SiO₂ contents which in some samples are too low and in others may be high owing to alteration; presence of plagioclase in many samples; absence of any relict orthopyroxene.

3) The Betts Cove ophiolite may have formed in a fore-arc basin. This interpretation is supported by the following: boninites are most commonly found in fore-arc basins; subducted material is a feasible source of water which according to many authors is required to promote melting of the source; a nearby arc is a plausible source of the sediments and pyroclastics of the overlying Snooks Arm Group; fore-arc basins should be relatively simple to obduct.

Chapter 4

MINERALIZATION AND RELATED ALTERATION

4.1. Introduction

The Betts Cove deposit and peripheral showings are described in this chapter. The study has concentrated on descriptions of the mineralization and its related alteration which is mineralogically and chemically distinct from the background greenschist facies alteration. Results of a fluid inclusion study are also presented here. The mineralization and alteration are described in light of previous studies of "Cyprus Type deposits", modern sub-sea hydrothermal systems and experiments in which seawater was reacted with basalt.

4.2. Outcrop Description

The old Betts Cove mine is located at the contact between the sheeted dyke and the pillow lava units of the Betts Cove Ophiolite. The location is given in Fig. 2-1 and an enlargement of the area is shown in Fig. 2-2. Rocks outcropping in the vicinity of the mine contain only minor sulphides and the underground workings are now inaccessible. Much of the immediate area is covered by debris from a rockfall that occurred during the last few years of the mining period, and by ore and waste dumps. Old reports are the only source of information about the shape or size of the orebody. Fig. 4-1 is a photo of the mine site as it is today.

Bainbridge Seymour and Co., in an August 1899 report to Reid Newfoundland Co., made some general observations about mineralization in the Betts Cove ophiolite: "From our study we find that a series of copper deposits exist more or

less broken from some distance east of Tilt Cove to ten or fifteen miles west of Betts Cove, the latter thus being apparently in the center of this mineralized belt or zone. The enclosing rocks are chiefly diorites and serpentines, with some other metamorphic formations, and belong to the Lower Silurian System. The cupriferous and pyritic ores are found in veins more or less continuous, and pockets or masses of varying sizes. In places the ore is free from any admixture of gangue filling, but where the latter is present it invariably consists of chloritic slate, often heavily charged with iron and sometimes copper. The Betts Cove ore deposit was crescent-shaped, others are basin-shaped, while others strongly resemble veins in appearance. Our general conclusions are however that none of them can by any means be considered fissure veins. The surface-indications of these ore-deposits generally consist of 'gossan' and ironstone, usually much weathered and decomposed. Too much reliance cannot however be placed on the appearance of these outcrops, as in the case of Betts Cove, a magnificent ore deposit was found underlying a comparatively insignificant outcrop."

Howley, in 1892, stated, "In the course of excavating some enormous pockets of ore were come across" (Murray and Howley, 1918).



Figure 4-1: Photograph of old mine site
Old mine site - large rock mass in center has fallen from cliff behind.
Slip-face is visible

Opinions vary as to the amount of known mineralization which remained upon closure of the mine. Bainbridge Seymour & Co. (1899) stated, "Opinions as to the present value of the old mine diverge, but from apparently the most reliable sources we gathered that very little ore remained for stoping and that the bottom was poor owing to the presence of slate which considerably disturbed and impoverished the ore."

Conversely, Howley, in 1892, wrote, "It is thought the ore was far from being exhausted at the time {of mine closure}" and in 1901, wrote, "The Newfoundland Copper Concentrating Company are now engaged at the Betts Cove Mine, and are now driving a tunnel from the waterside in towards the old workings with a view to unwatering the mine, and get out the ore still believed to exist in quantity below the original excavations, but which was rendered unreclaimable some years ago owing to the caving in of the entire roof of the mine" (Murray and Howley, 1918).

In 1905 another unsuccessful attempt was made to reopen the mine. Howley, in 1906, reported on the progress during the attempt, "So far as the work has progressed at Bett's Head, {the local name for the mine site, not to be confused with the coastal point of the same name} it is found that considerable ore still exists in the first and second levels, and it is generally believed that...bodies of ore occur below the lowest workings" (Murray and Howley, 1918).

Unfortunately such terms as enormous and considerable which were used to describe the orebody are relative and don't give any indication of its actual size. All that is known is that production amounted to about 130,000 tons.

At the mine site most of the sulphide in outcrop is stringer pyrite and chalcopyrite in stockwork quartz, and pyrite disseminations in the pillow lavas. These occurrences are concentrated in chloritic shear zones which strike southeast and dip 60 to 70 degrees northeast. Their locations are shown on Figs. 2-1 and 2-2. The stockwork mineralization outcrops along the old mine trail from CS-41

to the mine site. The quartz veins in the stockwork zone are commonly < 1 cm wide (Fig. 4-2a). The best outcrop of stockwork quartz (Fig. 4-2b) is located on Mt. Misery. In places, e.g. CS-62, the pillows are chloritic, sheared and flattened. Pyrite and chalcopyrite, associated with sugary white quartz, tend to be concentrated in the interstices. Locally, thin lenses of porous and crumbly pyrite with quartz are found in shear zones, e.g. at CS-138. Here, a 4 m wide zone of intensely sheared, pyritized, chloritic rock strikes 135 and dips 65 degrees southeast. This zone is weathered to a bright yellow, soft and crumbly gossan. Lavas adjacent to this zone are slightly mineralized, but are chloritized and sheared to a lesser extent such that deformed varioles are preserved. Another significant stringer zone outcrops at CS-149; mineralization here is concentrated in a 3 m wide zone of chloritized, sheared lavas.

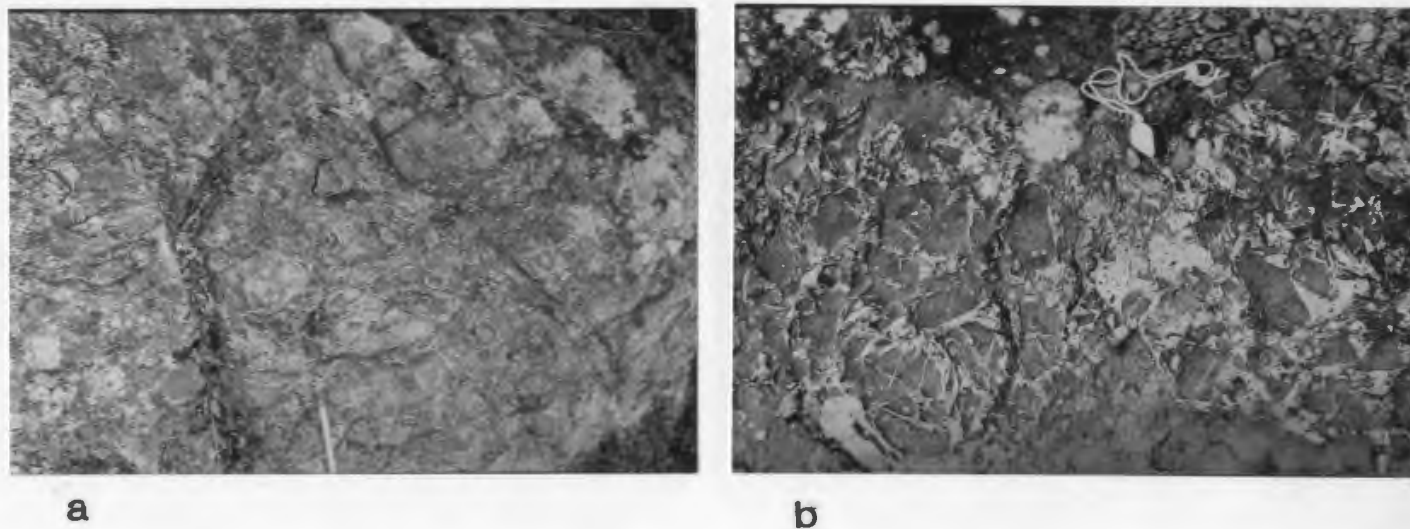


Figure 4-2: Photographs of outcrops of stockwork mineralization

- (a) Typical stockwork mineralization - very thin quartz veins (CS-60);
- (b) More well developed stockwork at Mount Misery.

Massive sulphide outcrops at only one place; a 1.5 m thick unit of massive banded pyrite intercalated with sheared chloritic pillow lavas outcrops at the entrance to, and for the length of, a 12 m long adit. Bainbridge Seymour & Co. (1899) described this occurrence: "A more recent fall of the bluff referred to on

page 3 has exposed a very promising looking body of pyrites, samples of which assayed from 43.75 to 46.74 % of Sulphur. This body has a vein-like appearance, possessing good walls with 'gossan' on each side, has practically no outcrop, and is in section in the shape of the letter 'A', thus promising to widen out in depth. It has already attained in a total depth of 20 ft a width of 8 ft. The only development work carried out consists of a drift measuring 36 ft long, in the face of which the ore continues strong in appearance. We estimate that there are already 600 tons of this ore in sight, and we would recommend its further development" (for sulphur).

The shear zone that contains this pyrite body is about 3 m wide, strikes 060 and dips 70 degrees north to 80 degrees south. The banding in the ore parallels the foliation of the shear zone and is of tectonic origin. The sulphide unit has a sharp contact with the sheared pillows which it contains lenses and fragments of. The pillows are variolitic and near the sulphides have well developed hyaloclastic texture. Red chert is found in the interstices and is remobilized in stringers which parallel the foliation.

In 1955, M.J. Boylen (Advocate Mines Ltd.) drilled eight holes in the Betts Cove area (Carrigan, 1955). Their location map is inadequate, but the holes appear to have been drilled in the immediate vicinity of the old mine. Six of the holes were vertical; maximum depth reached was 517 ft. (157 m). The other two holes were drilled at dips of 55 and 50 degrees with total depths of 712 ft. (217 m) and 466 ft. (142 m) respectively. Two holes had to be abandoned when the old workings were intersected at 408 ft. (124 m) and 325 ft. (99 m) and a third intersected a "foreign body that resisted diamond bit". None of the holes intersected massive sulphides but all intersected some disseminated and stringer mineralization associated with chloritic shear zones (dipping 60 to 70 degrees) and quartz and calcite veinlets. The results of the core assays are unavailable, but the highest sulphide concentrations estimated from visual inspection of the core by the logging geologist were 6 % pyrite over 19 ft. (5.8 m) and 3-4 % chalcopyrite over

26 ft. (7.9 m). Core which remains at the site at present is largely devoid of significant mineralization, but contains abundant quartz and calcite veins and variolitic sections.

Several small peripheral showings were also sampled. Several of these are located along the Fault Cove Fault (Fig. 2-1). They are all stringer chalcopyrite - pyrite associated with quartz and commonly calcite. The host rocks are chloritized, sheared pillow lavas and, at CS-197, sheeted dykes. Some of these shear zones have weathered to yellow-orange gossans. At CS-197 only minor mineralization outcrops, but there are three trenches at the showing indicating that much of the mineralization may have been excavated. At CS-198 chalcopyrite - quartz - calcite stringers cut chloritized pillow lavas which surround an old shaft. Nearby, at CS-202 minor mineralization is located in chloritized lavas but rubble removed from a pit at the showing contains significant stringer chalcopyrite - pyrite. At CS-205 several old pits or shafts are located. In this area dykes cut the pillow lavas on the north side of the fault; locally, they become sheeted. In places, screens of rubbly pillow breccia consisting of 2 mm to 15 cm sized rounded fragments occur between the dykes. Minor stringer mineralization is located in the lavas bordering the excavations, but the rubble lying about is heavily mineralized with stockwork chalcopyrite - pyrite associated with quartz and calcite.

The Betts Head showing (Fig. 2-1) consists of stockwork quartz with chalcopyrite - pyrite in sheared, chloritized variolitic pillows. Rubble lying about the shaft is stringer to semi-massive chalcopyrite and pyrite.

An adit and two pits or shafts are located at Mount Misery. Access to the adit is blocked by a shaft just inside the entrance. Disseminated and stringer pyrite, chalcopyrite and pyrrhotite are located in black, chloritic shear zones in dykes, dyke breccia and pillow lavas. In 1956, M.J. Boylen (Advocate Mines Ltd.) completed four drill holes in the immediate vicinity of the old workings (O'Toole, 1956). Three holes were drilled at a dip of 45 degrees; maximum footage 379 ft.

(115 m). The fourth was drilled at 60 degrees to a depth of 161 ft. (49 m). The rock in the core was reported to be characterized by abundant carbonate stringers and breccia and by carbonate amygdules. Sporadic red chert is reported in one hole. No core was found at the site, but the carbonate breccia is presumably similar to that in outcrop at CS-288 (Fig. 2-15c,d). The mineralization is reported as disseminations and wispy stringers of pyrite, pyrrhotite and chalcopyrite. Either pyrite or pyrrhotite may be locally dominant. The mineralization is, in places, associated with calcite stringers and chloritic zones. Sulphide content is generally minor to moderate but 11.5 ft. (3.5 m) of 25 % sulphides and 2 ft. (0.6 m) of 30 % sulphides (visual estimation) was reported from one hole.

At Foote Pond, disseminated pyrite and chalcopyrite occurs in the sheeted dyke unit. Prominent malachite and azurite staining is present.

A shaft at CS-9 near Betts Bight Pond is located in sheared, chloritized, mineralized (stringer pyrite) zones in variolitic pillow lavas. Dykes cut the lavas here and the sheeted dyke-pillow lava contact is nearby.

The Burtons Pond showing is located in the sheeted dyke member (Fig. 1-2; many gabbro screens (locally up to 50 %) characterize the unit here. The mineralization consists of pyrrhotite - marcasite - chalcopyrite stringers in chloritized rock. The pyrrhotite is non-magnetic, but its identity was confirmed by electron microprobe. Minor sphalerite and cobaltite (CoAsS) are also present. An inclined shaft and minor surface excavations are located at the showing.

4.3. Metal Contents of Sulphide Samples

During the mine's productive period the ore grade averaged 8 to 10 % Cu (Murray and Howley, 1918). Zinc was not recovered at the time and consequently many of the samples in the dumps contain abundant sphalerite. For this study, in order to determine whether banded ore is of sedimentary or tectonic origin, an effort was made to collect samples which clearly exhibit such banding ; such

samples are commonly sphalerite-rich. For these two reasons the samples are biased towards Zn.

Assays of ore samples were carried out at the laboratories of the Newfoundland Department of Mines and Energy. Twenty-one samples have been assayed for Cu, Zn and Pb; results, sample locations and sample descriptions are presented in Appendix D.

Massive samples contain variable proportions of pyrite, chalcopyrite and sphalerite; these proportions are reflected in the analyses. Although pyrite or chalcopyrite may be the only important sulphide in some samples, e.g. pyrite in sample A-6 and chalcopyrite in sample O-12, sphalerite never occurs without abundant pyrite.

Copper values range from 0.19 to 20.02 %; Zn values from 0.02 to 20.54 %. Only one sample had a significant amount of Pb (1.08 %). There is a tendency for Cu-rich samples to be deficient in Zn and vice-versa, e.g. sample O-12 has an average Cu content of 20.00 % and Zn content of 0.04 % whereas sample O-35 has a Cu content of only 0.37 % but a Zn content of 19.88 %. The two metals do occur together in significant amounts in some samples, e.g. O-9, O-2 and O-22, but one is always dominant over the other.

Cobalt and Ni concentrations range from < 0.01 to 0.04 % and < 0.01 to 0.05 % respectively. The Burtons Pond samples had the highest Ni contents, 0.05 % and three samples with 0.03 %, but were not higher in Co.

Ag values in the massive sulphide samples range from 10.1 to 36.3 ppm and average 20.1 ppm; those from the outcropping pyrite mass average 14.2 ppm. Bainbridge Seymour and Co. (1899) reported Ag assay results from this latter body of 10 dwts, 11 grs (16.0 ppm) and from a dump sample, which contained 17.64 % Cu, of 10 dwts, 0 grs (15.3 ppm). Snelgrove (1929) reported a Ag assay of 18 dwts (27.6 ppm) from a dump sample. Ag concentrations in the three stringer samples are lower and average 6.3 ppm.

Gold was analyzed by neutron activation at Chemex Labs in New Brunswick. Results range from < 1 ppb to $> 10,000$ ppb. There is no correlation between Au and Cu or Zn values; even the pyrite body is characterized by high Au concentrations. Unfortunately there are no Au analyses of the stringer sulphide samples but it is suspected that the results would be lower as for Ag. Bainbridge Seymour and Co. (1899) reported Au assay results of 1 dwt, 7 grs (1980 ppb) and 2 dwts, 10 grs (3700 ppb) from the same two samples they assayed for Ag. Snelgrove (1929) reported a Au assay of 6 dwts (9180 ppb) from a dump sample.

Some of the gold and silver is contained in electrum which was found in one sample (Fig. 4-3a). Au and Ag in this electrum occur in the ratio 60:40. It is not known if all the Au and Ag is contained in electrum but Au/Ag ratios of the sulphides are not constant. This means either Au/Ag ratios are not constant in the electrum or else Ag and/or Au occurs in another form.

4.4. Sulphide Textures

Most massive sulphide samples were collected from the dumps at the mine site (see Appendix D). Many samples exhibit banding which is clearly tectonic; in some samples two fabrics, at approximate right angles to one another, can be seen (Fig. 4-4a).

The dominant fabric (s in Fig. 4-4a) is that paralleling the direction of shearing. Fig. 4-4b and 4-3b illustrate that along this fabric pyrite augen are surrounded by sphalerite, chalcopyrite and gangue minerals (chlorite, stilpnomelane and/or actinolite). These minerals are also found in tension gashes and pressure shadows. This occurs because pyrite tends to deform brittly and chalcopyrite and sphalerite plastically (Upadhyay and Strong, 1973).

The second fabric (t in Fig. 4-4a) is defined by numerous small and discontinuous tension gashes filled with ribbon quartz (Fig. 4-4c). In some samples these gashes are present on a minute scale and are filled with sphalerite (Fig. 4-4d).

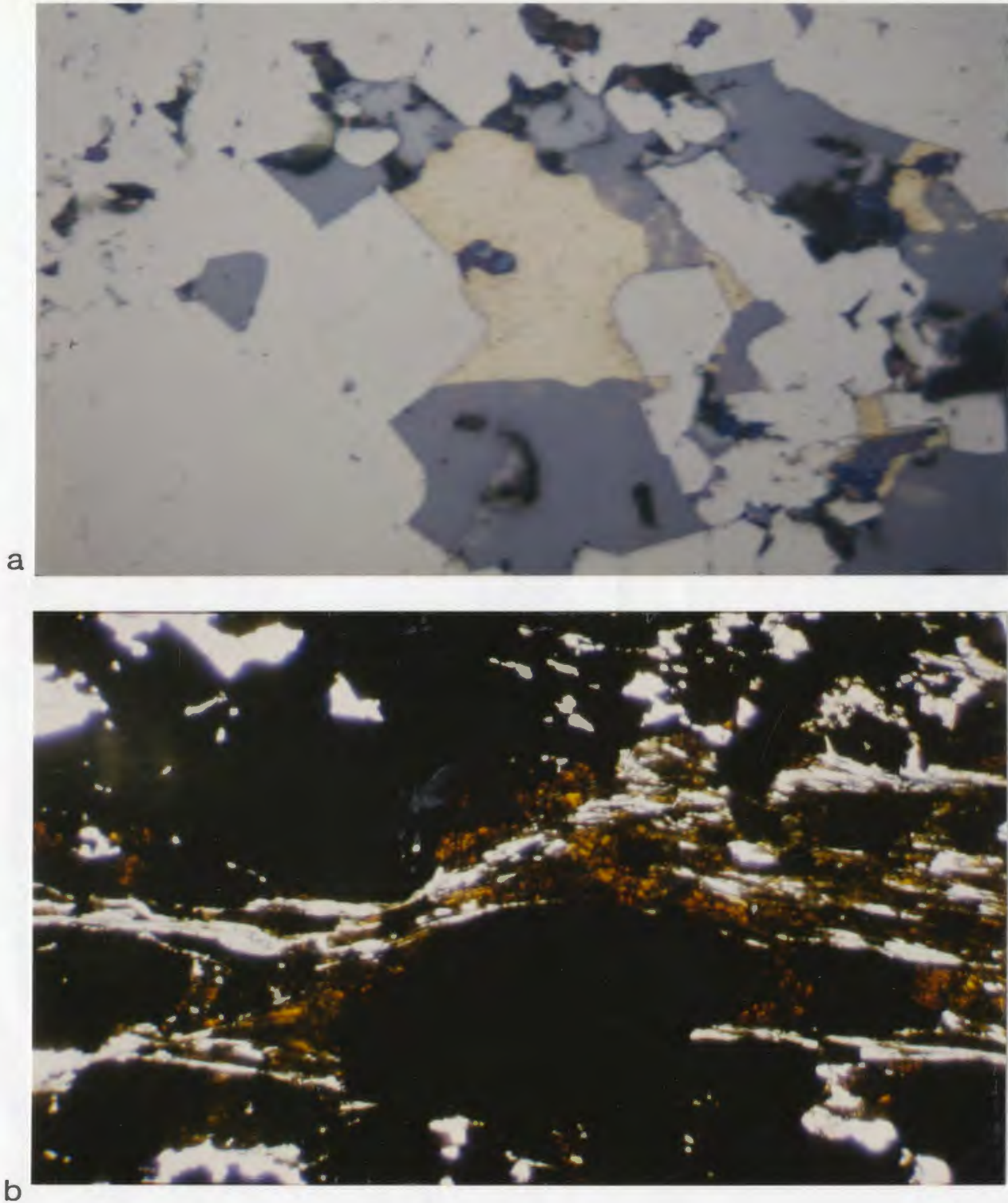


Figure 4-3: Photomicrographs of sulphide textures

(a) Sample O-11, RL, electrum - pitted, pale yellow - it occurs as a cement between pyrite grains. The blue colour in the center is the result of carbon coating; (b) Sample O-10, PL, sphalerite - red, surrounding pyrite - opaque; Photo widths: (a) 172 microns, (b) 2 mm.

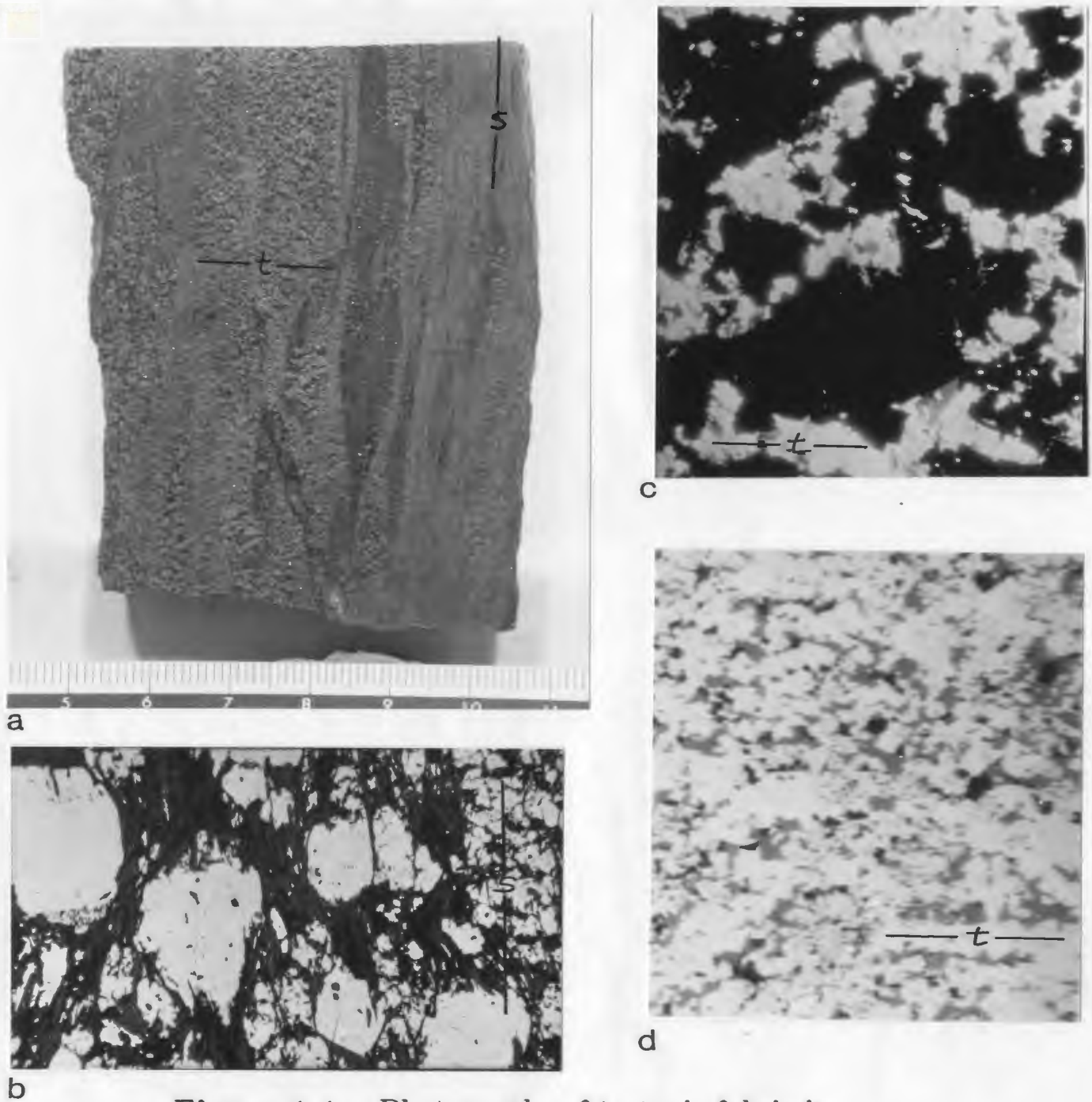


Figure 4-4: Photographs of tectonic fabric in sulphides

(a) Sample O-21, massive pyrite - dominant fabric "s" is result of shearing, subordinate fabric "t" is caused by tiny tension gashes; (b) O-8, RL, "s" fabric is outlined by pyrite augen - sphalerite, pyrite and chalcopyrite occur in pressure shadows; (c) O-20, XN, "t" fabric is outlined by ribbon quartz-filled tension gashes - opaque is pyrite; (d) Sample O-7, RL, minute tension gashes in pyrite filled with sphalerite. Photo widths (long dimensions): (b) 2 mm, (c) 1.5 mm, (d) 0.30 mm.

The tectonic fabric is best seen in samples which have abundant gangue; these are most commonly composed of pyrite with minor sphalerite or chalcopyrite. Samples with abundant sphalerite are very finely banded. In (Fig. 4-5a) banding has parted around a rock fragment augen. Textures in such samples appear to have been completely recrystallized as a result of extreme shearing. In Fig. 4-5b, for example, euhedral pyrite cubes are surrounded by and corroded by sphalerite. Yui (1983) interpreted this same texture (page 237, Fig. 10 and 11) to be the result of recrystallization.

Some samples contain chalcopyrite intergrown with chlorite (Fig. 4-5c,d). Minor albite occurs in veins and intergrown with chalcopyrite in such samples (Fig. 4-5d). These samples are not sheared and are very porous - possibly as a result of leaching of some mineral from the rock.

Chalcopyrite and sphalerite commonly surround euhedral to anhedral pyrite grains. Chalcopyrite is commonly found in fractures which cut pyrite and gangue, and in quartz - calcite veins which postdate much of the shearing. It appears to both predate and postdate sphalerite. Galena was found in sample O-16; it occurs interstitially to the other sulphides. The same sample contains several subhedral crystals of arsenopyrite. The only other sulphide mineral found was minor pyrrhotite, which commonly occurs as inclusions in chalcopyrite and pyrite. One sample of chloritic basalt from Mount Misery contains minor stringer pyrrhotite. Electrum was found in massive ore sample O-11 where it fills vugs and occurs as a cement in fractures in pyrite (Fig. 4-3a).

Textural evidence, outlined above, leads to the conclusion that banding is of tectonic origin. Features indentified as sedimentary slump folds (Upadhyay and Strong, 1973) may in fact be tectonically produced folds. The alternating layers of pyrite, chalcopyrite and sphalerite would therefore be the result of remobilization during shearing rather than the result of repeated precipitation of these minerals. The large scale separation of chalcopyrite and sphalerite is, however, a primary feature as is shown in section 4.5.

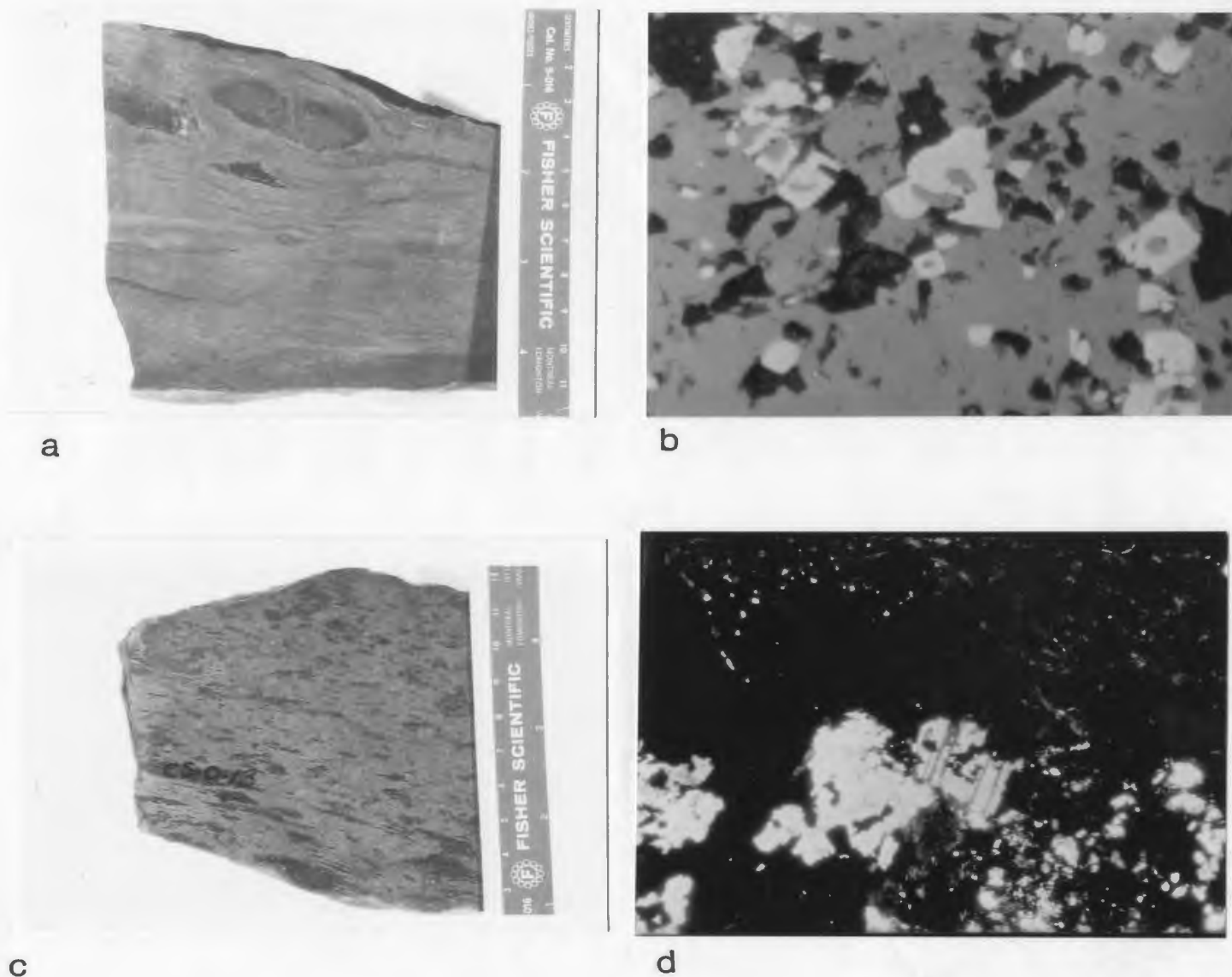


Figure 4-5: Photographs of sulphide textures

(a) Sample O-2, well developed tectonic banding in massive pyrite - sphalerite - chalcopyrite sample - note rock fragments augen; (b) Sample O-3, RL, pyrite grains (white) corroded by sphalerite (grey); (c) Sample O-13, semi-massive chalcopyrite intergrown with chlorite; (d) Sample O-18, XN, albite intergrown with chalcopyrite - chlorite is also intergrown with chalcopyrite in this sample. Rock in upper left corner of photo is a mosaic of quartz and chlorite. Photo widths: (b) 0.37 mm, (d) 1.5 mm.

Although extremely rare, primary sulphide textures were preserved in two samples. Fig. 4-6a,b show spheroidal and framboidal pyrite in massive, vaguely banded sulphide sample O-9. Most of the surrounding pyrite has been recrystallized. Fig. 4-6c is a photo of framboidal pyrite from a quartz - albite - calcite vein that cuts a mineralized variolitic pillow (sample 138a).

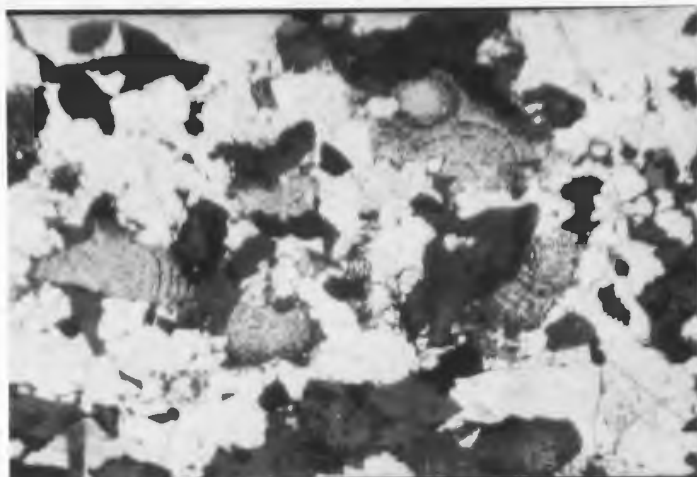
Gangue minerals (Fig. 4-7) associated with the sulphides are quartz, chlorite, calcite, stilpnomelane, epidote and actinolite. In sample 198b abundant talc is intergrown with chalcopyrite. Actinolite and chlorite are intergrown with sulphides in some samples.

The mineralogy of the Burtons Pond showing is somewhat different. The most abundant sulphide is stringer non-magnetic pyrrhotite (confirmed by electron microprobe) which has altered to marcasite on rims and along fractures (Fig. 4-6d). Stringer chalcopyrite with minor sphalerite inclusions is also present. Euhedral to subhedral grains of cobaltite were identified in several samples (Fig. 4-6d). Actinolite is commonly intergrown with the sulphides.

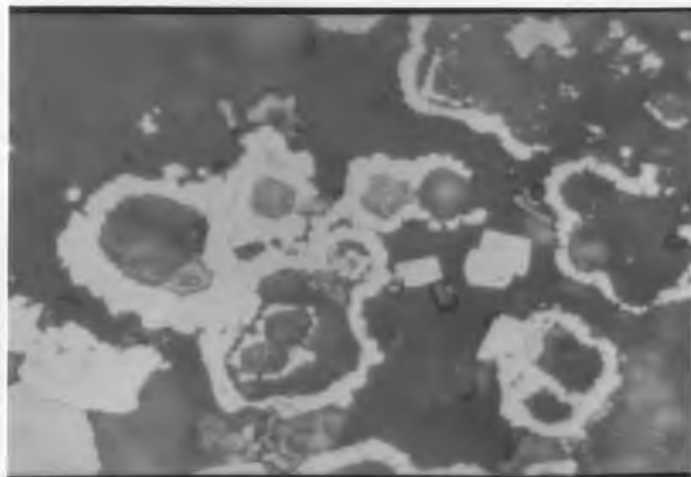
4.4.1. Comparison with Troodos and East Pacific Rise Deposits

The mineralogical composition and textural features show many similarities to and some differences from the classic Troodos and newly discovered East Pacific Rise deposits. The disposition of a massive sulphide body above a zone of stringer pyrite and chalcopyrite is characteristic of the Betts Cove deposit as it is of those in Cyprus. The Troodos deposits are composed mainly of pyrite and chalcopyrite, but sphalerite is a major component of some of the deposits, as it is at Betts Cove.

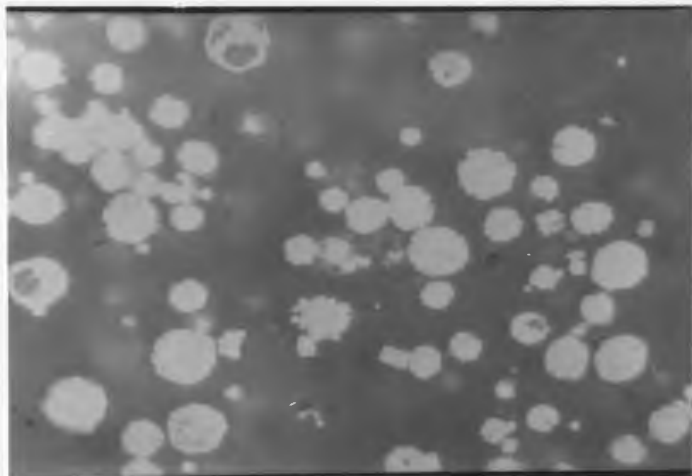
The East Pacific Rise sulphides are built into mounds or structures which are 15 by 30 m wide and 2 m high (Speiss et al., 1980) to 10 m high and 5 m in diameter (Francheteau et al., 1979). One to five metre tall chimneys surrounding individual vents are built upon the mounds. The following description is taken from the above two references plus Hekinian et al., 1980 and Oudin, 1983).



a



b



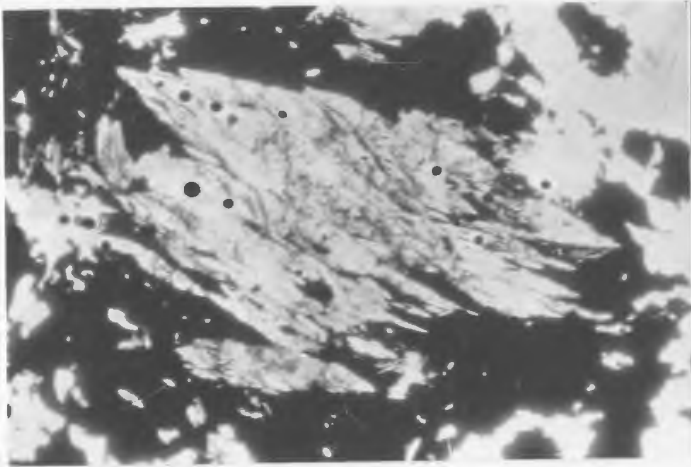
c



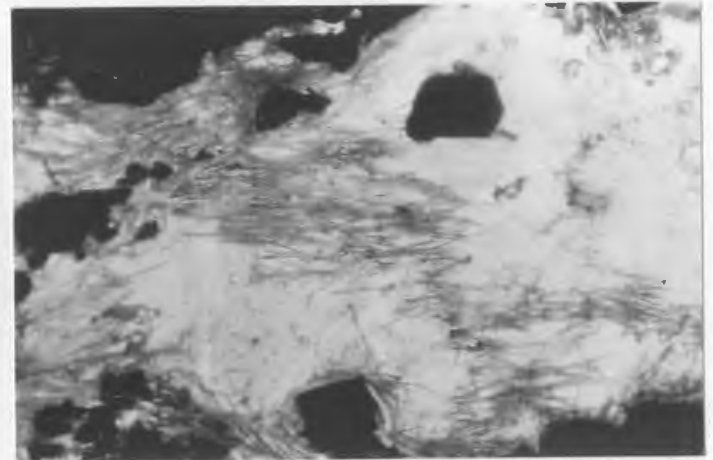
d

Figure 4-6: Photomicrographs of cobaltite and primary pyrite

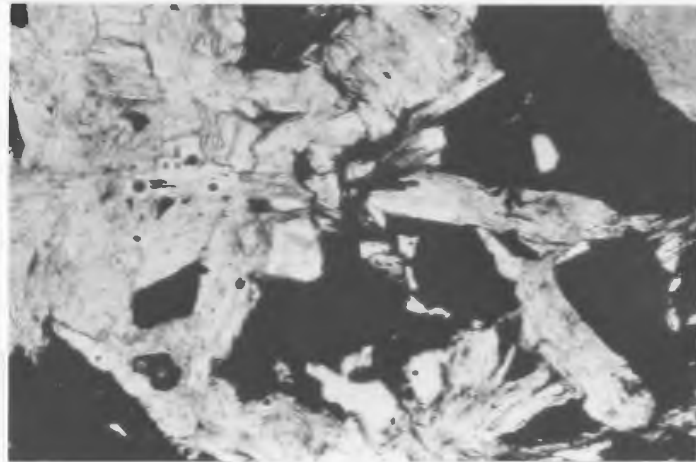
(a) Sample O-9, RL, spheroidal pyrite surrounded by recrystallized (whiter) pyrite; (b) Sample O-9, RL, framboidal pyrite in quartz gangue; (c) Sample 138a, RL, pyrite framboids in quartz - albite - calcite vein which cuts variolitic pillow; (d) Sample BP-1, RL, white grain in center is cobaltite, at lower left is marcasite after pyrrhotite. Photo widths: (a) 0.41 mm, (b,c) 150 microns, (d) 0.70 mm



a



b



c

Figure 4-7: Photomicrographs of gangue minerals

(a) Sample 282r, PL, actinolite intergrown with chalcopyrite; (b) Sample O-14, PL, stilpnomelane (fibrous mineral); (c) Sample 198b, PL, talc intergrown with chalcopyrite. Photo widths: (a,b) 0.75 mm; (c) 0.67 mm.

The primary ore minerals of the mounds are pyrite, sphalerite and chalcopyrite. Pyrrhotite is actually precipitating from the vent waters and wurtzite rather than sphalerite predominates in the chimney walls, but these minerals are unstable and are minor constituents of the mounds. Wurtzite is an isomorph of sphalerite that forms at low temperatures and pressures, probably in general from acid solutions (Ramdohr, 1969). Mound gangue minerals include anhydrite, gypsum, barite and hydrous amorphous silica (opal). Anhydrite is absent from inactive areas as it dissolves at about 140 °C when hydrothermal activity wanes (Haymon and Kastner, 1981). Inactive chimneys and mounds are characterized by alteration products such as hydrous iron oxides and Cu-Fe and Zn sulphates. The materials in the chimney walls are concentrically zoned, suggesting fluctuations in chemical and/or physical properties of the vent solutions.

Framboidal, collomorphic and spheroidal textures of pyrite, marcasite, wurtzite, sphalerite and chalcopyrite have been found in the EPR mounds (Hekinian *et al.* 1980; Oudin, 1983). Similar textures are also found in pyrite in Cyprus (Searle, 1972; Constantinou, 1976), Tilt Cove (Kanehira and Bachinski, 1967), several deposits in the Lushs Bight Group (Smitheringale and Peters, 1974), York Harbour (Duke and Hutchinson, 1974) and rarely in Betts Cove (Fig. 4-6a,b,c). At York Harbour and in Cyprus colloform sphalerite has been reported (Duke and Hutchinson, 1974 and Oudin, 1983 respectively). The textural similarity between these deposits and those from the EPR suggests they originated in the same manner.

Edmond (1982) proposed that the passage of hot hydrothermal fluids through previously deposited mounds serves to "zone refine" them by redissolving trace metals and moving them to the surface of the deposit. In this way the large scale zoning seen in ore deposits on land (i.e. pyrite - chalcopyrite in the lower parts of the deposit and sphalerite in the upper parts) is brought about. The oxidization and removal of the upper portions of an orebody before burial would result in a pyrite - chalcopyrite deposit. Sphalerite, being concentrated in the upper part,

would be absent (as it is for the most part in some of the Troodos deposits). At Betts Cove zoning of the deposit is implied by the negative sphalerite - chalcopyrite correlation, and although it is not known if the sphalerite was concentrated at the top of the deposit it might be suspected.

Edmond (1982) indicated that as the chimney components are the product of "shock precipitation", they represent highly disequilibrium assemblages. They are therefore subject to dissolution or transformation. Oudin (1983) has identified 33 minerals from the active sulphide deposits sampled by Alvin. She has outlined a complex series of mineral dissolutions and replacements. Such minerals as anhydrite, wurtzite, chalcopyrrhotite, and pyrrhotite are unlikely to be preserved. Of these the latter is the only one found in the Betts Cove deposit and then only in trace amounts. Some of the Lushs Bight deposits contain wurtzite, pyrrhotite, cubanite and pentlandite.

Banding such as is characteristic of the Betts Cove sulphides is not typical of the Cyprus deposits and is absent from the East Pacific Rise mounds. This further supports its interpretation as a result of tectonism.

The Burtons Pond showing differs from the Betts cove deposit and the other pyrite - chalcopyrite showings. Although it is mineralogically simpler, it shows similarities to the Cu-Ni-Co-Fe mineralization that occurs in ultramafic rocks of the Limassol Forest Plutonic Complex, Cyprus (Panayiotou, 1980) and in gabbros of the Troodos Plutonic Complex (Constantinou, 1980). Mineralization in the Limassol Forest occurs as lenticular or irregular bodies, veins and disseminations. There are two main occurrences at Lakxia tou Mavrou and Pevkos. Dominant minerals at the former are pyrrhotite and chalcopyrite. Other important minerals are cubanite, and loellingite (FeAs_2). Minor amounts of other arsenides and sulphides such as niccolite, valleriite and pentlandite occur. At Pevkos the dominant minerals are troilite (FeS), valleriite and maucherite (Ni_3As_2). Chalcopyrite and cubanite are common; pyrrhotite, pentlandite, gersdorffite ($(\text{Ni},\text{Co},\text{Fe})\text{AsS}$), oregonite (Ni_2FeAs_2) and cobaltite are minor to rare. Rare

electrum is found at both areas (Panayiotou, 1980). The mineralization in the gabbros consists of fracture fillings, pure sulphide veins and quartz sulphide veins. Pyrrhotite is the dominant mineral, followed by chalcopyrite, sphalerite, pyrite and marcasite. Bravoite ((Fe,Ni)S₂) valleriite, mackinawite and native gold have also been identified (Constantinou, 1980).

Panayiotou (1980) attributed the Limassol Forest mineralization to remobilization of primary sulphides which segregated from the magma by immiscibility. Constantinou (1980) interpreted the mineralization in the Troodos gabbros to be the result of hydrothermal activity. Mineralization was accompanied by chloritization and silicification of the host rocks. The Burtons Pond showing is also the result of hydrothermal activity. The host rocks have been chloritized, carbonatized and silicified.

4.5. Alteration

An area of mineralization-related alteration, which corresponds to the stockwork zone, has been outlined in the vicinity of the abandoned mine (Fig. 2-2). The alteration consists of two zones - an intensely altered core surrounded by a halo of less, and differently, altered rock.

Alteration in the core zone is uniformly pervasive and is characterized by distinctive mineralogical and geochemical signatures. The mineralogy is simple; chlorite and quartz +/- leucoxene (Fig. 4-8a and upper left hand corner of Fig. 4-5d). Sulphides and associated epidote are found sporadically in quartz veinlets and as disseminations. All primary features such as quench textures and varioles have been obliterated.

The rocks are characterized by anomalously high total iron, Cu and Zn and extreme depletion of CaO and Na₂O (table 4-1). K₂O may also have been leached from the rock but because background levels are so low it is difficult to tell. Iron contents increase from about 10 % Fe₂O₃(t) in background rocks to 17.00-19.48

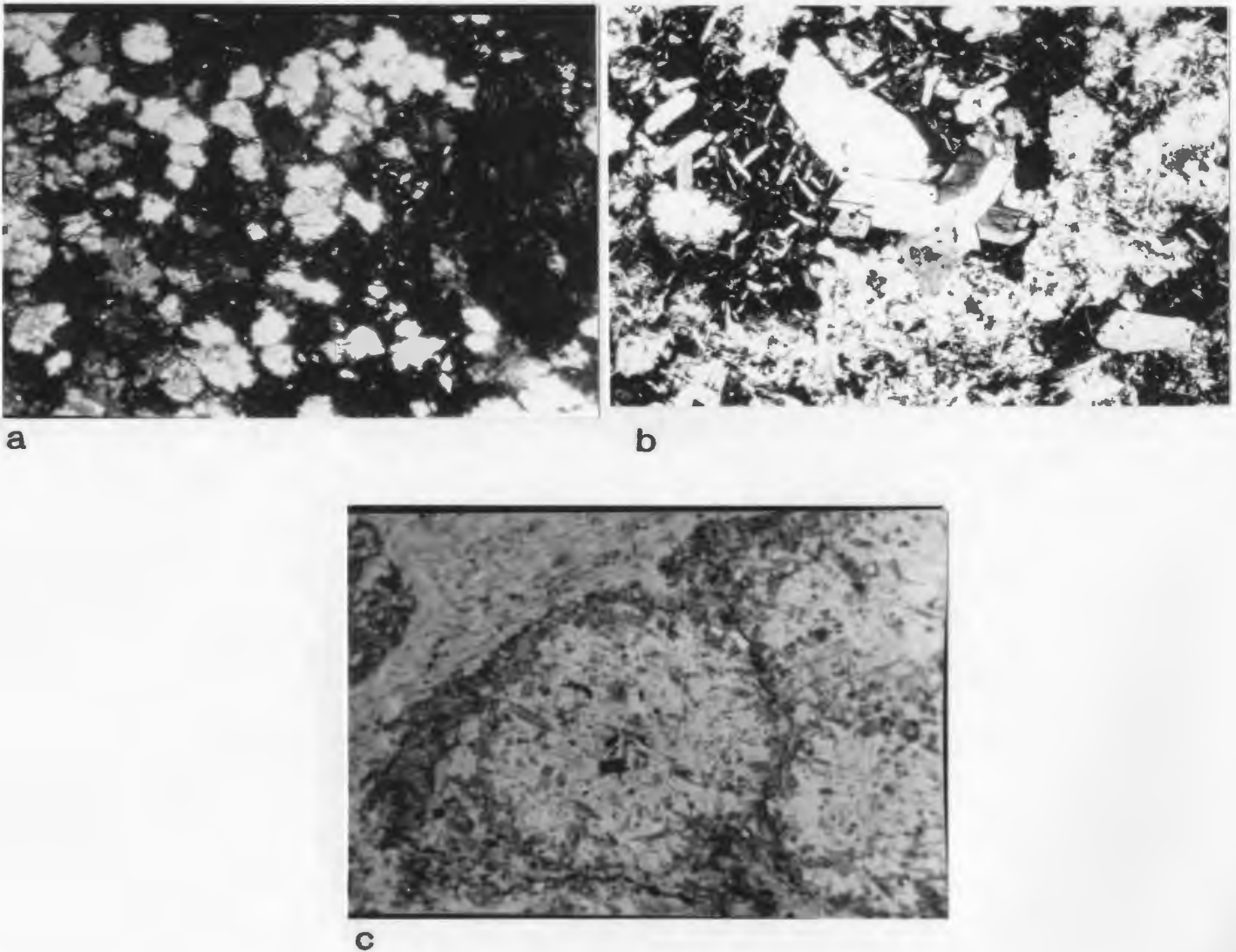


Figure 4-8: Photomicrographs of mineralization-related alteration

(a) Sample 1, XN, typical quartz - chlorite core zone alteration - quartz is commonly equant "popcorn-shaped" grains. Note chlorite pseudomorph of olivine at right side of photo; (b) Sample 137a, XN, quartz - albite - chlorite halo zone alteration - laths of albite, anhedral quartz, interstitial chlorite. (c) Sample 138a, PL, quartz - albite - chlorite alteration of variolitic pillow - variolites are rimmed by calcite and are composed of albite. Matrix and intravariolite clinopyroxene have been altered to chlorite. Photo widths: (a,c) 2.7 mm, (b) 2.0 mm.

% in the core zone samples. Copper and zinc values increase by variable amounts in the quartz - chlorite rocks, ranging from 115 ppm to 9793 ppm and from 71 to 359 ppm respectively. One exception is sample 289 which is of similar mineralogy but which has an extremely low Cu (2 ppm) concentration. Cu/Zn ratios range from 1.03 to 58.80. CaO and Na₂O values are < 0.40 % and as low as 0.04 %, a significant decrease from background levels. K₂O values range from 0.01 to 0.06 % except in one sample in which muscovite occurs in a quartz vein. These cations have been pervasively leached from the rock with the result that all feldspar has been converted to quartz, and pyroxene and actinolite to chlorite. A similar situation was found by Constantinou (1980) in footwall alteration zones of Cyprus massive sulphide deposits.

Alteration in the outer halo is dominated by an assemblage of chlorite, albite, quartz and calcite (Fig. 4-8b,c) but it is irregularly distributed and ranges from a more intense chlorite - quartz type along fractures to a background greenschist assemblage of albite, actinolite, chlorite, epidote and quartz in relatively impermeable zones. Variolitic textures have been preserved in this area but the enclosed pyroxenes have been altered to chlorite whereas background greenschist alteration has generally not affected variole-enclosed pyroxenes. In many samples patches of relict actinolite remain, most commonly in the matrix of variolitic samples. The actinolite is variably altered to chlorite. The varioles are commonly rimmed by calcite which presumably has formed from Ca²⁺ which was liberated from plagioclase during albitization. Although it has not been conclusively demonstrated it is assumed that the symmetrical zoning seen on a large scale would be duplicated on a small scale around fractures i.e. chlorite - quartz assemblages should pass outwards into chlorite - albite - quartz - calcite alteration and then to background greenschist facies alteration.

Rocks characterized by this chlorite - albite - quartz - calcite mineralogy differ from those in the core zone in having "normal" iron contents (8.23-11.71 %) and CaO and Na₂O values which range from strongly depleted to background levels

Table 4-1: Geochemical characteristics of alteration zones

sample	Fe ₂ O ₃ (%)	CaO(%)	Na ₂ O(%)	Cu(ppm)	Zn(ppm)	Cu/Zn

chlorite - quartz						

41C	18.53	0.04	0.04	4687	89	52.66
42A	17.90	0.21	0.24	4174	71	58.80
50A	19.06	0.32	0.13	115	108	1.06
60A	19.48	0.23	0.34	134	130	1.03
61	17.00	0.25	0.38	1796	148	12.13
198B	17.19	5.13	0.03	9793	359	33.76
289	17.16	0.72	0.02	2	114	0.02

chlorite - albite - quartz (+/- actinolite - calcite)						

62D	9.91	1.75	4.68	74	686	0.10
63C	8.72	7.05	4.46	65	365	0.17
127	8.23	5.40	5.40	11	62	0.18
136B	11.71	1.20	2.85	123	698	0.17
137A	11.62	1.11	4.36	403	169	2.38
137B	9.87	1.92	4.26	212	309	0.68
138A	11.38	3.85	4.01	88	1605	0.05
198A	11.28	4.80	3.18	59	835	0.07
198C	11.33	3.65	3.58	47	532	0.08
199A	10.93	1.74	1.64	90	108	0.83

misc.						

95B	15.95	0.55	1.59	951	134	7.09
101	15.56	1.98	2.51	640	107	5.98
117	10.10	3.72	3.94	370	236	1.56

total iron as Fe₂O₃

(table 4-1). Copper and Zinc concentrations are anomalously high but in this zone Zn is enriched preferentially to Cu; Cu/Zn ratios range from 0.05 to 0.83 with one exception at 2.38.

A few samples in table 4-1 have been classed as miscellaneous. One of these, 95b, contains chlorite, quartz and albite and has a geochemical signature with

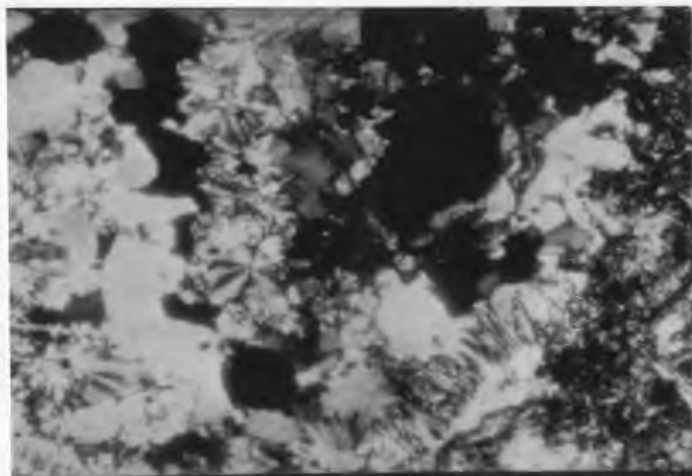
characteristics of both zones. Much of the albite in this sample has been replaced by quartz; it is taken as evidence that there is a gradational contact between the core and halo alteration zones. Sample 101 is from the halo zone, but it contains abundant actinolite, and has a geochemical signature like that of 95b. Sample 117 is also from the halo zone, but contains abundant epidote as well as chlorite, quartz and albite.

Rocks of the outer halo are cut by quartz, epidote, sulphide veinlets like those which cut the core area and also by quartz, albite, calcite, sulphide veinlets (Fig. 4-9a). Both types of veinlets also cut the rocks outside the core and halo zones. At sample location 121 the sheeted dyke unit is brecciated by veins of pure albite (Fig. 4-9b,c). The dykes here contain abundant actinolite and epidote; no relict pyroxene remains. At Lokken, an ophiolite deposit in Norway, the orebody is underlain by a lens of "felsite", a rock which varies from almost pure quartz to almost pure albite (Grenne *et al.*, 1980). Another Norwegian deposit, Hoidal, contains this quartz - albite unit in abundance. The albite veins at Betts Cove may be feeders for such a unit or at least may have originated from similar processes. Such albite veins may be generated by re-deposition of the Na_2O leached from the core zone.

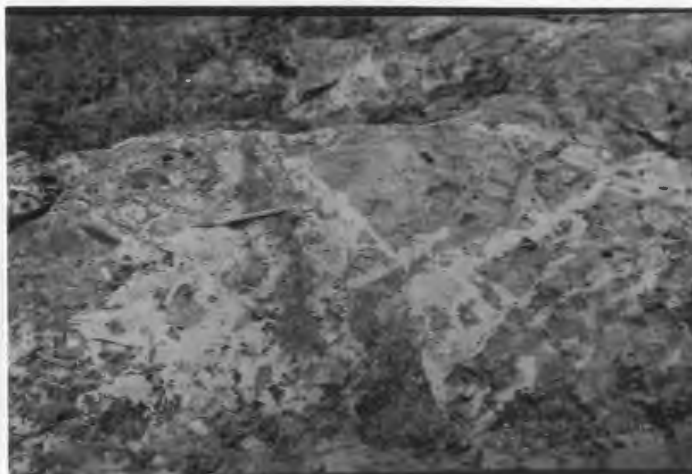
4.5.1. Variation Diagrams

The most important geochemical characteristics of the zones are illustrated in several variation diagrams (Fig. 4-10 and 4-11). Several samples have been somewhat arbitrarily, as opposed to statistically, defined as mineralized based on their Cu and Zn contents. Samples 127, 199a and 289 which have core and halo assemblages, have been excluded from this group due to their low metal contents.

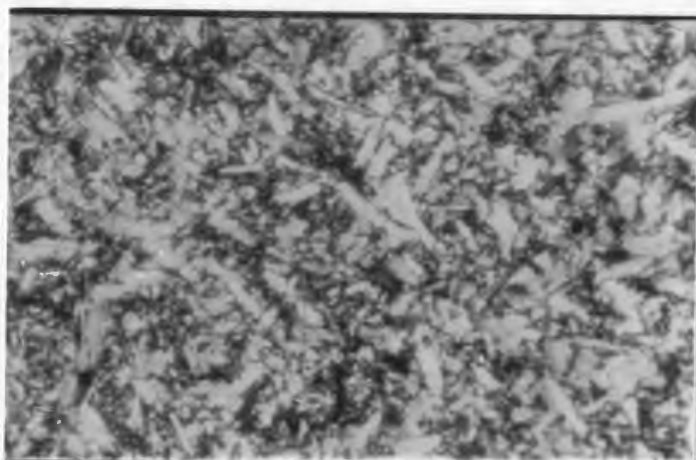
In Fig. 4-10a, Na_2O vs. $\text{FeO}(t)/\text{MgO}$, the mineralized samples fall into two groups which can be separated also on the basis of their Cu/Zn ratios. These groups do not correspond exactly to the two alteration zones but all the chlorite - quartz core rocks fall into the Cu-rich group along with some of the miscellaneous



a



b



c

Figure 4-9: Photographs of albite veins (in outcrop and thin-section)

(a) Sample 138a, XN, albite - quartz - calcite - sulphide vein - albite forms radial aggregates and needles which grow from the vein walls; (b) Pure albite veins brecciate sheeted dykes at CS-121; (c) Sample 121a, XN, thin-section of albite from these veins - minor relict actinolite in lower left-hand corner. Photo widths: (a,c) 0.75 mm.

samples. Copper-group rocks are those which have Cu/Zn ratios > 1 ; zinc-group rocks have Cu/Zn ratios < 0.18 . Any samples with Cu/Zn ratios between 1 and 0.18 would also belong to the Zn-group. The Cu-group samples have a high FeO(t)/MgO ratio and variable Na₂O contents. All samples from the core zone plot at the lower end of the trend. The Zn-group samples have about background FeO(t)/MgO ratios and more uniform high Na₂O values. The high FeO(t)/MgO ratios of the Cu-group rocks are responsible for their departure from the main trend on the Cr vs. FeO(t)/MgO diagram (Fig. 3-3d).

Some of this iron is contained in sulphides but most of it is contained in chlorite as evidenced by sample 289 which contains no visible sulphides but has a high iron content, and by the general correspondence between the FeO(t)/MgO ratios of the rocks and of the chlorites. The latter have been determined by electron microprobe and are presented in Appendix E. The FeO(t)/MgO ratios of the chlorites in the background rocks are largely related to the degree of maficity (as indicated by Cr) of the rocks. However, the chlorites of some samples are more iron-rich than would be expected for their Cr contents (Fig. 4-12). These samples are dominantly composed of chlorite and quartz with variable amounts of sulphide. They include several core area rocks and several sulphide-bearing samples collected from the dumps. Fig. 4-13 is a triangular plot of FeO vs. MgO vs. Al₂O₃ from the chlorites. The data points from background rocks generally plot nearer to the MgO corner; those from the mineralized samples plot over a wider range but tend to be iron-rich. Fields shown on the diagram are from Mottl (1983a). Chlorites from typical greenschist facies sea-floor basalts plot within field A. Field B represents greenstone breccias which consist of quartz, Fe-rich chlorite and minor sulphides. These breccias formed within an upflow zone of a hydrothermal system from fluids rich in Fe, Mn, Cu, Zn, H₂S, and SiO₂ and poor in Mg (Mottl, 1983).

Fig. 4-10b shows that the Cu-group samples are more depleted in CaO + Na₂O + K₂O than the Zn-group samples.

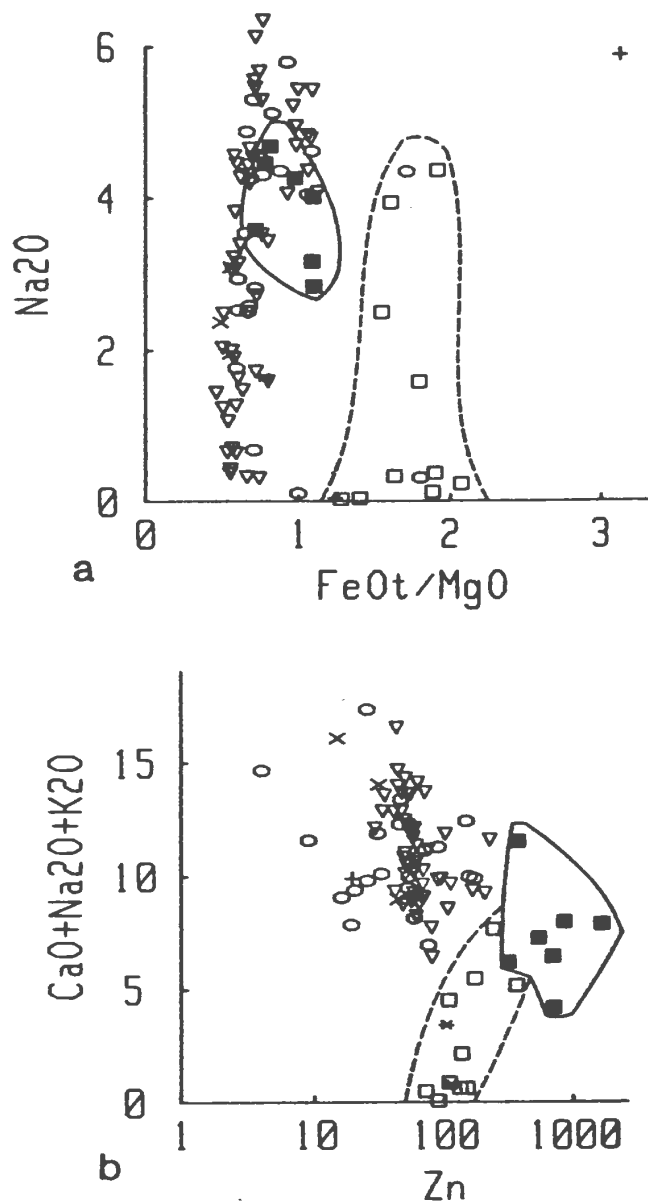


Figure 4-10: Variation diagrams

Symbols as for Fig. 3-1 except open squares are Cu-group and filled squares are Zn-group. (a) Na₂O vs. FeOt/MgO - Note high Na₂O contents and background FeOt/MgO of Zn-group rocks in contrast with variable Na₂O contents and high FeOt/MgO ratios of Cu-group rocks; (b) CaO+Na₂O+K₂O vs. log(Zn) - Note higher CaO+Na₂O+K₂O contents of Zn-group rocks.

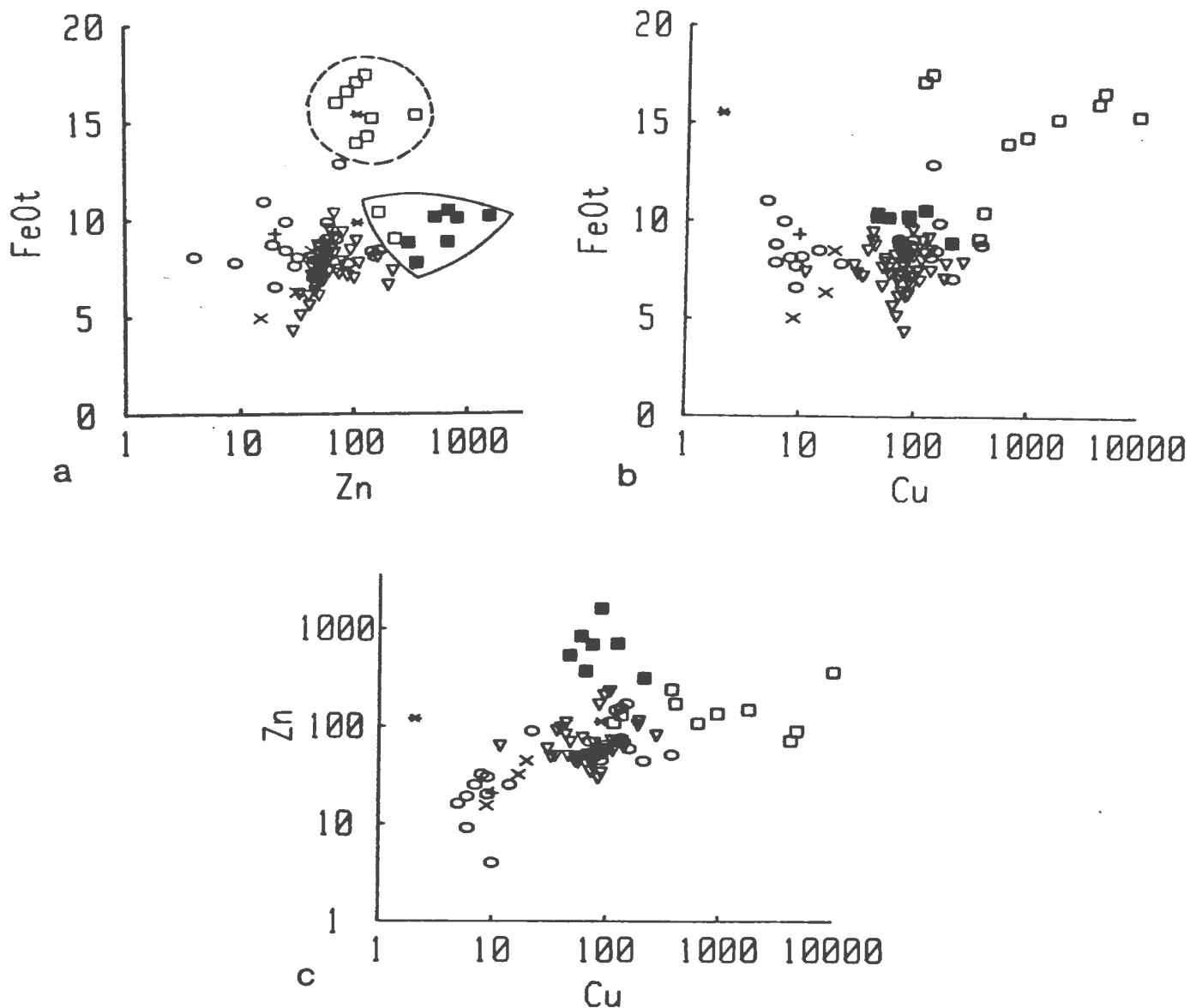


Figure 4-11: Variation diagrams

Symbols as for Fig. 4-10. (a) FeOt vs. $\log(\text{Zn})$ - Note high total FeO contents of most of the Cu-group samples and low Zn content of many of the dykes; (b) FeOt vs. $\log(\text{Cu})$ - Note low Cu content of many of the dyke samples; (c) $\log(\text{Zn})$ vs. $\log(\text{Cu})$ - Note negative relationship of Cu and Zn in mineralized samples in contrast with their positive relationship in background samples.

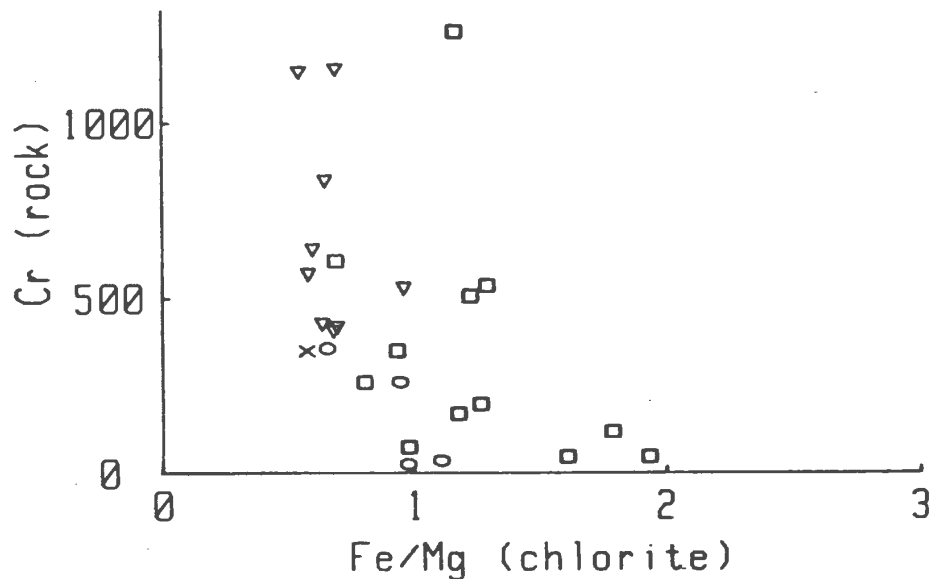


Figure 4-12: Cr (in whole rock) vs. Fe/Mg (in chlorites).

Symbols - triangles, background pillows; circles, dykes; x, gabbro; squares, core and halo alteration zone samples.

In Fig. 4-11a two of the Cu-group samples plot with those from the Zn-group because, although they have high FeO(t)/MgO ratios, they do not have the high total iron contents which characterize the core zone rocks. This diagram shows that there is a clearly defined trend of increasing iron with increasing Zn in the background pillow lavas. A similar trend is observed for the background pillow lavas in Fig. 4-10b. Samples with anomalously high Zn values plot to the right of this trend. There are also a number of samples which plot to the left of this trend. These are dyke samples plus two gabbro samples and a plagiogranite sample. Fig. 4-11b, log(Cu) vs. FeO(t), shows that although there is no clear trend involving the background pillows there are clearly anomalously low Cu concentrations among many of the dyke samples. The background pillow lavas have Cu values which average between 30 and 120 ppm. Copper values of dyke samples, excluding those denoted as mineralized (table 4-2), fall into three groups: (a) background - 70 to 93 ppm, (b) anomalously high - 133 to 372 ppm, (c)

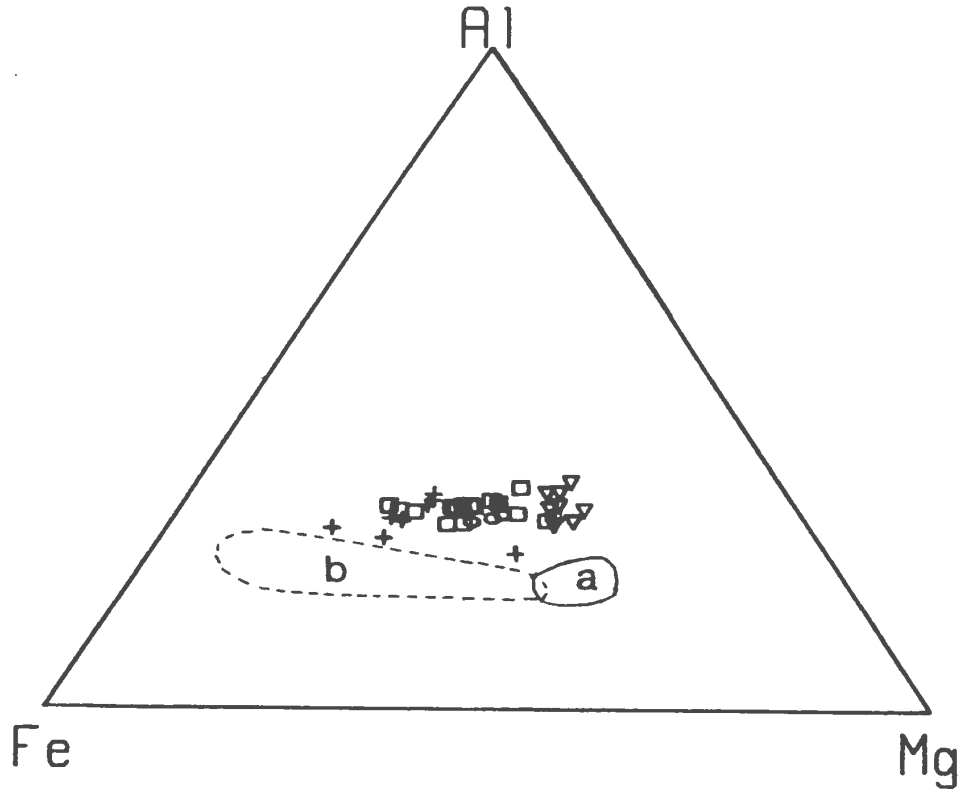


Figure 4-13: Triangular plot of FeO vs. Al_2O_3 vs. MgO in chlorites;

Symbols - triangles, background pillows; +, dykes; x, gabbro; squares, core and halo alteration zone samples; circles, massive and stringer sulphide samples from the dumps; Fields a and b from Mottl (1983a); Chlorites from typical greenschist facies sea-floor basalts plot within field a. Field b represents greenstone breccias which consist of quartz, Fe-rich chlorite and minor sulphides. (see text)

anomalously low - 5 to 22 ppm. Zn values of the latter group range from 4 to 32 ppm with one exception at 89 ppm.

Govett and Pantazis (1971) carried out a regional analysis of the distribution of Cu, Zn, Ni and Co in the pillow lavas and dykes of the Troodos Massif. They found that both Cu and Zn concentrations of background pillow lavas range from about 10 ppm to 160 ppm; the mean Cu and Zn concentrations ranged from 64 to 71 ppm and 51 to 59 ppm respectively. These values are similar to those denoted

Table 4-2: Cu and Zn concentrations in dykes

sample	Cu(ppm)	Zn(ppm)	act/cpx

anomalously low			

106a	5	16	act
121c	6	9	act
27a	6	19	act
121b	7	25	act
34b	8	32	act
273	9	20	act
129	9	30	act
106b	10	4	act
263a	14	25	act
89a	22	89	act

background			

89b	70	70	cpx
34a	89	52	cpx
251	90	45	cpx
269a	93	58	cpx

anomalously high			

197b	120	146	both
194	133	154	cpx
201a	134	75	act
197d	148	170	act
269d	157	59	act
112	209	44	cpx
130b	372	51	act

act = actinolite, cpx = clinopyroxene

as background in this study. The concentration of Cu and Zn in Group C dykes is clearly very low when compared to average values for Betts Cove and Troodos.

The low metal values of this group have been interpreted as the result of leaching of Cu and Zn from the rocks by circulating seawater, with the leached Cu and Zn re-deposited in the massive sulphide body. Support for this hypothesis lies in the alteration history of the samples. The metal-poor group of samples all

have actinolite predominant over clinopyroxene, but the background dyke samples have abundant clinopyroxene. The samples with high Cu values may have either mineral dominant. The implications of this are discussed in paragraph 4.5.4.2.

Fig. 4-11c illustrates the negative correlation between Cu and Zn in the core and halo alteration samples, which indicates that these elements were separated during the mineralizing process. This is important as it implies that the separation of Cu and Zn in the massive sulphides is a primary feature and not the result of remobilization by later shearing. Rocks in the alteration zones near the mine have not been tectonized.

4.5.2. Comparison With Other Deposits

4.5.2.1. Eurasian Ophiolite Deposits

The alteration in the core zone is very similar to that found in the stockwork zones of many massive sulphide deposits in Cyprus as described by Constantinou (1980). He found that an assemblage of chlorite, quartz, kaolinite and illite was prevalent in this zone and concluded that CaO, Na₂O and, to a lesser extent K₂O, had been leached from the rock. Varying amounts of alumina were also leached from the stockwork zone. Although the abundance of free silica in the rock increased, Constantinou (1980) attributed this to removal of CaO, Na₂O and K₂O and suggested that the rock may have actually lost silica. Iron, Cu, Zn and Co values increased considerably in the stockwork zone. The ratios of the minor elements in the stockwork zone are similar to their ratios in the overlying massive ore but quite different from their ratios in the background lavas. This supports the interpretation of the genetic relationship between the stockwork zone and the massive sulphide zone (Constantinou, 1980).

4.5.2.2. Newfoundland Ophiolite Deposits

The Ordovician Lushs Bight Group, which contains ophiolitic pillow lava and sheeted dyke units contains numerous massive sulphide deposits, some of which were once mined. The chlorite schists which characterize these deposits are enriched in iron and water and depleted in calcium and silica (Papezik and Fleming, 1967).

Gale (1969) studied dispersion patterns of Cu, Zn, Ni, Co, Mn, and Na in the chlorite schist wall rocks of three of the Lushs Bight Group sulphide deposits (the Lady Pond, Little Deer, and Little Bay deposits). He found that Na decreased significantly in the wall rocks and that this decrease is gradual as the sulphides are approached. Copper is erratically enriched in the chlorite schist and mineralized zones; it is commonly enriched by more than an order of magnitude. Copper aureoles are present around all zones of copper mineralization but they fall off sharply within a few feet of visible Cu mineralization. Zinc shows erratic distribution in the chlorite schist and mineralized zones; it is locally several times higher than background. In places, Zn forms aureoles around zones of Cu mineralization. In most cases Mn does not show anomalous behavior, but in two drill holes from two different deposits a narrow Mn aureole was found around the ore zone. Nickel and cobalt values fall within the same range in the country rock, wall rock and ore zone for each profile, but they are more erratically distributed in the ore zone and individual positive anomalies can be related to sulphides.

Gale (1969) concluded that the Na was being removed from the rock and carried away by epigenetic hydrothermal pre-ore and/or ore-forming fluids. He also concluded that Zn and Cu were introduced by epigenetic hydrothermal fluids and that Zn and Cu were dispersed from the ore zone into the wall rocks. However, Mn, Ni and Co abundances were interpreted to reflect mainly the primary magmatic distribution of these elements with perhaps some modification in the ore zone by hydrothermal fluids. By analogy with the situation at Betts Cove there is little doubt that the fluids responsible for the Na depletion were directly responsible for the sulphide deposition.

The overall zone of anomalous behavior of Zn, Cu and Na was found to be not much larger than the zone of visible mineralization (anomalies extend no more than 25 feet beyond the zone of economic mineralization). The hydrothermal alteration is therefore of little use as an exploration tool (Gale, 1969)

Bachinski (1977a) reported chlorite - quartz alteration accompanied by sporadic K_2O enrichment at the Whalesback deposit in the Lushs Bight Group. He concluded that the clay minerals that are found in the stockwork alteration zones of deposits on Cyprus are absent from the alteration zone at Whalesback because of the higher metamorphic grade of the latter.

Duke and Hutchinson (1974) described alteration of lavas near sulphide mineralization at the York Harbour deposit in the Bay of Islands ophiolite. The most intense alteration resulted in an assemblage of calcite, amorphous or cryptocrystalline quartz and sulphide mineralization. Other common constituents are chlorite, plagioclase, epidote and accessory Ti minerals.

4.5.2.3. Canadian Archean Deposits

Many Archean deposits exhibit footwall alteration patterns characterized by a central core surrounded by a halo of differing alteration assemblages. Alteration below many deposits in the Noranda district consists of a pipe-shaped body in which a central chloritic zone passes outwards into a sericitic halo. This zonation also occurs on a smaller scale around veins (Gibson, 1979; Riverin and Hodgson, 1980; Franklin *et al.*, 1981). At the Millenbach deposit, in the Noranda district, a chloritic Cu-rich core is surrounded by a narrow sericitic Zn-rich stringer halo. The core zone is enriched in MgO and FeO and depleted in CaO and Na_2O ; the halo is depleted in the latter two oxides and is enriched in K_2O . At the Garon Lake deposit MacGeehan (1978) has documented two types of alteration: (1) a spilitic type characterized by an assemblage of albite - actinolite - epidote - quartz - chlorite; (2) silicic veinlets surrounded by zones of quartz - albite and quartz - epidote and circular quartz - epidote patches. He suggested that the quartz - epidote zones were solution channels through which the heated fluids moved.

4.5.2.4. Summary

The similarity between alteration zones at Betts Cove and those of other deposits leads to the conclusion that these zones represent a footwall alteration pipe through which evolved hydrothermal solutions upwelled immediately prior to their exhalation onto the seafloor. Bachinski (1977a) reached a similar conclusion about the alteration zone at Whalesback.

The Archean alteration zones differ from those of the Betts Cove deposit in that they are enriched in K_2O and in MgO . The latter is found in chlorites which are Mg-rich whereas those at Betts Cove, Whalesback (Bachinski, 1977a) and other deposits in the Lushs Bight Group (B. Kean, pers. comm., 1984) are Fe-rich. Talc is an abundant constituent of some Archean footwall alteration zones, whereas it is rare in the footwall alteration at Betts Cove.

4.5.3. Discussion

4.5.3.1. Experimental Studies

Many geologists now accept the hypothesis that ocean floor, and hence ophiolitic, massive sulphide deposits form as a result of exhalation onto the seafloor of metal-bearing hydrothermal solutions which convectively circulate through the ocean crust; the fluids (initially cold seawater), which become heated and modified as they pass through the rock column, leach metals from the rocks and transport them to the surface where they precipitate as metalliferous deposits. These ideas have evolved through the work of Helgeson (1964, 1969), Bostrom and Peterson (1966), Bischoff (1969), Degens and Ross (1969), Bender *et al.* (1971), Corliss (1971), Sillitoe (1972), Upadhyay and Strong (1973), Spooner and Fyfe (1973), Dymond *et al.* (1973), Andrews and Fyfe (1976), Spooner (1977, 1980), Parmentier and Spooner (1978), Rona (1978, 1980) and Rona and Lowell (1980) among many others, on natural ridge systems, the Red Sea and ophiolites. Evidence that seawater is the dominant component of the hydrothermal fluids comes from hydrogen, oxygen, strontium and sulphur isotope studies on ophiolites

and their deposits e.g. Spooner et al. (1974), Chapman and Spooner (1977), Spooner (1977), Spooner et al. (1977a), Spooner et al. (1977b), Heaton and Sheppard (1977), and Bachinski (1977b).

Insight into the chemical exchanges which take place between seawater and the rock column as seawater circulates through the crust have come from experimental work. The experiments of Bischoff and Dickson (1975) and Hajash (1975) demonstrated that upon reaction with basalt rock or glass seawater changes from an oxygenated slightly alkaline Na-Mg-SO₄-Cl solution to a reducing, acidic, metal-bearing Na-Ca-Cl solution. Almost all Mg²⁺ and SO₄²⁻ are removed from solution. Bischoff and Dickson (1975) proposed that it is incorporation into montmorillonite of Mg²⁺ along with OH⁻, leaving H⁺ behind, that controls and lowers the pH. This idea was supported and refined by a series of later experiments, Seyfried (1977), Seyfried and Bischoff (1977, 1979, 1981), Mottl and Holland (1978), Mottl et al. (1979), Hajash and Chandler (1980), and Seyfried and Mottl (1982) in which rock and glass samples (dominantly of basaltic composition) were reacted with seawater and artificial solutions at varying temperatures and water/rock ratios of 1 to 125. The seawater/rock ratio as used in the experiments is the initial mass of unreacted seawater divided by the initial mass of fresh rock. It will be hereafter abbreviated "w/r".

The most important findings of the experiments are:

1) At temperatures from 150° to 300°C Mg²⁺ is rapidly removed from seawater and incorporated into alteration minerals most likely in the form of an Mg(OH)₂ component.

2) Removal of OH⁻ from solution into the rock results in production of H⁺ and a rapid drop in pH.

3) Addition of Mg²⁺ to the rock is accompanied by removal of Ca²⁺, K⁺, Fe²⁺, Mn²⁺, Cu²⁺, Zn²⁺ and Sr²⁺ into solution in response to charge balance constraints.

4) Na^+ is added to the rock at w/r ratios < 5 but is leached from the rock at w/r ratios > 10 .

5) SO_4^{2-} is removed from seawater by reduction and by combining with leached Ca^{2+} to form anhydrite.

6) Basaltic rock has the capacity to remove all Mg^{2+} from an amount of seawater 50 times its own mass. This has led to a distinction between rock-dominated conditions, which occur at w/r ratios < 50 , and seawater-dominated conditions, which occur at w/r ratios > 50 . A constant supply of Mg^{2+} is necessary to maintain a seawater-dominated system.

7) A low pH, which enhances metal solubility, is maintained under seawater-dominated conditions, but under rock-dominated conditions the initially produced H^+ is consumed by silicate hydrolysis reactions and pH rebounds to near neutrality.

8) Rock-dominated conditions result in a complex assemblage of secondary minerals whereas seawater-dominated conditions, because of the acidity, result in smectite, mixed layer clay, or chlorite, and quartz, hematite and anhydrite.

9) At higher temperatures, 400-500 °C, high acidity is maintained even under rock-dominated conditions. At these temperatures Ca^{2+} addition to secondary silicates produces H^+ in a manner analogous to Mg^{2+} addition at lower temperatures.

4.5.3.2. Application of Experimental Results to the Present Study

Assemblages in the Betts Cove alteration zones correspond remarkably well to those illustrated in Fig. 4-14 from Mottl (1983a). This diagram was constructed by Mottl based on chemical data from experiments in which basaltic rock and glass was reacted with seawater at a temperature of 300 °C, pressures of 500 to 600 bars and w/r ratios of 1, 3, 10, 50, 62 and 125 (Mottl and Holland, 1978;

Mottl *et al.*, 1979; Seyfried and Bischoff, 1981 and Seyfried and Mottl, 1982) combined with data on mineral assemblages and mineral compositions from rock at the Mid-Atlantic Ridge (Humphris and Thompson, 1978a). These experiments were successful in duplicating the chemistry of natural solutions from the Reykjanes Peninsula, the Galapagos Rift at 86 degrees west and the East Pacific Rise at 21 degrees north, but they failed to duplicate the mineralogical changes which occur in natural systems. Specifically, the experiments failed to produce epidote and produced smectite or mixed layer smectite-chlorite instead of the chlorite which forms in nature. Seyfried and Bischoff (1981) attributed these discrepancies to kinetic problems, i.e. more time would be needed to form these minerals. Mottl constructed the diagram in Fig. 4-14 to fit assemblages that form in nature rather than those that form in the laboratory. It "assumes that a rock sample can be treated as if it were altered over a restricted temperature range by a batch process" (Mottl, 1983a).

The diagram illustrates that at low w/r ratios (2-35) and a temperature of 300 °C an assemblage of chlorite - albite - epidote - actinolite - quartz is stable. This is the background spilitic alteration assemblage in the Betts Cove area. At w/r ratios from 35 to 50 an assemblage of chlorite - albite - quartz is stable. This plus calcite is the dominant assemblage in the outer halo of mineralization-related alteration. At w/r ratios > 50, an assemblage of chlorite - quartz, the core zone minerals, is stable.

The distribution of these zones at Betts Cove is readily explained by the geometry of sub-seafloor convection cells. Fig. 4-15 (Spooner, 1977) shows the typically envisioned system and Fig. 4-16 (Parmentier and Spooner, 1978) shows the flow geometry of the system. Flow through areas of downwelling or recharge is diffuse, whereas flow through areas of upwelling or discharge is commonly focussed along faults, fractures and permeable zones. Theoretically, highest fluid flux would occur in the core area of the zone of upwelling fluids; fluids in this core area would be hot and metal-rich (Parmentier and Spooner, 1978). The high flux

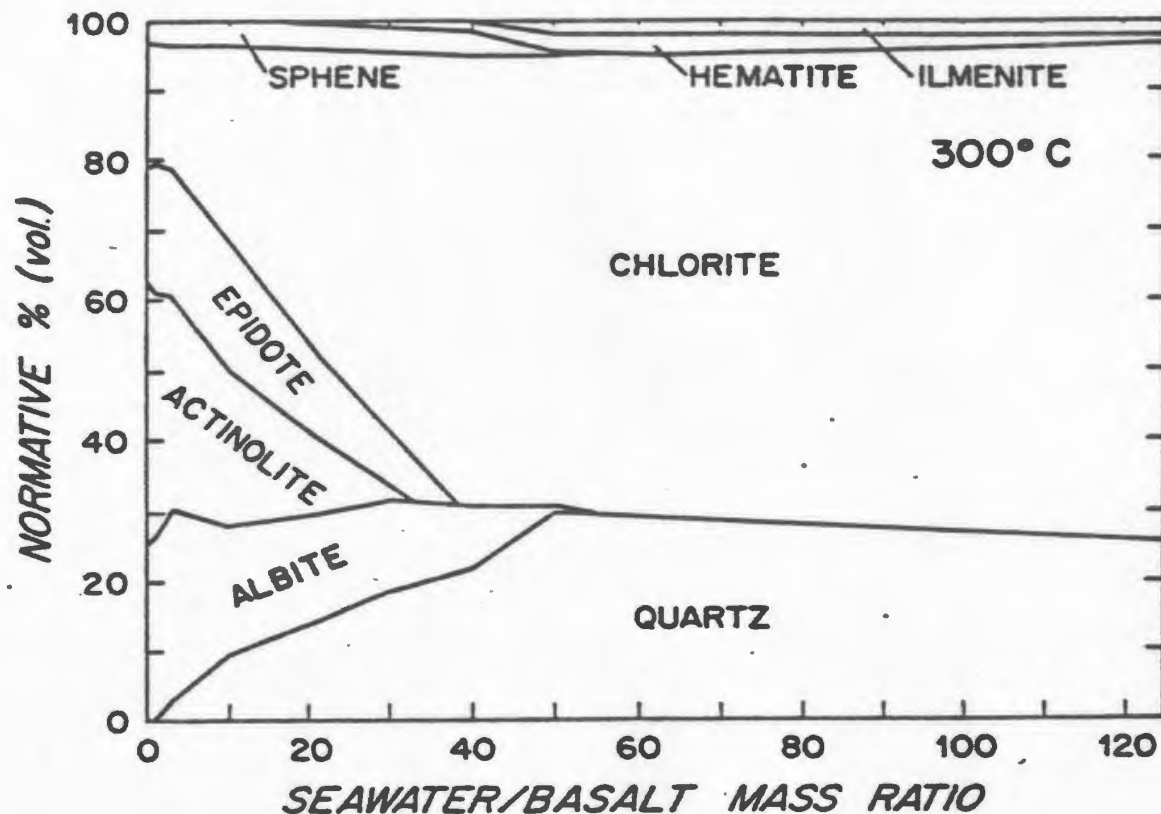


Figure 4-14: Alteration assemblages produced by varying water/rock ratios

From Mottl (1983a); based on experiments in which water and basaltic rock or glass were reacted at 300 °C, 500 to 600 bars and w/r ratios of 1, 3, 10, 50, 62 and 125. See text for explanation and references.

through the core zone at Betts Cove has resulted in seawater-dominated conditions i.e. a chlorite - quartz assemblage. Rocks in the halo zone were produced in an area of lower fluid flux and therefore a lower w/r ratio. Because flow through the downwelling part of the system was diffuse, the w/r ratio was low and the background spilitic assemblage was stable.

As discussed in paragraph 4.5.4.1, the incorporation of Mg^{2+} and Ca^{2+} into secondary silicates is important for H^+ generation and metal leaching. The dominance of actinolite over clinopyroxene in dykes which have anomalously low

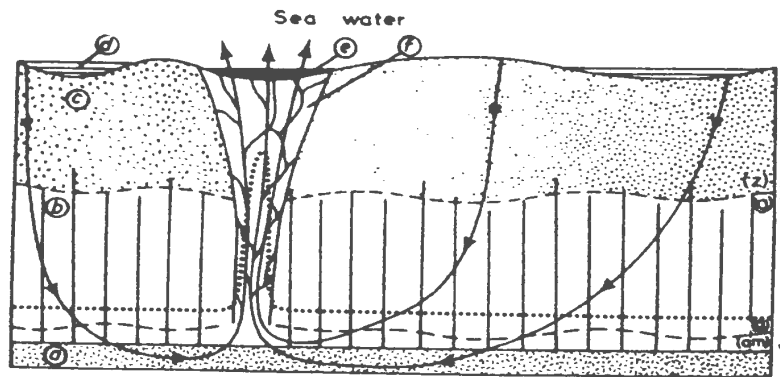


Figure 4-15: Sub-seafloor convection cell model

Model of Spooner (1977) for circulation of seawater through the ocean crust; (a) gabbro, metagabbro and variably altered trondhjemite; (b) sheeted dyke complex; (c) pillow lavas; (d) umbers; (e) massive sulphide ore; (f) mineralized stockwork. Dashed wavy lines indicate boundaries between zeolite (z), greenschist (g) and amphibolite (am) facies metamorphism. Lines with arrows outline pattern of hydrothermal convection. Dotted line is approximate form of isotherm produced by convection (Elder, 1967).

Cu and Zn values has also been demonstrated (Table 4-2). The obvious conclusion to be drawn from this is that the alteration of clinopyroxene to actinolite, glass to chlorite and plagioclase to albite was accompanied by H^+ formation and metal leaching. It is probable that most of the Cu was leached from pyroxene and basalt glass and most of the Zn from feldspar, as has been suggested by Graf (1977) for the Bathurst area. The normal background values of Cu and Zn in clinopyroxene-rich dykes is a result of their lower degree of alteration owing to their higher degree of impermeability. The alteration and metal-leaching were part of the same process - interaction of diabase with seawater along the downwelling limb of a sub-seafloor convection system.

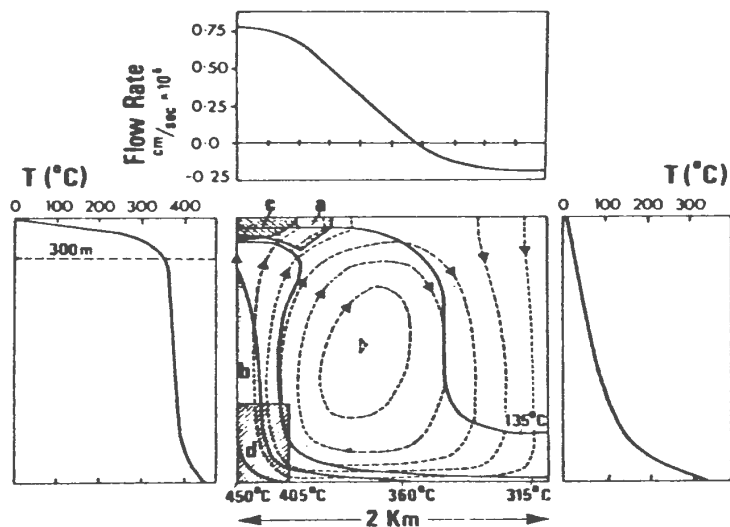


Figure 4-16: Flow geometry of sub-seafloor hydrothermal convection system

The central part of the diagram shows stream lines and isotherms for steady-state convection of a fluid with temperature dependent viscosity and coefficient of thermal expansion at a Rayleigh number of 50 (see Parmentier and Spooner, 1978 for mathematical calculations). Realistic absolute values of temperature are given for a maximum bottom temperature of 450°C . Area a = theoretical volume of most intense mineralization; area b = theoretical volume of maximum leaching; area c = approximate dimensions of the Limni mine (Troodos) stockwork; area d = approximate volume of basalt which would contain the copper contained in the Limni ore deposit. Temperature profiles along the vertical boundaries of the cell are shown on the left and right-hand sides of the central diagram. The vertical flow rate through the open upper boundary is shown above the central diagram. (from Parmentier and Spooner, 1978).

4.5.3.3. Natural Systems

The geochemical characteristics of fluids emanating onto the seafloor at Galapagos and the East Pacific Rise (EPR) have been described by Edmond et al. (1979a,b) and Von Damm et al. (1983) respectively. At Galapagos fluid samples were collected from four different fields each of which has many individual vents. At EPR three fields were sampled. Samples from both areas show many similarities and some important differences.

Because temperature measurements are imprecise (+/- 0.5 °C) due to variable entrainment of ambient seawater in the sampler, measured elements were normalised to SiO₂ concentration (Edmond et al. 1979a,b) and Mg concentration (Von Damm et al. 1983). These components were chosen because they are easy to measure and they behave in a regular and predictable manner.

Most components showed an increase or decrease in concentration with increasing temperature. This is due to mixing of hot end-member solutions with ambient seawater both above and below the rock-water interface. Extrapolation of a mixing line determines the concentration of the element in the end-member solution. These concentrations have been determined by Edmond et al. (1979a,b) and Von Damm et al. (1983) and are presented in Table 4-3.

Fluids from both areas are devoid of magnesium and sulphate; consequently, concentrations of these two elements show an increase with decreasing temperature in response to addition of seawater. Their concentrations extrapolate to zero at temperatures near 350 °C, the temperature of the uncontaminated end-member solution.

Silica increases regularly with increasing temperature at both EPR and Galapagos. Its concentration in the end-member solutions at both sites is about 1290 ppm.

Lithium, rubidium and potassium in fluids from the EPR all show well defined

Table 4-3: Concentrations (ppm) of components in modern vent solutions at EPR and Galapagos

Component	EPR	Galapagos
SiO ₂	1286	1310
Mg	0	0
SO ₄	0	0
Li	7.3	4.8-7.9
K	978	735
Rb	2.2	1.1-1.7
Ca	862	986-1611
Sr	8	
Mn	55	20-63
Fe	100	max-1.3
Zn	7.2	n.d.
Cu	max-0.95	0
Ni	n.d.	0
Ba	n.d.	2.3-5.9

References: EPR - Von Damm et al., 1983;
Galapagos - Edmond et al., 1979a,b

linear trends, increasing with increasing temperature. Results from Galapagos are similar except that increase of K and Rb is less pronounced. Von Damm et al. (1983) suggested that at Galapagos some of the K and Rb may have been removed into the sub-surface wall rocks prior to exhalation of the solution.

Calcium increases with increasing temperature, but its concentration at EPR is lower than at Galapagos where it varies from 986 to 1611 ppm in the four fields.

Edmond et al. (1979b) found that strontium remained constant within analytical resolution at Galapagos, but Von Damm et al. (1983) reported that it showed a small ($< 5\%$) increase with increasing temperature at EPR.

Barium was only reported from Galapagos where at one of the fields it increased very sharply with increasing temperature; its increase at the other fields was less pronounced and indistinguishable among the three fields.

Chlorine showed both increasing and decreasing trends in the different fields at both sites. Sodium is difficult to measure therefore Edmond et al. (1979b) and Von Damm et al. (1983) calculated it based on charge balance constraints. Both elements behave in a similar fashion; their absence from some of the measured solutions requires that there be a "sink" within the underlying rock column. At present the identity of the Cl sink is not known, although Von Damm et al. (1983) suggested that it is removed into an insoluble mineral with Fe or Mg as a cation. Sodium is added to the rock during normal sub-sea metamorphism.

Metal Contents

Galapagos

Edmond et al. (1979b) reported that at Galapagos measured concentrations of Cu, Ni and Cd decrease in vent waters with increasing temperature. Zinc was apparently not determined. Their concentrations extrapolate to zero at temperatures between 10° and 30° C. Edmond et al. (1979b) suggested that these elements are removed from the hydrothermal fluids into sulphides which precipitate as a result of their sub-surface mixing with cold groundwater. The extrapolated temperatures are thus interpreted as characteristic of a sub-surface reservoir of mixed fluids from which the vent waters have been drawn.

The behavior of Fe in the Galapagos vents was found to be highly variable. In two vents it increased with increasing temperature, but in the other two it increased to a maximum and then decreased. The interpretations of this behavior were hampered by lack of knowledge about the exact form of the Fe, whether reduced or oxidized, dissolved, particulate or colloidal, but it is evidently being precipitated in the conduit (Edmond et al., 1979b).

Manganese increases with increasing temperature in all four fields at Galapagos. It is not involved in sulphide precipitation in the conduit, but it may be scavanged by clays in the reaction zone (Edmond et al., 1979b).

East Pacific Rise

Fluids at EPR contain 7.2 ppm Zn and 0.95 ppm Cu. The Zn/Cu ratio is much higher than in average basalts where it is about unity. Von Damm et al. (1983) concluded that either Zn is being preferentially mobilized for reasons that are not clear or that Cu is being fractionated into sulphides which precipitate in the conduit. The latter process has occurred at Betts Cove.

Data for Fe from EPR show a degree of scatter as a result of sulphide precipitation after sampling, but its concentration in the endmember can be estimated at about 100 ppm. Mn concentration is about 55 ppm. The Fe/Mn ratio in the fluids at EPR is lower than it is in the average basalt. Von Damm et al. (1983) proposed that ferrous iron is incorporated into silicates or chlorides or precipitated as insoluble oxides during sulphate reduction but that its separation from Mn is unlikely to be a primary hydrothermal effect due to their similar behavior. However, there is a big difference in their behavior depending on oxidation state. Iron forms sulphides easily whereas Mn does not, therefore the Fe is probably being removed into sulphides in the conduit.

4.5.3.4. Implications for Betts Cove

At Betts Cove almost all of the Na_2O , CaO and Sr have been removed from the rocks in the core of the conduit. Hydrothermal fluids emanating from the conduit during the leaching process would be expected to be enriched in these components. Ca increases with increasing temperature in the modern vents and Sr shows a slight increase at EPR. This means that they are being removed from some portion of the rock column. The emanating fluids as predicted have a low pH; this is consistent with leaching of these components from the alteration pipe. However, although Na_2O increases with increasing temperature in some vents, it shows the opposite behavior in others which indicates that the fluids are completely devoid of it. This may be because all the Na_2O has already been completely removed from the conduit. It may also mean that it is being precipitated in the sub-surface, perhaps in a unit such as the "felsite" of Grenne *et al.* (1980) or in veins such as those found near the mine site at Betts Cove (Fig. 4-9b).

Barium concentrations increase with increasing temperature in the Galapagos vents. Barite is actually being precipitated from white smokers on the EPR (Edmond, 1982). The behavior of Ba in the alteration pipe at Betts Cove is unexpected. It should be leached from the conduit along with Ca , Na and Sr but it does not show any depletion.

K_2O values in the core of the alteration pipe are very low, but the background levels are also very low so it is difficult to accurately judge its behavior.

The pattern of mineralization at Betts Cove is consistent with the arrival of hot, relatively undiluted acid metal-bearing solutions at the seafloor. There was some degree of metal precipitation in the conduit itself and in its halo of alteration.

The formation of massive sulphide deposits implies that flow rates were high enough to enable the fluids to locally dominate conditions; thus, in the immediate area of the vents reducing conditions would prevail (Edmond *et al.*, 1979b).

The return to oxidizing conditions upon cessation of hydrothermal activity would result in corrosion of the sulphides; preservation would consequently require rapid burial. Burial of the Betts Cove deposit by pillow lavas must have taken place soon after it formed. This is supported by the apparent absence of an ochre horizon and the general lack of sedimentation within the ophiolitic pillow lava unit.

4.6. Fluid Inclusions

4.6.1. Introduction

Over 30 fluid inclusion sections were cut (see Appendix F). Although quartz in most of the sections contains fluid inclusions only seven sections contain inclusions large enough for microthermometric studies. However, inclusions in the other sections and in several polished thin-sections were observed under high magnification using an oil immersion lens. Quartz in samples 202b, 9d, 2, 1, 59, 117, 61 and 200a occurs with sulphides or with the distinctive alteration assemblages associated with mineralization. Quartz in samples 202a, 138b and 200a has been affected by later tectonism. Samples 139c, 139d, and 51a are from open space-filling vuggy quartz veins which are located in the mineralization-related alteration zone. Sample 141 is calcite from a tension gash in the same area. Samples 269e and 216d are from similar veins outside this zone. Such vuggy quartz appears to be filling tensional regimes which developed as a result of post-mineralization faulting.

4.6.2. Description of Inclusions

Most of the quartz samples examined contain abundant small fluid inclusions. The largest inclusions seen were about 70-80 microns across but most range between 5 and 20 microns. Those smaller were not even large enough for visual examination. An effort was made to determine whether the inclusions were primary or secondary but this was not always possible. In some samples the inclusions are aligned along growth zones (Fig. 4-17) and in others their long axes

are aligned (showing the growth direction) but not along one plane (Fig. 4-20a). The relationship of these inclusions to the growth direction of the crystal indicates that they are primary. Secondary inclusions concentrated on fractures occur in most samples and are generally too small to examine. In other samples inclusions are randomly distributed with no obvious planar arrangement; this may indicate that they are primary (Roedder, 1967a).

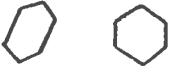
There are basically two types of fluid inclusions in the samples (1) simple two phase liquid-vapour inclusions (Fig. 4-18); (2) liquid-vapour plus one or more solid phases (Fig. 4-19 - 4-22). The former are always more abundant. Table 4-3 contains descriptions of the various solid phases.

The most commonly observed intra-inclusion solid phase is an acicular to prismatic crystal that exhibits moderate to high birefringence and moderate relief. It may be anhydrite. Another similar shaped mineral with little or no birefringence is also common. Both of these minerals were observed in the same inclusion in several samples (e.g. Fig. 4-21a). A more rectangular mineral with bright birefringence is probably a carbonate. A euhedral rhombohedral carbonate was seen in one inclusion in sample 269e but anhedral to subhedral carbonate crystals are more common. Several subhedral to euhedral hexagonal platelets (no birefringence-basal?) were observed especially in sample 202b. They may be bassanite ($\text{CaSO}_4 \cdot 1/2\text{H}_2\text{O}$) a close relative of anhydrite or they may be accidental inclusions of chlorite. An equant isotropic solid phase that resembles halite, although uncommon, was seen within fluid inclusions in various samples. An opaque euhedral hexagonal platelet (hematite) was seen in one inclusion in sample 269e. Another inclusion in this sample contains one, possibly two, opaque solid phases.

Table 4-4 summarizes the characteristics of the inclusions in the various samples.

In order to assess the importance of the solid phases it is necessary to determine

Table 4-4: Characteristics of fluid inclusion solid phases

No.	Shape	Biref.	Relief	Possible Minerals
1		med, high	high	anhydrite
2		low	med	unknown
3		med, high	med	carbonate, anhydrite
4		high	high	carbonate
5		none	med	bassanite, chlorite
6		none	high	halite
7		high	high	carbonate
8		opaque	high	hematite

All solid phases except #8 are colourless but may appear green (an artifact of the high magnifications used to examine them).

whether they were precipitated from the solution after trapping (in which case they are daughter minerals) or whether they were merely accidentally enclosed within the inclusion. Some of the solid phases found in the inclusions are obviously accidental but this cannot be conclusively demonstrated in all cases. Roedder (1967a, 1972) suggested that the best criterion for determining that a solid phase is actually a daughter mineral is regularity of phase ratios among a majority of inclusions. Each inclusion should contain one crystal of each daughter phase with which it is saturated. In some small inclusions supersaturation may

Table 4-5: Characteristics of fluid inclusions

Sample	solid phases	zoned or aligned	prim. sec.	sulph. related
216d	1,2,3,4,6			3,t
139d	1,2,3,6			2,t
139c	1,2,3,6			2,t
51a	3,6	g.z.	p	2,t
138b			s	2,sh
O-32		g.z.	p	2
141		cleavage	s	3,t
269e	1,4,7,8			3,t
200a	1,4,5,6		s	2,sh
202b	1,2,5,6	g.z.	p	1
202a	1,2	fractures	s	3,sh
1	1,4	g.z.	p	1
2	1,2			1
59	1			1
117	1			1
61	1			1
9d	1			1

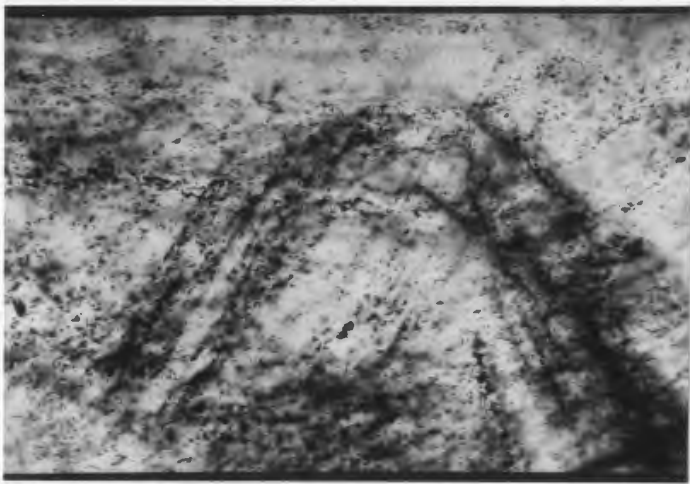
Numbers for solid phases refer to Table 4-3. g.z.-growth zones, sh-subjected to later shearing, t-fills tensional area of uncertain age w.r.t. mineralization, probability of inclusions being related to mineralization: 1-high, 2-uncertain, 3-low p-primary, s-secondary (where known)

persist but nucleation of the daughter should be able to be effected by cooling (Roedder, 1967a, 1972), or for carbonate or sulphate, heating the inclusion. Irregularity of phase ratios may mean that the solid phases are accidental especially if they are present as "free" solid inclusions in the host mineral.

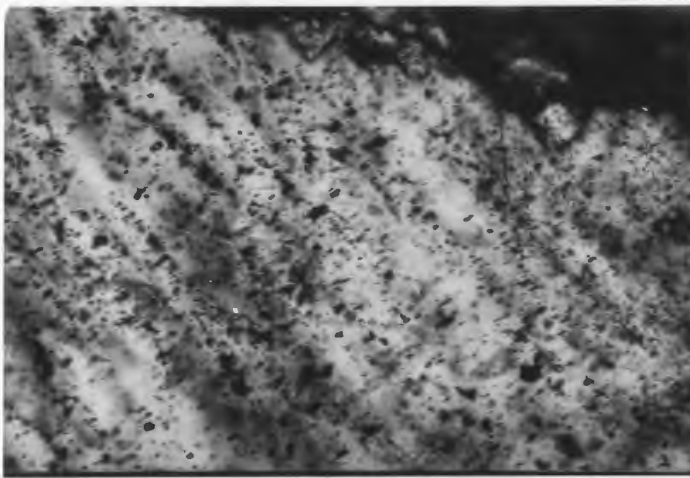
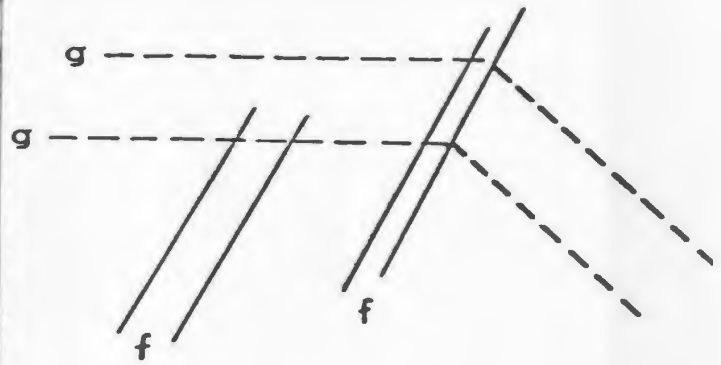
Solid phases in inclusions observed in this study exhibit variable phase ratios (Fig. 4-19 - 4-22). Rare inclusions contain three (or more ?) solid phases; others contain two, one or no solid phases. Heating or cooling the inclusions did not bring about nucleation of any additional phases. Higgins (1980) suggested that variations in ratios of solid phases could result from their dissolution with falling temperature but more probably mean that they are accidental inclusions.

This conclusion is favoured for this study for several reasons. First of all it is unlikely that the large variations observed could result from dissolution with falling temperature; such dissolution would affect all carbonate or sulphate daughter minerals. Secondly, calcite occurs alone as solid inclusions in quartz in many samples. "Free" sulphate or halite inclusions in quartz would be expected to dissolve if the quartz was subsequently bathed by fluids, hence their absence is not surprising. Thirdly, the variable phase ratios cannot be accounted for by different inclusion populations, because the homogenization and final melting temperatures fall into one population (Fig. 4-23a,b). Lastly, there is a problem in precipitating minerals which have retrograde solubility from cooling fluids. According to Holland (1967) in many situations calcite or sulphates cannot be precipitated from solutions by simple cooling but require loss of CO_2 or SO_2 from the system. If a homogenous fluid of moderate salinity was trapped and sealed by quartz then presumably carbonates or sulphates would not generally precipitate with falling temperature.

If a mineral is precipitated from a solution after trapping then it should be in equilibrium with that solution. For example, halite would be expected to dissolve with increasing temperature, whereas carbonate or sulphate would be expected to grow larger. During this study there was no observed change in size or shape of



a



b



Figure 4-17: Photomicrographs of growth zones in quartz

(a) Sample 202b, PL, growth zones {g} and fractures {f} in quartz; (b) Sample 51a, PL, growth zones in quartz. Photo widths: (a,b) 0.67 mm.

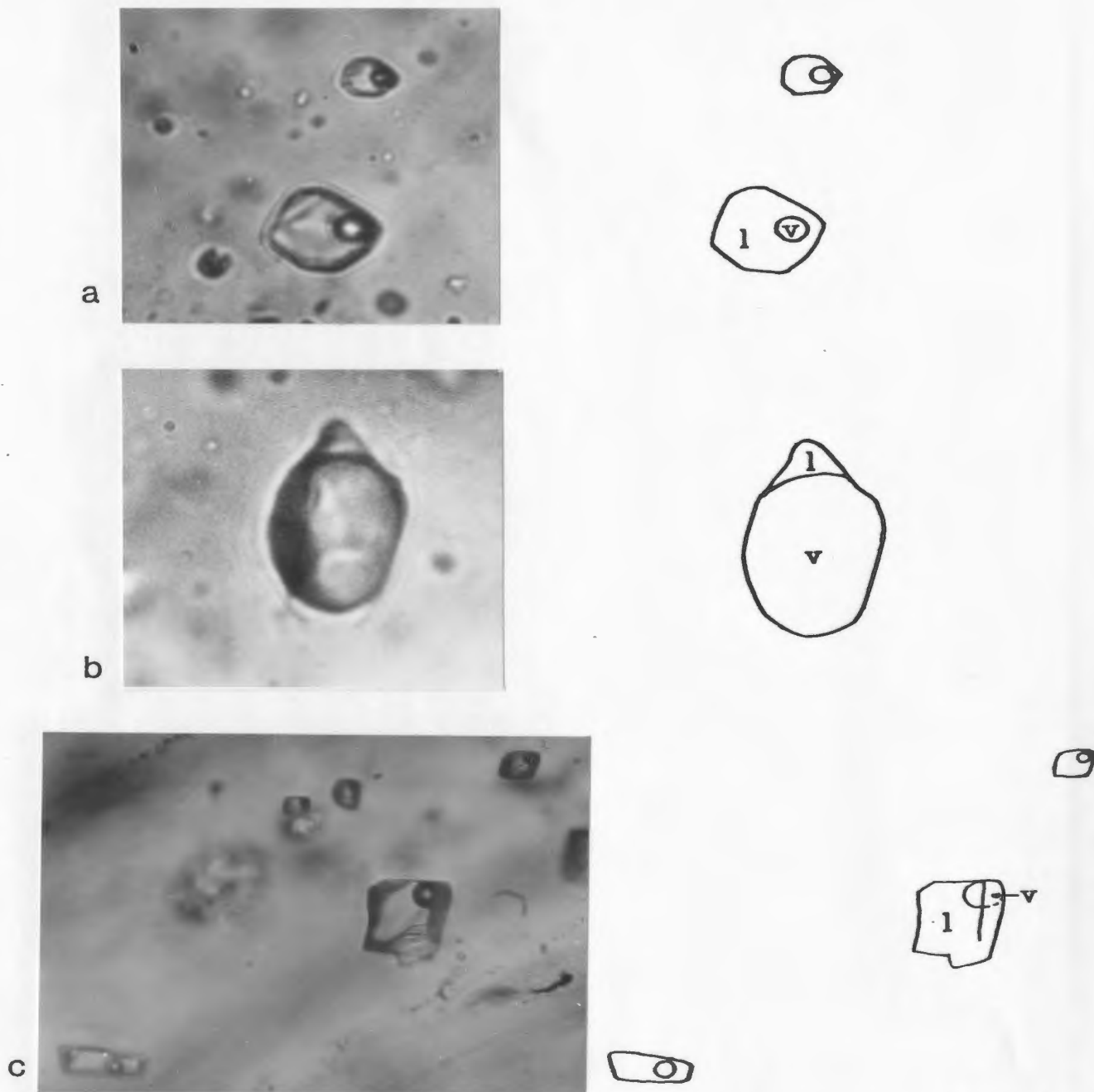


Figure 4-18: Photomicrographs of two-phase inclusions

(a) Sample 138b, PL, typical liquid-vapour {l-v} inclusions; (b) Sample 216d, PL, l-v inclusion with anomalously high v content; (c) Sample 141, PL, l-v inclusions in calcite. Photo widths: (a) 32 microns, (b) 23 microns, (c) 110 microns.

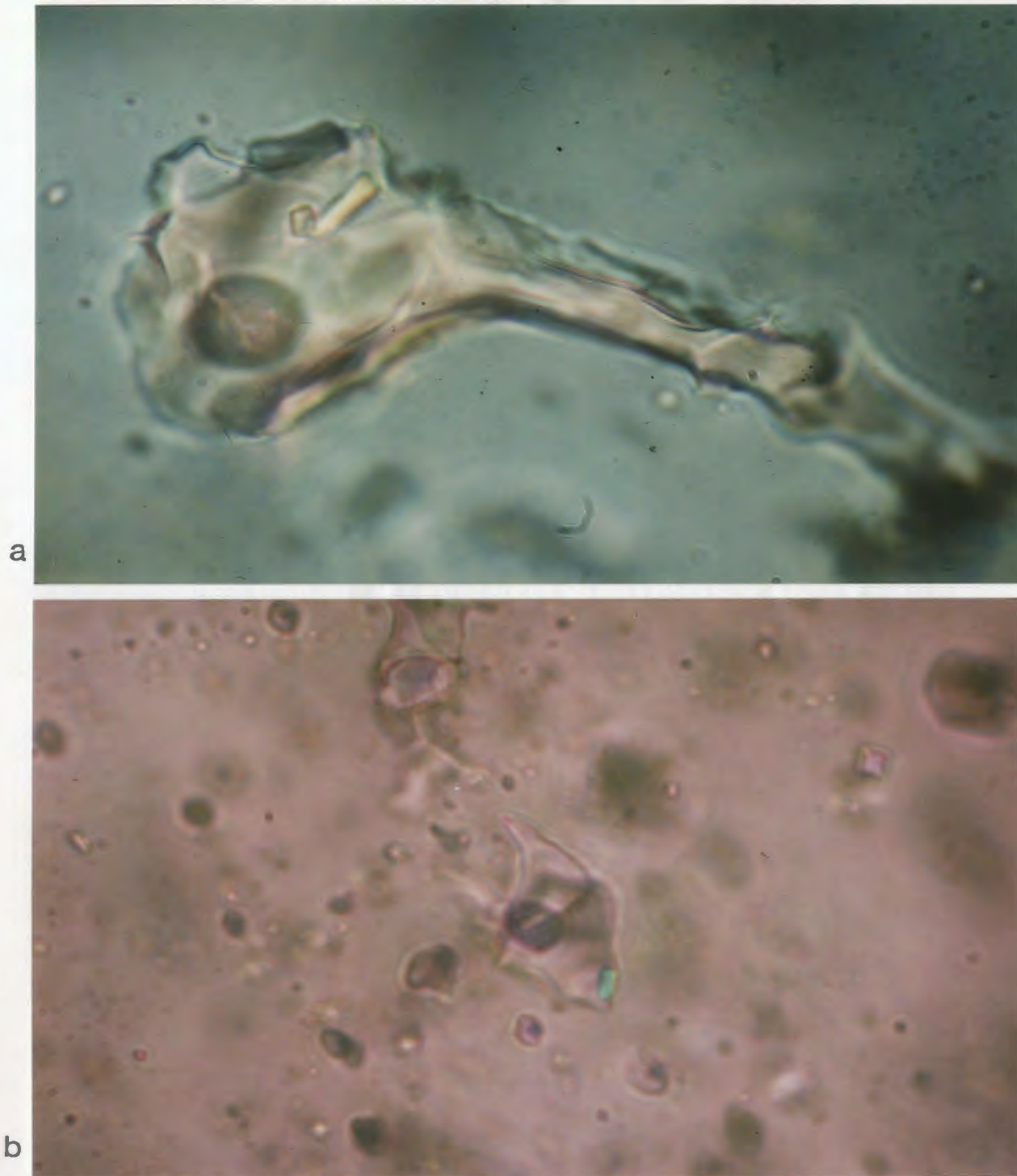


Figure 4-19: Photomicrographs of multiphase inclusions

(a) Sample 139c, XN, anhydrite (yellow) and halite (green) solid phases;
(b) Sample 216d, XN, anhydrite solid phase (green). Photo widths: (a,b) 78 microns.

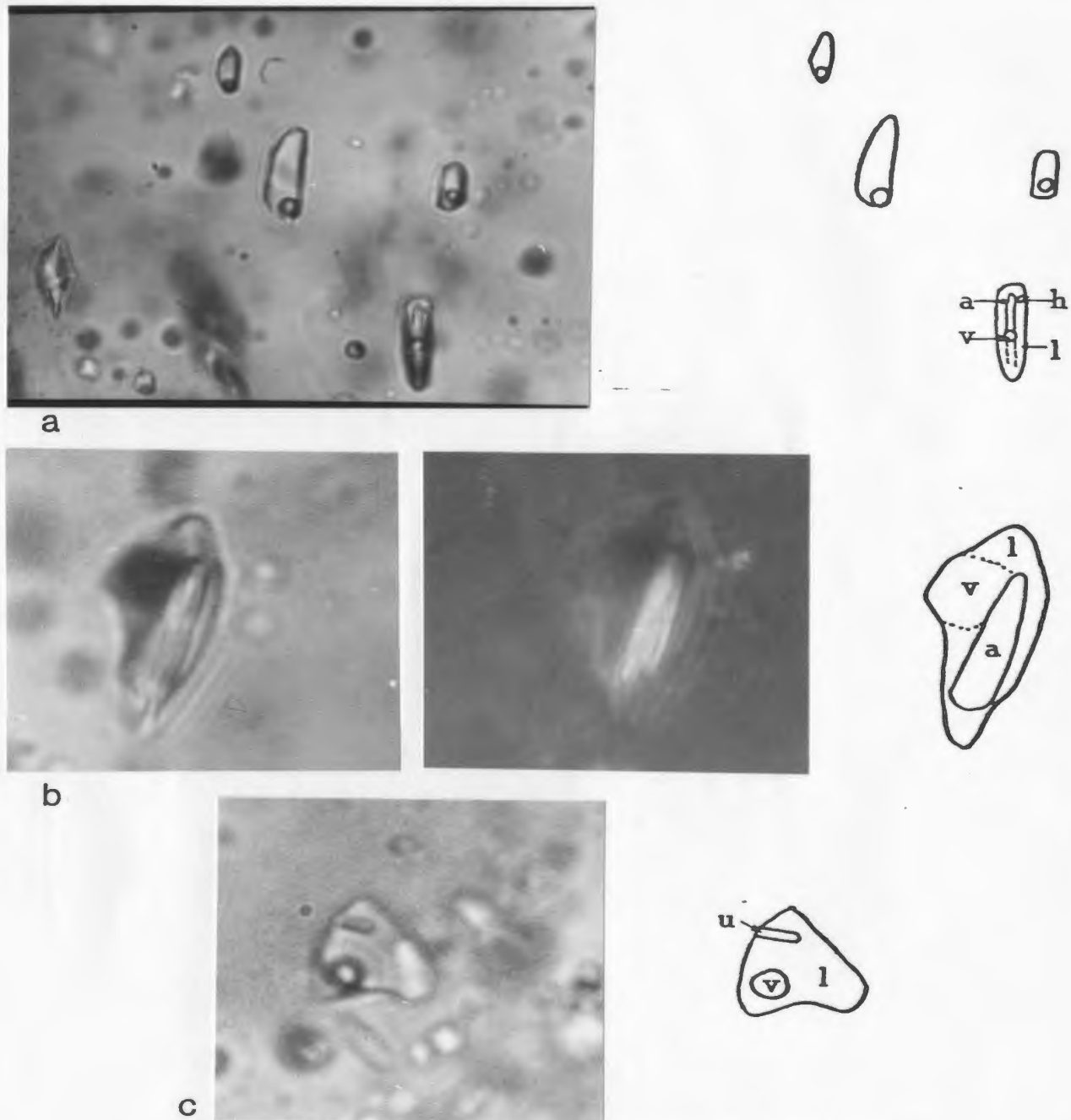


Figure 4-20: Photomicrographs of multiphase inclusions

(a) Sample 216d, PL, primary alignment of inclusions. Lowermost inclusion has an acicular {a} (anhydrite or the unknown) and an equant {h} (halite?) solid phase; (b) Sample 202b, left - PL, center - XN, anhydrite {a} solid phase in inclusion - bubble is out of focus behind solid; (c) Sample 202b, PL, acicular crystal {u} the unknown. Photo widths: (a) 55 microns, (b) 23 microns, (c) 15 microns.

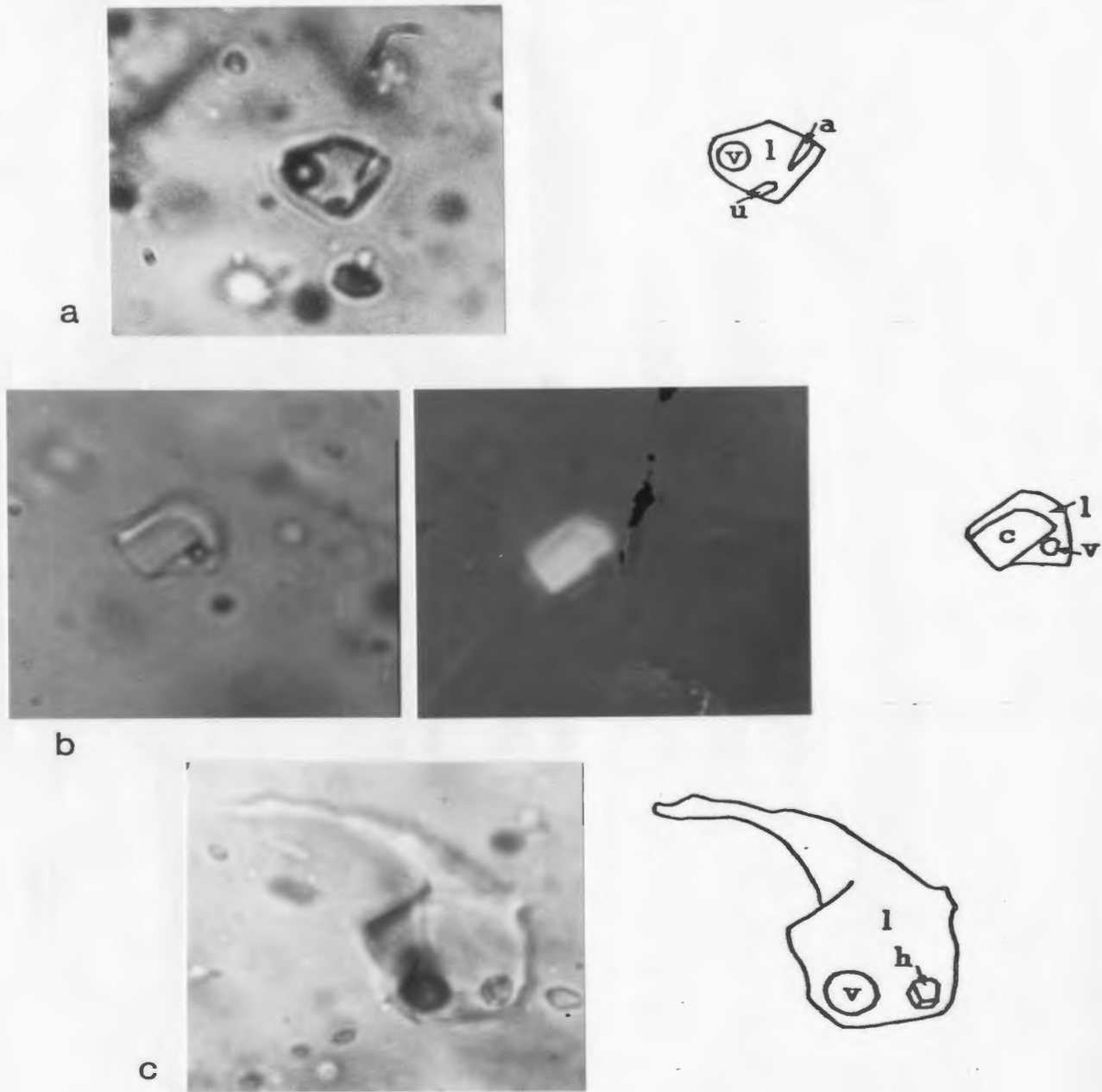


Figure 4-21: Photomicrographs of multiphase inclusions

(a) Sample 202b, PL, two solid phases - anhydrite {a} and the unknown {u}; (b) Sample 216d, left - PL, center - XN, rectangular platelet {c} (carbonate or anhydrite) in fluid inclusion; (c) Sample 216d, PL, inclusion containing halite cube {h}. Photo widths: (a) 23 microns, (b) 17 microns, (c) 27 microns.

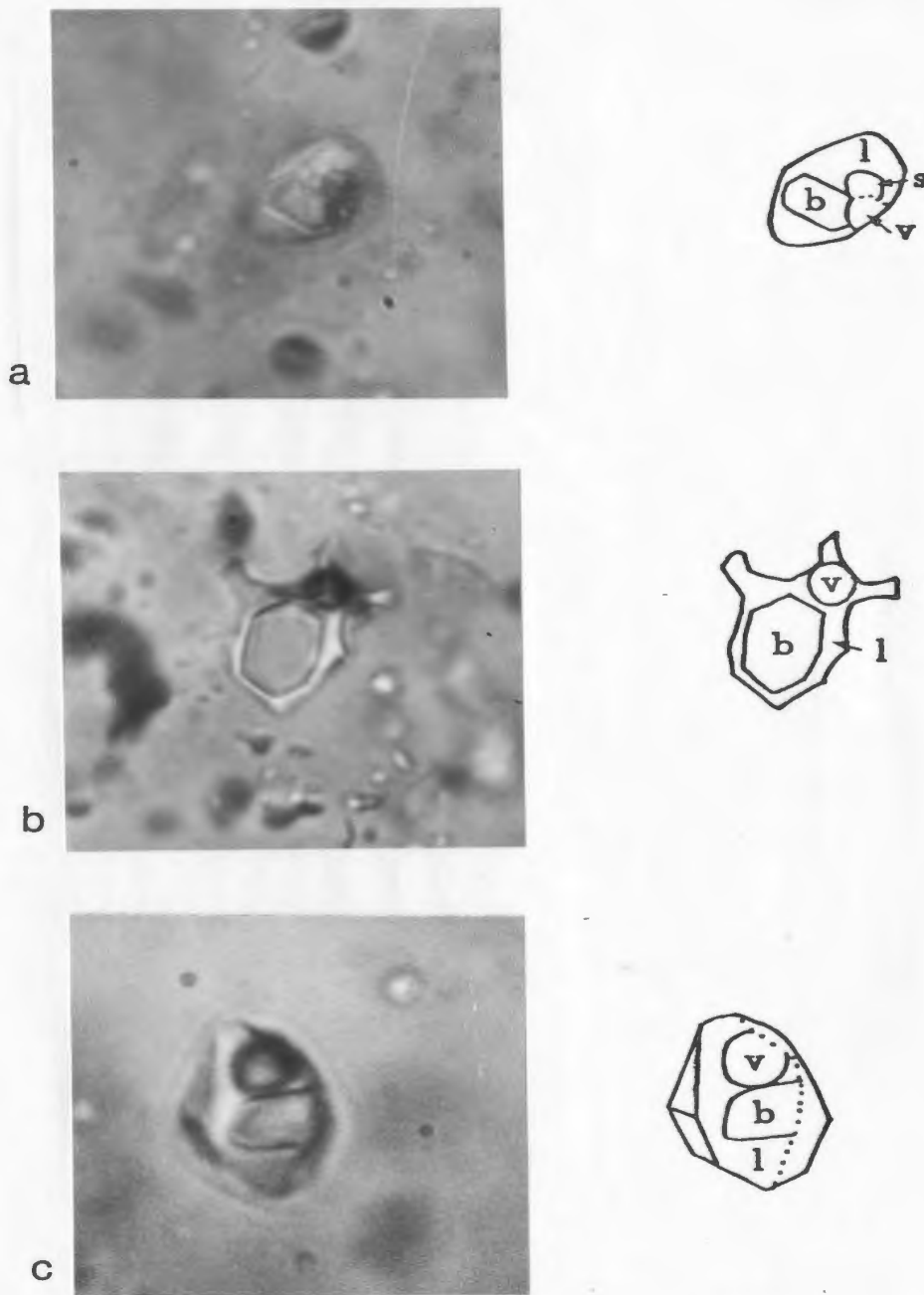


Figure 4-22: Photomicrographs of multiphase inclusions

(a) Sample 202b, PL, hexagonal platelet {b} (bassanite or chlorite) - there appears to be another solid phase as well {s}; (b) Sample 202b, hexagonal platelet {b} (bassanite or chlorite); (c) Sample 202b, PL, platelet {b} (bassanite or chlorite). Photo widths: (a,b) 27 microns, (c) 19 microns.

any of the solid phases upon heating and freezing of the inclusions. If the solid phases are indeed carbonates and sulphates then they should show an increase in size with increasing temperature even if they are accidental inclusions. Their failure to do so may mean the fluid is deficient in some components necessary for their growth (in which case they are certainly accidental inclusions). However, it is also possible that growth did occur but was undetectable due to the small size of the solid phases. Addition of even a slight, undetectable layer around the outside of a crystal of such small proportions would result in a large percentage increase in the volume of the phase.

4.6.3. Freezing Results

4.6.3.1. Fluid Composition

The most common ionic species in fluid inclusions are Na^+ , K^+ , Ca^{2+} , Mg^{2+} , Cl^- , SO_4^{2-} , CO_3^{2-} and HCO_3^- (Roedder, 1972), which are all components of seawater. It is not expected that there are any substantial amounts of any other ions in the fluid inclusions from the Betts Cove samples. Observation of the inclusions has shown no evidence for the presence of CO_2 as a separate liquid phase. Some limits can be placed on the composition of the fluids by observation of the initial melting temperature of the frozen material within the inclusion.

For natural chloride solutions the temperature of first melting should correspond to a eutectic, however, if the composition of the fluid lies far from the eutectic composition the amount of melt which forms may be very small and may be difficult to see (Crawford, 1981). For this reason the initial melting temperatures quoted here may in some cases only be upper limits on the eutectic temperature. The freezing temperatures of the solutions upon cooling, although affected by supercooling, can be thought of as a lower limit on the eutectic temperature and have been recorded for such purposes. They are hereafter referred to as spontaneous freezing temperatures to avoid confusion with final melting temperatures.

Eutectic temperatures for common chloride species are given in Table 4-6.

Table 4-6: Eutectic temperatures of aqueous chloride systems

Dissolved Species	Te ° C	Ref	Dissolved Species	Te ° C	Ref
NaCl	-20.8	1	NaCl-CaCl ₂	-52.0	2
KCl	-10.6	1	NaCl-MgCl ₂	-35	1
CaCl ₂	-49.8	1	NaCl-CaCl ₂ -MgCl ₂	-57	3
MgCl ₂	-33.6	1	NaCl-KCl-CaCl ₂	-56	1
NaCl-KCl	-22.9	1			

Ref. (1) Linke, 1965 (2) Yanatieva, 1946
(3) Luzhnaya and Vereshtchetina, 1946

Inclusions were cooled to temperatures of about -60° to -70° C. Inclusions froze spontaneously after a degree of supercooling. Spontaneous freezing temperatures, which were recorded for 21 inclusions, ranged between -33° and -52° C.

Recorded initial melting temperatures fall between -20° and -51° C. The fluids therefore are complex and contain CaCl₂, (and probably MgCl₂ and KCl although this can not be proven) as well as NaCl as would be expected of natural solutions. Moreover, fluid compositions differ from inclusion to inclusion. This is known because many inclusions completely froze at temperatures above the eutectic for CaCl₂ at -49.8° C and the eutectic for NaCl-CaCl₂ at -52.0° C precluding the presence of CaCl₂. However, in other inclusions initial melting temperatures between -40° and -50° C were recorded, implying the presence of CaCl₂.

Spooner and Bray (1977) published results of a fluid inclusion study on samples from stockwork zones of Troodos deposits. They did not report initial melting temperatures but they did report that most inclusions froze completely at about -30° C, a temperature which precludes the presence of CaCl₂ in the fluids.

4.6.3.2. Salinity

Final melting temperatures of ice were recorded for 54 inclusions. Ice and NaCl may react upon cooling to form the metastable phase hydrohalite --NaCl.2H₂O. Both hydrohalite and ice are characterized by similar final melting temperatures. The salinities inferred from the final melting temperatures for the two phases will differ widely, therefore recognition is crucial. In this study the solid is known to be ice rather than hydrohalite because of its low negative relief and its tendency to recrystallize into a few coarse grains during heating (see Roedder, 1972; Crawford, 1981).

The final melting temperature of ice ranged between +2° and -10° C, corresponding to salinities of 0 to 14 wt. % NaCl (Fig. 4-23a). The mode occurs between -3° and -4° C, i.e. between 6 and 7 equiv. wt. % NaCl, which is about twice the salinity of seawater; the mean is 6 equiv. wt. % NaCl. The positive melting temperatures may be the result of leakage metastability of ice. If the gas bubble is eliminated by expansion of the liquid on freezing, negative pressure may result, causing metastable superheated ice to persist at temperatures as high as +6° C (Roedder, 1967b). For example ice in one inclusion melted at -1.2° C. When the experiment was repeated the ice melted at +0.2° C and the bubble did not reappear.

4.6.4. Homogenization Temperatures

Fig. 4-23b is a histogram of the homogenization temperatures for all data. The data fall into a normal distribution with a mean at 160° C. Most of the samples homogenized between 150° and 170° C. Several anomalously high homogenization temperatures are probably the result of heating of previously decrepitated inclusions. Leroy (1979) has demonstrated that heating of inclusions may result in decrepitation such that when the inclusion is cooled a larger vapour bubble forms. Reheating of the inclusion will then result in homogenization at the former decrepitation temperature. Such an enlargement of vapour bubbles after heating of inclusions was noticed in this study. Natural decrepitation may explain

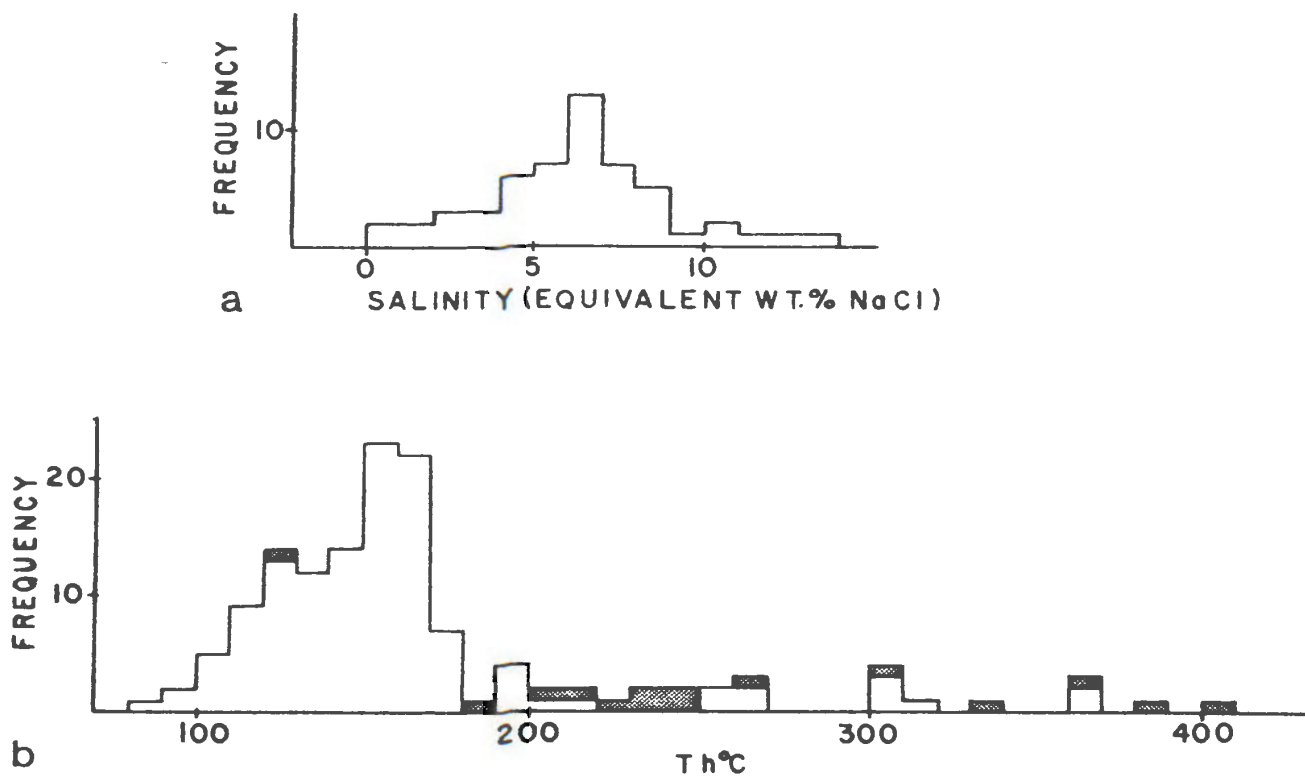


Figure 4-23: Fluid inclusion salinity and homogenization temperature histograms

(a) Histogram of salinity (equiv. wt. % NaCl). Salinity is derived from final melting temperature of ice from 54 inclusions; (b) Histogram of homogenization temperatures of 124 fluid inclusions. Stippled areas indicate decrepitation temperatures of unhomogenized inclusions i.e. a lower limit on the homogenization temperature.

several anomalous vapour rich inclusions which were observed in various samples (Fig. 4-18b).

The majority of modern day seafloor hydrothermal deposits are situated beneath about 1600 to 5800 m of water (water depths for sixty-three deposits are tabulated by Rona, (1984)). Precise water depths for the Betts Cove deposit cannot be determined but for a 5 % NaCl solution, water depths of 2500 and 5000 m would result in pressure corrections of +27° and +45° C respectively (diagrams of Potter, 1977) for a homogenization temperature of 160° C.

These temperatures are substantially lower than the 350° C temperatures of end-member hydrothermal solutions which are currently emanating from fumaroles on the seafloor. The values found by Spooner (1980) for fluid inclusions from stockworks of Troodos ore deposits are comparable to those of the modern systems.

The lower values cannot be due to mixing of the fluids with cold, less saline seawater near the seafloor. Such a lowering of temperature would be accompanied by a lowering of the salinity but a plot of salinity vs. homogenization temperature showed that there is no relationship between the two in inclusions from the Betts Cove samples.

The salinities are substantially higher than that of seawater and the possibility exists that this may be the result of boiling; determination of such a phenomenon would have important implications for sulphide deposition. But, in order for boiling to have occurred at the temperature and salinities measured, water depth would have to have been less than 100 metres (Haas, 1971 - Fig. 2). In addition, no evidence for boiling was observed during the fluid inclusion study. The liquid-vapour ratio in the inclusions appeared to be relatively constant. The rare vapour-rich inclusions which were seen decrepitated upon heating, supporting the idea that they may have originated by natural decrepitation.

The lower temperatures may represent deposition from a waning hydrothermal system. Edmond (1984) suggested that the quartz in the stockworks below hydrothermal seafloor deposits precipitated near the end of the lifespan of the system. Presumably the temperatures of fluids in the system at this point should be lower than they would have been when the system operated at peak efficiency. This would explain the discrepancy between observed temperatures in this study and those from the East Pacific rise where quartz is not at present forming, but not the differences between the Betts Cove and Troodos samples.

There is however, another possible and more probable explanation, i.e. that none of the measured fluid inclusions are related to the mineralizing event. Sample 216d and three of the samples from within the mineralization-related alteration zone are "vuggy" quartz. This quartz is open space filling and may have filled fractures or tension gashes that formed in response to fault movements. Much of this faulting postdates the emplacement of the orebody, thus the quartz segregations may be later phenomena. Sample 138b is from a 4 cm wide vein of dense quartz which cuts slightly sheared chloritic pillows and the inclusions it contains may have been affected by this shearing. It is thus not possible to conclusively demonstrate that any of the salinity or temperature data derived from inclusions in these samples reflects the nature of the mineralizing fluids.

4.7. Structural and Stratigraphic Control

The localization of Newfoundland ophiolitic deposits into chloritic shear zones is an almost ubiquitous phenomenon. Such instances have been documented in the Betts Cove Ophiolite (Snelgrove, 1931; Upadhyay and Strong 1973), the Lushs Bight Group (Kanehira and Bachinski, 1968; Gale, 1969; West, 1972; Smitheringale and Peters, 1974; Papezik and Fleming, 1967; DeGrace, 1971; Kennedy and DeGrace, 1972) and at the York Harbour deposit (Duke and Hutchinson, 1974). Most of the above authors contended that the shear zones were the result of post-ore tectonics and that their common association with mineralization is a result of the ease of deformation of massive sulphide bodies.

Duke and Hutchinson (1974) suggested that at York Harbour the ore-fluids were localized along ocean-floor faults which were characterized by post-ore movement.

The mapping of Upadhyay (1973) showed that for much of its length the Betts Cove Ophiolite and overlying Snooks Arm Group exhibits uniform (albeit incomplete) "layer-cake stratigraphy", but at the two extremes, Betts Cove and Tilt Cove, the ophiolite is dismembered and highly faulted. The faults are internal, i.e. they do not extend beyond the ophiolite and Snooks Arm Group, suggesting they are original ocean floor faults.

Strong (1980, 1984), pointed out that at Tilt Cove there is a strong stratigraphic control of the mineralization, which occurs in breccia zones at the sheeted dyke-pillow lava contact. At Betts Cove the mineralization also occurs at contacts between the pillow lava unit and the sheeted dyke unit. These contacts are commonly faulted, and at Mount Misery and along the Fault Cove Fault they are characterized by abundant pillow breccia. The block of pillow lavas which hosts the mineralization may be downfaulted into the sheeted dyke unit.

The relationships between the mineralization, the breccia zones, the pillow lava-sheeted dyke contact and the fault zones are not completely clear. Nevertheless it is apparent that (a) the contact between the pillow lava and sheeted dyke units is commonly characterized by abundant pillow lava and dyke breccia; this is not unexpected as this contact represents the extrusion of hot lava into cold seawater; (b) contacts are commonly faulted, but there may not have been a great deal of movement along the faults; (c) mineralization has an affinity for both the fault zones and the contact zones, which is not surprising since the two are commonly paired.

The stratigraphy may have originally dictated sites of fault initiation, i.e. weak zones in the rock (contact zones or breccia zones for example), may have been the preferred sites of faulting. Alternatively, movement of fluids along the faults may have been responsible for some of the brecciation. Breccias are characterized by both rounded and hyaloclastic fragments (see subsection 2.4.1).

Structural control of sub-seafloor hydrothermal ore deposits is being increasingly recognized (e.g. Adamides, 1980; Franklin *et al.*, 1981; Rona, 1984). The hydrothermal mounds at the East Pacific Rise and Galapagos sites are located along faults and fractures (Francheteau *et al.*, 1979; Speiss *et al.*, 1980; Corliss *et al.*, 1978; Hekinian *et al.*, 1978). Rona (1978, 1980, 1984) described structural control of mineralization at the TAG Hydrothermal Field on the Mid-Atlantic Ridge.

Some structural control of the ore fluids can be demonstrated at Betts Cove. The main alteration zone at Betts Cove is a relatively broad feature which has an outer halo. The alteration along the Fault Cove Fault, which is a sharp, well-defined feature, is much narrower and does not extend significantly outside the fault zone. This can be interpreted to be a result of highly efficient focussing of fluids along the fault such that the wall rocks were not greatly affected. The main alteration zone would be the result of less concentrated flow along a less well-defined permeable zone.

Adamides (1980) proposed fault control of ophiolitic deposits at Kalavassos, Cyprus (Fig. 4-24a). Fig. 4-24b illustrates the similarly envisioned geometry of the Betts Cove hydrothermal system. The most intensive flow occurs along the core of the system and produces the quartz - chlorite alteration, which passes outward into the halo quartz - albite - chlorite assemblage.

4.8. Summary

The Betts Cove deposit and peripheral showings occur along faults at the contact between the pillow lava and sheeted dyke units of the Betts Cove Ophiolite. The main deposit is a massive pyrite - chalcopyrite - sphalerite body, which overlies an intensely altered stockwork feeder zone. The peripheral showings, which occur mainly along the Fault Cove Fault are of the stringer chalcopyrite - pyrite type. Although there are differences in degree of preservation the massive sulphide and its stockwork zone are morphologically,

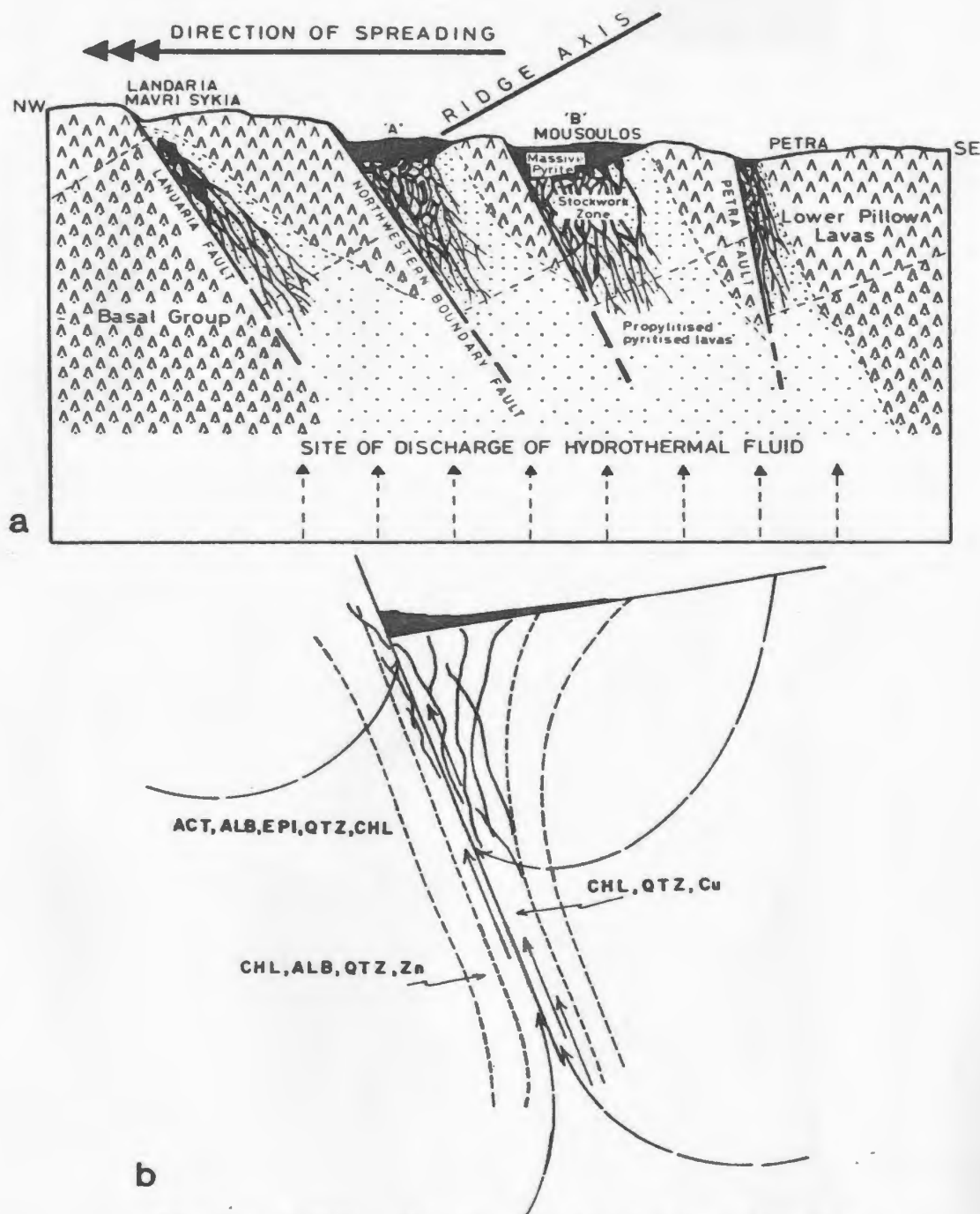


Figure 4-24: Fault control of mineralization

(a) Fault control of mineralization at Kalavassos, Cyprus (Adamides, 1980); mineralizing fluids moved up along fault zones, producing stockwork zones and altering the lavas; (b) Fault control at Betts Cove; mineralizing fluids produced a central stockwork zone characterized by quartz - chlorite alteration surrounded by a zone of quartz - chlorite - albite mineralization; background rocks have an assemblage of actinolite - albite - epidote - quartz - chlorite.

texturally and chemically similar to the deposits of the Troodos Ophiolite in Cyprus.

Much of the massive ore is strongly tectonically banded, but primary framboidal textures in pyrite do occur. Copper and zinc values are to some extent inversely related, indicating that the deposit may be zoned.

The footwall alteration zone consists of a core iron-copper-enriched chlorite - quartz zone from which almost all Na_2O and CaO have been leached. This is surrounded by a zinc-enriched chlorite - albite - quartz halo. The mineralogy of the two zones can be related to the amount of hydrothermal fluids which have passed through the rock. The more intensely altered core has been the site of maximum focus of the flow of hydrothermal fluids. It grades outwards over a short distance into the less-altered chlorite - albite - quartz zone and then into a background greenschist assemblage of actinolite - chlorite - albite - epidote - quartz.

The sulphides were precipitated from the same fluids that caused the footwall alteration. The metals were leached from the rocks by fluids on the downwelling limb of a hydrothermal system. At the same time the rock and seawater exchanged other elements, notably Mg, Na, and Ca to produce a background alteration assemblage, which at Betts Cove is now represented by the greenschist assemblage described above. Alteration in the stockwork zone was caused by passage of evolved hydrothermal fluids through the rock. Precipitation of sulphides was brought about by the mixing of cold, alkaline, oxidizing seawater with the hot, acid, reducing hydrothermal fluids.

Temperatures and salinities derived from fluid inclusions are interpreted to represent later passage of fluids through the rock. These fluids were concentrated along fractures and tension cracks which postdate the mineralization and are probably related to later movement along the faults which host the mineralization. Although much of the movement along the faults postdates the

mineralization, the faults themselves may actually have preceded ore formation and may have served as a site of localization of upwelling metal-bearing solutions.

Chapter 5

CONCLUSIONS

The Betts Cove Complex is a Lower Ordovician ophiolite suite, in which the four main constituents of an ophiolite, the ultramafic, gabbroic, sheeted dyke and pillow lava members, are represented. Individual members may be locally absent, but the complete sequence is exposed in the Betts Cove-Kitty Pond area. The ophiolite is conformably overlain by the Snooks Arm Group, a series of interbedded pillow basalts, sills and sediments. It is unconformably overlain by and in fault contact with the Silurian Cape St. John Group, and is intruded by the Burlington Granodiorite and the Cape Brule Porphyry.

The map area contains representatives of three of the members of the ophiolite. The ultramafic member is absent from the area studied. Contacts between the units are generally faulted, but locally gradational contacts occur. Where these gradational contacts exist, they occur over a short distance, commonly several metres.

Gabbro pods that occur within the sheeted dyke member are in part intrusive into the sheeted dyke unit and to a lesser extent the pillow lava unit. They are cut by later dykes which become sheeted near the edges of the pods.

The pillow lava member is characterized by extensive development of variolitic textures. These textures are the result of quenching of the lavas as they erupted onto the seafloor. Where quench textures are not apparent, i.e. in some pillows and in 99 % of the dykes, variolitic textures are absent. Variolitic textures are controlled by both degree of supercooling and lava composition.

The pillow lavas and dykes of the map-area are chemically very different from average MORB. They are characterized by anomalously high MgO, Ni and Cr, and extremely low TiO_2 and incompatible element contents. Their chemistry is most compatible with an island arc-related environment. Chemically similar rocks, "boninites", from the Western Pacific are found in fore-arc basins. The ophiolite may have formed at a spreading center in a fore-arc basin.

Massive sulphide deposits are located along faults near the pillow lava-sheeted dyke interface in the Betts Cove and Tilt Cove areas. The main deposit at Betts Cove is a massive pyrite - chalcopyrite - sphalerite body, which overlies an intensely altered stockwork feeder zone. The peripheral showings, which occur mainly along the Fault Cove Fault are of the stringer pyrite - chalcopyrite type. Although there are differences in degree of preservation, the massive sulphide and its stockwork zone are morphologically, texturally and chemically similar to deposits in other Newfoundland ophiolites and in the Troodos, Oman and Norwegian ophiolites.

Much of the massive ore is strongly tectonically banded, but primary framboidal textures in pyrite do occur. Copper and zinc concentrations are to some extent inversely related, indicating that the deposit may be zoned.

The footwall alteration zone consists of a core of iron-copper-enriched chlorite - quartz from which almost all Na_2O and CaO have been leached. This is surrounded by a zinc-enriched chlorite - albite - quartz halo. The mineralogy of the two zones can be related to the amount of hydrothermal fluids which have passed through the rock. The more intensely altered core has been the site of maximum focus of the flow of hydrothermal fluids. It grades outwards over a short distance into the less-altered chlorite - albite - quartz zone and then into a background greenschist assemblage of actinolite - chlorite - albite - epidote - quartz.

The sulphides were precipitated from the same fluids that caused the footwall

alteration. The metals were leached from the rocks by fluids on the downwelling limb of a hydrothermal system. At the same time the rock and seawater exchanged other elements, notably Mg, Na, and Ca to produce a background alteration assemblage. At Betts Cove this alteration is now represented by the greenschist assemblage described above, but it may have originally been lower (zeolite facies) grade. Alteration in the stockwork zone was caused by passage of evolved metal-bearing hydrothermal fluids through the rock. Precipitation of sulphides was brought about by the mixing of cold, alkaline, oxidizing seawater with the hot, acid, reducing hydrothermal fluids. The mineralization and the background alteration are therefore contemporaneous and are products of the same process-- circulation of seawater through the ocean crust in response to temperature anomalies over magma chambers at spreading centers.

Temperatures and salinities derived from fluid inclusions are interpreted to represent later passage of fluids through the rock. These fluids were concentrated along fractures and tension cracks which postdate the mineralization and are probably related to later movement along the faults which host the mineralization. Although much of the movement along the faults postdates the mineralization, the faults themselves may actually have preceded ore formation and may have served as a site of localization of upwelling metal-bearing solutions.

In the Lushs Bight Group there seems to be an association of variolitic textures in the pillow lavas with mineralization (B. Kean, P. Dean, pers. comm., 1983). The association may be fortuitous in that it may be high heat flow at the spreading ridge that produces both phenomena. This would result in rapid extrusion of hot lava, and hence a greater degree of supercooling and development of quench textures. They would therefore not be intrinsically related, but end-results of the same cause-- heat generated by a magma chamber underlying the spreading center.

It is this heat which is responsible for generating seawater circulation cells in the crust, thereby substantially altering the rock column and producing massive sulphide deposits.

REFERENCES

- Adamides, N. G. 1980. The form and environment of formation of the Kalavassos ore deposits--Cyprus. in: Ophiolites, ed. A. Panayiotou, Proceedings International Ophiolite Symposium, Nicosia, Cyprus, April 1979, Geological Survey Cyprus, p. 117-127
- Andrews, A. J. 1977. Low temperature fluid alteration of oceanic layer 2 basalts, DSDP Leg 37. *Canadian Journal Earth Sciences*, 14, p. 911-926
- Andrews, A. J. and Fyfe, W. S. 1976. Metamorphism and massive sulphide generation in oceanic crust. *Geoscience Canada*, 3, p. 84-94
- Arndt, N. T. and Brooks, C. 1980. Komatiites. *Geology*, 8, p. 155-166
- Arndt, N. T. and Nesbitt, R. W. 1982. Geochemistry of Munro Township basalts. in: Komatiites, eds. N. T. Arndt and E. G. Nisbet, George Allen and Unwin, London, England, p. 309-329
- Bachinski, D. J. 1977a. Alteration associated with metamorphosed ophiolitic cupriferous iron sulfide deposits: Whalesback Mine, Notre Dame Bay, Newfoundland. *Mineralium Deposita*, 12, p. 48-63
- 1977b. Sulfur isotopic composition of ophiolitic cupriferous iron sulfide deposits, Notre Dame Bay, Newfoundland. *Economic Geology*, 72, p. 243-257
- Bainbridge Seymour and Co. 1899. Unpublished report to Reid Newfoundland Co. on the Betts Cove Mine. Reid Newfoundland Co. Report 37, Newfoundland Department Mines and Energy, Mineral Development Division Open File
- Baird, D. M. 1947. The geology of the Burlington Peninsula, Newfoundland. Ph. D. thesis, McGill University, Montreal
- 1948. Copper mineralization in the Bett's Cove-Stocking Harbour district, Notre Dame Bay, Newfoundland. *Canadian Mining and Metallurgical Bulletin*, April, p. 211-213

- _____. 1951. The geology of the Burlington Peninsula, Newfoundland. Geological Survey Canada, paper 51-21, 70 p.
- Baker, J. H. and de Groot, P. A. 1983. Proterozoic seawater - felsic volcanics interaction, W. Bergslagen, Sweden. Evidence for high REE mobility and implications for 1.8 Ga seawater compositions. *Contributions Mineralogy Petrology*, 82, p. 119-130
- Baragar, W. R. A. 1954. Betts Pond area, Burlington Peninsula, Newfoundland. Unpublished report, Falconbridge Nickel Mines Ltd. Newfoundland Department Mines and Energy, Mineral Development Division, Open File 2E/13(91)
- Bell, K. and Blenkinsop, J. 1977. Geochronological evidence of Hercynian activity in Newfoundland. *Nature*, 265, p. 616-618
- Bender, M., Broecker, W., Gornitz, V., Middel, V., Kay, R. and Sun, S. 1971. Geochemistry of three cores from the East Pacific Rise. *Earth Planetary Science Letters*, 12, p. 425-433
- Bichan, W. J. 1958. Summary reports on the ore zones, structural controls for mineralization, the post-ore dislocations and the overall economic potential of the Tilt Cove Mine. Unpublished report, Maritime Mining Corp. Ltd., 16 p.
- Bird, J. M. and Dewey, J. F. 1970. Lithospheric plate-continental margin tectonics and the evolution of the Appalachian Orogen. *Geological Society America Bulletin*, 81, p. 1031-1060
- Bischoff, J. L. 1969. Red Sea geothermal brine deposits. in: *Hot Brines and Heavy Metal Deposits of the Red Sea*, eds. E. T. Degens and D. A. Ross, Springer, New York, N. Y., p. 348-401
- Bischoff, J. L. and Dickson, F. W. 1975. Seawater-basalt interaction at 200 C and 500 bars: implications for origin of sea-floor heavy-metal deposits and regulation of seawater chemistry. *Earth Planetary Science Letters*, 25, p. 385-397
- Bostrom, K. and Peterson, M. N. A. 1966. Precipitates from hydrothermal exhalations on the East Pacific Rise. *Economic Geology*, 61, p. 1258-1265
- Brock, P. W. G. 1974. The sheeted dike layer of the Betts Cove Ophiolite Complex does not represent spreading. *Canadian Journal Earth Sciences*, 11, p. 208-210

- Bryan, W. B., 1972. Morphology of quench crystals in submarine basalts. *Journal Geophysical Research*, 29, p. 5812-5819
- Burnsall, J. T. 1975. Stratigraphy, structure and metamorphism west of Baie Verte, Burlington Peninsula, Newfoundland. Ph. D. thesis, Cambridge University, 337 p.
- Burnsall, J. T. and de Witt, M. J. 1975. Timing and development of the orthotectonic zone in the Appalachian orogen of northwest Newfoundland. *Canadian Journal Earth Sciences*, 12, p. 1712-1722
- Burnsall, J. T. and Hibbard, J. 1980. Fleur de Lys (12I/1) and Horse Islands (2L/4) map areas. Newfoundland Department Mines and Energy, Mineral Development Division, Map 80-30
- Cameron, W. E. and Nisbet, E. G. 1982. Phanerozoic analogues of komatiitic basalts. in: *Komatiites*, eds. N. T. Arndt and E. G. Nisbet, George Allen and Unwin, London, England, p. 29-50
- Cameron, W. E., Nisbet, E. G. and Dietrich, V. J. 1979. Boninites, komatiites and ophiolitic basalts. *Nature*, 280, p. 550-553
- _____ 1980. Petrographic dissimilarities between ophiolitic and ocean-floor basalts. in: *Ophiolites*, ed. A. Panayiotou, Proceedings International Ophiolite Symposium, Nicosia, Cyprus, April 1979, Geological Survey Cyprus, p. 182-192
- Cann, J. R. 1970. Rb, Sr, Y, Zr and Nb in some ocean floor basaltic rocks. *Earth Planetary Science Letters*, 10, p. 7-11
- Carmichael, I. S. E., Turner, F. J. and Verhoogen, J. 1974. *Igneous Petrology*. McGraw-Hill Inc., New York, N. Y., 739 p.
- Carrigan, D. G. 1955. Diamond Drill logs, Betts Cove area. M. J. Boylen Engineering (Advocate Mines Ltd.), Unpublished report. Newfoundland Department Mines and Energy, Mineral Development Division, Open File 2E/12(153)
- Chapman, H. J. and Spooner, E. T. C. 1977. ^{87}Sr enrichment of ophiolitic sulphide deposits in Cyprus confirms ore formation by circulating seawater. *Earth Planetary Science Letters*, 35, p. 71-78
- Church, W. R. 1965. Structural evolution of northeast Newfoundland - comparison with that of the British Caledonides. *Maritime Sediments*, 1, p. 10-14

- 1966. Geology of the Burlington Peninsula, northeast Newfoundland. Geological Association Canada and Mineralogical Association Canada, Technical Program, p. 11-12
- 1969. Metamorphic rocks of Burlington Peninsula and adjoining areas of Newfoundland and their bearing on continental drift in the North Atlantic. in: North Atlantic Geology and Continental Drift, ed. M. Kay. American Association Petroleum Geologists, Memoir 12, p. 212-233
- Church, W. R. and Coish, R. A. 1976. Oceanic versus island arc origin of ophiolites. *Earth Planetary Science Letters*, 31, p. 8-14
- Church, W. R. and Riccio, L. M. 1974. The sheeted dike layer of the Betts Cove Ophiolite Complex does not represent spreading: discussion. *Canadian Journal Earth Sciences*, 11, p. 1499-1502
- 1977. Fractionation trends in the Bay of Islands ophiolite, Newfoundland: polycyclic cumulate sequences in ophiolites and their classification. *Canadian Journal Earth Sciences*, 14, p. 1156-1165
- Church, W. R. and Stevens, R. K. 1971. Early Paleozoic ophiolite complexes of the Newfoundland Appalachians as mantle-oceanic crust sequences. *Journal Geophysical Research*, 76, p. 1460-1466
- Clark, L. A. 1971. Volcanogenic ores: comparison of cupriferous pyrite deposits of Cyprus and Japanese Kuroko deposits. in: IAGOD volume, ed. Y. Takeuchi, Society Mining Geologists Japan, Special Issue 3, p. 206-215
- Coish, R. A. 1977a. Ocean floor metamorphism in the Betts Cove Ophiolite, Newfoundland. *Contributions Mineralogy Petrology*, 60, p. 255-270
- 1977b. Petrology of the mafic units of west Newfoundland ophiolites. Ph. D. thesis, University of Western Ontario, London, Ontario, 227 p.
- Coish, R. A. and Church, W. R. 1978. The Betts Cove ophiolite, Newfoundland: some unusual chemical characteristics. [abstract] EOS, Transactions American Geophysical Union, 59, p. 408
- 1979. Igneous geochemistry of mafic rocks in the Betts Cove Ophiolite, Newfoundland. *Contributions Mineralogy Petrology*, 70, p. 29-39
- Coish, R. A., Hickey, R. and Frey, F. A. 1982. Rare earth element geochemistry of the Betts Cove Ophiolite, Newfoundland: complexities in ophiolite formation. *Geochimica Cosmochimica Acta*, 46, p. 2117-2134

- Constantinou, G. 1972. The geology and genesis of the sulphide ores of Cyprus. Ph. D. thesis, University of London, 275 p.
- — — — — 1976. Genesis of conglomerate structure, porosity and collomorphic textures of the massive sulphide ores of Cyprus. in: *Metallogeny and Plate Tectonics*, ed. D. F. Strong, Geological Association Canada Special Paper 14, p. 187-210
- — — — — 1980. Metallogenesis associated with Troodos ophiolite. in: *Ophiolites*, ed. A. Panayiotou, Proceedings International Ophiolite Symposium, Nicosia, Cyprus, April 1979, Geological Survey Cyprus, p. 663-674
- Constantinou, G. and Govett, G. J. S. 1972. Genesis of sulphide deposits, ochre and umber of Cyprus. *Institute Mining Metallurgy Transactions, Section B*, 81, p. B34-46
- — — — — 1973. Geology, geochemistry and genesis of Cyprus sulphide deposits. *Economic Geology*, 68, p. 843-858
- Corliss, J. B. 1971. The origin of metal-bearing submarine hydrothermal solutions. *Journal Geophysical Research*, 76, p. 8128-8138
- Corliss, J. B., Lyle, M., Dymond, J. and Crane, K. 1978. The chemistry of hydrothermal mounds near the Galapagos Rift. *Earth Planetary Science Letters*, 40, p. 12-24
- Corliss, J. B., Dymond, J., Gordon, L. I., Edmond, J. M., Von Herzen, R. P., Ballard, R. D., Green, K., Williams, D., Bainbridge, A., Crane, K. and Van Andel, T. H. 1979. Submarine thermal springs on the Galapagos Rift. *Science*, 203, p. 1073-1083
- Craig, H., Clarke, W. B. and Beg, M. A. 1975. Excess ^3He in the deep water on the East Pacific Rise. *Earth Planetary Science Letters*, 26, p. 125-132
- Craig, P. M. 1967. The geology of the East Mine, Tilt Cove, Newfoundland. B. Sc. Honours thesis, University of Aberdeen, Scotland, 92 p.
- Crawford, A. J., Beccaluva, L. and Serri, G. 1981. Tectono-magmatic evolution of the West Phillipine-Mariana region and the origin of boninites. *Earth Planetary Science Letters*, 54, p. 346-356
- Crawford, M. L. 1981. Phase equilibria in aqueous fluid inclusions. in: *Fluid Inclusions: Applications to Petrology*, eds. L. S. Hollister and

M. L. Crawford, Mineralogical Association Canada Short Course Handbook, 6, p. 75-100

Dean, P. 1978. The volcanic stratigraphy and metallogeny of Notre Dame Bay, Newfoundland. M. Sc. thesis, Memorial University of Newfoundland, St. John's, Newfoundland, 204 p. (published as Memorial University of Newfoundland Geology Report 7)

Degens, E. T. and Ross, D. A. 1969. (eds.) Hot Brines and Recent Heavy Metal Deposits in the Red Sea. Springer, New York, N. Y., 600 p.

DeGrace, J. R. 1971. Structural and stratigraphic setting of sulphide deposits in Ordovician volcanics South of King's Point, Newfoundland. M. Sc. thesis, Memorial University of Newfoundland, St. John's, Newfoundland, 62 p.

DeGrace, J. R., Kean, B. F., Hsu, E. and Green, T. 1976. Geology of the Nippers Harbour map area (2E/13), Newfoundland. Newfoundland Department Mines and Energy, Mineral Development Division, Report 76-3, 73 p.

Dewey, J. F. 1969. Evolution of the Appalachian/Caledonian Orogen. *Nature*, 22, p. 124-129

Dewey, J. F. and Bird, J. M. 1971. Origin and emplacement of the ophiolite suite. Appalachian ophiolites in Newfoundland. *Journal Geophysical Research*, 76, p. 3179-3206

de Wit, M. J. 1972. The geology around Bear Cove, eastern White Bay, Newfoundland. Ph. D. thesis, Cambridge University, England, 232 p.

— — — — — 1974. On the origin and deformation of the Fleur de Lys metaconglomerate, Appalachian fold belt, northwest Newfoundland. *Canadian Journal Earth Sciences*, 11, p. 1168-1180

— — — — — 1980. Structural and metamorphic relationships of pre-Fleur de Lys and Fleur de Lys rocks of the Baie Verte Peninsula, Newfoundland. *Canadian Journal Earth Sciences*, 17, p. 1559-1575

Donaghue, H. G., Adams, W. S. and Harper, C. E. 1959. Tilt Cove copper operation of the Maritimes Mining Corporation Limited, *Canadian Institute Mining Metallurgy, Journal*, 62, p. 54-73

Douglas, V. G., Williams, D., Rove, O. N. and others 1940. Copper deposits of Newfoundland. *Geological Survey Newfoundland, Bulletin* 20, 176 p.

- Drever, H. I., Johnston, R. and Brebner, G. 1973. Radiate texture in lunar igneous rocks and terrestrial analogs [abs]. in: Lunar Science IV, eds. J. W. Chamberlain, and C. Watkins, Lunar Science Institute, Houston, p. 187-189
- Drever, H. I., Johnston, R., Butler, P. Jr. and Gibb, F. G. F. 1972. Some textures in Apollo 12 lunar igneous rocks and in terrestrial analogs. in: Proceedings of the Third Lunar Science Conference, ed. E. A. King, Massachusetts Institute of Technology Press, Cambridge, Massachusetts, p. 171-184
- Duke, N. A. and Hutchinson, R. W. 1974. Geological relationships between massive sulphide bodies and ophiolitic volcanic rocks near York Harbour, Newfoundland. Canadian Journal Earth Sciences, 11, p. 53-69
- Dunning, G. R. 1984. The geology, geochemistry, geochronology and regional setting of the Annieopsquotch Complex and related rocks of southwest Newfoundland. Ph. D. thesis, Memorial University of Newfoundland, St. John's, Newfoundland, 402 p.
- Dymond, J., Corliss, J. B., Heath, J. R., Field, C. W., Dasch, E. J. and Veeh, H. H. 1973. Origin of metalliferous sediments from the Pacific Ocean. Geological Society America Bulletin, 84, p. 3355-3372
- Edmond, J. M. 1980. Ridge crest hot springs: the story so far. EOS, Transactions American Geophysical Union, 61, p. 129
- _____ 1982. The chemistry of ridge crest hot springs. Marine Technology Society Journal, 16, n. 3, p. 23-25
- _____ 1984. Hydrothermal ore generation within sediment starved and sediment covered ridge areas. Geological Association Canada, Newfoundland Branch, Spring Meeting, April 5-6, 1984.
- Edmond, J. M., Measures, C., McDuff, R. E., Chan, L. H., Collier, R., Grant, B., Gordon, L. I. and Corliss, J. B. 1979a. Ridge crest hydrothermal activity and the balances of the ocean: the Galapagos data. Earth Planetary Science Letters, 46, p. 1-18
- Edmond, J. M., Measures, C., Mangum, B., Grant, B., Sclater, F. R., Collier, R., Hudson, A. Gordon, L. I. and Corliss, J. B. 1979b. On the formation of metal-rich deposits at ridge crests. Earth Planetary Science Letters, 46, p. 19-30
- Edmond, J. M. and Von Damm, K. 1983. Hot springs on the ocean floor. Scientific American, 248, n. 4, p. 78-93

- Einstein, A. 1956. Investigation of the theory of the Brownian movement. translator, A. D. Cowper, Dover, New York, N. Y.
- Elder, J. W. 1965. Physical processes in geothermal areas. American Geophysical Union Monograph Series, 8, p. 211-239
- — — — — 1967. Steady free convection in a porous medium heated from below. *Journal Fluid Mechanics*, 27, p. 29-48
- — — — — 1977. Model of hydrothermal ore genesis. in: *Volcanic Processes in Ore Genesis*, Geological Society London, Special Publication 7, p. 4-13
- Epstein, R. S. 1983. The eastern margin of the Burlington Granodiorite, Newfoundland. M. Sc. thesis, University of Western Ontario, 188 p.
- Finlow-Bates, T. and Stumpfl, E. F. 1981. The behaviour of so-called immobile elements in hydrothermally altered rocks associated with volcanogenic submarine-exhalative ore deposits. *Mineralium Deposita*, 16, p. 319-328
- Floyd, P. A. and Winchester, J. A. 1975. Magma type and tectonic setting discrimination using immobile elements. *Earth Planetary Science Letters*, 27, p. 211-218
- Francheteau, J., Needham, H. D., Choukroune, P., Juteau, T., Seguret, M., Ballard, R. D., Fox, P. J., Normark, W., Carranza, A., Cordoba, D., Guerrero, J., Rangin, C., Bougault, H., Cambon, P., and Hekinian, R. (CYAMEX Scientific Team) 1979. Massive deep-sea sulphide ore deposits discovered on the East Pacific Rise. *Nature*, 277, p. 523-528
- Franklin, J. M., Lydon, J. W. and Sangster, D. F. 1981. Volcanic-associated Massive Sulfide Deposits. in: *Economic Geology Seventy-fifth Anniversary Volume*, ed. B. J. Skinner, The Economic Geology Publishing Co., El Paso, Texas, p. 485-627.
- Fryer, B. J. 1977. Rare earth evidence in iron-formations for changing Precambrian oxidation states. *Geochimica Cosmochimica Acta*, 41, p. 361-367
- Fryer, B. J. and Hutchinson, R. W. 1976. Generation of metal deposits on the seafloor. *Canadian Journal Earth Sciences*, 13, p. 126-135
- Gale, G. H. 1969. The primary dispersion of Cu, Zn, Ni, Co, Mn, and Na adjacent to sulfide deposits, Springdale Peninsula, Newfoundland. M. Sc. thesis, Memorial University of Newfoundland, St. John's, Newfoundland, 143 p.

- _____. 1973. Paleozoic basaltic komatiite and ocean floor type basalts from northeast Newfoundland. *Earth Planetary Science Letters*, 18, p. 22-28
- Gary, M., McAfee, R. and Wolf, C. L. 1972. (eds.) *Glossary of Geology*, American Geological Institute, Washington, D. C., 805 p.
- Gass, I. G. 1980. The Troodos massif: Its role in the unravelling of the ophiolite problem and its significance in the understanding of constructive plate margin processes. in: *Ophiolites*, ed. A. Panayiotou, Proceedings International Ophiolite Symposium, Nicosia, Cyprus, April 1979, Geological Survey Cyprus, p. 23-35
- Gealey, W. K. 1980. Ophiolite obduction mechanism. in: *Ophiolites*, ed. A. Panayiotou, Proceedings International Ophiolite Symposium, Nicosia, Cyprus, April 1979, Geological Survey Cyprus, p. 228-243
- Gelinas, L., Brooks, C. and Trzcieski, W. E., Jr. 1976. Archean variolites - quenched immiscible liquids. *Canadian Journal Earth Sciences*, 13, p. 210-230
- Gibson, H. L. 1979. *Geology of the Amulet Rhyolite Formation, Turcotte Lake section, Noranda area, Quebec*. M. Sc. thesis, Carlton University, Ottawa, 154 p.
- Govett, G. J. S. and Pantazis, T. M. 1971. Distribution of Cu, Zn, Ni and Co in the Troodos pillow lava series, Cyprus. *Institute Mining Metallurgy Transactions*, 80, Section B, p. 1327-1346
- Graf, J. L. 1977. Rare earth elements as hydrothermal tracers during the formation of massive sulfide deposits in volcanic rocks. *Economic Geology*, 72, p. 527-548
- Grenne, T., Grammeltvedt, G. and Vokes, F. M. 1980. Cyprus type sulphide deposits in the western Trondheim district, central Norwegian Caledonides. in: *Ophiolites*, ed. A. Panayiotou, Proceedings International Ophiolite Symposium, Nicosia, Cyprus, April 1979, Geological Survey Cyprus, p. 727-743
- Haas, J. L. Jr. 1971. The effect of salinity on the maximum thermal gradient of a hydrothermal system at hydrostatic pressure. *Economic Geology*, 66, p. 940-946
- Hajash, A. 1975. Hydrothermal processes along Mid-Ocean Ridges: an experimental investigation. *Contributions Mineralogy Petrology*, 53, p. 205-226

- Hajash, A. and Chandler, G. W. 1980. An experimental investigation of high temperature interactions between seawater and rhyolite, andesite, basalt and peridotite. *Contributions Mineralogy Petrology*, 78, p. 240-254
- Hart, R. 1970. Chemical exchange between sea water and deep ocean basalts. *Earth Planetary Science Letters*, 9, p. 269-279
- Haymon, R. M. and Kastner, M. 1981. Hot spring deposits on the East Pacific Rise at 21° N: preliminary description of mineralogy and genesis. *Earth Planetary Science Letters*, 53, p. 363-381
- Heaton, T. H. E. and Sheppard, S. M. F. 1977. Hydrogen and oxygen isotope evidence for sea-water hydrothermal alteration and ore deposition, Troodos complex, Cyprus. in: *Volcanic Processes in Ore Genesis*, Geological Society London, Special Publication 7, p. 42-57
- Hekinian, R., Fevreir, N., Bischoff, J. L., Picot, P. and Shanks, W. C. 1980. Sulfide deposits from the East Pacific Rise near 21° N. *Science*, 207, p. 1433-1444
- Hekinian, R., Rosendahl, B. R., Cronan, D. S., Dimitriev, Y., Fodor, R. V., Goll, R. M., Hoffert, M., Humphris, S. E., Matten, D. P., Natland, J., Petersen, N., Roggenthen, W., Schrader, E. L., Srivastava, R. K. and Warren, N. 1978. Hydrothermal deposits and associated basement rocks from the Galapagos spreading center. *Oceanologica Acta*, 1, p. 473-482
- Hekinian, R., Fevrier, M., Avedik, F., Cambon, P., Charlou, J. L., Needham, H. D., Raillard, J., Boulegue, J., Merlivat, L., Moinet, A., Manganini, S. and Lange, J. 1983. East Pacific Rise near 13° N: geology of new hydrothermal fields. *Science*, 219, p. 1321-1324
- Helgeson, H. C. 1964. *Complexing and Hydrothermal Ore Deposition*. Pergamon Press, New York, N. Y., 128 p.
- _____ 1969. Thermodynamics of hydrothermal systems at elevated temperatures and pressures. *American Journal Science*, 267, p. 724-804
- Hibbard, J. 1982. Significance of the Baie Verte Flexure, Newfoundland. *Geological Society America Bulletin*, 93, p. 790-797
- _____ 1984. Geology of the Baie Verte Peninsula, Newfoundland. Newfoundland Department Mines and Energy, Mineral Development Division, Memoir 2, 279 p.

- Hibbard, J. and Gagnon, J. 1980. Geology of the Jackson's Arm (east) and Baie Verte map sheets. Newfoundland Department Mines and Energy, Mineral Development Division, Map 80-03
- Hibbard, J., Muggridge, W. and Gagnon, J. 1980a. Hampden (east)(12H/10E) and King's Point (west)(12H/9W) map areas. Newfoundland Department Mines and Energy, Mineral Development Division, Map 80-09
- — — — — 1980b. Sheffield Lake (12H/7) map area. Newfoundland Department Mines and Energy, Mineral Development Division, Map 80-18
- Hickey, R. L. and Frey, F. A. 1982. Geochemical characteristics of boninite series volcanics: implications for their source. *Geochimica Cosmochimica Acta*, 46, p. 2099-2115
- Higgins, N. C. 1979. Theory, methods and application of fluid inclusion research. Geological Association Canada, Newfoundland Section, Short Course Notes, St. John's, Newfoundland, November 17, 1979, 74 p.
- — — — — 1980. The genesis of the Grey River tungsten prospect: a fluid inclusion, geochemical and isotopic study. Ph. D. thesis, Memorial University of Newfoundland, St. John's, Newfoundland, 539 p.
- Holland, H. D. 1967. Gangue minerals in hydrothermal deposits. in: *Geochemistry of Hydrothermal Ore Deposits* (1st ed.), ed. H. L. Barnes, Holt, Rhinehart and Winston, p. 382-436
- Hudson, L. 1953. Diamond Drill logs, Betts Pond area. Falconbridge Nickel Mines Ltd., Unpublished report. Newfoundland Department Mines and Energy, Mineral Development Division, Open File Nfld(1269)
- Humphris, S. E. and Thompson, G. 1978a. Hydrothermal alteration of oceanic basalts by seawater. *Geochimica Cosmochimica Acta*, 42, p. 107-125
- — — — — 1978b. Trace element mobility during hydrothermal alteration of oceanic basalts. *Geochimica Cosmochimica Acta*, 42, p. 127-136
- Humphris, S. E., Morrison, M. A. and Thompson, R. N. 1978. Influence of rock crystallization history upon subsequent lanthanide mobility during hydrothermal alteration of basalts. *Chemical Geology*, 23, p. 125-137
- Hutchinson, R. W. 1973. Volcanogenic sulfide deposits and their metallogenic significance. *Economic Geology*, 68, p. 1223-1247

- Hutchinson, R. W. and Searle, D. L. 1971. Stratabound pyrite deposits in Cyprus and relations to other sulphide ores. in: IAGOD volume, ed. Y. Takeuchi, Society Mining Geologists Japan, Special Issue 3, p. 198-205
- Hynes, A. 1980. Carbonatization and mobility of Ti, Y and Zr in Ascot Formation metabasalts, S. E. Quebec. Contributions Mineralogy Petrology, 75, p. 79-87
- James, W. F., Buffam, B. S. W. and Cooper, M. A. 1963. unpublished report on the Tilt Cove property of Maritimes Mining Corporation Ltd., 10 p.
- Jenner, G. A. 1977. Geochemistry of the Upper Snooks Arm Group, Newfoundland. M. Sc thesis, University of Western Ontario, London, Ontario, 134 p.
- Jenner, G. A. and Fryer, B. J. 1980. Geochemistry of the upper Snooks Arm Group basalts, Burlington Peninsula, Newfoundland: evidence against formation in an island arc. Canadian Journal Earth Sciences, 17, p. 888-900
- Johannsen, A. 1939. A Descriptive Petrography of the Igneous Rocks, Volumes 1-4, (2nd ed.). University of Chicago Press, Chicago, Illinois.
- Kanehira, K. and Bachinski, D. J. 1967. Framboidal pyrite and concentric textures in ores of the Tilt Cove Mine northeastern Newfoundland. Canadian Mineralogist, 9, p. 124-128
- — — — — 1968. Mineralogy and textural relationships of ores from the Whalesback Mine, northeastern Newfoundland, Canadian Journal Earth Sciences, 5, p. 1387-1395
- Keith, H. D. and Padden, F. J. Jr. 1963. A phenomenological theory of spherulitic crystallization. Journal Applied Physics, 34, p. 2409-2421
- Kennedy, M. J. 1971. Structure and stratigraphy of the Fleur de Lys Supergroup in the Fleur de Lys area, Burlington Peninsula, Newfoundland. Geological Association Canada Proc., 24, p. 59-71
- — — — — 1975a. Repetitive orogeny in the northeastern Appalachians - New plate models based upon Appalachian examples. Tectonophysics, 28, p. 39-87
- — — — — 1975b. The Fleur de Lys Supergroup: stratigraphic comparison of Moine and Dalradian equivalents in Newfoundland with the British Caledonides. Geological Society London, 131, p. 305-310

- Kennedy, M. J. and DeGrace, J. 1972. Structural sequence and its relationship to sulphide mineralization in the Ordovician Lush's Bight Group of Western Notre Dame Bay, Newfoundland. *Canadian Institute Mining Metallurgy Transactions*, 75, p. 300-308
- Kennedy, M. J. and Phillips, W. E. 1971. Ultramafic rocks of the Burlington Peninsula, Newfoundland. *Geological Association Canada, Proc.*, 24, p. 35-46
- Kennedy, M. J., Phillips, W. E. D. and Neale, E. R. W. 1972. Similarities in the early structural development of the northwestern margin of the Newfoundland Appalachians and Irish Caledonides. 24th International Geological Congress, Montreal, Report, Section 3, p. 516-531
- Kidd, W. S. F. 1974. The evolution of the Baie Verte lineament, Burlington Peninsula, Newfoundland. Ph. D. thesis, Cambridge University, England, 294 p.
- 1977. The Baie Verte Lineament: ophiolite complex floor and mafic volcanic fill of a small Ordovician marginal basin. in: *Island Arcs, Deep Sea Trenches and Back Arc Basins*, eds. M. Talwani and W. C. Pittman, Maurice Ewing Series, 1, p. 407-418
- Kidd, W. S. F., Dewey, J. F. and Bird, J. M. 1978. The Ming's Bight Ophiolitic Complex: Appalachian oceanic crust and mantle. *Canadian Journal Earth Sciences*, 15, p. 781-804
- Kusmirski, R. and Norman, R. 1982. Geology between Tilt Cove and East Pond, east Burlington Peninsula Newfoundland. Assessment report, Newmont Mining Canada Ltd. Newfoundland Department Mines and Energy, Mineral Development Division, Confidential File 2E/13(434)
- Leroy, J. 1979. Contribution a l'etalonnage de la pression interne des inclusions fluides lors de leur decrepitation. *Bulletin de Mineralogie*, 102, p. 584-593
- Linke, W. F. 1965. Solubilities of inorganic and metal-organic compounds. (4th ed.), American Chemical Society, 1914 p.
- Lister, C. R. 1974. On the penetration of water into hot rock. *Royal Astronomical Society Geophysical Journal*, 39, p. 465-509
- Lofgren, G. 1974. An experimental study of plagioclase crystal morphology: isothermal crystallization. *American Journal Science*, 274, p. 243-273

- Ludden, J. N. and Thompson, G. 1979. An evaluation of the behaviour of the rare earth elements during the weathering of sea-floor basalt. *Earth Planetary Science Letters*, 43, p. 85-92
- Luzhnaya, N. P. and Vereschchetina, I. P. 1946. Sodium, calcium, magnesium chlorides in aqueous solutions at -57° to $+25^{\circ}$ C (polythermic solubility). *Zhurnl. Prikl. Khimii*, 19, p. 723-733
- MacGeehan, P. J. 1978. The geochemistry of altered volcanic rocks at Matagami, Quebec: a geothermal model for massive sulfide genesis. *Canadian Journal Earth Sciences*, 15, p. 551-570
- Malpas, J. G. and Strong, D. F. 1975. A comparison of chrome-spinels in ophiolites and mantle diapirs of Newfoundland. *Geochimica Cosmochimica Acta*, 39, p. 1045-1069
- Martin, W. 1983. Once Upon a Mine: Story of Pre-Confederation Mines on the Island of Newfoundland. *Canadian Institute Mining Metallurgy, Special Volume 26*, 98 p.
- Mattinson, J. M. 1975. Early Paleozoic ophiolite complexes of Newfoundland: Isotopic ages of zircons. *Geology*, 3, p. 181-183
- Miyashiro, A. 1973. The Troodos ophiolite complex was probably formed in an island arc. *Earth Planetary Science Letters*, 19, p. 218-224
- Moore, J. G. and Vogt, P. G. 1976. Hydrothermal manganese crusts from two sites near the Galapagos spreading axis. *Earth Planetary Science Letters*, 29, p. 349-356
- Mottl, M. J. 1983a. Metabasalts, axial hot springs, and the structure of hydrothermal systems at mid-ocean ridges. *Geological Society America Bulletin*, 94, p. 161-180
- Mottl, M. J. 1983b. Hydrothermal processes at seafloor spreading centres: application of basalt-seawater experimental results. in: *Hydrothermal Processes at Seafloor Spreading Centers*, eds. P. A. Rona, K. Bostrom, L. Laubier and K. L. Smith. NATO Conference Series IV, Marine Sciences, Plenum Press, New York, N. Y. p. 199-224
- Mottl, M. J. and Holland, H. D. 1978. Chemical exchange during hydrothermal alteration of basalt by seawater - I. Experimental results for major and minor components of seawater. *Geochimica Cosmochimica Acta*, 42, p. 1103-1115

- Mottl, M. J., Holland, H. D. and Corr, R. F. 1979. Chemical exchange during hydrothermal alteration of basalt by seawater - II. Experimental results for Fe, Mn and sulfur species. *Geochimica Cosmochimica Acta*, 43, p. 869-884
- Mottl, M. J. and Seyfried, W. E. 1980. Sub-seafloor hydrothermal systems: rock- vs. seawater-dominated. in: *Seafloor Spreading Centers: Hydrothermal Systems*, eds. P. A. Rona and R. P. Lowell, Dowden, Hutchinson and Ross Inc., Stroudsburg, Pa., p. 66-82
- Murray, A. and Howley, J. P. 1881. Report of the Geological Survey of Newfoundland from 1864 to 1880. Geological Survey Newfoundland, Publication, 536 p.
- — — — — 1918. Report of the Geological Survey of Newfoundland from 1881 to 1909. Geological Survey Newfoundland, Publication, 725 p.
- Neale, E. R. W. 1957. Ambiguous intrusive relationship of the Betts Cove-Tilt Cove serpentinite belt, Newfoundland. *Geological Association Canada, Proc.*, 9, p. 95-107
- — — — — 1958a. Baie Verte, Newfoundland. Geological Survey Canada, Map 10-1958
- — — — — 1958b. Nippers Harbour, Newfoundland. Geological Survey Canada, Map 22-1958
- — — — — 1959. Fleur de Lys, Newfoundland. Geological Survey Canada, Map 16-1959
- — — — — 1967. Burlington (Baie Verte) Peninsula, Newfoundland. Geological Survey Canada, Paper 67-1A, p. 183-186
- Neale, E. R. W., Kean, B. F. and Upadhyay, H. D. 1975. Post-ophiolite unconformity, Tilt Cove-Betts Cove area, Newfoundland. *Canadian Journal Earth Sciences*, 12, p. 880-886
- Neale, E. R. W. and Kennedy, M. J. 1967. Relationship of the Fleur de Lys Group to younger groups of the Burlington Peninsula, Newfoundland. in: *Geology of the Atlantic Region*, eds. E. R. W. Neale and H. Williams. Geological Association Canada Special Paper 4, p. 139-169
- Neale, E. R. W. and Nash, W. A. 1963. Sandy Lake (east half), Newfoundland. Geological Survey Canada, Paper 62-28, 40 p.

- Neale, E. R. W., Nash, W. A. and Innes, G. M. 1960. Kings Point, Newfoundland. Geological Survey Canada, Map 35-1960
- O'Toole, K. 1956. Diamond Drill logs, Mt. Misery area. M. J. Boylen Engineering (Advocate Mines Ltd.), Unpublished report. Newfoundland Department Mines and Energy, Mineral Development Division, Open File 2E/12(153)
- Oudin, E. 1983. Hydrothermal sulfide deposits of the East Pacific Rise (21° N), Part 1: descriptive mineralogy. *Marine Mining*, 4, p. 39-72
- Panayiotou, A. 1980. Cu-Ni-Co-Fe sulphide mineralization, Limassol Forest, Cyprus. in: *Ophiolites*, ed. A. Panayiotou, Proceedings International Ophiolite Symposium, Nicosia, Cyprus, April 1979, Geological Survey Cyprus, p. 102-116
- Papezik, V. S. 1964. Nickel minerals at Tilt Cove, Notre Dame Bay, Newfoundland. *Geological Association Canada, Proc.*, 15, part 2, p. 27-32
- Papezik, V. S. and Fleming, J. M. 1967. Basic volcanic rocks of the Whalesback area, Newfoundland. *Geological Association Canada Special Paper* 4, p. 181-192
- Parmentier, E. M. and Spooner, E. T. C. 1978. A theoretical study of hydrothermal convection and the origin of the ophiolitic sulphide deposits of Cyprus. *Earth Planetary Science Letters*, 40, p. 33-44
- Pearce, J. A. 1975. Basalt geochemistry used to investigate past tectonic environments on Cyprus. *Tectonophysics*, 25, p. 41-67
- _____. 1980. Geochemical evidence for the genesis and eruptive setting of lavas from Tethyan ophiolites. in: *Ophiolites*, ed. A. Panayiotou, Proceedings International Ophiolite Symposium, Nicosia, Cyprus, April 1979, Geological Survey Cyprus, p. 261-272
- Pearce, J. A. and Cann, J. R. 1973. Tectonic setting of basic volcanic rocks determined using trace element analyses. *Earth Planetary Science Letters*, 19, 290-300
- Potter, R. W. II. 1977. Pressure corrections for fluid-inclusion homogenization temperatures based on the volumetric properties of the system NaCl-H₂O. *Journal Research-United States Geological Survey*, 5, p. 603-607
- Ribando, R. J., Torrance, K. E. and Turcotte, D. L. 1976. Numerical models for hydrothermal circulation in the oceanic crust. *Journal Geophysical Research*, 81, p. 3007-3012

- Riccio, L. M. 1972. The Betts Cove ophiolite, Newfoundland. M. Sc. thesis, University of Western Ontario, London, Ontario, 91 p.
- — — — — 1975. Report of mineral exploration on the Burlington Peninsula for 1975. Unpublished report, Phillips Management Inc., Newfoundland Department Mines and Energy, Mineral Development Division, Open File Nfld (929)
- Riverin, G. and Hodgson, C. J. 1980. Wall-rock alteration at the Millenbach Cu-Zn mine, Noranda, Quebec. *Economic Geology*, 75, p. 424-444
- Roedder, E. 1967a. Fluid inclusions as samples of ore fluids. in: *Geochemistry of Hydrothermal Ore Deposits* (1st ed.), ed. H. L. Barnes, Holt, Rhinehart and Winston, p. 515-574
- — — — — 1967b. Metastable "Superheated" ice in liquid-water inclusions under high negative pressure. *Science*, 155, p. 1413-1417
- — — — — 1972. Composition of Fluid Inclusions. *Data of Geochemistry* (6th ed.), Chapter JJ, United States Geological Survey Professional Paper 440 JJ, 164 p.
- Rona, P. A. 1978. Criteria for recognition of seafloor hydrothermal mineral deposits. *Economic Geology*, 73, p. 135-160
- — — — — 1980. TAG Hydrothermal Field: Mid-Atlantic Ridge crest at latitude 26 N. *Journal Geological Society London*, 137, p. 385-402
- — — — — 1984. Hydrothermal mineralization at seafloor spreading centers. *Earth Science Reviews*, 20, p. 1-104
- Rona, P. A. and Lowell, R. P. 1980. (eds.) *Seafloor Spreading Centers: Hydrothermal Systems. Benchmark Papers in Geology*, 56, Dowden, Hutchinson and Ross, Stroudsburg, Pennsylvania, 424 p.
- Sampson, E. 1923. The ferruginous chert formations of Notre Dame Bay, Newfoundland. *Journal Geology*, 3, p. 571-598
- Saunders, C. M. 1983. The Betts Cove sulphide deposit. in: *Current Research*, eds. M. J. Murray, P. D. Saunders, W. D. Boyce, and R. V. Gibbons, Newfoundland Department Mines and Energy, Mineral Development Division, Report 83-1, p. 175-181
- Schroeter, T. G. 1971. Geology of the Nippers Harbour area, Newfoundland. M. Sc. thesis, University of Western Ontario, London, Ontario, 88 p.

- Scott, M. R., Scott, R. B., Rona, P. A., Butler, L. W. and Nalwalk, A. J. 1974. Rapidly accumulating manganese deposit from the median valley of the Mid-Atlantic Ridge. *Geophysical Research Letters*, 1, p. 355-358
- Searle, D. L. 1972. Mode of occurrence of the cupriferous pyrite deposits of Cyprus. *Institute Mining Metallurgy Transactions*, 81, Section B, p. 189-197
- Seyfried, W. E. Jr. 1977. Seawater-basalt interaction from 25-300 °C and 1500 bars: implications for the origin of submarine metal-bearing hydrothermal solutions and regulation of ocean chemistry. Ph. D. thesis, University of Southern California, Los Angeles, 242 p.
- Seyfried, W. E. and Bischoff, J. L. 1977. Hydrothermal transport of heavy metals by seawater: the role of seawater-basalt ratio. *Earth Planetary Science Letters*, 34, p. 71-77
- _____ 1979. Low temperature basalt alteration by seawater: an experimental study at 70 °C and 150 °C. *Geochimica Cosmochimica Acta*, 43, p. 1937-1947
- _____ 1981. Experimental seawater-basalt interaction at 300 °C, 500 bars, chemical exchange, secondary mineral formation and implications for the transport of heavy metals. *Geochimica Cosmochimica Acta*, 45, p. 135-147
- Seyfried, W. E. and Mottl, M. J. 1982. Hydrothermal alteration of basalt by seawater under seawater-dominated conditions. *Geochimica Cosmochimica Acta*, 46, p. 985-1002
- Sillitoe, R. H. 1972. Formation of certain massive sulphide deposits at sites of sea-floor spreading. *Institute Mining Metallurgy Transactions*, 81, Section B, p. 141-148
- Simonian, K. O. and Gass, I. G. 1978. Arakapas fault belt, Cyprus: a fossil transform fault. *Geological Society America Bulletin*, 89, p. 1220-1230
- Sleep, N. H. and Wolery, T. J. 1978. Egress of hot water from mid-ocean ridge hydrothermal systems: some thermal constraints. *Journal Geophysical Research*, 83, p. 5913-5922
- Smewing, J. D., Simonian, K. O. and Gass, I. G. 1975. Metabasalts from the Troodos Massif, Cyprus. Genetic implications deduced from petrography and trace element geochemistry. *Contributions Mineralogy Petrology*, 51, p. 49-64

- Smitheringale, W. G. and Peters, H. R. 1974. Volcanogenic copper deposits in probable ophiolite rocks, Springdale Peninsula. in: Geological Association Canada/Mineralogical Association Canada Fieldtrip Manual B-3, St. John's, p. 35-48
- Snelgrove, A. K. 1929. Geological report on Betts Cove Copper Mine. Unpublished report, Norseman Corporation Limited, Newfoundland Department Mines and Energy, Mineral Development Division, Open File 2E/13(23)
- 1931. Geology and ore deposits of Betts Cove-Tilt Cove area, Notre Dame Bay, Newfoundland. Ph. D. thesis, Princeton University, New Jersey. (published in Canadian Mining Metallurgical Bulletin, 24, 43 p.)
- Snelgrove, A. K. and Baird, D. M. 1953. Mines and mineral occurrences of Newfoundland. Newfoundland Department Mines and Energy, Mineral Development Division, Information Circular 4, 149 p.
- Speiss, F. N., MacDonald, K. C., Atwater, T., Ballard, R., Carranza, A., Cordoba, D., Cox, C., Diaz Garcia, V. M., Francheteau, J., Guerrero, J., Hawkins, J., Hayman, R., Hessler, R., Juteau, T., Kastner, M., Larson, R., Luyendyk, B., Macdougall, J. D., Miller, S., Normark, W., Orcutt, J. and Rangin, C. (RISE Group) 1980. East Pacific Rise: hot springs and geophysical experiments. *Science*, 207, p. 1421-1444
- Spooner, E. T. C. 1977. Hydrodynamic model for the origin of the ophiolitic cupriferous pyrite ore deposits of Cyprus. in: *Volcanic Processes in Ore Genesis*, Geological Society London, Special Publication 7, p. 58-71
- 1980. Cu-pyrite mineralization and seawater convection in oceanic crust - the ophiolitic ore deposits of Cyprus. in: *The Continental Crust and its Mineral Deposits*, ed. D. W. Strangway, Geological Association Canada Special Paper 20, p. 685-704
- Spooner, E. T. C. and Bray, C. J. 1977. Hydrothermal fluids of seawater salinity in ophiolitic sulphide deposits in Cyprus. *Nature*, 266, p. 808-812
- Spooner, E. T. C. and Fyfe, W. S. 1973. Sub-sea metamorphism, heat and mass transfer. *Contributions Mineralogy Petrology*, 42, p. 287-304
- Spooner, E. T. C., Beckinsale, R. D., Fyfe, W. S. and Smewing, J. D. 1974. O¹⁸ enriched ophiolite metabasic rocks from E. Liguria (Italy), Pindos (Greece) and Troodos (Cyprus). *Contributions Mineralogy Petrology*, 47, p. 41-62

- Spooner, E. T. C., Beckinsale, R. D., England, P. C. and Senior, A. 1977a. Hydration, O-18 enrichment and oxidation during ocean floor hydrothermal metamorphism of ophiolitic metabasic rocks from E. Liguria, Italy. *Geochimica Cosmochimica Acta*, 41, p. 857-871
- Spooner, E. T. C., Chapman, H. J. and Smewing, J. D. 1977b. Strontium isotopic contamination and oxidation during ocean floor hydrothermal metamorphism of the ophiolitic rocks of the Troodos Massif, Cyprus. *Geochimica Cosmochimica Acta*, 41, p. 873-890
- Squires, G. C. 1981. The distribution and genesis of the Tilt Cove sulphide deposits. B. Sc. thesis, Memorial University of Newfoundland, St. John's, Newfoundland, 115 p.
- Strong, D. F. 1974. Plate tectonic setting of Appalachian - Caledonian mineral deposits as indicated by Newfoundland examples. Society Mining Engineers, AIME Transactions, 255, p. 121-128
- Strong, D. F. 1977. Volcanic regimes of the Newfoundland Appalachians. in: *Volcanic Regimes in Canada*, eds. W. R. A. Baragar, L. C. Coleman and J. M. Hall, Geological Association Canada Special Paper 16, p. 61-90
- _____ 1980. Geology of the Long Pond-Tilt Cove-Beaver Cove Pond area, western Notre Dame Bay, Newfoundland. Unpublished report, Newmont Mining Canada Ltd., Newfoundland Department Mines and Energy, Mineral Development Division, Confidential File 2E/13(408), 75 p.
- _____ 1984. Geological relationship of alteration and mineralization at Tilt Cove Newfoundland. in: *Mineral Deposits of Newfoundland - A 1984 Perspective*, ed. H. S. Swinden, Newfoundland Department Mines and Energy, Mineral Development Division, Report 84-3, p. 81-90
- Strong, D. F. and Malpas, J. G. 1975. The sheeted dike layer of the Betts Cove ophiolite complex does not represent spreading: further discussion. *Canadian Journal Earth Sciences*, 12, p. 894-896
- Sun, S. S. and Nesbitt, R. W. 1978. Geochemical regularities and significance of ophiolitic basalts. *Geology*, 6, p. 689-693
- Taylor, R. P. and Gorton, M. P. 1977. Geochemical application of spark source mass spectrography. III. Element sensitivity, precision and accuracy. *Geochimica Cosmochimica Acta*, 41, p. 1375-1380
- Upadhyay, H. D. 1973. The Betts Cove Ophiolite and related rocks of the Snooks

Arm Group, Newfoundland. Ph. D. thesis, Memorial University of Newfoundland, St. John's, Newfoundland, 224 p.

— — — — — 1974. Geology and mineral potential of Betts Cove - Tilt Cove area, Newfoundland. Unpublished report, Consolidated Morrison Explorations Ltd., Newfoundland Department Mines and Energy, Mineral Development Division, Open File 2E/12 (329)

— — — — — 1978. Phanerozoic peridotitic and pyroxenitic komatiites from Newfoundland. *Science*, 202, p. 1192-1195

— — — — — 1982. Ordovician komatiites and associated boninite-type magnesian lavas from Betts Cove, Newfoundland. in: *Komatiites*, eds. N. T. Arndt and E. G. Nisbet. George Allen and Unwin, Boston, p. 187-198

Upadhyay, H. D., Dewey, J. F. and Neale, E. R. W. 1971. The Betts Cove ophiolite complex, Newfoundland: Appalachian oceanic crust and mantle. *Proc. Geological Association Canada*, 24, No. 1, July 1971

Upadhyay, H. D. and Neale, E. R. W. 1976. The Betts Cove - Tilt Cove ophiolite and associated rocks, Newfoundland. *Geological Society America Abstracts with Program*, 8, p. 290

— — — — — 1979. On the tectonic regimes of ophiolite genesis. *Earth Planetary Science Letters*, 43, p. 93-102

Upadhyay, H. D. and Strong, D. F. 1973. Geological setting of the Betts Cove copper deposits, Newfoundland: an example of ophiolite sulphide mineralization. *Economic Geology*, 68, p. 161-167

Von Damm, K. L., Grant, B. and Edmond, J. M. 1983. Preliminary report on the chemistry of hydrothermal solutions at 21 North, East Pacific Rise. in: *Hydrothermal Processes at Seafloor Spreading Centers*, eds. P. A. Rona, K. Bostrom, L. Laubier and K. L. Smith. NATO Conference Series IV, Marine Sciences, Plenum Press, New York, p. 369-390

Watson, K. de P. 1943. Mafic and ultramafic rocks of the Baie Verte area, Newfoundland. *Journal Geology*, 51, p. 116-130

— — — — — 1947. Geology and mineral deposits of the Baie Verte - Ming's Bight area, Newfoundland. *Geological Survey Newfoundland, Bulletin*, 21, 48 p.

Weiss, R. F., Lonsdale, P., Lupton, J. E., Bainbridge, A. E. and Craig, H. 1977. Hydrothermal plumes in the Galapagos Rift. *Nature*, 267, p. 600-603

- West, J. M. 1972. Structure and ore-genesis: Little Deer Deposit, Whalesback Mine, Springdale, Newfoundland. M. Sc. thesis, Queen's University, Kingston, Ontario, 80 p.
- White, D. E., Anderson, E. T. and Grubbs, D. K. 1963. Geothermal brine well: Mile deep hole may tap ore-forming magmatic water, rocks undergoing metamorphism. *Science*, 139, p. 919-922
- Williams, C. T. and Floyd, P. A. 1981. The localized distribution of U and other incompatible elements in spilitic pillow lavas. *Contributions Mineralogy Petrology*, 78, p. 111-117
- Williams, D. L., Von Herzen, R. P., Sclater, J. G. and Anderson, R. N. 1974. The Galapagos spreading center: lithospheric cooling and hydrothermal circulation. *Royal Astronomical Society Geophysical Journal*, 38, p. 587-608
- Williams, H. 1976. Tectonic stratigraphic subdivision of the Appalachian orogen. *Geological Society America Abstracts with Program*, 8, p. 1279-1295
- — — — — 1977. Ophiolitic melange and its significance in the Fleur de Lys Supergroup, northern Appalachians. *Canadian Journal Earth Sciences*, 14, p. 987-1003
- — — — — 1978. Tectonic lithofacies map of the Appalachian orogen. Memorial University of Newfoundland, Map 1
- Williams, H., Hibbard, J. and Bursnall, J. T. 1977. Geologic setting of asbestos-bearing ultramafic rocks along the Baie Verte Lineament, Newfoundland. *Geological Survey Canada, Paper 77-1A*, p. 351-360
- Williams, H. and Hibbard, J. 1977. Geology of the Baie Verte Peninsula and western White Bay. Newfoundland Department Mines and Energy, Mineral Development Division, Map 77-29, 12H (529)
- Williams, H. and St. Julien, P. 1978. The Baie Verte - Brompton Line in Newfoundland and regional correlations in the Canadian Appalachians. *Geological Survey Canada, Paper 78-1A*, p. 225-229
- — — — — 1982. The Baie Verte-Brompton Line: early Paleozoic continent-ocean interface in the Canadian Appalachians. in: *Major Structural Zones and Faults of the Northern Appalachians*, eds. P. St. Julien and J. Beland, *Geological Association Canada Special Paper 24*, p. 177-207
- Winchester, J. A. and Floyd, P. A. 1976. Geochemical magma type

discrimination: application to altered and metamorphosed basic igneous rocks. *Earth Planetary Science Letters*, 28, p. 459-469

Wolery, T. J. and Sleep, N. H. 1976. Hydrothermal circulation and geochemical flux at mid-ocean ridges. *Journal Geology*, 84, p. 249-275

Yanatieva, O. K. 1946. Solubility polytherms in the systems $\text{CaCl}_2\text{-MgCl}_2\text{-H}_2\text{O}$, and $\text{CaCl}_2\text{-NaCl-H}_2\text{O}$. *Zhurnl. Prike. Khimii.*, 19, p. 709-722 (in Russian)

Yui, S. 1983. Textures of some Japanese Besshi-Type ores and their implications for Kuroko deposits. in: *The Kuroko and Related Volcanogenic massive sulfide deposits*, eds. H. Ohmoto and B. J. Skinner, *Economic Geology Monograph* 5, p. 231-240

Appendix A

Petrographic Table Illustrating Mineralogy of Samples

Section A - minerals found in the rock; section B - minerals found in veins and vesicles; x - rare to minor; X - common; XX - abundant; olv - olivine pseudomorphs (no olivine preserved), cpx - clinopyroxene, fld - plagioclase (dominantly albite), qtz - quartz, act - actinolite, chl - chlorite, clz - clinozoisite (grades into epidote), epi - epidote, cal - calcite, mus - muscovite, chr - chromite, py - pyrite, cp - chalcopyrite, sl - sphalerite.

SECTION A: ROCK

sample	background pillow lavas													
	olv	cpx	fld	qtz	act	chl	clz	epi	cal	mus	chr	py	cp	sl
45		X	X	X	XX	X		x		x		x		
49	x	X	-	X	X	x	X		X		x			
51b				X	X	X	X		x					
53	X	X	X	x	X	X	X		x				x	
55	X	X	X	X	X	X	X			x	x	x		
65		X	X		X	X	X				x	x		
66		X	X	x	X	X	X	X					x	
68		X	X		X	X	X	x		x			x	x
69b	X	X	X	X	X	X	X				x			
80a				X	X	x	X	x	XX			x	x	
82a		X	X	X	X	X	X				x	x		
82b		X	X	X	x	X	X					x	x	
83a	XX	X	X	X	X	X	X		X		X			
84	X	X	x		X	X	x							
85	X	X	X		X	x	X		X	x		x		x
104a		X	X	x	X	X	X	X	X					
105a		X	X	X	x	x	X					x		
105b		X	x	X	x	XX	X							
116	x	X	X	x	X	X	X	x			x	x		
141	x		X	X	XX	x	X					x	x	
144a	X	X	X	x	X	x	X	x	X		x	x		
145	x		X	X	X	X	X		XX	x	x	x		
149c		X	X	X	X		X	x					x	x
153a	X			x	XX	X	X		x		x	x		
157	x	X	X		X	X	x		x					
166		X	X		X	X	X	X	X			x		
168b	x	X	XX	X	X	X	X	x			x			

sample	olv	cpx	fld	qtz	act	chl	clz	epi	cal	mus	chr	py	cp	sl
	background pillow lavas													
170	X	X	X	x	XX	X	X			x	x			
179a		X	X	X	x	X		x				x	x	
181	X	X	x	x	X	X	x				x			
183	X	X	X	x		x	X				x			
184		X	XX			X		X			x			
186		X	X	X		X		X						
203	x	X	X		X	X		x				x		
204b		X	XX		X	X			x					
205g	x	X	X	X	X	X					x			
210a		X	X	x	X	X								
211		x	x	X	XX	X		X				x		
216a	x			x	X	X					x			
221b	X	X	x	X	X	X		X	x			x		
237	X	XX	X		XX	X	X				x			
238	x	X	X		X	X		X			x			
249	X	X	X		X	X	X		x	x				
252	X	XX	x	x		x	X				x			
253			X	X	X	X		x						
255a	X	XX	X		X	x	X							
255b	X	X	X		X	x	X		X		x	x		
256		X	X		X	x		X						
257	x	X	X	x	X	X	X						x	
259	X	X	X	X	X	X	X		X	x	x	x		
261a				X		X			XX				x	
278c	x	X	X		X	X		X			x			
281			X		X	X			XX		x	x	x	
282a	x				X	X			X		x			
286a	X		X	X	X	X		X	X	x	x			
286b	X		x	X	XX	X		X	X		x	x		
288	X		x	X	X	X		x	X		x			

sample	olv	cpx	fld	qtz	act	chl	clz	epi	cal	mus	chr	py	cp	sl
	chlorite-quartz alteration													
1	x			XX	x	XX						X	X	
2				XX		XX						X	x	
41c				XX		XX						X	X	
42a				XX		XX						X	X	
50a				XX		XX						X	x	
60a				XX		XX		x						
61				XX		XX						X	x	
197e				XX	X	X								x
198b	x			XX		XX			X		x	X	x	
200b				XX		XX					x	X	x	
205s				XX		XX						x		
289				XX	X	XX								
	chlorite-albite-quartz alteration													
59			X	XX		XX		x						x
62d			XX	X	X	X						X	x	x
63c			X	x	X	X		x	X			x		x
95b			X	XX		XX		X				X	x	
101			XX	X	X	X						X		
117			X	X		X		XX				X	x	
127			XX	X		XX			X			X	x	
136b			X	XX		XX		x	x			X	x	
137a			XX	XX		XX		X				X	x	x
137b			XX	X	x	X		x				X	x	
138a	x		XX	x	X	X			X		x	X		x
164			X	X	x	X								
198a	x		X		X	X			XX		x			
198c			X		X	X			X			x		
199a			X	XX		XX			X			X		

sample	olv	cpx	fld	qtz	act	chl	clz	epi	cal	mus	chr	py	cp	sl
	dykes													
27a			XX		X	X								
34a		X	X	x	x	x								
34b			X	x	X	x				XX	x			
89a			X	X	X		X							
89b	X	X	X	X	X	X	X				x			
106a	x		X		XX	x					X	x		
106b			XX	X	X			XX					x	
112		XX	XX		X	x							x	x
121a			XX		x									
121b			X		X	X		XX	x				x	x
121c			X	x	XX			x					x	x
129			X		XX			x						
130b			X	x	XX	x		X						
194	X	X	X	X	X	X		x			x	x	x	
197b			X	X	x	X								
197d		X	X	x	X	X					x	x	x	
201a			x	X	X	X			X					
220		X	X	X	X	x							x	
229			XX		X	X		x						
230a			X		X	X		X	X				x	x
251		XX	XX			x			X				x	
263a		X	XX		X	x			X					
267c			X	X	X	X		x	XX				x	
268a			XX	XX					X	X				
268c		X	XX	X	x	X			x					
269a		X	X	x		X			X					
269c		X	X		X	x	X							x
269d			X		XX	x								x
273			XX	X	X	X			X					x
	gabbro													
216b			X	X	X	X				x	x	x		
234		X	X	x	X				x	XX				
241		X	X	x		X								
	plagiogranite													
223a			XX	X	x	X		X						

SECTION B: VEINS AND VESICLES

	qtz	alb	chl	epi	cal	pre	mus	py	cp	sl
sample	background pillow lavas									
45	X	X	x	X	X		x	x		
49		x	x		x	x				
51b	X			X	X					
53		X				x				
55	X	X	X							
65	X			X						
66	x	X	X	X	X	XX	x			
68			x	X						x
69b	X	X	X				x			
80a	X	X	x	X	X			x	x	x
82a										
82b	X	X		X	X			X		
83a	X		X	X	X			x		
84					x					
85		x	X	x	X			x		x
104a	X			X	X			X		
105a	X			X	X			X		
105b	X	X	X	x				X		
116	x									
141	X	X	X	X	X			x	x	
144a	x	x	XX	x	X					
145			X		X					
149c	X		X	X						
153a	X		X		X			x		
157		x	X	X	X					
166			x	X	X			x		
168b	X	X				x				

	qtz	alb	chl	epi	cal	pre	mus	py	cp	sl
sample	background pillow lavas									
170	X	x	x		x					x
179a	X	X	x	x	X					x
181	X	X	X	x	X					x
183	x	X	X		X	x				x
184		X	X							
186	x		X							x
203		X	X		x	x				x
204b										
205g	X	X			X					x
210a		X								
211	x				XX					
216a	x		X							
221b	X		X	X	X		x			x
237	X		X							
238			x		x					
249	X		X							
252		X	X			X	x			x
253	X	X	x	X	X					
255a	X		X		X	x				
255b	x		X		X	x				
256	X		X							x
257	X		X		x	x				x
259			X		x					x
261a										
278c	X	X	X	X	X	x	x			x
281	X	X	X		X					x
282a					X					
286a	x	x	x	x	X					
286b	X	x	x	x	X					
288	X	x	x	x	XX					

sample	qtz	alb	chl	epi	cal	pre	mus	py	cp	sl
	chlorite-quartz alteration									
1	X							X	X	
2	X									
41c										
42a	X		X	X				X	X	
50a	X	X	X	X			X	X	X	
60a										
61				x				x	x	
197e	XX		X		X			x	XX	
198b	X				XX			X	XX	x
200b	XX							X		
205s	XX				XX			X	XX	
289	x		x							
	chlorite-albite-quartz alteration									
59	X			X			x	X	x	
62d	x	x		X				X	x	x
63c	X	XX	x		X		x			x
95b	x	X		x			x	x		
101	X	X		X	X			X		
117	X			XX				X		
127	x				XX					
136b	X		X	X			x	X	x	
137a	X		X	X			x	X	x	x
137b	X	X	X	X				X	x	
138a	X	XX			X			X	x	x
164	X	X	x	X				X	x	
198a	X			x				x		x
198c	X	X			X			x		
199a	x				X					

Appendix B

Analytical Methods

Ninety-nine samples were analyzed for major and trace elements. Major elements were analyzed by atomic absorption. For each sample 0.1000 gm of 100 mesh rock powder was weighed into a flask. The samples were dissolved in 5 ml concentrated HF + 50 ml of saturated Boric Acid solution; 145 ml distilled water was then added to each flask. Analysis of MgO and CaO requires further dilution of the sample solution with lanthanum oxide solution and distilled water. The samples were compared to standards containing known amounts of the major oxides. The standards were first run to get rough readings for % absorption. Then a reading was obtained for the sample and for the standards just lower and just higher than the sample. The amount of a particular oxide can then be worked out by the following formula:

$$\% \text{ oxide} = \% \text{ LS} + \frac{\% \text{A sample} - \% \text{A LS}}{\% \text{A HS} - \% \text{A LS}} * (\% \text{ HS} - \% \text{ LS}) * 2$$

(A = Absorption; LS = low standard; HS = high standard)

Loss on ignition was determined by weighing a known amount of rock powder in a crucible before and after ignition at 1000 ° C.

Trace elements were analyzed by X-ray fluorescence of pressed pellets. The pellets were made by the following technique: 10 +/- 0.1 gm of rock powder was combined with 1.4 to 1.5 gm binder (Bakelite brand phenyl resins) and mixed thoroughly on a mechanical shaker. The mixture was poured into a press and formed into pellets which were baked 10-20 minutes at 200 ° C.

Rare-earth analyses were also carried out using the technique of Fryer (1977) but abundances were found to be too low (generally 5 to 10 times chondrites) to be analysed accurately by the method used. Thus the results are not included.

Appendix C

Major and Trace Element Analyses

	SAMPLE NUMBER				
	45	49	51B	53	55

MAJOR ELEMENTS					

SiO ₂	49.30	54.90	54.80	51.80	60.00
TiO ₂	.17	.25	.27	.25	.10
Al ₂ O ₃	14.10	13.10	15.30	13.70	10.30
Fe ₂ O ₃	9.64	6.94	8.75	7.54	6.68
MnO	.15	.12	.24	.16	.11
MgO	11.71	8.75	8.00	11.19	9.69
CaO	8.61	7.96	4.60	10.07	6.78
Na ₂ O	.27	5.39	4.50	3.06	3.27
K ₂ O	2.12	.05	.04	.30	.25
P ₂ O ₅	.01	.01	.01	.02	.06
LOI	3.92	2.89	3.39	2.53	2.53

TOTAL	100.00	100.36	99.90	100.62	99.77

TRACE ELEMENTS					

Rb	30	2	0	3	1
Sr	209	99	36	86	91
Y	8	9	12	10	4
Zr	19	12	27	17	9
Nb	1	2	3	1	2
Zn	61	46	166	54	50
Cu	113	76	82	87	82
Ni	138	188	53	183	203
Ba	135	44	51	84	31
V	246	192	332	248	207
Cr	448	437	27	464	832
Ga	13	9	12	8	6

SAMPLE NUMBER

65 68 69B 80A 82A

MAJOR ELEMENTS

	65	68	69B	80A	82A
SiO2	57.30	54.90	50.00	55.60	52.60
TiO2	.10	.23	.17	.09	.13
Al2O3	12.10	15.30	11.70	13.80	13.40
Fe2O3	6.84	9.93	8.98	8.35	8.73
MnO	.15	.12	.15	.16	.13
MgO	9.03	7.94	16.00	9.38	10.34
CaO	8.58	4.73	7.18	3.90	6.40
Na2O	4.09	3.94	1.16	3.23	3.34
K2O	.04	.25	.39	.29	.49
P2O5	.01	.01	.01	.02	.03
LOI	1.58	3.05	4.70	4.98	2.74
TOTAL	99.82	100.40	100.44	99.80	98.33

TRACE ELEMENTS

Rb	0	4	7	2	6
Sr	40	140	99	76	82
Y	7	10	7	7	6
Zr	13	17	27	15	22
Nb	1	1	5	4	2
Zn	33	70	56	80	58
Cu	86	129	82	261	95
Ni	126	36	346	70	120
Ba	37	54	106	72	58
V	230	342	218	298	272
Cr	457	5	1099	209	451
Ga	12	11	8	7	8

SAMPLE NUMBER

82B 83A 84 85 104A

MAJOR ELEMENTS

SiO ₂	56.90	62.30	51.00	53.90	57.20
TiO ₂	.13	.03	.44	.34	.11
Al ₂ O ₃	14.40	9.81	14.50	16.40	12.40
Fe ₂ O ₃	8.40	6.12	8.11	5.56	7.78
MnO	.16	.10	.13	.11	.24
MgO	6.92	9.53	11.72	7.34	9.36
CaO	4.13	5.87	7.37	7.63	7.36
Na ₂ O	5.20	3.10	4.14	4.48	4.43
K ₂ O	.07	.16	.26	1.12	.04
P ₂ O ₅	0.00	.01	0.00	.04	0.00
LOI	3.22	3.14	3.11	3.01	2.09
TOTAL	99.53	100.17	100.78	99.93	101.01

TRACE ELEMENTS

Rb	0	1	8	27	0
Sr	82	81	225	123	79
Y	8	3	13	8	4
Zr	14	11	16	15	11
Nb	1	1	0	0	1
Zn	112	41	53	34	102
Cu	184	63	87	69	178
Ni	35	347	194	182	85
Ba	35	35	53	97	41
V	311	187	214	186	253
Cr	2	1145	406	417	254
Ga	8	7	9	10	10

SAMPLE NUMBER

105A

116M

116V

141

144A

MAJOR ELEMENTS

	105A	116M	116V	141	144A
SiO ₂	55.10	51.40	54.40	58.00	54.20
TiO ₂	.20	.20	.23	.20	.27
Al ₂ O ₃	14.50	13.60	14.50	12.40	11.30
Fe ₂ O ₃	8.22	11.19	7.96	7.20	7.91
MnO	.18	.17	.12	.15	.15
MgO	6.85	10.86	9.60	9.66	10.61
CaO	8.87	5.47	5.08	4.74	7.05
Na ₂ O	4.69	3.90	5.50	4.25	4.09
K ₂ O	.04	.04	.05	.05	.05
P ₂ O ₅	.03	.02	.02	.01	0.00
LOI	1.96	3.16	2.83	2.99	2.74
TOTAL	100.64	100.01	100.29	99.65	98.37

TRACE ELEMENTS

	105A	116M	116V	141	144A
Rb	1	3	0	1	0
Sr	66	62	69	68	37
Y	6	10	7	6	1
Zr	17	12	12	14	16
Nb	0	4	1	0	2
Zn	71	68	48	206	225
Cu	105	46	31	91	101
Ni	48	156	141	83	335
Ba	43	41	45	53	65
V	238	323	240	278	195
Cr	13	578	478	394	872
Ga	11	10	9	10	9

SAMPLE NUMBER

145

149C

153A

157

166

MAJOR ELEMENTS

	145	149C	153A	157	166
SiO2	48.00	56.20	50.80	53.50	56.40
TiO2	.13	.23	.17	.36	.20
Al2O3	10.10	15.10	10.70	12.50	14.90
Fe2O3	7.13	7.94	9.43	7.26	7.61
MnO	.14	.12	.17	.13	.14
MgO	11.09	7.26	15.02	11.26	7.09
CaO	10.69	6.17	6.25	8.18	6.72
Na2O	1.67	4.82	1.86	4.42	5.10
K2O	.16	.04	.07	.04	.05
P2O5	0.00	.03	.01	0.00	.04
LOI	10.19	2.47	5.47	2.40	2.24
TOTAL	99.30	100.38	99.95	100.05	100.49

TRACE ELEMENTS

	145	149C	153A	157	166
Rb	6	1	2	0	1
Sr	50	105	39	89	86
Y	4	9	5	12	9
Zr	16	18	20	16	10
Nb	4	4	2	0	0
Zn	43	75	107	46	55
Cu	71	59	42	51	108
Ni	370	48	330	208	48
Ba	67	37	52	44	39
V	205	299	262	186	281
Cr	819	33	1104	440	26
Ga	8	11	7	7	12

SAMPLE NUMBER

168B 170 179A 181 183F1

MAJOR ELEMENTS

SiO ₂	52.30	51.30	54.80	52.30	50.00
TiO ₂	.07	.12	.10	.12	.30
Al ₂ O ₃	10.80	9.71	13.80	10.60	12.50
Fe ₂ O ₃	8.09	8.85	8.61	9.14	8.28
MnO	.16	.16	.14	.16	.18
MgO	14.46	17.28	7.31	15.28	12.34
CaO	6.79	7.17	7.12	7.11	11.76
Na ₂ O	1.90	1.36	4.63	1.00	1.57
K ₂ O	.16	.10	.03	.41	.72
P ₂ O ₅	.01	0.00	0.00	.01	0.00
LOI	3.89	3.72	2.14	3.92	2.77
TOTAL	98.63	99.77	98.68	100.05	100.42

TRACE ELEMENTS

Rb	4	6	2	7	9
Sr	90	172	51	53	109
Y	4	7	7	4	11
Zr	11	19	13	16	19
Nb	0	2	1	2	1
Zn	57	55	59	64	49
Cu	79	87	111	136	58
Ni	333	338	58	311	200
Ba	43	51	58	78	158
V	208	202	266	228	215
Cr	913	858	51	954	418
Ga	9	5	8	9	11

	SAMPLE NUMBER				
	183F2	183M	184	186	204B
MAJOR ELEMENTS					
SiO2	51.90	51.20	51.20	55.60	52.80
TiO2	.26	.33	.08	.11	.50
Al2O3	10.20	16.50	13.80	13.80	15.70
Fe2O3	8.32	7.84	8.27	8.94	7.61
MnO	.20	.11	.14	.14	.14
MgO	12.66	10.53	12.48	7.57	8.88
CaO	12.57	5.01	5.59	7.26	3.41
Na2O	1.22	2.34	4.24	4.23	6.00
K2O	.66	.51	.05	.05	.05
P2O5	0.00	0.00	.06	0.00	0.00
LOI	2.60	5.63	3.62	2.47	4.11
TOTAL	100.59	100.00	99.53	100.17	99.20

TRACE ELEMENTS					
Rb	9	7	2	0	2
Sr	80	133	62	78	79
Y	11	9	11	1	15
Zr	16	14	17	9	22
Nb	2	0	1	1	1
Zn	43	61	58	57	89
Cu	51	135	29	88	35
Ni	189	249	221	44	59
Ba	166	106	41	50	52
V	198	177	231	273	286
Cr	392	588	701	52	122
Ga	7	13	7	12	12

	SAMPLE NUMBER				
	205G	210A	211	216A	221B

MAJOR ELEMENTS					

SiO ₂	53.20	54.60	55.50	50.50	47.60
TiO ₂	.03	.20	.10	.37	.10
Al ₂ O ₃	8.90	14.10	10.00	13.30	11.60
Fe ₂ O ₃	10.01	7.79	7.98	8.82	9.14
MnO	.22	.12	.13	.15	.19
MgO	16.90	9.75	8.99	13.56	14.90
CaO	5.60	5.48	6.53	4.95	10.77
Na ₂ O	.60	5.29	1.42	3.62	.33
K ₂ O	.02	.04	.06	.21	.67
P ₂ O ₅	0.00	.01	0.00	.03	0.00
LOI	5.09	2.25	9.46	4.20	4.99

TOTAL	100.57	99.63	100.17	99.71	100.29

TRACE ELEMENTS					

Rb	2	1	0	1	9
Sr	6	66	47	91	110
Y	4	9	2	13	5
Zr	8	12	7	19	17
Nb	2	1	0	0	2
Zn	81	49	47	67	51
Cu	42	34	54	74	76
Ni	427	139	125	221	363
Ba	24	35	24	63	91
V	249	236	273	258	235
Cr	1637	465	547	636	916
Ga	9	9	7	10	6

	SAMPLE NUMBER				
	237	238	249	252	253

MAJOR ELEMENTS					
SiO2	50.20	53.60	51.80	47.40	53.20
TiO2	.07	.36	.33	.35	.09
Al2O3	12.40	14.40	17.10	12.90	12.20
Fe2O3	9.11	7.90	6.65	8.95	8.91
MnO	.19	.14	.12	.16	.15
MgO	14.62	9.35	8.54	14.24	11.12
CaO	6.58	6.80	7.56	12.28	8.10
Na2O	2.92	5.15	4.37	.66	1.62
K2O	.11	.07	.62	.41	.18
P2O5	.02	.02	0.00	0.00	.01
LOI	3.46	2.47	2.86	3.56	3.97

TOTAL	99.68	100.26	99.95	100.91	99.55

TRACE ELEMENTS					
Rb	1	0	9	8	3
Sr	76	103	161	73	222
Y	6	15	13	11	4
Zr	16	21	18	14	12
Nb	2	1	2	1	2
Zn	95	52	40	51	69
Cu	38	76	71	66	117
Ni	250	173	183	236	148
Ba	60	53	97	66	68
V	268	224	205	241	242
Cr	693	444	426	567	562
Ga	9	8	12	11	14

SAMPLE NUMBER

255A 257AV 257AW 259 261

MAJOR ELEMENTS

SiO ₂	49.10	61.40	46.50	49.30	44.70
TiO ₂	.46	.13	.16	.16	.11
Al ₂ O ₃	13.60	13.40	12.30	11.30	14.90
Fe ₂ O ₃	9.42	4.73	10.40	9.26	7.58
MnO	.19	.09	.16	.16	.17
MgO	11.69	5.90	14.16	14.98	6.98
CaO	9.10	5.79	13.39	8.95	9.53
Na ₂ O	2.60	5.95	.29	.38	.09
K ₂ O	.42	.16	.18	.50	2.74
P ₂ O ₅	.04	.02	.02	0.00	0.00
LOI	3.11	1.39	3.30	5.03	12.42
TOTAL	99.73	98.96	100.86	100.02	99.22

TRACE ELEMENTS

Rb	6	0	3	10	30
Sr	110	138	139	120	18
Y	14	6	4	7	5
Zr	21	11	14	15	12
Nb	1	0	2	1	2
Zn	49	29	62	57	214
Cu	44	81	93	82	129
Ni	165	97	116	425	89
Ba	85	35	52	73	73
V	257	220	273	221	271
Cr	392	387	382	1016	106
Ga	9	10	10	8	9

SAMPLE NUMBER

278C

282A

286A

288

41C

MAJOR ELEMENTS

	278C	282A	286A	288	41C
SiO2	53.50	53.80	55.40	45.60	52.00
TiO2	.61	.13	0.00	.13	.17
Al2O3	14.30	9.36	9.96	9.19	11.90
Fe2O3	7.64	7.71	8.22	8.18	17.18
MnO	.14	.16	.15	.16	.22
MgO	9.48	13.66	11.66	12.48	11.12
CaO	7.94	9.14	7.56	14.23	.04
Na2O	4.32	2.38	1.38	.56	.04
K2O	.04	.31	.74	.31	.01
P2O5	.01	.04	0.00	.01	.02
LOI	2.62	2.92	5.78	7.62	6.32
TOTAL	100.60	99.61	100.85	98.47	99.02

TRACE ELEMENTS

Rb	2	7	11	5	2
Sr	126	64	40	272	1
Y	17	3	4	3	4
Zr	27	14	6	15	19
Nb	3	3	3	2	3
Zn	48	53	49	42	89
Cu	69	93	76	54	4687
Ni	96	298	254	339	61
Ba	49	58	50	29	57
V	270	200	238	178	349
Cr	281	792	1152	900	300
Ga	12	8	3	10	9

SAMPLE NUMBER

42A 50A 60A 61 198B

MAJOR ELEMENTS

	42A	50A	60A	61	198B
SiO2	58.00	54.40	52.20	60.00	49.40
TiO2	.10	0.00	.03	.15	.07
Al2O3	10.40	12.60	12.60	10.20	8.41
Fe2O3	16.66	18.08	18.36	16.14	15.31
MnO	.14	.23	.20	.15	.39
MgO	7.27	8.69	10.21	7.69	10.88
CaO	.20	.30	.22	.24	4.57
Na2O	.22	.12	.32	.36	.03
K2O	.06	.42	.08	.02	.02
P2O5	.01	.02	.03	.01	0.00
LOI	5.10	5.54	5.98	4.83	7.91
TOTAL	98.16	100.40	100.23	99.79	96.99

TRACE ELEMENTS

Rb	0	6	4	1	3
Sr	6	4	5	8	22
Y	1	5	6	6	3
Zr	13	16	14	12	12
Nb	1	2	2	1	4
Zn	71	108	130	148	359
Cu	4174	115	134	1796	9793
Ni	34	43	77	24	290
Ba	65	71	55	49	65
V	317	353	394	317	254
Cr	45	45	186	0	1260
Ga	8	11	8	7	4

	SAMPLE NUMBER				
	289	62D	63C	95B	101
MAJOR ELEMENTS					
SiO ₂	55.00	52.50	52.40	57.20	53.20
TiO ₂	.11	.13	.17	.29	.16
Al ₂ O ₃	10.10	15.30	13.30	12.50	13.90
Fe ₂ O ₃	16.16	9.29	8.29	15.18	14.83
MnO	.11	.12	.28	.21	.20
MgO	11.93	10.36	9.65	7.67	8.70
CaO	.68	1.64	6.70	.52	1.89
Na ₂ O	.02	4.39	4.24	1.51	2.39
K ₂ O	.03	.04	.04	.04	.04
P ₂ O ₅	.02	.02	.01	.07	0.00
LOI	6.04	4.92	5.19	4.61	4.65
TOTAL	100.20	98.71	100.27	99.80	99.96
TRACE ELEMENTS					
Rb	0	0	1	0	0
Sr	1	92	81	29	87
Y	8	9	6	11	9
Zr	13	11	16	20	22
Nb	2	1	5	3	2
Zn	114	686	365	134	107
Cu	2	74	65	951	640
Ni	102	77	96	51	72
Ba	48	52	41	40	44
V	314	377	302	344	369
Cr	534	259	349	119	197
Ga	7	11	6	11	11

SAMPLE NUMBER

117 127 136B 137A 137B

MAJOR ELEMENTS

SiO2	59.80	53.40	56.00	59.20	57.10
TiO2	.20	.12	.16	.36	.16
Al2O3	14.60	14.90	13.70	13.60	14.60
Fe2O3	9.88	7.68	11.03	11.02	9.52
MnO	.14	.14	.21	.16	.18
MgO	5.57	6.93	9.11	5.21	8.85
CaO	3.64	5.04	1.13	1.05	1.85
Na2O	3.85	5.04	2.68	4.13	4.11
K2O	.02	.03	.15	.03	.04
P2O5	.08	.01	0.00	.04	.02
LOI	3.39	7.18	5.00	3.99	3.69
TOTAL	101.17	100.47	99.17	98.79	100.12

TRACE ELEMENTS

Rb	0	0	3	0	0
Sr	91	50	50	66	76
Y	10	9	8	16	9
Zr	20	13	16	32	18
Nb	1	1	2	1	2
Zn	236	62	698	169	309
Cu	370	11	123	403	212
Ni	34	56	36	15	72
Ba	46	58	66	57	56
V	296	308	401	429	335
Cr	12	73	2	1	169
Ga	11	11	9	11	11

	SAMPLE NUMBER				
	138A	198A	198C	199A	27A

MAJOR ELEMENTS					

SiO2	54.40	52.80	48.40	54.60	50.20
TiO2	.08	.54	.54	.13	.06
Al2O3	13.20	13.40	14.60	12.30	15.60
Fe2O3	10.84	10.62	10.82	10.13	9.19
MnO	.20	.39	.44	.22	.13
MgO	8.98	8.85	13.70	12.06	12.48
CaO	3.67	4.52	3.49	1.61	2.80
Na2O	3.82	2.99	3.42	1.52	4.63
K2O	.04	.03	.05	.07	.04
P2O5	0.00	.03	.04	0.00	0.00
LOI	4.48	7.47	5.23	6.60	4.91

TOTAL	99.71	101.64	100.73	99.24	100.04

TRACE ELEMENTS					

Rb	0	1	0	0	2
Sr	53	46	39	28	31
Y	7	18	17	8	6
Zr	17	22	25	13	12
Nb	3	1	3	2	2
Zn	1605	835	532	108	19
Cu	88	59	47	90	6
Ni	116	169	184	121	96
Ba	31	61	50	55	55
V	339	328	355	386	363
Cr	504	445	513	603	178
Ga	9	11	15	9	11

	SAMPLE NUMBER				
	34A	34B	89A	89B	106A

MAJOR ELEMENTS					

SiO2	52.80	52.20	56.70	50.40	51.00
TiO2	.03	.03	.03	.03	.09
Al2O3	13.80	12.70	14.40	11.10	9.66
Fe2O3	9.36	8.57	8.38	9.67	11.78
MnO	.15	.16	.13	.21	.19
MgO	10.98	12.72	6.94	14.68	15.62
CaO	5.38	6.04	6.36	8.98	6.18
Na2O	4.16	2.43	4.50	1.71	2.51
K2O	.11	1.23	.14	.09	.10
P2O5	0.00	.04	.01	.02	0.00
LOI	3.23	3.94	2.04	3.98	3.33

TOTAL	100.00	100.06	99.63	100.87	100.46

TRACE ELEMENTS					

Rb	0	19	4	3	1
Sr	97	57	64	61	58
Y	4	8	4	4	1
Zr	8	13	12	15	11
Nb	0	3	2	3	3
Zn	52	32	89	70	16
Cu	89	8	22	70	5
Ni	102	207	56	462	321
Ba	57	110	36	51	42
V	351	280	280	257	261
Cr	262	704	36	835	1118
Ga	10	7	8	8	9

	SAMPLE NUMBER				
	106B	112	121B	121C	129

MAJOR ELEMENTS					

SiO2	56.30	55.90	45.00	57.80	58.00
TiO2	.11	.10	.14	.03	.20
Al2O3	14.60	13.00	18.60	9.90	11.40
Fe2O3	8.91	7.67	10.58	8.55	8.35
MnO	.09	.16	.11	.11	.15
MgO	4.69	9.78	5.29	11.12	9.06
CaO	10.22	6.84	16.40	7.19	6.63
Na2O	4.31	5.23	.30	4.21	5.06
K2O	.02	.04	.01	.05	.05
P2O5	.08	.01	.06	0.00	.01
LOI	1.18	1.74	2.94	1.63	1.58

TOTAL	100.51	100.47	99.43	100.59	100.49

TRACE ELEMENTS					

Rb	1	1	4	0	2
Sr	215	33	71	35	63
Y	8	3	8	4	11
Zr	23	9	21	7	16
Nb	3	0	2	1	0
Zn	4	44	25	9	30
Cu	10	209	7	6	9
Ni	29	85	66	115	80
Ba	39	31	38	38	39
V	280	250	323	282	260
Cr	7	196	38	539	257
Ga	9	8	20	7	6

	SAMPLE NUMBER				
	130B	194	197B	197D	201A

MAJOR ELEMENTS					
SiO2	55.00	53.00	53.30	52.00	44.50
TiO2	.03	.13	.27	.10	.10
Al2O3	10.40	11.20	14.00	11.90	12.20
Fe2O3	9.39	8.59	8.99	8.86	13.39
MnO	.19	.25	.33	.33	.21
MgO	12.62	12.83	8.12	12.21	17.05
CaO	6.68	6.50	11.94	6.00	5.08
Na2O	2.43	2.81	.10	3.35	.64
K2O	.06	.22	.01	.03	.81
P2O5	.05	0.00	.03	.01	0.00
LOI	3.19	3.78	3.64	4.59	6.05

TOTAL	100.04	99.31	100.73	99.38	100.03

TRACE ELEMENTS					
Rb	0	3	1	0	7
Sr	61	42	560	71	7
Y	5	7	7	8	4
Zr	13	22	17	10	5
Nb	3	0	3	1	0
Zn	51	154	146	170	75
Cu	372	133	120	148	134
Ni	167	307	100	215	185
Ba	50	74	33	37	69
V	237	240	265	274	372
Cr	649	1033	358	761	829
Ga	5	12	19	12	11

	SAMPLE NUMBER				
	251	263A	269A	269D	273

MAJOR ELEMENTS					

SiO ₂	52.80	52.80	51.60	52.00	59.10
TiO ₂	.72	.16	.18	.13	.16
Al ₂ O ₃	12.90	15.90	14.60	13.50	13.30
Fe ₂ O ₃	7.67	8.96	9.56	10.44	6.80
MnO	.12	.10	.14	.17	.10
MgO	9.36	8.68	12.00	10.64	5.77
CaO	8.20	3.78	4.23	4.40	4.36
Na ₂ O	4.41	5.56	2.70	4.16	3.80
K ₂ O	.31	.05	.87	.18	.65
P ₂ O ₅	.20	0.00	.02	.01	.01
LOI	3.65	4.72	4.34	3.41	4.38

TOTAL	100.34	100.71	100.24	99.04	98.43

TRACE ELEMENTS					

Rb	1	1	13	1	7
Sr	157	57	65	57	95
Y	19	9	8	7	5
Zr	64	19	17	8	19
Nb	2	3	2	1	1
Zn	45	25	58	59	20
Cu	90	14	93	157	9
Ni	30	75	93	91	60
Ba	129	46	63	35	57
V	275	377	308	311	277
Cr	187	25	250	266	45
Ga	10	12	9	11	8

SAMPLE NUMBER

	216B	234	241	223A
--	------	-----	-----	------

MAJOR ELEMENTS

SiO ₂	52.30	52.80	47.60	60.50
TiO ₂	.10	.29	.14	.43
Al ₂ O ₃	10.50	12.30	17.70	13.80
Fe ₂ O ₃	8.96	6.83	5.37	10.04
MnO	.17	.16	.11	.10
MgO	14.62	11.02	9.88	2.91
CaO	6.15	9.50	12.31	3.79
Na ₂ O	1.86	3.00	2.28	5.75
K ₂ O	.51	1.08	.86	.16
P ₂ O ₅	0.00	.03	.01	.04
LOI	5.01	3.25	3.82	1.61
TOTAL	100.18	100.26	100.08	99.13

TRACE ELEMENTS

Rb	4	13	12	3
Sr	54	96	150	84
Y	4	13	5	22
Zr	8	27	8	43
Nb	0	1	1	2
Zn	43	31	15	20
Cu	20	17	9	10
Ni	336	121	110	11
Ba	58	87	90	56
V	252	205	133	366
Cr	1111	415	352	0
Ga	9	8	12	12

Appendix D

Sulphide Analyses

*	*	*	*	*	*	*	*	*
Sample	Cu	Zn	Pb	Ag	Ag	Ag	Ag	Au

A-3	0.91	1.45	0.02				16.9	6650
repeat	0.91	1.45	0.02					

A-6	0.20	0.37	0.02				13.3	>10000
repeat	0.19	0.36	0.02					

O-12	19.97	0.04	<0.01	12.8	11.4		12.7	
dupl.	20.02	0.04	<0.01	12.9			12.8	1600

O-9	7.01	2.12	0.02	31.6	26.5		30.9	

O-16	0.19	4.55	1.08	37.1	38.1		39.5	

O-4	0.47	0.55	0.02	4.9	4.5		5.3	

O-33	0.20	7.96	0.22				16.6	<1
repeat	0.20	7.57	0.22					

O-34	1.18	6.91	0.02				20.4	4100
repeat	1.19	6.69	0.02					

O-35	0.37	20.54	0.06				16.5	>10000
repeat	0.36	19.22	0.06					

O-2	1.89	5.05	0.03				11.1	7100
repeat	1.81	4.79	0.03					

* Sample	* Cu	* Zn	* Pb	* Ag	* Ag	* Ag	* Au	*
O-6	0.97	2.06	0.08			30.1	9600	
repeat	1.00	2.12	0.07					
O-22	4.26	1.82	0.02			24.9	7050	
repeat	4.13	1.71	0.02					
O-3	0.52	11.80	0.07			25.5	>10000	
repeat	0.51	11.56	0.07					
O-7	0.98	1.98	0.14			29.6	>10000	
282r	16.21	0.13	0.01	25.3	21.9	23.3		
205s	2.39	0.32	<0.01	7.8	7.6	8.9		
3	3.79	0.02	<0.01	7.0	6.3	6.8		
BP-6	0.19	0.01	<0.01	1.7	2.1	2.2		
BP-4	3.74	0.02	<0.01	5.5	5.0	5.6		
BP-1	0.87	0.01	<0.01	6.4		6.8	245	
BP-8	1.85	0.04	<0.01	12.2		16.8	2600	

Cu,Zn,Pb in percent; Ag in ppm; Au in ppb

SAMPLE LOCATIONS

Samples A-3 & A-6 are from the outcropping massive pyrite lens.

Samples prefixed by an "0" are from the main mine site dumps.

Samples prefixed by "BP" are from the dump at the Burtons Pond showing.

Samples 282r, 205s and 3 are from rubble brought up from shafts at the Betts Head, Fault Cove and Mount Misery showings respectively.

Sample 277 is from a dump (location given in Fig. 2-1).

SAMPLE DESCRIPTIONS

A-3, A-6: Crumbly, porous, banded massive pyrite.

All "0" samples except 0-4, 0-12, 0-13 and 0-18: Banded to homogeneous massive sulphide; pyrite with variable amounts of chalcopyrite and sphalerite.

0-4, 3, 205s: Stringer chalcopyrite and/or pyrite in chloritic basalt.

0-12, 0-13, 0-18, 282r: Semi-massive chalcopyrite and minor pyrite in chloritic basalt.

277: Disseminated pyrite in a quartz, actinolite-rich rock.

Appendix E

Electron Microprobe Data - Chlorites

```
*****
p 83a(9)      p 252(10)      p 249(4)      p 216a(3)
-----
```

Si	31.80	3.085	29.66	2.892	29.71	2.950	31.13	3.104
Al	16.93	1.936	20.15	2.316	18.61	2.177	15.84	1.860
Mg	25.47	3.684	24.44	3.554	23.39	3.462	25.03	3.718
Fe	13.85	1.121	14.09	1.148	14.79	1.227	14.88	1.240
Mn	0.20	0.013	0.13	0.010	0.22	0.017	0.17	0.011
Ca	0.20	0.019	0.05	0.003	0.22	0.023	0.08	0.005
Na	0.01	0.001	-	0.001	0.01	-	0.03	0.005
K	0.02	0.001	0.01	0.001	0.02	-	0.02	0.002
Ti	-	-	0.01	-	0.03	0.005	-	-
Cr	0.53	0.040	0.10	0.007	0.04	0.002	0.13	0.011
Ni	0.20	0.011	0.04	0.002	0.01	-	0.01	-

t	89.21	9.911	88.68	9.934	87.05	9.863	87.32	9.956

Numbers in brackets indicate number of analyses averaged to get results. Letters preceding sample number indicate rock type: p, background pillows; d, dykes; g, gabbro; a, core and halo alteration zone rocks; s, massive and stringer sulphide samples from dumps; t, total. For each sample first column is percent and second column is stoichiometric proportions.

	p 55(2)		p 85(3)		p 286a(4)		p 84(2)	
Si	29.92	2.965	28.33	2.866	29.60	2.942	31.14	3.082
Al	17.81	2.081	18.92	2.256	17.64	2.064	15.94	1.859
Mg	24.31	3.594	23.03	3.473	24.05	3.564	24.63	3.633
Fe	15.67	1.298	15.93	1.348	16.52	1.372	16.67	1.379
Mn	0.17	0.011	0.23	0.018	0.28	0.021	0.18	0.014
Ca	0.13	0.011	0.08	0.008	0.10	0.010	0.08	0.005
Na	-	-	0.02	0.004	0.02	0.001	-	-
K	0.04	0.002	0.04	0.004	0.01	-	-	-
Ti	-	-	-	-	-	-	-	-
Cr	0.19	0.017	0.21	0.021	0.40	0.040	0.02	-
Ni	0.01	-	0.01	-	0.01	-	0.01	-

t 88.25 9.979 86.80 9.998 88.63 10.014 88.67 9.972

	p 116(3)		d 197b(2)		d 268c(2)		d 34a(2)	
Si	29.93	3.006	29.91	3.036	30.14	3.023	28.82	2.901
Al	17.86	2.113	16.54	1.979	17.27	2.040	18.46	2.189
Mg	20.34	3.044	23.59	3.570	21.42	3.203	21.25	3.188
Fe	19.44	1.633	15.45	1.311	19.55	1.639	20.04	1.687
Mn	0.23	0.018	0.50	0.042	0.20	0.015	0.21	0.018
Ca	0.80	0.085	0.08	0.006	0.09	0.009	0.04	0.003
Na	0.11	0.018	0.02	0.003	0.06	0.009	-	-
K	0.01	-	0.02	0.003	0.02	0.003	0.02	0.003
Ti	-	-	-	-	-	-	-	-
Cr	0.15	0.015	0.18	0.018	0.02	-	0.01	-
Ni	-	-	-	-	-	-	-	-

t 88.87 9.932 86.29 9.968 88.77 9.941 88.85 9.989

	d 263a(2)		d 89a(2)		g 241(2)	
Si	29.48	2.968	28.55	2.913	31.63	3.126
Al	17.26	2.049	17.21	2.069	16.45	1.914
Mg	21.24	3.188	20.42	3.104	24.79	3.651
Fe	20.72	1.746	22.61	1.928	14.30	1.180
Mn	0.16	0.012	0.12	0.009	0.22	0.170
Ca	0.26	0.028	0.05	0.003	0.11	0.011
Na	0.02	0.002	0.02	0.003	0.02	0.002
K	0.10	0.012	0.05	0.006	0.10	0.011
Ti	-	-	-	-	-	-
Cr	0.04	-	-	-	0.02	-
Ni	-	-	-	-	0.01	-

t 89.28 9.995 89.03 10.035 87.65 10.065

	a 199a(2)		a 62d(1)		a 1(2)		a 63c(3)	
Si	31.40	3.115	28.59	2.871	29.50	2.999	28.13	2.891
Al	16.17	1.890	19.88	2.352	16.96	2.032	18.25	2.210
Mg	23.76	3.514	21.67	3.242	21.89	3.315	20.61	3.158
Fe	16.35	1.355	17.36	1.456	18.52	1.573	19.20	1.650
Mn	0.32	0.024	0.25	0.021	0.26	0.021	0.45	0.037
Ca	0.12	0.011	0.05	0.003	0.03	0.003	0.34	0.036
Na	0.02	0.004	0.01	-	0.05	0.009	0.02	0.003
K	0.03	0.002	0.04	0.003	0.10	0.012	0.02	0.001
Ti	-	-	-	-	-	-	-	-
Cr	0.18	0.017	-	-	0.07	0.006	0.07	0.018
Ni	-	-	0.01	-	-	-	-	-

t 88.35 9.932 87.86 9.948 87.38 9.967 87.09 10.004

```

*****
      a 127(7)      a 197e(5)      a 105b(2)      a 137b(2)
-----
Si  28.09  2.836  27.65  2.874  27.45  2.864  28.93  2.934
Al  19.24  2.288  17.87  2.187  18.05  2.221  18.55  2.219
Mg  20.87  3.138  19.52  3.023  19.25  2.993  18.93  2.862
Fe  20.41  1.722  21.36  1.855  21.59  1.884  22.23  1.885
Mn   0.25  0.020   0.64  0.055   0.28  0.024   0.34  0.026
Ca   0.03  0.001   0.03  0.003   0.03  0.003   0.06  0.006
Na   0.01  0.003   0.04  0.007   -      -      0.03  0.003
K    -      -      0.03  0.002   0.03  0.003   0.01  -
Ti   0.01  -      -      -      -      -      -      -
Cr   0.02  -      0.12  0.012   0.14  0.012   0.02  -
Ni   0.03  -      -      -      -      -      0.01  -
-----
t   88.96 10.008  87.26 10.018  86.82 10.004  89.11  9.935
*****
      a 138a(4)      a 198b(2)      a 101(2)      a 289(3)
-----
Si  28.15  2.925  28.66  2.970  27.39  2.863  29.23  3.009
Al  17.70  2.168  16.53  2.018  18.28  2.252  16.67  2.021
Mg  18.32  2.836  19.38  2.995  18.14  2.826  18.59  2.853
Fe  22.39  1.946  22.55  1.954  22.91  2.004  23.93  2.061
Mn   0.35  0.030   0.48  0.040   0.30  0.024   0.14  0.012
Ca   0.06  0.006   0.11  0.009   0.07  0.006   0.02  -
Na   -      -      0.01  -      0.03  0.003   0.04  0.006
K    0.09  0.012   0.01  -      -      -      0.04  0.003
Ti   -      -      -      -      -      -      -      -
Cr   0.55  0.058   0.24  0.024   0.18  0.018   0.13  0.012
Ni   0.01  -      0.01  -      -      -      -      -
-----
t   87.62  9.981  87.98 10.010  87.30  9.996  88.79  9.977
*****

```

	a 50a(2)		a 95b(3)		a 42a(5)		s 0-10b(2)	
Si	27.26	2.859	26.68	2.844	26.81	2.831	33.44	3.355
Al	18.23	2.253	18.30	2.300	19.00	2.363	12.86	1.520
Mg	16.29	2.545	15.09	2.396	14.47	2.276	22.37	3.347
Fe	26.15	2.293	26.94	2.400	27.97	2.470	19.48	1.635
Mn	0.37	0.031	0.38	0.034	0.28	0.022	0.08	0.006
Ca	0.03	0.003	0.02	-	0.03	0.001	0.02	-
Na	0.04	0.006	0.01	-	0.02	0.003	0.07	0.012
K	0.04	0.003	0.01	-	0.01	0.001	0.07	0.009
Ti	-	-	-	-	-	-	-	-
Cr	0.04	0.003	0.09	0.009	0.12	0.004	-	-
Ni	-	-	-	-	-	-	-	-

t	88.45	9.996	87.52	9.983	88.71	9.971	88.39	9.884
---	-------	-------	-------	-------	-------	-------	-------	-------

	s 282r(2)		s 0-18(2)		s 9d(2)		s 0-19(4)	
Si	28.45	2.955	26.95	2.819	28.02	2.895	28.09	2.978
Al	19.11	2.339	19.14	2.361	18.71	2.277	17.00	2.122
Mg	16.02	2.479	16.77	2.613	16.63	2.559	15.23	2.406
Fe	23.64	2.052	24.70	2.159	25.32	2.186	27.02	2.395
Mn	0.20	0.015	0.33	0.027	0.32	0.027	0.12	0.009
Ca	0.03	0.003	0.01	-	0.01	-	0.02	0.002
Na	0.04	0.006	0.06	0.012	0.04	0.006	0.02	0.002
K	0.04	0.003	0.01	-	0.02	-	0.04	0.003
Ti	0.02	-	-	-	0.01	-	0.01	-
Cr	0.01	-	-	-	-	-	0.20	0.017
Ni	-	-	0.02	-	-	-	-	-

t	87.56	9.852	87.99	9.991	89.08	9.950	87.75	9.934
---	-------	-------	-------	-------	-------	-------	-------	-------

	s 0-20(3)		s 202a(5)		s 0-14(5)		s 277(2)	
Si	26.43	2.857	27.55	2.919	29.22	3.057	26.79	2.919
Al	17.11	2.181	17.40	2.173	15.60	1.923	16.82	2.158
Mg	15.47	2.496	14.62	2.303	15.08	2.337	11.32	1.835
Fe	27.59	2.496	28.16	2.494	29.52	2.598	33.30	3.035
Mn	0.14	0.013	0.94	0.083	0.07	0.002	0.29	0.025
Ca	-	-	0.04	0.002	0.14	0.014	0.04	0.003
Na	-	-	0.02	0.002	0.09	0.015	0.04	0.006
K	0.02	0.003	0.03	0.001	0.04	0.005	0.05	0.006
Ti	0.01	-	-	-	0.02	-	0.01	-
Cr	0.01	-	0.05	0.002	0.12	0.009	-	-
Ni	0.04	-	0.02	0.001	-	-	0.03	-
t	86.82	10.046	88.83	9.980	89.90	9.960	88.69	9.987

Appendix F

Fluid Inclusion Methodology

Fluid inclusion sections are doubly polished and are ideally between 0.5 and 0.2 mm thick. Cutting and grinding of the sections must be carried out carefully and slowly to insure that frictional heating does not decrepitate the inclusions. A complete listing of the preparation procedure is given in Higgins (1979).

Microthermic studies were carried out on a Chaixmeca Heating/Freezing Stage which consists of three components: (a) a heating freezing stage attached to a petrographic microscope stage; (b) a temperature monitor/control unit; (c) a pressurized liquid nitrogen container. To prevent icing up of the sample and the objective lens Higgins (1979) devised an adaption: dry nitrogen gas is fed into a tube which is placed along-side the sample and the lens. Higgins (1979) provides a more detailed description of the system complete with diagrams.

The stage was calibrated for the heating runs by melting a small amount of several standard chemicals (in powder form) between glass cover slips and comparing the measured melting temperature with the actual melting temperature of each compound. The resulting calibration curve is presented in Fig. F-1. Past experience has shown that it is not necessary to calibrate for the cooling runs (D.F. Strong, pers. comm., 1982).

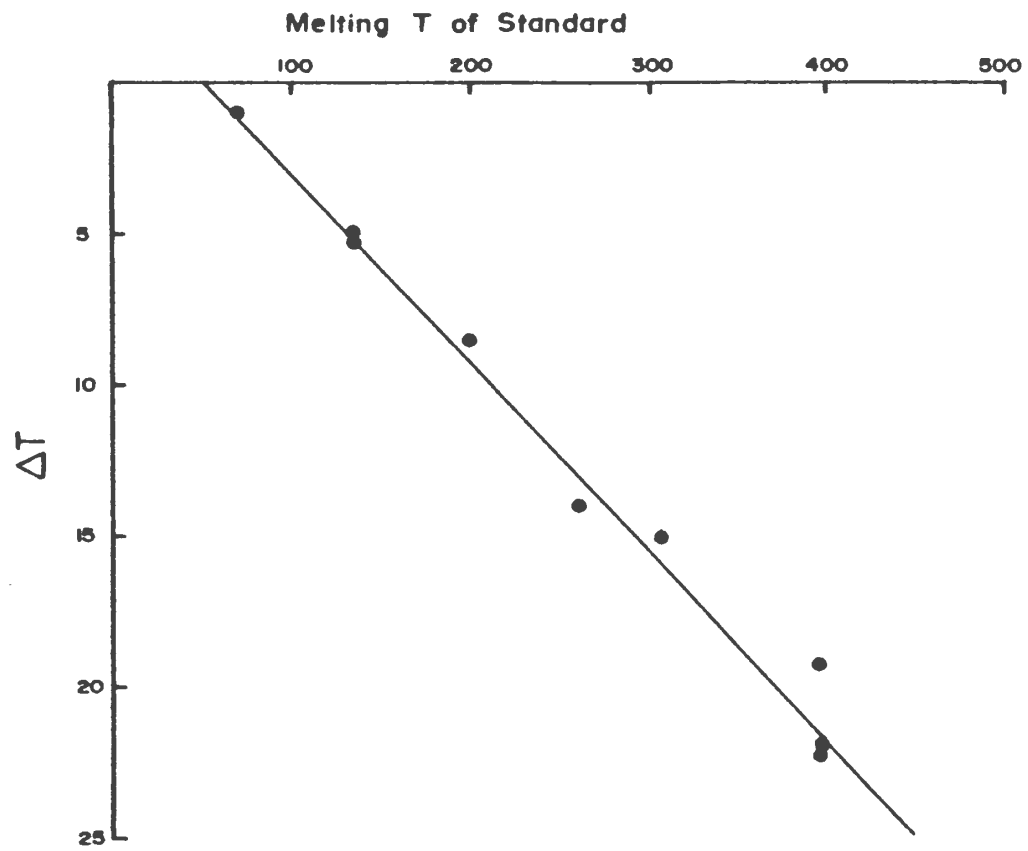


Figure F-1: Calibration curve for fluid inclusion heating runs

